



UNIVERSITAT
POLITÈCNICA
DE VALÈNCIA

UNIVERSITAT POLITÈCNICA DE VALÈNCIA

INSTITUTO INTERUNIVERSITARIO DE INVESTIGACIÓN DE RECONOCIMIENTO
MOLECULAR Y DESARROLLO TECNOLÓGICO

DEPARTAMENTO DE QUÍMICA

Tesis Doctoral

**SCREENING METHODOLOGIES FOR THE DETERMINATION OF
WATER CONTAMINANT RESIDUES BY COMPACT DISK
TECHNOLOGY**

Presentada por **Paulina Dobosz** para optar al grado de Doctor por la Universitat Politècnica
de València

Directores

Dr. Àngel Maquieira Catalá

Dr. Sergi Morais Ezquerro

Valencia, Enero 2017

D. Ángel Maquieira Catalá, Catedrático de Universidad del Departamento de Química de la Universitat Politècnica de València.

D. Sergi Morais Ezquerro, Profesor Contratado Doctor del Departamento de Química de la Universitat Politècnica de València.

CERTIFICAN: Que el trabajo que presenta Paulina Dobosz, en esta memoria, con el título “*Screening methodologies for the determination of water contaminant residues by compact disk technology*” ha sido realizado bajo nuestra dirección en el Instituto Interuniversitario de Investigación de Reconocimiento Molecular y Desarrollo Tecnológico (IDM) de la Universitat Politècnica de València para optar al grado de Doctor por la Universitat Politècnica de Valencia. Para que así conste, firman el presente certificado en Valencia, 18 de enero de 2017.

Dr. Ángel Maquieira Catalá

Dr. Sergi Morais Ezquerro

Dla mamy

Resumen

La contaminación de aguas superficiales causada por plaguicidas y productos industriales es actualmente, uno de los grandes problemas medioambientales. Aunque estas sustancias están presentes a niveles muy bajos, tienen efectos perjudiciales en el medio en general y especialmente en humanos. Por este motivo, diferentes instituciones han regulado los niveles de contaminantes en áreas de control de la calidad de las aguas, creando listas prioritarias de sustancias peligrosas y tóxicas para el medio ambiente.

Actualmente, la monitorización de los contaminantes incluidos en las listas oficiales se realiza mediante técnicas cromatográficas y espectrometría. Estos métodos analíticos están aprobados como técnicas de referencia para la determinación de residuos orgánicos presentes en aguas naturales. A pesar de ser técnicas fiables, reproducibles y sensibles, los métodos cromatográficos no están exentos de inconvenientes. Este tipo de metodologías requiere una instrumentación costosa y una laboriosa preparación de muestra, que hacen que el análisis sea en general complejo.

Por ello, el desarrollo de métodos analíticos alternativos que faciliten hacer medidas in-situ a bajo coste y con gran capacidad de trabajo es de gran utilidad. En este sentido, las técnicas inmunoquímicas tienen un gran potencial analítico ya que son en general sensibles y selectivas, se pueden utilizar en el lugar de la toma de muestra y tienen capacidad multianalito.

Esta tesis se ha centrado en el desarrollo de un sistema biosensor, basado en la tecnología de disco compacto, para la detección multianalito de diversos contaminantes prioritarios en aguas naturales.

Las limitaciones más críticas para el desarrollo de un biosensor multianalito mediante métodos inmunoquímicos son los relacionados con su sensibilidad y selectividad. Por lo tanto, una parte importante de la tesis se ha centrado en la selección de inmunoreactivos, formato y optimización de diferentes parámetros claves del ensayo.

Una estrategia utilizada para aumentar la sensibilidad de los ensayos ha consistido en marcar la inmunoreacción con nanopartículas de oro. Para ello, se ha estudiado diferentes tipos (esféricas y cilíndricas) de distinto tamaño y se han comparado sus prestaciones analíticas (relación señal ruido, sensibilidad etc.) También, se han desarrollado inmunoensayos cuantitativos sin necesidad de amplificación de la señal.

Por otro lado, se ha desarrollado una aproximación que hemos denominado “inmuncaptura” basada en el uso de nanopartículas de oro como especie de captura de analitos en disolución y que actúa como marcador de la inmunointeracción que tiene lugar en la fase sólida.

Finalmente, se han analizado muestras de agua naturales dopadas con distintos niveles de los analitos objeto de estudio para evaluar la utilidad de las metodologías desarrolladas como

herramienta de screening masivo en el área medioambiental. Los resultados obtenidos han sido comparados con los obtenidos mediante las técnicas de referencia.

Las investigaciones realizadas han permitido desarrollar nuevos formatos de ensayo y conocimientos inmunoquímicos aplicados a la tecnología de disco compacto, aportando nuevas herramientas de screening que permiten la determinación simultánea de contaminantes en aguas naturales por debajo de las concentraciones establecidas en la normativa europea de calidad de agua.

Resum

La contaminació d'aigües superficials causada principalment per plaguicides i altres productes industrials és un dels grans problemes mediambientals actuals. Malgrat que aquestes substàncies estan presents en nivells molt baixos, tenen efectes perjudicials en humans i animals. Per aquest motiu, diferents institucions estatals han regulat els nivells de contaminants en àrees de control de la qualitat de l'aigua, creant llistes prioritàries de substàncies perilloses i tòxiques per al medi ambient.

Actualment, la monitorització dels contaminants inclosos en les llistes oficials es realitza mitjançant tècniques cromatogràfiques i d'espectroscòpia de masses. Aquests mètodes analítics estan aprovats com a tècniques de referència per a la determinació de residus orgànics presents en aigües naturals. Malgrat ser tècniques fiables, reproduïbles i sensibles, els mètodes cromatogràfics no estan exempts d'inconvenients. Aquest tipus de metodologies requereix una instrumentació costosa i una laboriosa preparació de mostres que fan que l'anàlisi sigui, en general, complex.

Per això, el desenvolupament de mètodes analítics alternatius que facilitin la possibilitat de fer mesures in-situ a baix cost i amb gran capacitat analítica és de gran utilitat. En aquest sentit, les tècniques immunoquímiques tenen un gran potencial analític ja que són, en general, sensibles i selectives, es poden utilitzar en el lloc de presa de la mostra i tenen capacitat multianalítica.

Aquesta tesi s'ha centrat en el desenvolupament d'un sistema biosensor, basat en la tecnologia de disc compacte, per a la detecció multianalítica de diversos contaminants prioritaris en aigües naturals.

Les limitacions més crítiques per al desenvolupament d'un biosensor multianalític mitjançant mètodes immunoquímics són sensibilitat i selectivitat. Per tant, una part important de la tesi es va centrar en la selecció de immunoreactius, format i optimització de diferents paràmetres clau de l'assaig.

La detecció es va dur a terme mitjançant l'ús de nanopartícules d'or com a marcadors de la immunointeracció i amplificació de la senyal analítica. S'han estudiat diferents estructures d'or (esferes i cilindres) de diferents tamanys, i s'han comparat les seves prestacions analítiques (relació senyal-soroll, sensibilitat, etc.). També s'han desenvolupat immunoassaigs quantitius sense necessitat d'amplificació del senyal.

Per altra banda, s'ha desenvolupat una aproximació que hem denominat "immunocaptura", basada en l'ús de nanopartícules d'or com a espècie de captura d'analits en dissolució i que actua com a marcador de la immunointeracció que té lloc en la fase sòlida.

Finalment, s'han analitzat mostres d'aigües naturals dopades amb diferents nivells dels analits objecte d'estudi per avaluar la utilitat de les metodologies desenvolupades com a eina de

"screening" massiu en l'àrea mediambiental. Els resultats obtinguts han sigut avaluats per comparació amb els obtinguts mitjançant tècniques de referència.

Les investigacions realitzades han permès desenvolupar nous formats d'assaig i coneixements immunoquímics aplicats a la tecnologia de disc compacte, aportant noves eines de "screening" que permetin la determinació de contaminants en aigües naturals per sota dels límits de concentració establerts per les normes internacionals de la qualitat de l'aigua.

Abstract

The contamination of water resources with many industrial, agricultural and other chemicals is one of the key environmental problems that humanity is facing nowadays. Despite the fact that they are usually present at very low concentration, they possess a significant risk to aquatic and human life.

To address this issue many national and international institutions set different regulations to monitor and control the water quality.

Currently, the monitoring of compounds included in official watch lists is conducted by chromatographic and mass spectroscopic methods. These techniques are approved as “gold standards” for analytical quantitation of organic residues in water. Although they are sensitive and reproducible, cannot be used on-site. The need of sampling and centralized laboratory measurements makes not only the overall cost high but lowering the efficiency of the analysis.

Therefore, there is an urgent need to develop suitable field methods to facilitate the *in situ* measurements at a low cost. Biosensors are therefore an alternative technology that can provide sensitive results in a fast and affordable way.

This thesis has focused on the development of a biosensor based on immunoassays and compact disk technology, for the multiplex detection of priority water contaminants.

As the methods based on the immunorecognition events are challenging in terms of the selectivity and sensitivity, the major part of the thesis was the selection of the immunoreagents, assay form and procedure.

For the detection part, gold nanostructures were selected as sensitive tags for signal enhancement. Therefore, different nanoparticles were studied in order to select the optimal size in terms of the signal enhancement, sensitivity and antibody amount used. Also, the assays performances with signal enhancement and without any amplification were evaluated. The best immunoassay was selected for developing the multiplexed assay.

Furthermore, an approach to improve the readout sensitivity of microimmunoassays based on used of gold nanoparticles as both capture and detection species was demonstrated. The method is based on the performance of the immunorecognition event in a homogeneous mode and detection part in the heterogeneous format.

Finally, representative water samples were analysed to confirm the applicability of the multi-residue assay. The analytical properties have been established for each methodology and the obtained results have been validated by comparison with reference techniques.

The investigations carried out in this work, have resulted in new insights in immunoassay technique that could be useful for screening applications.

Publications:

Dobosz, P.; Morais, S.; Puchades, R.; Maquieira, Á. *Nanogold bioconjugates for direct and sensitive multiplexed immunosensing*, Biosens. Bioelectron. **2015**, 69, 294–300

Dobosz, P.; Morais, S.; Bonet, E.; Puchades, R.; Maquieira, Á., *Massive Immuno Multiresidue Screening of Water Pollutants*, Anal. Chem., **2015**, 87, 9817–9824

Dobosz, P.; Morais, S.; Puchades, R.; Maquieira, A *homogeneous immunocapture assay as a practical approach to increase immunoassay sensitivity* (In preparation)

Participation in scientific conferences:

Dobosz, P.; Morais, S.; Puchades, R.; Maquieira, Á., *A gold nanoparticle-based immunoassay: the influence of nanoparticle size on assay sensitivity*, VII Workshop on Sensors and Molecular Recognition, ISBN 978-84-695-8811-6, Valencia, **2013**.

Dobosz, P.; Morais, S.; Puchades, R.; Maquieira, Á., *Gold nanoparticle-based immunoassay on a Digital Versatile Disk for the determination of priority pollutants residues in water*, XVII euroAnalysis, Analytical chemistry for human well-being and sustainable development, Warsaw, **2013**.

Dobosz, P.; Morais, S.; Puchades, R.; Maquieira, Á., *Rapid Screening Test on DVD-R for Priority Water Pollutants*, I Encuentro de Doctorandos de UPV, Valencia, **2014**.

Dobosz, P.; Morais, S.; Puchades, R.; Maquieira, Á., *Nanogold conjugates for direct biosensing of small organic molecules*, VIII Workshop on Sensors and Molecular Recognition, ISBN 978-84-697-1302-0, Valencia, **2014**.

Dobosz, P.; Morais, S.; Puchades, R.; Maquieira, Á., *A homogeneous immunocapture as a practical approach to increase immunoassay sensitivity*, VIII Workshop on Sensors and Molecular Recognition, ISBN 978-84-697-1302-0, Valencia, **2014**.

Dobosz, P.; Morais, S.; Puchades, R.; Maquieira, Á., *Antibody-Functionalized Nanoparticles For Multi-Residue Screening of Water Pollutants*, IX International Workshop on Sensors and Molecular Recognition, Valencia, **2015**.

Table of Contents

I Introduction.....	27
1.1 Water contamination.....	27
1.2 Gold standard methods used for water monitoring.....	32
1.3 Monitoring and screening systems.....	33
1.4 Rapid assays for detection of pollutant residues in water.....	38
1.5 Multiplex bioanalytical methods for environmental monitoring.....	40
1.5.1 Planar arrays.....	42
1.5.2 Suspension arrays.....	44
1.5.3 Automated multi-analyte systems.....	46
1.6 Biosensing.....	48
1.6.1 Biorecognition elements.....	49
1.6.2 Signal tags.....	51
1.6.3 Assay formats.....	58
1.6.4 Supports.....	61
1.6.5 Techniques for detection of the immunointeraction events.....	64
1.7 Compact Disk technology.....	67
1.7.1 Analytical applications of disks as analytical platform.....	69
1.7.1.1 Lab-on-a-CD.....	70
1.7.1.2 Compact disk technology as analytical tool.....	70
II Objectives.....	77
III Materials and Methods.....	91
3.1 Reagents.....	91
3.2 Instruments.....	92
3.3 Antibody purification.....	93
3.4 Preparation of coating conjugates.....	93
3.5 Gold colloid titration procedure.....	94
3.6 Preparation of antibody-nanogold conjugates (Ab-AuNPs).....	95
3.7 Preparation of antibody-gold nanorod conjugates (Ab-AuNRs).....	96
3.8 Preparation of antigen-nanogold tracers (OVA-H-AuNPs).....	97
3.9 Preparation of hapten-nanogold tracers (H-AuNPs).....	98
3.10 Microarraying.....	99
3.11 Microimmunoassay protocols.....	101
3.11.1 Two-step antigen-coated microimmunoassay using antibody-nanogold conjugates.....	101
3.11.2 One-step antigen-coated microimmunoassay using antibody-nanogold conjugates.....	102
3.11.3 One-step antigen-coated microimmunoassay using antibody-gold nanorod conjugates.....	102

3.11.4 Two-step antibody-coated microimmunoassay using antigen-nanogold tracers.....	103
3.11.5 Two-step antibody-coated microimmunoassay using hapten-nanogold tracers	104
3.11.6 Immunocapture microimmunoassay	104
3.12 Analysis of water samples	105
3.13 Compact disk scanning and data acquisition	105
IV Results and Discussion.....	109
4.1 Purification of antibodies.....	109
4.2 Characterization of gold nanoparticles.....	111
4.3 Optimization of antibody-gold nanoparticles conjugation.....	113
4.4 Selection of the nanoparticle size.....	118
4.4.1 Two-step antigen-coated microimmunoassay using antibody-nanogold	118
4.4.2 One-step antigen-coated microimmunoassay using antibody-nanogold	120
4.5 Two-step antibody-coated microimmunoassay using antigen – nanogold tracers.....	122
4.6 One-step microimmunoassay using antibody-gold nanorods	125
4.6.1 Titration experiments of the antibody-gold nanorods conjugates.....	128
4.6.2 Competitive immunoassays using antibody-gold nanorod conjugates	129
4.7 Two-step antigen-coated microimmunoassay using hapten nanogold tracers.....	130
4.8 Optimization of the performances of microimmunoassay	134
4.9 Individual calibration curves	140
4.10 Selection of the antibodies for the development of a multiplex assay	144
4.11 Multiplex calibration curves	156
4.12 Study of the assay controls	160
4.13 Study of the antibody-gold nanoparticles stability	163
4.14 Immunocapture microimmunoassay.....	164
4.14.1 Selection of the optimal conditions for homogeneous immunocapture step.....	164
4.14.2 Competitive assays using immunocapture step.....	168
4.15 Determination of the potential of the developed methodology. Analysis of water samples..	173
V Conclusions	183
VI References.....	189

List of Figures

Figure 1. The selection role of a screening approach. Samples in black contain the analyte at a level above the pre-set cut-off value.	36
Figure 2. Overview of multiplex bioanalytical technologies currently applied for food and environmental analysis (adapted from ⁶²).	41
Figure 3. Different capture agents and detection methods applied in microarray immunoassays (adapted from ⁷⁴).	48
Figure 4. Overview of a single IgG structure. Left view shows the three-dimensional structure of an IgG1 molecule determined by X-ray crystallography. The heavy chains (H) are shown in dark-blue and the light chains (L) are seen as light-blue. Right view shows a simplified model of IgG structure using the same colour coding as left view. (CDR – complementary determining region, C _H – constant region on heavy chain, C _L – constant region on light chain, V _H – variable region on heavy chain, V _L – variable region on light chain).	49
Figure 5. Schematic representations of (a) localized surface plasmon resonance, (b) electric oscillation of gold nanosphere (c) electric oscillation of gold nanorods (adapted from ⁹⁸).	53
Figure 6. (A) Relative size of nanoparticles and biomolecules, drawn to scale. Schematic representation of a nanoparticle with 5 nm core diameter, 10 nm shell diameter, with PEG molecules of 2000 and 5000 g mol ⁻¹ (on the left, light grey), streptavidin (green), transferrin (blue), antibody (IgG, purple), albumin (red), single-stranded DNA (20mer, cartoon and space filling). Proteins are crystal structures taken from the Protein Data Bank (http://www.rcsb.org) and displayed as surfaces; PEG and DNA have been modelled from their chemical structure and space filling (from ¹⁰⁹). (B) Protein attachment modes on AuNPs.	57
Figure 7. Scheme of the most commonly employed heterogeneous immunoassay configurations (adapted from ¹²⁰) A. Immobilized antigen format; B. Immobilized antibody format.	60
Figure 8. Dose-response curve for a competitive immunoassay.	61
Figure 9. DVD cross section representing pits and lands.	67
Figure 10. Characteristics of compact disks and lasers used in disk drives.	68
Figure 11. Schematic representation of disc reading process.	69
Figure 12. Chemical structure of 2-(2,4,5 trichlorophenoxy)propionic acid.	78
Figure 13. Chemical structure of 3-phenoxybenzoic acid.	78
Figure 14. Chemical structure of 4-nitrophenol.	79
Figure 15. Chemical structure of alachlor.	79
Figure 16. Chemical structure of atrazine.	80
Figure 17. Chemical structure of azoxystrobin.	80
Figure 18. Chemical structure of chlorpyrifos.	81
Figure 19. Chemical structure of diazinon.	81

Figure 20. Chemical structure of diuron.	82
Figure 21. Chemical structure of endosulfan.	82
Figure 22. Chemical structure of fenthion.....	83
Figure 23. Chemical structure of forchlorfenuron.....	83
Figure 24. Chemical structure of imidacloprid.	84
Figure 25. Chemical structure of malathion.	84
Figure 26. Chemical structure of pentachlorophenol.	85
Figure 27. Chemical structure of pyraclostrobin.....	85
Figure 28. Chemical structure of sulfasalazine.	86
Figure 29. Chemical structure of triclosan	86
Figure 30. Antibody gold nanoparticles conjugation protocol.....	95
Figure 31. Antibody gold nanorods conjugation protocol.....	97
Figure 32. Coating antigen gold nanoparticles conjugation protocol.....	98
Figure 33. Scheme of the conjugation protocol for the preparation of hapten-nanogold tracers. .	99
Figure 34. Non-contact printer used for microarraying.....	99
Figure 35. DVD microarray layout used for the optimization steps.	100
Figure 36. DVD microarray layout.	100
Figure 37. Scheme of the two step antigen-coated microimmunoassay using antibody-nanogold conjugate.	101
Figure 38. Scheme of one step antigen-coated microimmunoassay using antibody-nanogold conjugates.....	102
Figure 39. Scheme of the one step microimmunoassay with antibody-gold nanorod conjugate.	103
Figure 40. Scheme of the antibody-coated two-step micro immunoassay using antigen-nanogold tracer.....	103
Figure 41. Scheme of two-step antibody-coated immunoassay using hapten-nanogold tracers.	104
Figure 42. Scheme of the immunocapture procedure.....	105
Figure 43. Scheme of the detection system.	106
Figure 44. Elution profile for the purification of anti-atrazine serum using protein G column. .	110
Figure 45. Surface plasmon resonance bands for studied nanoparticles.	111
Figure 46. UV/VIS spectra of colloidal gold (5 nm) and the antibody conjugate. The inset graph shows the λ_{max} for the gold absorption peaks and the resulting red-shift upon antibody conjugation. The peak at 280 nm corresponds to protein absorption.	112
Figure 47. Scheme of the aggregation test.	113
Figure 48. Gold aggregation tests performed to evaluate the minimal antibody concentration required to avoid aggregation of gold nanoparticles of different size.	114
Figure 49. Optimization of pH of the conjugation for all studied AuNPs size.	117

Figure 50. Size profile of AuNPs before and after incubation with antibodies (A-bare AuNPs, B-AuNPs incubated with 2.5 $\mu\text{g}/\text{mL}$ of IgGs, C-AuNPs incubated with 30 $\mu\text{g}/\text{mL}$ of IgGs).....	118
Figure 51. Titration experiment of different gold conjugates performed to evaluate the amplification yields of different sized gold nanoparticles.....	119
Figure 52. Titration experiment of AbAuNPs performed to evaluate their applicability in immunoassays without signal amplification.	121
Figure 53. Evaluation of the optimal competition conditions using antigen-tracer dilutions 1/200 (A) and 1/1000 (B).	123
Figure 54. A. Competition curve for antigen-nanogold atrazine tracers. B. Analytical features for both assays.	125
Figure 55. Optimization of the PEG concentration for nanorod stabilization. Left and right panels show the changes in the absorbance and in the SPR_{max} for different PEG concentrations, respectively.	126
Figure 56. UV/VIS spectra of gold nanorods and the antibody conjugate. The inset graph shows the λ_{max} for the gold absorption peaks and the resulting red-shift upon PEG and antibody conjugation.....	127
Figure 57. Titration experiment for antibody-nanorod conjugates.....	128
Figure 58. Antibody-gold nanorod competitive assays for imidacloprid.....	130
Figure 59. PEGylated gold nanoparticles.....	131
Figure 60. Titration experiments using Au atrazine hapten tracer.	132
Figure 61. Competition curve for atrazine using Au-hapten tracer. The standard curves are the mean of 10 curves performed in different days and on different discs averaging four points per analyte concentration.	133
Figure 62. Signal intensities values obtained for different printing carbonate buffer concentrations.	134
Figure 63. Different ways of applying the sample onto the microarray.....	135
Figure 64. Comparison of signal intensities for different droplets volumes for three analytes. (A) – Signal intensities for tested analytes; (B) – Signal intensities for control (GAR-Au).....	136
Figure 65. Comparison of signal intensities for different sample volumes using cover glass slides. (A) Signal intensities for tested analytes (A) and (B) for the positive control (GAR-Au).....	137
Figure 66. Optimization of the incubation time of the chlorpyrifos immunoassay.....	138
Figure 67. Analytical response of silver (A) and copper (B) enhancement reagents.....	139
Figure 68. Spot diameter profile upon increment of development time.....	140
Figure 69. Influence of the coating antigen concentration on the assay sensitivity for atrazine.	141
Figure 70. Influence of the nanogold bioconjugate optical density on sensitivity of the immunoassay for atrazine.....	143

Figure 71. (A) The binding of two antibodies with shared-reactivity to one immobilized coating conjugate.(B) The binding of antibody to two different analytes. Antibody B binds to both analytes, whereas antibody A only to analyte A.	145
Figure 72. Effect of antigens with shared (B) or cross-reactivity (C) on the displacement of antigen from the immune complex represented as a curve A.....	146
Figure 73. A) Layout of the 10-plex immuno multi-residue assay. B) Images showing the selectivity of antibody-nanogold conjugates. (1. Alachlor; 2. Atrazine; 3. Azoxystrobin; 4. Chlorpyrifos; 5. Diuron; 6. Forchlorfenuron, 7. 3-Phenoxybenzoic acid, 8. Pyraclostrobin; 9. Sulfasalazine, 10. Triclosan).	152
Figure 74. Alternative array configurations (Green and grey arrays correspond to positive and negative controls, respectively).....	153
Figure 75. Competition curves for the 10-plex assay. Panel A and B represent sigmoidal curves, whereas panels C and D show the linear working ranges for 10-plex assays.	157
Figure 76. Competitive curves for eight analytes that were not included in the 10-plex assay. .	159
Figure 77. Images of the 10-plex microimmunoassay after reading the disk. Panel A represent the matrix layout, whereas panels 1, 2 and 3 show the spots intensity. The concentration of the mixture analytes in panels 1, 2 and 3 is 0, 1.0 and 16.0 $\mu\text{g/L}$, respectively; see Figure 36 for the layout.	160
Figure 78. Comparison of the signal intensities of first step control for individual assays.....	161
Figure 79. Signal variability for the second positive control (GAR-IgG-Au).....	162
Figure 80. Time stability profile of the nanogold bioconjugates and batch to batch variability. 163	
Figure 81. Recovery of the signals after centrifugation of the samples (A: without centrifugation, B: after centrifugation).	165
Figure 82. Comparison of the sensitivity between assays with pre-incubation step (PI) and using immunocapture concept (IC).....	166
Figure 83. Signal intensity profile for different nanogold bioconjugate-sample volume ratios..	167
Figure 84. Competitive assays in immunocapture format. Curves obtained using 1.0 μL (A) and 0.5 μL (B) of nanogold conjugate.	168
Figure 85. Competitive curves for different immunoassay approaches (SI – standard immunoassay; PI – preincubation immunoassay, IC – immunocapture step) for chlorpyrifos...	169
Figure 86. Pyraclostrobin titration experiments to evaluate the optimal AuNPs dilution for immunocapture step.	171
Figure 87. Calibration curves for three different one step immunoassays approaches (SI –standard immunoassay; PI – preincubation immunoassay, IC – immunocapture step).....	172

List of Tables

Table 1. Emerging contaminants included in the EU Watch list ²³	29
Table 2. Priority substances list under Water Framework Directive ¹⁵	31
Table 3. Rationale for the updating of water quality monitoring and technologies aiming to rectify these insufficiencies (adapted from ⁴⁶).....	34
Table 4. Characteristics of selected types of prototype or commercially available tools and technologies for chemical and biological monitoring requirements within the WFD (adapted from ⁴⁶).....	37
Table 5. Selected suppliers of immunoassay test-kits for environmentally relevant compounds (adapted from ⁶⁰)	39
Table 6. A list of AWACSS compounds monitored in the surface water, groundwater, municipal/industrial wastewater and sediment samples within the years 2001–2003.....	47
Table 7. Properties of polyclonal, monoclonal and recombinant Abs.....	50
Table 8. a) Enzymes commonly used as labels in heterogeneous immunoassays.....	51
Table 9. Types of conjugations between biomolecules and noble metal NPs (adapted from ¹⁰²)	55
Table 10. Chemical and physical characteristic of solid phases (Adapted from ^{128–130})	62
Table 11. Labels used in immunoassays	65
Table 12. Systems studied for the multiplex immunoassay	92
Table 13. Centrifugation conditions for all studied nanoparticle sizes	95
Table 14. Minimum antibody concentration needed to stabilize gold nanoparticles from aggregation and comparison between theoretical calculation and experimental results	116
Table 15. Optimal concentration of the coating conjugates and nanogold bioconjugate dilution and its optical density for the eighteen analytes studied	144
Table 16. Colour coded shared reactivity of antibody-functionalized nanoparticles	148
Table 17. Reactivity for gold labelled 4NP, TPA and CLP antibodies	150
Table 18. Forchlorfenuron hapten structures	151
Table 19. Cross-reactivity values for structurally related compounds in the ten-plex immunoassay.....	155
Table 20. Limit of detection (LOD; IC ₁₀), sensitivity (IC ₅₀), working range (WR), slope, and linear regression coefficient (r ²) for all tested analytes.....	158
Table 21. Immunizing proteins used for the preparation of the antibodies integrated in 10-plex immunoassay.....	161
Table 22. Analytical parameters of chlorpyrifos immunoassays for immunocapture, preincubation and standard immunoassay approaches with signal amplification.....	170
Table 23. Comparison of analytical parameters for standard immunoassay and immunocapture without signal amplification.....	172
Table 24. Results obtained for the immuno multi-residue ^a and chromatographic ^b analysis (GC-MS or HPLC-MS) of spiked water sample	175

Abbreviations and Acronyms

4NP	4-Nitrophenol
Ab	Antibody
ALA	Alachlor
ATZ	Atrazine
AuNP	Gold nanoparticle
AuNR	Gold nanorod
AZB	Azoxystrobin
BSA	Bovine serum albumin
BD	Blu-ray disk
CD	Compact disk
CTAB	Cetyltrimethylammonium bromide
DCC	N, N'-Dicyclohexylcarbodiimide
DLS	Dynamic light scattering
DNA	Deoxyribonucleic acid
DIU	Diuron
DVD	Digital versatile disk
DZN	Diazinon
EC	European Commission
ECD	Electron capture detector
ELISA	Enzyme-linked immunosorbent assay
EPA	Environmental protection agency
FCF	Forchlorfenuron
FNT	Fenthion
FPD	Flame photometric detector
GC	Gas chromatography
HPLC	High performance liquid
HRP	Horseradish peroxidase
HSA	Human serum albumin
IC	Immunocapture assay
IgG	Immunoglobulin G
IMD	Imidacloprid

LC	Liquid chromatography
LOD	Limit of detection
MLT	Malathion
MS	Mass spectrometry
MR	Microcystin
mAb	Monoclonal antibody
NHS	N-Hydroxysuccinimide
NPD	Nitrogen phosphorus detector
OVA	Ovalbumin
OD	Optical density
pAb	Polyclonal antibody
PAHs	Polyaromatic hydrocarbons
PBA	3-phenoxybenzoic acid
PC	Polycarbonate
PCP	Pentachlorophenol
PEG	Polyethylene glycol
PI	Preincubation immunoassay
PYS	Pyraclostrobin
QD	Quantum dot
rAb	Recombinant antibody
SDWA	Safe drinking water act
SERS	Surface enhanced Raman spectroscopy
SI	Standard immunoassay
SNS	Silver nanospheres
SPR	Surface plasmon resonance
SSZ	Sulfasalazine
TCA	2-(2,4,5-trichlorophenoxy) propionic
TCS	Triclosan
TEM	Transmission electron microscopy
UN	United Nations
UV-vis	Ultraviolet-visible
WFD	Water framework directive

1

Introduction

I Introduction

1.1 Water contamination

Many of the major problems that humanity is facing in the twenty-first century are related to water quality issues. Key forms of water pollution come from human and industrial activities, misuse of chemicals, agricultural pesticides and fertilizers. It has been estimated that half of the population of the developing world is exposed to polluted sources of water. As a consequence, it has effect on environment in general and in the human health, in particular.^{1,2}

Currently, more than 85,000 chemicals are produced worldwide, of which more than 2200 in amounts exceeding 450 tons of active substances per year.³ Pesticides are second in the amount, after the fertilizers, chemicals applied and use in the environment. In 2013, the total quantity of pesticide sales amounted to close to 360 000 tonnes. Spain (19.5 %), France (18.7 %), Italy (13.8 %), Germany (12.3 %) and Poland (6.2 %) were the Member States in which the highest quantities of pesticides were sold.⁴

According to European Union Pesticide Database, 1331 active substances are recognized with 482 compounds being approved to be used in crop protection.⁵ The majority of them are used as herbicides, fungicides and insecticides. There are also several plant growth regulators and repellents. These substances belong to more than 100 different classes. Europe accounts for nearly one-third of the world pesticide market (\$30 billion/year) whereas North America and Asia each share approximately 25% of the world market. The United States is the leading consumer of pesticides, followed by India and France, the main European consumer. Per hectare, Japan uses 12 kg, Europe 3 kg, and the United States 2.5 kg, far surpassing India (0.5 kg), which is also one of the world's primary producers.⁶ It is estimated that EU countries consume more than 300,000 tons of pesticides per annum for crop protection alone. Globally, the market is dominated by fungicides, accounting for over 40% of the total demand for pesticides in 2010. The global market for herbicides is expected to reach 1,351.3 kilotons by 2016.⁷

Pesticides are currently considered as one of the most harmful compounds causing important risks to surface waters, particularly insecticides impact the ecosystem functions.^{8,9} As a consequence, the monitoring of water quality has become an important issue.

Different legislation schemes are currently being set worldwide in order to improve water quality. These are based on lists of pollutants that are used in industrial processes or pesticides applied in the environment. Governments and organizations have established their own lists for different water systems (e.g., the European Union (EU)'s Water Framework Directive (WFD),¹⁰ OSPAR, International Cooperation for the Protection of the Marine Environment of the North-East Atlantic, the Convention for the Protection of the Danube, the Barcelona Convention concerning the Protection of the Mediterranean Sea, and the International Commission for the

Protection of the Rhine). The lists are continually updated to take into consideration new emerging pollutants, since usually only the compounds listed in normatives are monitored.¹¹

Currently, many chemicals that were not traditionally considered contaminants can be found in various environmental compartments and in areas where they were never used, mainly due to their persistence during their transport over long distances. The sources of these emerging contaminants are usually waste and wastewaters coming from industrial, agricultural or municipal activities.

Nowadays, more than 700 emerging pollutants, their metabolites and transformation products, are listed as present in the European aquatic environment.¹²

Emerging pollutants (EPs) are defined as synthetic or naturally occurring chemicals that are not commonly monitored but which enter the environment and have the potential to cause known or suspected adverse ecological and (or) human health effects. To the current emerging pollutants list, other products of daily use could be added; pharmaceuticals, personal care products, surfactants, gasoline additives, flame retardants, drinking water and swimming pool disinfection by-products, nitrosamines, drugs of abuse and their metabolites, hormones and other endocrine disrupting compounds, plasticisers, nanomaterials (nanosilver and nanogold, fullerenes and other carbon-based nanomaterials), artificial sweeteners (sucralose, acesulfame, saccharin, cyclamate, aspartame), perfluorinated compounds (PFOA, PFOS, and others), polar pesticides and their degradation/transformation products, algal toxins, siloxanes, perchlorate, benzotriazoles, and many others, which shows the magnitude of the problem.

Large numbers of non-regulated EPs have been detected in the ng to $\mu\text{g/mL}$ range in surface waters throughout the UK¹³ and across the rest of Europe.¹⁴ To date more than 200 different pharmaceuticals alone have been reported in river waters, with concentrations up to $6.5 \mu\text{g/L}$ for the antibiotic ciprofloxacin.¹⁵

The presence of EPs in the environment is mainly attributed to the discharge of from wastewaters treatment plants (WwTPs).

In 2013, EU-wide monitoring survey was conducted where 90 WwTPs were sampled, 156 chemicals were measured and four different toxicity assays were conducted on selected samples. The samples came from Austria (number of samples: 6), Belgium (18), Czech Republic (7), Cyprus (2), Finland (6), France (5), Germany (2), Greece (2), Hungary (2), Ireland (2), Italy (2), Lithuania (3), Netherlands (11), Portugal (2), Slovenia (1), Spain (3), Sweden (11), and Switzerland (5). The single maximum concentration found for the contaminants were relevant, as they exceeded maximum allowable concentration values (MAC-EQS) set by Water Framework Directive. These MAC-EQS values are acute toxicity standards which must not be exceeded in the water samples. The highest concentrations were found for such chemicals as triclosan ($4.3 \mu\text{g/l}$), linuron ($3.2 \mu\text{g/L}$), terbutylazine ($2.4 \mu\text{g/L}$), mecoprop ($2.2 \mu\text{g/L}$), ibuprofen

(2.1 µg/L) and diuron (1.4 µg/L), amongst many others. The maximum effluent concentrations were for most compounds in quite good agreement with a study in seven WWTPs in the main cities along the Ebro river basin (north-east of Spain).¹⁶

Also, approximately 70 pharmaceuticals belonging to a variety of therapeutic classes have been reported in UK environmental waters. The most studied were non-steroidal anti-inflammatory drugs, β-blockers, anti-depressants and the antiepileptic carbamazepine. These are highly prescribed drugs (>1000 kg per annum) and frequently found in wastewaters.¹⁷

It is possible that some of the emerging pollutants have been released to the environment, but the presence of many of them has not been neither identified nor detected, due to the lack of sensitive methodologies and the absence of reference standards. On the other hand, new chemicals that are being synthesized can create new sources of emerging pollutants. The presence of these chemicals in the environment is more problematic, considering that they do not appear individually, but as a complex mixture, which could lead to unwanted synergistic effects. Therefore, detailed information on the concentration of the most relevant EPs for risk assessment is needed.

In the European Union, a watch list of EPs was elaborated from national monitoring programs, because it is required by the WFD. This list presents emerging substances requiring further attention due to their possible risk to human health. In 2015 a watch list of emerging contaminants was launched and includes 25 compounds to be monitored routinely (Table 1).¹⁸

Table 1. Emerging contaminants included in the EU Watch list¹⁸

#	Substance	#	Substance
1	Acetamidiprid	14	2-Ethylhexyl 4-methoxycinnamate
2	Aminotriazole	15	Erythromycin
3	Azithromycin	16	Formaldehyde
4	Ciprofloxacin	17	Imidacloprid
5	Chromium trioxide	18	Methiocarb
6	Clarithromycin	19	Oxadiazon
7	Clothianidin	20	Thiacloprid
8	Cyanide-Free	21	Thiamethoxam
9	Cyclododecane	22	Tolyfluanid
10	Dichlofluanid	23	Tri-allate
11	Diflufenican	24	Trichlorfon
12	Dimethenamid-P	25	Triphenyl phosphate
13	2,6-di-tert-butyl-4-methylphenol		

Water monitoring is an analytical practice set by governments under the established regulations to control water pollution. It is estimated that the impact of pollution caused by industrial discharges of toxic substances in European surface waters has decreased 70% over the past 30 years.¹⁹ This reduction is a result of the implementation of strict regulations along with the development of cleaner technologies.

In Europe, the first list of water priority pollutants was established in 2001 by way of Decision 2455/2001/EC (Annex X) under the *Water Framework Directive* (2000/60/EC). The substances listed were selected from amongst those presenting a significant risk to or via the aquatic environment.

This first list was replaced by the one described in the Annex II of the (EQSD), also known as the Priority Substances Directive, which set environmental quality standards (EQS) for the substances in surface waters. The list encompasses 45 substances shown to be of major concern for European Waters (Table 2).

These substances are named either as priority or priority hazardous substances, depending on their toxicity level.

Concerning the quality of water intended for human consumption, another important legislation is the *Drinking Water Directive* (Council Directive 98/83/EC). According to the Directive, a total of 48 microbiological, chemical and indicator parameters must be monitored and tested regularly. As far as the level of pesticides is concerned, the highest permitted concentration of individual pesticides in drinking water was set to 0.10 µg/L, whereas the total amount cannot exceed 0.5 µg/L.

On the other hand, in USA, the United States Environmental Protection Agency (US EPA) sets legal limits on the levels of certain contaminants in drinking water under the *Safe Drinking Water Act* (SDWA).²⁰

These rules regulate over 65 contaminants in three pollutants groups: Inorganic Contaminants (IOCs), Volatile Organic Contaminants (VOCs), and Synthetic Organic Contaminants (SOCs). The rules apply to all public water systems. The current list contains 126 priority pollutants. Moreover, EPA sets a list of acceptable techniques for treating contaminated water.

Table 2. Priority substances list under Water Framework Directive¹⁰

#	Name of priority substance	MAC (µg/L)
1	Alachlor	0.7
2	Anthracene	0.4
3	Atrazine	2.0
4	Benzene	50
5	Brominated diphenylethers	Not applicable*
6	Cadmium and its compounds	Depending on
6a	Carbon-tetrachloride	Not applicable
7	C10-13 Chloroalkanes	1.4
8	Chlorfenvinphos	0.3
9	Chlorpyrifos (Chlorpyrifos-ethyl)	0.1
9a	Cyclodiene pesticides (Aldrin, Dieldrin,	Not applicable
9b	DDT	Not applicable
10	1,2-Dichloroethane	Not applicable
11	Dichloromethane	Not applicable
12	Di(2-ethylhexyl)phthalate (DEHP)	Not applicable
13	Diuron	1.8
14	Endosulfan	0.01
15	Fluoranthene	1
16	Hexachlorobenzene	0.05
17	Hexachlorobutadiene	0.6
18	Hexachlorocyclohexane	0.04
19	Isoproturon	1.0
20	Lead and its compounds	Not applicable
21	Mercury and its compounds	0.07
22	Naphthalene	Not applicable
23	Nickel and its compounds	Not applicable
24	Nonylphenol (4-Nonylphenol)	2.0
25	Octylphenols	Not applicable
26	Pentachlorobenzene	Not applicable
27	Pentachlorophenol	1.0
28	Polyaromatic hydrocarbons (PAH)	Not applicable
29	Simazine	4.0
29a	Tetrachloroethylene	Not applicable
29b	Trichloroethylene	Not applicable
30	Tributyltin compounds	0.0015
31	Trichlorobenzenes	Not applicable
32	Trichloromethane	Not applicable
33	Trifluralin	Not applicable
34	Dicofol	Not applicable
35	Perfluorooctane sulfonic acid and its	36
36	Quinoxifen	2.7
37	Dioxins and dioxin-like compounds	Not applicable
38	Aclofenin	0.12
39	Bifenox	0.04
40	Cybutryne	0.016
41	Cypermethrin	6·10 ⁻⁴
42	Dichlorvos	7·10 ⁻⁴
43	Hexabromocyclododecane (HBCDD)	0.05
44	Heptachlor and heptachlor epoxide	3·10 ⁻⁴
45	Terbutryn	0.34

* Not applicable means that the annual average values are not harmful as they are significantly lower than values derived on the basis of acute toxicity; MAC – maximum allowable concentration

1.2 Gold standard methods used for water monitoring

Currently, the monitoring of compounds included in official watch lists is conducted by chromatographic and mass spectroscopic methods. These techniques are approved as “gold standards” by European and American environmental communities for analytical separation, identification and quantitation of organic residues in different matrices, including water.

These methods are used for the analysis of various classes of substances, and the results obtained are of high analytical value. However, the sampling procedures still are sources of errors, as samples are taken at set points, meaning that the analysis will represent the water quality status at one particular region.¹⁹

Despite their high sensitivity and reproducibility, chromatographic methods cannot be used on-site and still require the collection of spot samples and their transport to a laboratory for analysis, making not only the overall cost high but lowering the efficiency of the analysis.

The low concentration of organic pollutants and the complexity of the environmental water samples make necessary to include preconcentration and clean-up steps in the analysis procedure. Solvent extraction (SE) is among the oldest of the preconcentration and matrix isolation techniques used in analytical chemistry. SE is time consuming and involves high reagent consumption. Currently, QuEChERS technique (quick, easy, cheap, effective, rugged and safe) is between the most used for multiresidue analysis.²¹ The main advantages of QuEChERS extraction are the high recovery of compounds with a wide range of polarity and volatility, high sample throughput, non-sophisticated equipment, smaller volume of organic solvent, low cost per sample^{22,23} and possibility to determine hundreds of different compounds per run.

Also, other extraction techniques have been used, including supercritical fluid extraction (SFE), pressurized-liquid extraction (PLE), microwave-assisted extraction (MAE), solid-phase extraction (SPE), and matrix solid phase dispersion (MSPD), but these approaches are more costly and require skilled personnel.

Micro-extraction methods have been also used for contaminants analysis. Among these techniques, solid-phase microextraction (SPME),²⁴ head-space (HS)-SPME²⁵ and stir-bar-sorptive extraction (SBSE),²⁶ and variants of the liquid-phase microextraction technique (LPME); for example, dispersive liquid-liquid microextraction (DLLM) and hollow-fibre microporous membrane liquid-liquid extraction (HF-MMLLE) seem very useful.^{27,28} Despite the advances in analytical instrumentation, sample pre-treatment for analyte concentration and matrix removal is frequently the bottleneck in the overall analytical method.

Liquid chromatography (LC) is a powerful tool enabling effective separation of non-volatile and thermally labile compounds, including pesticides, incompatible with gas chromatography (GC).²⁹

Liquid chromatography is usually coupled to mass spectrometry (LC-MS) and is a commonly hyphenated method for non-volatile pollutants.^{30,31} Liquid chromatography–tandem mass spectrometry (LC–MS²) is most widely used for simultaneous qualitative and quantitative profiling of several classes of compounds, because of its high sensitivity and selectivity.^{23,32–34}

GC separation depends on the compound boiling point and molecular polarity, and different physicochemical interactions with the GC column. Selective but not specific detectors, for example NPD, FPD, and ECD are still used to determine different classes of pollutants.^{35,36} If this selective detection methods are replaced by the universal and specific quadruple mass spectrometer many classes of contaminants can be analysed in a single run.

Gas chromatography-mass spectrometry has been proposed and demonstrated as a powerful tool for profiling many compounds and their metabolites, and it is the system most frequently used owing to its high sensitivity and selectivity.^{37–40}

The cost of the analysis that would truly represent the overall water quality status using mentioned techniques would be high, since chemically different compounds should be analysed in a single run. This is the reason why new alternative techniques are emerging to deal with this problem.

The alternative monitoring tools would complement or even partially replace the current gold standard methods. Some of them provide rapid, on-site measurements, whilst others still require the collection of spot samples and their transport to a laboratory for analysis. These methods can offer important advantages, in terms of cost as well as efficiency of the analysis.

1.3 Monitoring and screening systems

The implementation of the European Union's Water Framework Directive requires all Member States to implement water monitoring programs. Thus, the activities that are necessary to comply with the regulations make the water quality actions more costly. Therefore, there is an urgent need to develop monitoring tools and methodologies that are able to provide the necessary information at a lower cost. Since the WFD does not specify the methods that have to be used, there are opportunities to modify existing methods and/or to develop new approaches with the aim of obtaining the necessary chemical and biological data.

The procedure to monitor the content of pollutants involves taking water samples at specified intervals of time and places and transport them back to the laboratory for analysis.

A significant research effort in the area of analytical chemistry is currently taking place to develop suitable field methods to facilitate the *in situ* measurements. The on-site analysis is a more efficient approach than taking a sample and transporting it to a laboratory and then performing all the steps to get final results. The main advantage is to reduce the probability of

sample change associated with its transport and storage. The major drawback of this approach is that the performance characteristics of on-site instrumentation are usually poorer compared to laboratory instrumentation.

On the other hand, in most cases the collected water sample is analysed directly to measure the 'total' concentration of a particular analyte. This methodology is well established and validated and therefore it has been accepted for regulatory and legal purposes. However, this approach is valid only if it provides a truly representative picture of the chemical quality of water at a particular sampling site, which is generally assumed. Unfortunately, it was shown that spot sampling can alter the determination of total pollutant amount, as the presence pollutants can vary temporally and spacially.⁴¹ The highest levels of contaminant concentration are obtained when the active compounds are applied to the crop. Water sampling at specific spots, therefore provides only a 'snapshot' of the temporary situation when the sample is taken and fails to give a general water quality status. Some limitations of spot sampling are given in Table 3.

Table 3. Rationale for the updating of water quality monitoring and technologies aiming to rectify these insufficiencies (adapted from ⁴²)

Rationale	Appropriate technologies
Standard spot sampling is costly and labour-intensive	Passive samplers, immunoassays, sensors and biosensors
The collection of bottle or spot samples allows the determination of total contaminant concentrations: fails to account for the bioavailability of pollutants in water (especially for non-polar organics and certain heavy metals)	Biosensors, passive samplers, and in certain circumstances immunoassays
Certain situations/sites such as drinking water intakes or wastewater effluents require results from monitoring to be obtained rapidly, however, standard spot sample collection, transport to the laboratory before processing and analysis is a lengthy procedure	On-line monitoring systems, sensors or biosensors
Screening methodologies including sampling and analytical steps need to be implemented by relatively unskilled monitoring personnel	Immunoassay test kits, passive sampling, bottle sampling, whole-organism bioassays, certain sensors and biosensors

Techniques that already exist combined with new emerging technologies may give additional information in order to obtain a more realistic picture of the biological and chemical water quality.

From a practical point of view, it is important to think if quantitative results are always necessary. In routine laboratories, it is quite usual to first determine whether one or more analytes are present/absent in a sample and then, if some of the analytes are present the next action is to confirm and quantify the positives. Therefore, instead of trying to determine the pollutant concentrations in all samples, it could be enough, as a first step, just to assure if they are present above or below the permitted concentration level. Semi-quantitative or even qualitative methods are used in these cases, being very advantageous for many reasons. For example, as the number of samples for further more expensive analysis would be reduced, the overall cost of the analysis would decrease. Also, as these techniques are much cheaper, the number of samples pre-screened would be higher. Other great advantages are rapidity, simplicity, and minimization of errors, owing to delays between sampling and analysis. These types of assays are the commonly called “screening methods”, differing from traditional analytical ones in the following aspects:

- a. Little or no sample treatment.
- b. Qualitative or semi-quantitative rather than quantitative output.
- c. Rapidity and cost-effective (immediate decision making).
- d. The binary response obtained sometimes requires confirmation by using a reference method.

Not every screening system presents all performances, although most exhibit three or more. The primary objective of sample screening systems is to provide an efficient, reliable response in order to get requested information to avoid the need to processing a large number of samples and to make timely decisions. Another important aspect is the minimization of the preliminary steps of a conventional analytical process, which are usually tedious, time-consuming, and sources of major systematic and random errors. In fact, preliminary operations are the 'weaknesses' of the analytical process.

Figure 1 illustrates the selecting role of a sample screening system used to “filter” a sample set. From the analytical point of view, a screening analysis discriminates samples from a large group that contain certain analytes above or below a cut-off value. This value is usually a concentration level, set commonly by the legal regulations. This pre-set concentration is also called the specification limit, threshold value; maximum permitted level or maximum allowable concentration among other names. Usually only a small number of samples provides a “yes” response and must thus be subjected to the standard analytical process, both to confirm the response of the screening system and to obtain additional analytical information.

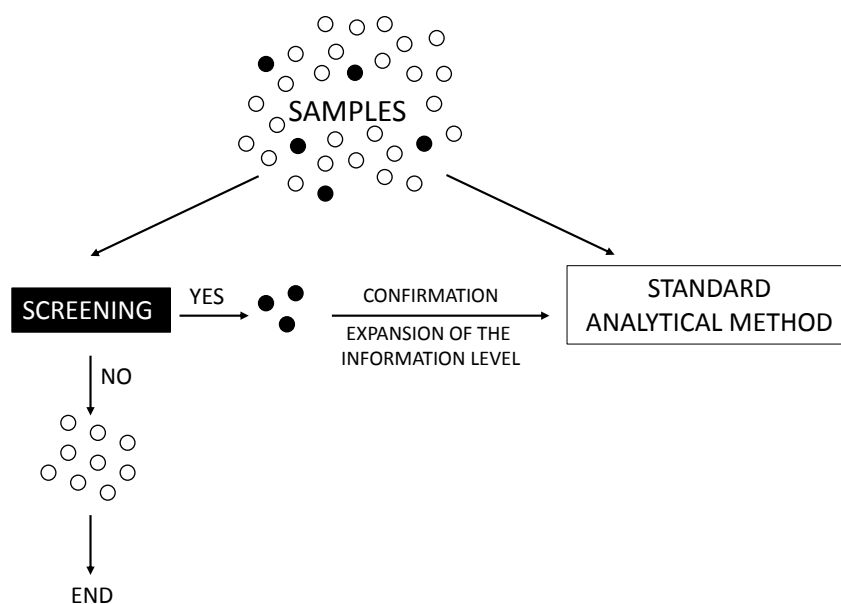


Figure 1. The selection role of a screening approach. Samples in black contain the analyte at a level above the pre-set cut-off value.

Approaches based on sensors (whether chemical, biological or biochemical) are of great practical interest, as they may be useful in providing a more realistic assessment of impacts and exposure of aquatic organisms to specific mixture of contaminants present in water.

Some examples of such techniques are presented in Table 4. As it can be noticed, only chemical analysis requires taking the samples from the field to the laboratory. On the other hand, screening methods can be performed on site with little or no sample treatment. Apart from such important advantage, alternative techniques possess some drawbacks such as restriction to only certain types of compounds, cross-reactivity commonly being a bottleneck of the assay. Nevertheless, combination of both standard and alternative techniques for water quality monitoring is of great value for true understanding of water pollution.

Table 4. Characteristics of selected types of prototype or commercially available tools and technologies for chemical and biological monitoring requirements within the WFD (adapted from ⁴²)

Tools	Principle	Value measured	Deployment characteristics	Applicability	Advantages	Drawbacks
Spot sampling + chemical analysis	Collection of a water sample followed by extraction/filtration and chemical analysis (GC, ICP-MS)	Total contaminant Concentrations	Bottle sampling	All types of waters Most chemicals	Accuracy may be determined relatively easily	Labour-intensive Provide a snapshot of the situation at sampling time Does not account for Bioavailability
Biosensors	Analytical device incorporating a combination of a specific biological element (recognition event) and a physical element (transducing this event)	Total and bio-available pollutant concentrations	In situ, laboratory-based and continuous monitoring	Priority pollutants	May be based on continuous and on-site monitoring	Often requires skilled operators
Sensors	Detection and quantitation based on physico-chemical characteristics of contaminants	Contaminant Concentrations	In situ, laboratory-based and continuous monitoring	Most types of waters Heavy metals, PAHs, and certain pesticides	Handheld instruments	Not applicable to all pollutants
Immunoassay test kits	Highly selective pollutant extraction and/or quantitation based on antigen/antibody interactions	Pollutant concentrations	Field or laboratory assays based on spot-sampling	Many organic pollutants e.g. pesticides, PAHs Certain metals	Rapid and easy to employ Very sensitive, selective and inexpensive assays Ability to process many samples	Unit: analyte equivalents Cross-reactivity with analogues and metabolites False positives Positive results may require further confirmation analysis

1.4 Rapid assays for detection of pollutant residues in water

There is an increasing need of developing fast, reliable, sensitive and cheap monitoring methods for in situ water analysis.^{43,44} The primary function of such rapid assays is to provide a quantitative or qualitative screening to detect the presence or absence of a targeted chemical or chemical family. For example, if the purpose of a study is to detect atrazine in a specific water setting, a rapid assay can be used with great benefit to screen water samples over time and space. A water sample could be analysed in the field to decide whether or not it should be sent to the centralized laboratory for confirmatory quantitative analysis. In this way, samples containing the target pollutant below the cut-off value are not further analysed by the reference methods. In this line, almost real-time information would be provided in the field about the presence or absence of the targeted compound. Nevertheless, these on-site techniques are not meant to replace standard laboratory analysis methods but contribute in faster water quality assessment of particular region.⁴⁵

For monitoring residues of contaminants, the techniques that can work include the use of chemical sensors, biosensors and immunoassay test kits. On-line, in situ and laboratory-based tools are analytical approaches that have become available to environmental monitoring programmes. Much work has been conducted recently with the aim of developing electrochemical sensors for detection and quantitation of chemical pollutants.⁴⁶ For example, electrochemical based devices have been miniaturised into screen-printed electrodes that are incorporated in hand-held equipment that may be used for rapid on-site monitoring of many heavy metals and certain pesticides.⁴⁷

The term *biosensor* is applied to describe analytical devices used for the determination of analytes containing a biological element (antibody,⁴⁸ enzymes,⁴⁹ DNA⁵⁰, whole-organisms⁵¹ or aptamers⁵²) in contact with a physiochemical detector. The main advantages of the biosensors over other kinds of sensors are selectivity and sensitivity, and in some cases, the ability to work in dull working environments.⁵³ In the literature, there are many examples of biosensors able to determine many environmental contaminants.⁵⁴ In the latter case, many of the biosensors developed aim to detect priority substances established in the WFD. Also, the analysis of new emerging pollutants, such as surfactants, hormones and antibiotics, is being approached.

Among many different tests, immunoassays are common analytical tools for environmental monitoring. The immunoassays approach began to be used in the environmental field in the early 1990s, when test kits became commercially available. Nowadays, immunoassay is a widely accepted methodology for the analysis of many organic contaminants. Several immunoassay kits have been developed to detect specific classes of environmental pollutants. For example, EPA has approved immunoassay methods for a number of contaminants, most of which are published

in EPA SW-846.⁵⁵ For example, for atrazine determination there are four immunoassay test kits commercially available approved by EPA, three of which provide quantitative results, while the fourth gives qualitative data. For the tests that provide quantitative results, the sensitivity of the kits allows for determination of atrazine residues at levels set by water normatives. WFD for environmental water sets the maximum allowable concentration for atrazine at 2 µg/L, whereas EPA maximum contaminant level for atrazine is 3 µg/L. For drinking water the limit cannot exceed 0.5 µg/L. All three tests are able to provide results in approximately one hour. On the other hand, the test strip takes only ten minutes to perform but gives only qualitative information.

Apart from those for atrazine detection, different test-kits are commercially available for a variety of pesticide residues, industrial contaminants, toxins, hormones and other residues of interest as it is presented in Table 5.

Table 5. Selected suppliers of immunoassay test-kits for environmentally relevant compounds (adapted from⁵⁶)

Company	Analytes
Abraxis LLC Warminster, PA, USA	Pesticide residues: Acetochlor; Alachlor; Atrazine; Carbendazin/Benomyl; Cyclodienes, 2,4-D; DDE; Diuron; Glyphosate; Metolachlor; Organophosphate/Carbamate; Pyrethroids; Spynosyn Industrial chemicals: Bisphenol A; Coplanar PCBs; PCBs higher chlorinated; PCBs lower chlorinated; PCBs broad reactivity; Polycrominated diethyl ether (PBDE); Triclosan
Beacon Analytical Systems Portland, ME, USA	Pesticide residues: Alachlor; Atrazine; 2,4-D; r-Metolachlor; s-Metolachlor Industrial contaminants: Cyclodienes; Petroleum Fuels; Toxaphene
Coring System Diagnostix GmbH Gernsheim, Germany	Pesticide residues: 2,4-D; Alachlor; Atrazine; Benomyl/Carbendazim; Carbofuran; Chlordan; Chlorpyrifos; Cyanazine; Diazinon; Hydroflour; Isoproturon; Metolachlor; Simazine; Triazines; Triclopyr Industrial contaminants: Inquest OP/Carbamat; MKW (TPH); PAHs; PCBs; PCP; RDX; TNT
EnviroLogix Portland, ME, USA	Pesticide residues: Imidacloprid; Isoproturon; Synthetic Pyrethroid, Organochlorines (Endosulfan)
Strategic Diagnostics Inc. Newark, DE, USA	Pesticide residues: 2,4-D; Alachlor; Aldicarb; Atrazine; Carbofuran; Benomyl/Carbendazim; Chlorothalonil; Chlorpyrifos; Cyanazine; Cyclodienes; Methomyl; Metolachlor; Procymidone; Simazine; Spinosad; Triclopyr DDT; Lindane; Toxaphene; Triazines Industrial contaminants/remediation: BTEX; PAHs, cPAHs; PCBs; PCP; TPH; TNT; RDX

With some exceptions, most test-kits use polyclonal antisera working in heterogeneous, competitive format in ELISA plate or in dipstick supports. Usually, test-kits for environmental applications are still very expensive, because the development costs are high and the market is, even after 15 years of applications, still small. Generally, it needs some practice and skills to use them properly. Also, the cost of analyzing one sample can be estimated in 20 euros, since on average 30 samples by triplicate are analysed in a 96 well-plate. All the kits available usually aim the determination of only one analyte, therefore the rapid monitoring system is restricted, as for each analyte separately a test-kit must be run, which is time and money consuming.

1.5 Multiplex bioanalytical methods for environmental monitoring

The Water Framework Directive includes a number of water pollutants that should be controlled. It recommends the necessity of providing novel monitoring methods for a future application in the field of water analysis. These methods should meet the performance criteria required by the European Union in terms of sensitivity, selectivity and reproducibility so that pollutant concentrations could be reliably measured at concentration levels below a limit known as the environmental quality standards (EQS). EQS are limits on the concentration of the priority substances which must not be exceeded if good chemical status must be achieved.

The EU requires from the Member States to select analytical tools that meet a minimum performance criteria, such as a limit of quantification equal or below a value of 30% of EQS. Additionally, it should be ensured that setting up monitoring tools is cost-effective. The regulation is quite strict and setting approaches or the adaptation of existing ones that fulfil these criteria is a difficult task that highlights the need for new devices.⁵⁷

This section provides an outlook on the recent developments in bioanalytical multiplex technologies and their applications for environmental monitoring. Figure 2 shows the most common approaches for the simultaneous detection of multiple target analytes in environmental analysis.

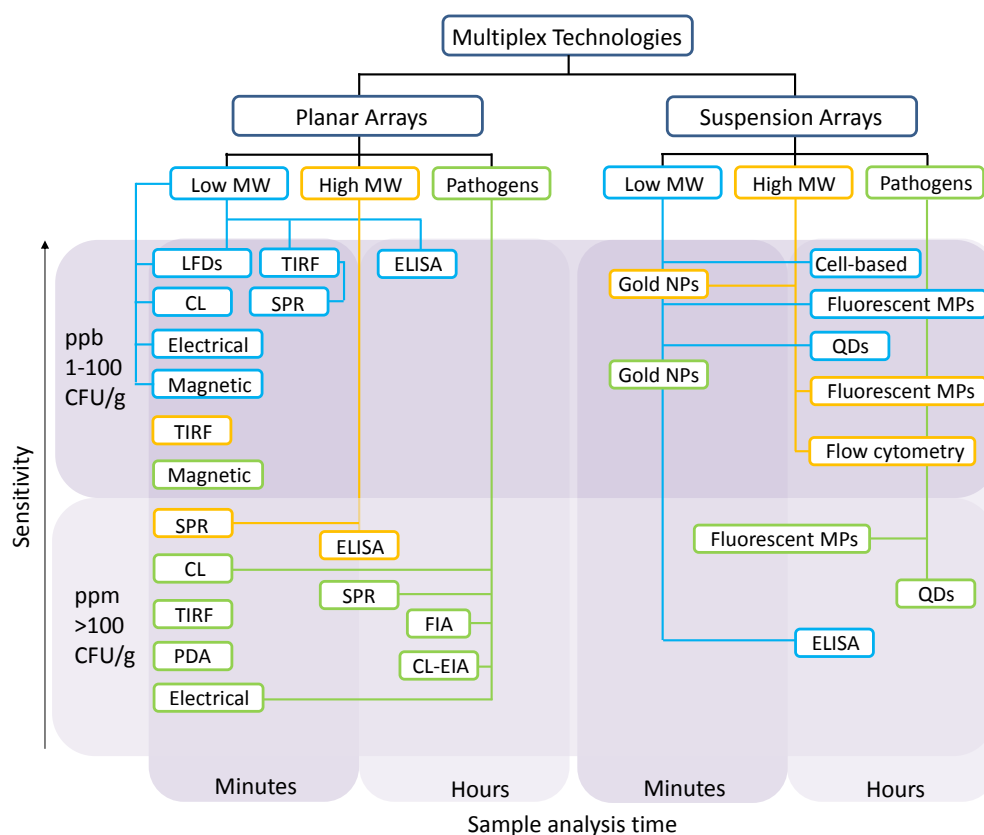


Figure 2. Overview of multiplex bioanalytical technologies currently applied for food and environmental analysis (adapted from⁵⁸).

Multiplex bioanalytical technologies can be classified in two large groups depending on the platform used: planar and suspension arrays. Planar arrays use a solid support (2D or 3D) for capture probe immobilization, whereas for suspension arrays the biorecognition occurs in solution. The methods can be classified also depending on the analyte size (low and high molecular weights and pathogens), sensitivity (parts per billion; $\mu\text{g/L}$ or parts per million; mg/L) and according to the assay time, which can take from minutes to hours. As shown in the Figure 2, for low molecular weight compounds, such as environmental pollutants, planar arrays are the most common configuration formats. The sensitivity is usually high (in order of $\mu\text{g/L}$) and the assay time can vary depending on the particular method.

1.5.1 Planar arrays

Planar arrays are miniaturized formats in which high-affinity capture molecules are immobilized in parallel assays as microspots on a solid support. The capture molecule will depend on the application and format of the assay, for instance, antibody, haptenized protein, DNA, aptamer, peptide etc. In the most frequent working mode, the target analyte is captured by the immobilized probe and unbound molecules are removed by washing. The bound analyte is usually detected by using labelled reporter molecules (e.g. enzyme, fluorophore, gold). Although, the use of labelled molecules to detect the immunoreaction is the most common procedure, some label-free detection strategies already exist. The signals are registered to relate the analytical measurement with the analyte concentration.

Microarrays are very useful approaches when multi-analyte high-throughput is needed. Short measurement times, automation, reduced sample volumes and good sensitivity are among the main advantages offered by planar arrays.

As it is shown in Figure 2, different planar arrays are used for analytical purposes. Usually the difference is in probe/target nature, support type, format assay and the detection method. Some recent examples of microarray planar immunoassays will be discussed below.

Marquette *et al.*⁵⁹ developed a microarray-based ELISA plate for the detection of five different pollutants such as pesticides, explosives and toxins in water. In this approach, numerous probes are immobilized in a matrix of spots in the same well on the optical-clear adhesive. The microarray proposed by Marquette group allows for testing many parameters all together, thus this microarray system is compatible with high-throughput requirements. Detection limits obtained were 0.01, 100, 0.02, 0.02 and 0.01 $\mu\text{g/L}$ for 2,4-dichlorophenoxyacetic acid (2,4D), trinitrotoluene (TNT), okadaic acid (OA), 1,3,5-trinitroperhydro-1,3,5-triazine (RDX) and atrazine, respectively.

Also, multiplexed immunoassay method was developed for the determination of endocrine disrupting compounds (EDCs) based on disposable screen-printed carbon electrodes.⁶⁰ Different capture antibodies were separately immobilized on the carbon electrodes to form an immunosensor array. Functionalized mesoporous silica nanoparticles were used as catalytic labels of secondary antibodies. Due to the catalytic activities of the platinum nanoparticles and the large surface area of SBA-15, a strong electrical response towards the analytical antigens was achieved. The multiplexed immunoassay array enabled the simultaneous determination of different analytes. Using diethylstilbestrol and estradiol as model analytes, this multiplexed immunoassay method showed wide linear ranges with detection limits down to 0.28 and 1.2 pg/mL for diethylstilbestrol and estradiol, respectively.

In another work, an automated array biosensor based on evanescent-wave excitation was developed for the detection of microcystins (MCs) in freshwater samples.⁶¹ The sensing surface consisted of microcystin-leucine-arginine (MCzLR) covalently immobilized onto a planar waveguide (microscope slide). The assay was performed in a competitive format. The immobilized MCLR and MCLR in solution were competing for binding sites of the antibody spiked in the sample. The amount of antibody bound to the antigens was revealed using Cy5-labeled rabbit anti-mouse IgG. The biosensor was successfully applied to the direct analysis of surface water samples without any clean-up or preconcentration steps, and the results were fully comparable to those obtained by LC-MS². The optimized biosensor assay presents an IC₅₀ value of $0.34 \pm 0.01 \mu\text{g/L}$, a detection limit of $0.016 \pm 0.003 \text{ ng/L}$ and a dynamic range from 0.06 to $1.50 \mu\text{g/L}$ MCLR.

Immunochromatography is widely used as a rapid and simple technique. However, immunochromatographic tests are only suitable for the detection of one or few substances in a row. This is due to the fact that it is difficult to apply a large number of reagent lines having different specificities on the membrane of the test strip. If there is an intention to setup a multiplex assay, there are two possibilities to attempt it: multiple analytes on one strip or whether multiple strips within a single cartridge. For example, gold-based lateral-flow strips were investigated for simultaneous detection of carbofuran and triazophos.⁶² The strength of the portable one-step strip assay was in the simultaneous screening for two pesticides within a short time (8–10 min) without any equipment.

Also, a lateral flow assay using antibodies tagged with quantum dots as fluorescent indicators was patented.⁶³ The invention provides for spatial and spectral multiplexing of quantum dot lateral flow assays. The tests employ fluorescence detection to determine the presence of microorganisms, proteins, polysaccharides, drugs, or nucleic acid molecules. This multiplex assay is a water monitoring assay, capable of detecting microorganisms for instance, *E. coli*, *Streptococcus group A*, *Pseudomonas aeruginosa*, *S. aureus*, and *S. maltophilia*.

There are some commercially available test strips for pesticide detection, but usually they aim to detect only one analyte per strip, like for example atrazine test strip developed by Abraxis (Table 5), which detects atrazine and simazine at 3 and 4 $\mu\text{g/L}$, respectively.

Multiplexed lateral flow assays, are not very easy to develop due to non-specific binding and “cross-talk” between tests. As a consequence, multiplexed assays tend to have higher background signals that limit parameters as dynamic range, sensitivity and selectivity.

1.5.2 Suspension arrays

Three-dimensional suspension arrays use microspheres as the solid support to which different capture ligands are covalently coupled. Compared to planar arrays, in which analyte identification relies on spatial position, in suspension arrays capture ligands are immobilized on colour- or size-coded microspheres. To generate the results flow cytometry principles are used: assay-specific microspheres are distinguished by either light scattering or internal fluorescent ratio and the signal is generated by additional fluorophore labels.

The suspension assays offer some advantages over planar microarrays, such as fast reaction kinetics and shortening assay time, based on the much higher surface to volume ratio as well as short diffusion distance. Another additional advantage is the high precision as a multiple (50-100) independent measurements are conducted within each microsphere population. On the contrary, this format of work needs a flow cytometer, a reader that is expensive and not easily adaptable for the use out of the laboratory.

Some recent examples of suspension multiplex arrays for environmental analysis will be discussed.

A multiplex bead-based competitive immunoassay using suspension array technology for the simultaneous detection of the pesticides triazophos, carbofuran and chlorpyrifos was developed.⁶⁴ Three hapten-protein conjugates were covalently bound to carboxylated fluorescent microspheres as probes. The fluorescent signals were measured by a suspension array reader. The multi-analyte assay has dynamic ranges of 0.02-50 ng/mL, 0.5-500 ng/mL and 1.0-1000 ng/mL and the detection limits were 0.024, 0.93 and 1.68 ng/mL for triazophos, carbofuran and chlorpyrifos, respectively. The bead-array method was highly selective for the three target pesticides and no cross-reactivity was observed from structurally related compounds. The method was applied to analyse vegetables spiked with the three pesticides, and the recoveries were between 70% and 120% with mean coefficients of variation of < 15%. This method proved to have wider dynamic range and reproducibility compared to traditional ELISA.

In another work, a multiplex assay for organophosphorus and carbamate pesticides was developed using a suspension array based on silica-hydrogel hybrid microbeads (SHHMs).⁶⁵ There are two advantages of SHHMs as microcarriers for suspension array. They have characteristic reflection peaks used for encoding, which come from the stop-band of the photonic crystal. Also, blended hydrogel composed of PEG-DA and acrylic acid could supply the functional carboxyl groups for anchoring antigens or antibodies. To check the feasibility and capability of the suspension array fenitrothion, chlorpyrifos-methyl, fenthion, carbaryl and metolcarb were selected as model analytes. The suspension array was based on indirect

competition immunoassay using the specific monoclonal antibodies, antigens conjugated to BSA which are immobilized on different types of SHHMs in solution and the biotin–streptavidin signal amplification using fluorescent detection. The LODs for fenitrothion, chlorpyrifos-methyl, fenthion, carbaryl and metolcarb were 0.02, 0.012, 0.04, 0.05 and 0.1 ng/mL, respectively. The suspension array was specific and no significant cross-reactivity was observed. The results for the detection of pesticide residues collected from agricultural samples (fruits and vegetables) using this method agreed well with those from liquid chromatography–tandem mass spectrometry.

Aptamer-based suspension assay for detection of six different organophosphorus pesticides (isocarbophos, phosalone, methamidophos, acephate trichlorfon, chlorpyrifos) was also developed.⁶⁶ In this study, organophosphorus pesticide aptamers were adsorbed on the surface of AuNPs to stabilize the AuNP solution against high concentrations of salt to prevent AuNP aggregation. After the addition of targets, the aptamers binding to the targets are detached from the AuNPs, resulting in aggregation of AuNPs and a colour change from red to purple-blue. The proposed method can detect 6 organophosphorus pesticides with good recoveries from 72% to 135% in environmental river water samples. Though the assay showed low sensitivity as a result of the low affinity of the aptamers, it allowed the simple, rapid, and multiplex detection of organophosphorus pesticides.

The Multi Analyte Profiling (xMAP) technology from Luminex Corporation is the most prominent suspension microarray commercially available. This technology employs small carboxylated polystyrene microspheres (5.6 μm), which are internally dyed with a red fluorophore and an infrared fluorophore. Up to 100 different color-coded bead sets can be distinguished by varying the ratio of the two fluorophores. Each bead set can be coupled to a different biological probe, allowing simultaneous measurements of up to 100 different biomolecular interactions in a single well.

Recently, a MagPix instrument was launched by Luminex, offering a low-cost, compact alternative for multi-analyte diagnostic and environmental testing. It moves away from a flow-cytometry-based system to an instrument based on magnetic bead array analysed on a magnet in a 2D readout with light emitting diodes (LEDs) and a CCD camera, offering a more robust system suitable for in-field measurements.

1.5.3 Automated multi-analyte systems

Despite the fast developments of previously mentioned techniques over the past decades, there is still much room for developing attractive water-monitoring devices. One of the important assets of such device would be the automation and remote control as well as generation of alarm signals when pollutant's concentration exceeds the pre-set threshold value.

In this line, two research projects supported by European Commission developed fast and cost-effective devices for the simultaneous detection of diverse organic pollutants – from pesticides to new emerging contaminants such as pharmaceuticals or endocrine disrupting compounds.

The first one, a biosensor RIANA consists of a flow injection system, a transducer mounted in a flow cell and an optical excitation and detection system. A solid phase fluoroimmunoassay was selected where the analyte derivate was immobilized on the solid support. Polyclonal antibodies were labelled with fluorescent dyes for the detection of immunoreaction event.⁶⁷

On the basis of the same immunoassay and optical detection principle, the new device AWACSS was designed ten years ago to overcome RIANA drawbacks. The major improvement of this new approach was the expansion of multi-analyte analysis capability that allowed the simultaneous measurements of up to 32 analytes, whereas RIANA biosensor determined simultaneously up to six different targets.

Different assays using the RIANA and AWACSS biosensors were developed in Milli-Q water in order to optimise the analytical method. In multi-analyte determinations using the river analyser (RIANA) the sensitivities (IC_{50}) were 0.35, 0.54, 1.5, 0.53, 0.89 and 81 $\mu\text{g/L}$ for atrazine, simazine, isoproturon, alachlor, 2,4-D and pentachlorophenol.⁶⁸ Also, three analytes estrone, atrazine and isoproturon were analysed in real water samples, and the sensitivity expressed as IC_{50} was 0.79, 1.84 and 0.47 $\mu\text{g/L}$, respectively.⁶⁹ For AWACSS project different polyclonal antibodies were isolated and their corresponding analyte derivatives were synthesized. AWACSS project prioritized the determination of pesticides, endocrine disrupting compounds, WFD priority substances, industrial pollutants and pharmaceuticals. The list of AWACSS compounds is presented in Table 6.

Table 6. A list of AWACSS compounds monitored in the surface water, groundwater, municipal/industrial wastewater and sediment samples within the years 2001–2003

Compound	Concentration ^a	Matrix ^b
Alachlor	0.11	SED
Pyrene	0.05–633	SED
Benzo[a]pyrene	0.15–36.94	SED
Fluorene	0.09–267	SED
Fluoranthene	0.02–717	SED
DEHP	1–2115	SED
Bisphenol A	0.06–35.19	SW, GW, WW
Nonylphenol	0.35–87.57	SW, GW, WW
Benzene	0.6–177.5	SW, GW, WW
Toluene	1.1–447.3	SW, GW, WW
Xylene	1.0–31.9	SW, GW, WW
Trichloroethylene	0.1–22852	SW, GW, WW
Atrazine	0.2–4.46	SW, GW, WW
Prometryn	0.13–1252	SW, GW, WW
Ametryn	0.22	SW, GW, WW
Terbuthylazine	0.14	SW, GW, WW
Simazine	0.1–0.5	SW, GW, WW
Benzenesulfonamide	0.42–4.86	SW, GW, WW
Caffeine	1.3–112	SW, GW, WW

^aConcentration range in mg/kg for sediment samples (SED) and in µg/L for water samples (SW, GW, and WW).

^bSED: sediment; SW: surface water; GW: ground water; WW: waste water

Another achievement of the AWACSS project was the establishment of an early warning system based on the network concept (remote measurement stations and an internet-accessible database on the server station). The measurement station uploads the data to the server and downloads new parameters for the next measurement. The AWACSS system not only meets the market demand but exceeds the current competitive detection methods in terms of meeting end-user requirements for current and future expectations. A system like AWACSS, equipped to measure up to 32 top compounds, could be well placed to the market due to its flexibility of adaptation of new compounds as well as the capability of online, unattended and centrally controlled monitoring. Till now, there are no news about the commercialization of this system.

1.6 Biosensing

Biosensors are gaining a lot of attention in the environmental research, as they fulfil all the requirements needed for on-site water monitoring. The concept of the biosensor is based on the integration of a biorecognition molecule (enzyme, antibody, receptor, microorganisms, nucleic acid, protein, etc.) with a transducer (electrochemical, gravimetric, optical, thermal, etc.) to generate a signal. The examples of capture agents and detection methods commonly applied in microarray format are presented in Figure 3. The biorecognition is based on the specific interaction between the capture molecule and the analyte, for example antigen-antibody, DNA hybridization, protein-protein, etc. The recognition event is then converted by a transducer into a measurable response such as adsorption of light, current, potential, mass, temperature change, etc. through electrochemical, thermal, optical, piezoelectric and other approaches. In this section all necessary elements required for building up biosensors will be discussed.

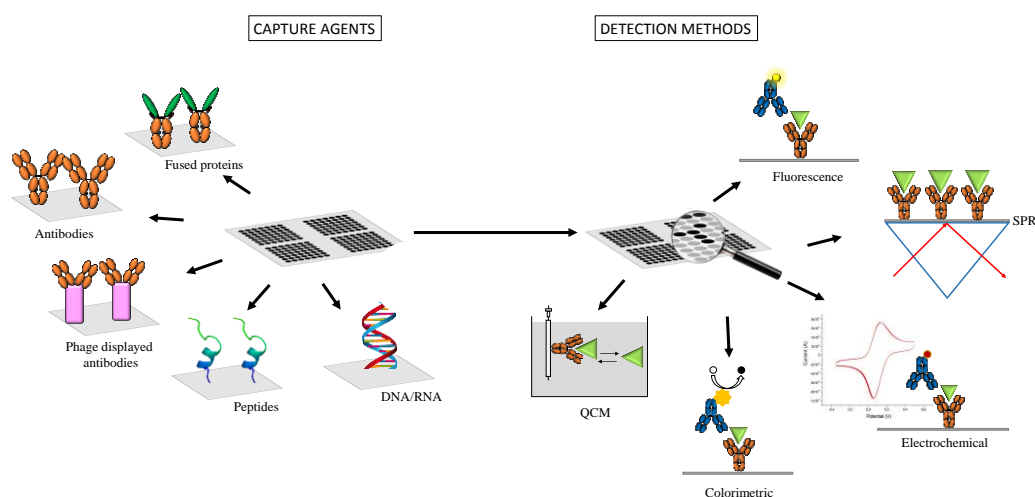


Figure 3. Different capture agents and detection methods applied in microarray immunoassays (adapted from⁷⁰).

1.6.1 Biorecognition elements

The most crucial element of a biosensor is the sensing molecule. This molecule might show high affinity and selectivity to the target analyte, thus enabling the identification and quantification of the compound. In the planar arrays, the biorecognition element is immobilized on a solid surface. The most common capture molecules are proteins such as antibodies, or nucleic acids. In this section only antibodies will be discussed.

The immunoglobulins are the most employed biorecognition elements for environmental analysis. The five primary classes of immunoglobulins are IgG, IgM, IgA, IgD and IgE. These are distinguished by the type of heavy chain found in the molecule. Differences in heavy chain polypeptides allow these immunoglobulins to function in different types of immune responses. Immunoglobulin G (IgG) is the predominant Ig class present in human serum. IgGs are produced as part of the secondary immune response to an antigen and represent 75% of total serum immunoglobulins. Because of its relative abundance and excellent selectivity toward antigens (both large molecular weight compounds, e.g. proteins, and small molecular weight compounds such as hormones, pesticides, antibiotics), IgGs are the main antibody class used in immunoassay methods.

Immunoglobulin G, as it is shown in Figure 4, consists of two identical heavy chains (H), each of 450 amino-acid residues, and of two light chains (L), each of 212 amino acid residues. The two H chains are held together by disulphide (-S-S-) linkages. L chains are also attached to H chains by disulphide bonds so that one L chain associates with one H chain. Both the H and L chains are divided into structural domains based on amino acid sequence.

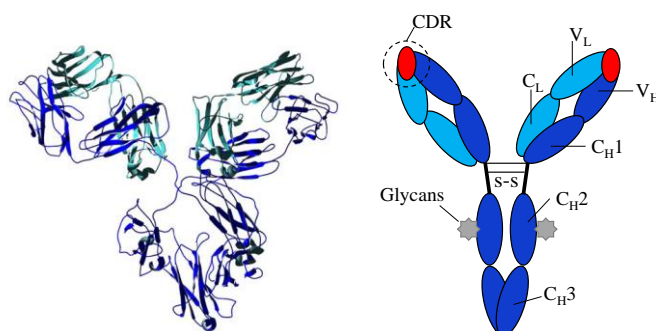


Figure 4. Overview of a single IgG structure. Left view shows the three-dimensional structure of an IgG1 molecule determined by X-ray crystallography. The heavy chains (H) are shown in dark-blue and the light chains (L) are seen as light-blue. Right view shows a simplified model of IgG structure using the same colour coding as left view. (CDR – complementary determining region, C_H – constant region on heavy chain, C_L – constant region on light chain, V_H – variable region on heavy chain, V_L – variable region on light chain).

Immunochemical analysis is based upon the specific reaction between an antibody (Ab) and its corresponding antigen. Small molecular mass compounds (e.g. pesticides) have to be coupled to a carrier molecule, usually a protein, in order to induce an antibody response in the immune system. Antibody production is mainly but not only carried out in warm-blooded animals, such as rabbits, sheep, mice or chicken. Polyclonal antibodies (pAb) are obtained from the blood and comprise a mixture of different Ab populations. Monoclonal antibodies (mAb) consist of a single monospecific Ab population. They are produced by hybridoma technology⁷¹ to guarantee unlimited production keeping constant affinity and selectivity. Typical properties of different antibodies are shown in Table 7.

Table 7. Properties of polyclonal, monoclonal and recombinant Abs

Properties	pAb (Ab from blood serum)	mAb (Ab from hybridoma cells)	rAb (Ab produced by gene technology)
Supply	Limited and variable	Unlimited production possible	Unlimited production possible, immunization not mandatory
Uniformity	Changing properties with different sera and bleedings	Constant properties of a mAb	Constant properties of a rAb, can be changed by genetic manipulations
Affinity	Mixture of Ab with different affinities, affinity often higher with pAb	Uniformly high or low, can be selected by testing	Uniformly high or low, can be selected by testing and can be Modified
Cross-reactivity	Results from different selectivity and low affinity interactions	Different, dependent upon the individual Ab	Different, dependent upon the individual Ab, can be modified
Classes and Subclasses	Typical spectrum	One defined isotype	Different, depending on molecular design
Demands on the antigen	High purity required for specific antisera	Impure Ags or mixture of Ags can be used for immunization, pure Ags necessary for screening	Impure Ags or mixture of Ags can be used for immunization, pure Ags necessary for screening, immunization not mandatory
Costs	Low	High	Once established, low

1.6.2 Signal tags

To know the extension of the recognition event between the antigen and the antibody, different techniques can be employed depending on the detection mode. In this way, the bound fraction can be quantified, so the analyte concentration. To achieve this, one of the components of the system must be labelled to act as a “tracer”. This tracer can be the labelled antigen or antibody. Any substance which can be measured accurately by simple methods can work as the label. In this section some of the most commonly used labels will be discussed.

Enzymes are perhaps the most varied class of labelling substances. Table 8 lists a selection of the most common enzymes. Enzymes are suitable labels because their catalytic properties, generating more than 10^5 product molecules per minute. Also, they offer easy detection, simple labelling methods and inexpensive and stable substrates. Horseradish peroxidase and alkaline phosphatase have been the most commonly used in heterogeneous assays while lysozyme and glucose-6-phosphate dehydrogenase are mainly used in the homogeneous EIAs. The enzyme labels are usually measured by visible or ultraviolet spectrophotometry, fluorescence or luminescence.

Table 8. a) Enzymes commonly used as labels in heterogeneous immunoassays.

Enzyme	Source	Chromogenic substrates
Alkaline phosphatase	Calf intestine	p-nitrophenyl- β -D-galactopyranoside, $\lambda = 420$ nm
β -D-Galactosidase	<i>Escherichia coli</i>	o-nitrophenyl- β -D-galactopyranoside (oNPG), $\lambda = 420$ nm Chlorophenolic red- β -D galactopyranoside (CPRG), $\lambda = 574$ nm
Glucose oxidase	<i>Aspergillus niger</i>	Coupled enzyme reaction glucose+chromogen for HRP
Peroxidase	Horseradish	H ₂ O ₂ /2,2'-azino-di(3-ethylbenzthiazoline sulfonic acid-6) (ABTS), $\lambda = 415$ nm H ₂ O ₂ /3,3',5,5'-tetramethylbenzidine (TMB), $\lambda = 450$ nm H ₂ O ₂ / o-phenylenediamine (OPD), $\lambda = 492$ nm
Urease	Jack bean	Urea/bromocresol yellow, $\lambda = 588$ nm

Table 8. b) Enzymes commonly used as labels in homogeneous immunoassays.

Enzyme	Source	Chromogenic substrates
Glucose-6-phosphate dehydrogenase	Leuconostoc mesenteroides	NADP glucose 6-phosphate, $\lambda = 340$ nm
Lysozyme	Egg white	Fragmentation of cell walls (<i>Micrococcus lysodeikticus</i>), $\lambda = 450$ nm
Malate dehydrogenase	Pig heart	NAD/malate, $\lambda = 340$ nm

Latex beads are still used in agglutination tests for the detection of small quantities of specific antibodies or antigens in a fluid test sample.⁷² Some advantages of these assays are that the procedures are simple, non-hazardous, and the results are obtained in short times. The agglutination reaction involves in vitro aggregation of microscopic carrier particles. The attachment of molecules to latex particles can be achieved through physical adsorption or covalent coupling. The major problem of particle-based assays, which require careful attention, is the nonspecific agglutination, reason why, for a long time, latex immunoagglutination tests were considered to be semiquantitative.

Semiconducting nanoparticles or *quantum dots* (QDs) refer to fluorescent nanocrystals made mainly from compounds of group II and VI elements of the periodic table. They serve as labels in bioassays due to their excellent fluorescence properties.^{73,74} They are a substitute for classical dyes or fluorophores since they exhibit very narrow, symmetric, bright and size-dependent emission and broad absorption spectra.⁷⁵ They are more resistant to photo bleaching compared to many other fluorophores. However, there are some limitations such as toxicity, inability to have perfect control over their size, agglomeration, surface oxidation, and non-specific binding. Functionalized semiconductor QDs have been used as fluorescence labels in numerous biorecognition events such as immunoassays for protein detection or the analysis of nucleic acids.^{76–78}

Among the pool of metallic nanoparticles available, the inorganic ones such as silver and gold have been most widely employed for signal amplification.

The properties of colloidal gold were not properly examined and understood until the days of Michael Faraday, who is considered to be the founding father of modern metal nanoparticle physics.^{79,80} In the late 20th century colloidal gold found use as a contrast enhancement agent for different biomedical imaging techniques. Recently, nanoscale properties of gold nanoparticles

(AuNPs) have attracted a lot of interest.⁸¹ Currently the AuNPs are used in different fields like optics,⁸² electronics,⁸³ optoelectronics,⁸⁴ and biosensing techniques.⁸⁵

Depending on the synthesis method, different shaped gold nanoparticles can be obtained. The most popular in biosensing applications are spherical gold nanoparticles and rod-shaped ones. However, many other shapes such as octahedrons,⁸⁶ tetrahedrons,⁸⁷ icosahedrons,⁸⁸ nanocubes⁸⁹ and nanoflowers⁹⁰ have been synthesized by changing the reducing agent, capping agent, and solvent.

Here, only the properties of spherical and rod-shaped nanoparticles will be discussed.

Spherical gold nanoparticles have a broad absorption band in the visible region of the electromagnetic spectrum. Mie was the first researcher to formulate the nature of the optical band as a surface plasmon effect, in the so-called “Mie theory”.⁹¹ The characteristics of the band arise from the collective oscillation of free-conduction electrons induced by an interacting electromagnetic field, and their resonances are noted as surface plasmon (SPR) (Figure 5a).

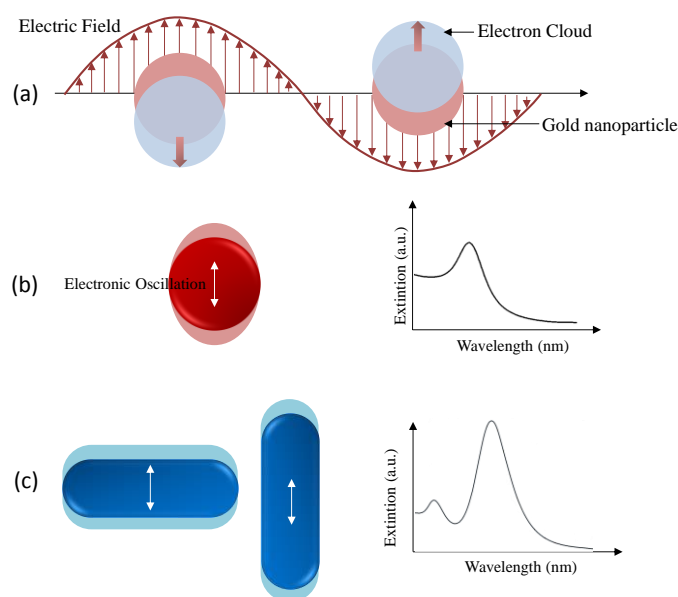


Figure 5. Schematic representations of (a) localized surface plasmon resonance, (b) electric oscillation of gold nanosphere (c) electric oscillation of gold nanorods (adapted from⁹²).

In fact, the electric field of the incoming radiation causes the formation of a dipole in the NP. A compensation force results in a resonance wavelength, as shown in Figure 5b. The specific resonance frequency depends on a number of parameters such as nanoparticle composition, morphology, concentration, solvent refractive index, surface charge, and temperature.^{93,94} Meanwhile, such a resonance wavelength for rod-shaped NPs depends on the angle of the electric

field. This results in two oscillations, transverse and longitudinal, that lead to two plasmon bands, as shown in Figure 5c. The transverse SPR band occurs at a wavelength close to that of spherical AuNPs (500-550 nm), while the longitudinal band is in the region 600–900 nm, depending on their aspect ratio (length/width).

The second type of selected gold nanoparticles are *gold nanorods*. As it was presented in Figure 5c, gold nanorods possess two plasmon bands, which are the result of their shape. The unique gold nanorods properties make them excellent nanoparticles for many different sensing applications. The main modalities where gold nanorods are used as sensing specie can be divided into several groups. First, changes in the optical absorbance of gold nanorods can be a sensitive marker of chemistry happening on their surface. Changes in the environment around the gold nanorods have an effect on the local refractive index (RI) which alters the position of the plasmon resonance peaks (mainly longitudinal). This phenomenon is called localized surface plasmon resonance (LSPR). Also, self-assembly of nanorods can be used for sensing. In this approach, aggregation of the nanorods in solution occurs by biorecognition, resulting in the plasmon changes. Another property of gold nanorods that can be useful for sensing applications is their strong ability to scatter light, which can be employed as optical sensing principle.⁹⁵ The plasmonic properties can be employed for SERS purposes as well.⁹⁶

The interaction between the particles and substrate is one of the key factors for surface modification, and the surface charge of AuNPs, therefore, plays a critical role. Most of the charges of metal NPs are fixed on the particle surface through the adsorption of a reducing agent in the preparation. Organic acid reductants, such as citric acid and ascorbic acid, yield negatively charged AuNPs; the anionic carboxylate added in the synthetic process adsorbs onto the surface of AuNPs as a protective layer, thereby imparting a negative charge. In particular, citrate capped particles are suitable for further bioconjugation, since the citrate layer is quite loosely bound to the particle.⁹⁷

Table 9 summarizes the different approaches for the biofunctionalization of noble metal NPs, including the main pros and cons of each approach.

Table 9. Types of conjugations between biomolecules and noble metal NPs (adapted from⁹⁸)

Type of interaction	Pros	Cons
Electrostatic (e.g., adsorption of negative charged DNA to positive charged gold NP)	Very simple and straightforward	Restricted to opposite charged biomolecules and NPs; Very sensitive to environmental properties (e.g., pH, ionic strength, <i>etc.</i>); Weak functionalization
Chemisorption (e.g., quasi-covalent binding of thiol functionalized biomolecule to gold NP)	Allows oriented functionalization; Very robust functionalization.	Requires NPs with capping agents with weaker adsorption than the derivatization moiety; Usually requires modification of the biomolecule; Subject to interference by other chemical groups available for adsorption within the biomolecule; Affected by chemical degradation and surface oxidation of some NPs (e.g., silver).
Covalent binding	Possibility to prepare NP with different functional groups Steric stabilization of NP	Ligand exchange is usually needed in order to attach the biomolecules Inter-particle crosslinking can occur
Affinity-based (e.g., His-tag protein binding to Ni-NTA derivatized gold NP)	Allows oriented functionalization; Very straightforward binding between affinity pairs.	Requires modification of both NPs and biomolecules with an affinity pair; Limited to availability of suitable binding affinity pairs.

Conjugation of inorganic nanoparticles to biomolecules generates hybrid materials that can be used to let the nanoparticles interact specifically with biological systems. Nanoparticle–biomolecule conjugates bring together the unique properties and functionality of both materials, e.g. fluorescence or magnetic moment of the inorganic particles and e.g. the ability of biomolecules for highly specific binding by molecular recognition.

The strategy for the conjugation of biomolecules to nanoparticles generally falls into four classes:

1. Electrostatic adsorption of positively charged biomolecules to negatively charged nanoparticles or vice versa,
2. Ligand-like binding to the surface of the inorganic particle core, commonly by chemisorption of e.g. thiol groups,
3. Covalent binding by conjugation chemistry, exploiting functional groups on both particle and biomolecules, and
4. Non-covalent, affinity-based receptor-ligand systems

Electrostatic adsorption (Figure 6B1) is a physical approach to attach biomolecules on the surface of nanoparticles. The nanoparticles and biomolecules with opposite charges will form the nanoparticle-biomolecule system. The biomolecule will be adsorbed to the nanoparticles by electrostatic attraction if both partners are oppositely charged.⁹⁹ Traditionally, the immobilization strategy have been exploited for the preparation of the so-called antibody immunogold conjugates¹⁰⁰ that have been used as labels for immunostaining in electron microscopy.^{101–104} Electrostatic adsorption is a simple and convenient method to build nanoparticle-biomolecule hybrids; however, it possesses some drawbacks. The systems obtained using this method are unstable after some time and will induce a slight change in the conformation of the biomolecules.

Since the discovery of immunogold labelling in 1971 by Faulk and Taylor, huge amount of information about the nature of bonding between gold nanoparticles and antibodies is known. It was suggested that interaction between proteins and AuNPs depends on three separate but dependent phenomena:

- (a) Ionic attraction between the negatively charged gold (e.g. citrate ions used as stabilizing agent) and the positively charged antibody;
- (b) Hydrophobic attraction between the antibody and the gold surface;
- (c) Dative binding between the gold conducting electrons and amino acid sulphur atoms of the antibody

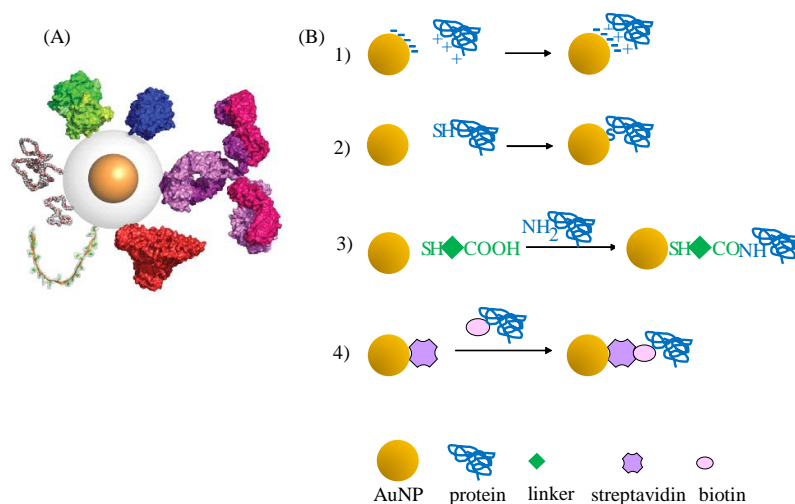


Figure 6. (A) Relative size of nanoparticles and biomolecules, drawn to scale. Schematic representation of a nanoparticle with 5 nm core diameter, 10 nm shell diameter, with PEG molecules of 2000 and 5000 g mol⁻¹ (on the left, light grey), streptavidin (green), transferrin (blue), antibody (IgG, purple), albumin (red), single-stranded DNA (20mer, cartoon and space filling). Proteins are crystal structures taken from the Protein Data Bank (<http://www.rcsb.org>) and displayed as surfaces; PEG and DNA have been modelled from their chemical structure and space filling (from¹⁰⁵). (B) Protein attachment modes on AuNPs.

Direct chemisorption (Figure 6B2) of thiol derivatives on nanoparticles is a simple chemical reaction that occurs between the surface of a nanoparticle and thiol group of a biomolecule. Thiol groups can be introduced in biomolecules to allow interaction with the surface of nanoparticles. In this situation, the thiol groups in the biomolecules are derived from amino acid residues or are incorporated by chemical functionalization methods. In contrast to electrostatic adsorption, direct chemisorption of thiol derivatives can produce a more stable noble metal nanoparticle-biomolecule complex because it involves a chemical reaction. However, it still induces a slight change in the conformation of the biomolecule.

Covalent binding (Figure 6B3) through bifunctional linkers uses bifunctional molecules of low molecular weight to conjugate biomolecules with noble metal nanoparticles. Such bifunctional linkers contain both anchor groups to attach to the surface of nanoparticles and functional groups that allow covalent binding to the target biomolecule.^{106,107} An important advantage of this approach is that retains the stability and activity of biomolecules to allow further conjugation with other biomolecules.^{108,109}

Affinity-based systems (Figure 6B4) found in nature have attracted increasing attention during last years. The most well-known example is the avidin–biotin system.¹¹⁰ The strong bond and specificity of the biotin–avidin system are the most important advantages of using this approach and has found a large number of applications in bio(nano)technology.

1.6.3 Assay formats

Immunoassays can be classified into two groups depending where the biorecognition event takes place.

Homogeneous immunoassays that could be also named as “mix and measure” technique does not require neither reagent immobilization on the surface no washing-steps. Therefore, homogeneous assays, in an ideal case are performed in one step, so they are more time effective. Since homogeneous immunoassays are simple to perform, they could be easily automated which makes them appropriate for high throughput applications. The crucial part of designing a homogeneous immunoassay is to find a method to detect the antibody–antigen binding in solution. Several approaches in order to detect the antigen-antibody binding can be employed. For example, enzymatic detection commonly used in heterogeneous format can be applied in the homogeneous format as well. In this case, the enzyme is conjugated to a small molecule, and when the antibody reacts with the tracer the enzymatic reaction is modified. If a sample with free analyte is added to the system, the analyte would react with the antibodies leading to a release of the enzyme-conjugates from the antibodies and a reconstitution of the enzyme reactivity occurs.

Fluorescence polarization immunoassay (FPIA) is one of the most popular homogeneous techniques currently used for the determination of small molecules. FPIA is a homogenous, competitive method based on detection of the fluorescence polarization (FP) of reaction mixtures containing the sample analyte, fluorescent-labelled tracer, and specific antibody. At fixed temperature and viscosity of the solution, the FP value will be directly dependent on the effective molecular size of the fluorophore. For small molecules (such as unbound tracer) with fast Brownian rotation in solution, FP is low, while for larger molecules (such as tracer bound to antibody) the values are higher. If the analyte is not present in the sample, the tracer will be bound to antibody and the FP will be high (typically about 150 to 300 mP, where mP are millipolarization units, equivalent to $1,000 \times \text{FP}$). If the analyte concentration in the sample is significantly higher than the concentration of the tracer, the antibody binding site will be preferentially occupied by analyte and most of the tracer will be free in solution. The FP of the reaction mixture will then be lower (typically about 30 to 60 mP).¹¹¹ The advantages of the technique are the high stability of tracers and the simplicity and reproducibility of the method. However, FPIA is susceptible to interference from light scattering and endogenous fluorophores in samples, and from tracer binding to sample matrix components.

In the field of environmental monitoring, Knopp *et al.*¹¹² developed a FPIA for detection of polycyclic aromatic hydrocarbons (PAHs) in natural water. Fluorescein-labelled tracers based on different PAHs were synthesized and studied in order to achieve a high sensitivity using both monoclonal and polyclonal antibodies. The application of different combinations of antibody

tracer pairs allows to separately determine groups of small and large PAHs or to realize a class-specific assay. The limits of detection of PAHs were 0.9, 1.1, and 3.4 ng/ml for benzo[a]pyrene, naphthalene, and anthracene, respectively. Despite the many advantages that FPIA technique has, it is not possible to apply it for simultaneous analysis of multiple analytes, and there is not yet applications developed for water pollutant residues analysis.

Another approach of an homogeneous assay technique is the gold-nanoparticle aggregation.¹¹³ Usually antibodies (or DNA strands) are attached to gold nanoparticles and in presence of target molecules the aggregation of nanoparticles occurs. The aggregation of AuNPs induces an electric dipole–dipole interaction and coupling between the plasmons of neighbouring particles, causing the colour change to purple or blue. Based on this principle, many different sensors have been developed. This kind of sensing can be used both for large (proteins, nucleic acids)¹¹⁴ and small organic molecules and even metal ions.¹¹⁵ The main advantage is that typically they consist in one step measurements, using a UV spectrophotometer to detect the aggregation. Also, the low concentration of gold nanoparticles is sufficient to generate visible colour changes due to the extremely high extinction coefficients. Also, the target concentration can be qualitatively estimated from the colour change directly by the naked eye. Despite the many advantages, some drawbacks are still present. For example, a suspension of the aggregates is unstable in solution due to the increased particle size and reduced surface repelling force. Thus, the colour of the suspension diminishes over time, becoming colourless in a few hours. Also, the sensitivity is much lower comparing to other techniques.

Homogeneous immunoassays are strong competitors for heterogeneous formats as they are easy to perform and usually faster. However, still much effort needs to be done to reach the sensitivity of the heterogeneous formats.

If the capture probe is immobilized on the support surface, it is referred to the heterogeneous format. The main advantage of this format is that the separation of bound and unbound molecules is very easy by simple washing step. The drawbacks of this immunoassay type would be the multiple incubation and washing steps, which makes this technique time consuming.

Most of the developed heterogeneous immunoassays are based either on competitive or sandwich assay, when applied to the detection of low and high molecular weight molecules. Two approaches could be considered when dealing with competitive immunoassays. In a first one (Figure 7A), protein antigens are immobilized directly on solid supports. Next, the sample and the specific compete with the immobilized analyte for a limited number of antibody binding sites. The reaction is finished by washing the solid support.

In a second one, the immobilized antibodies react with free antigens in competition with labelled antigens (Figure 7B). The sample is dispensed onto the support along with the tracer, where they compete for a limited number of antibody binding sites. After a certain incubation period, the unbound reagents are removed by washing the solid phase, and the signal from the bound tracer is measured.

In both cases, the signal is inversely related to the analyte concentration.

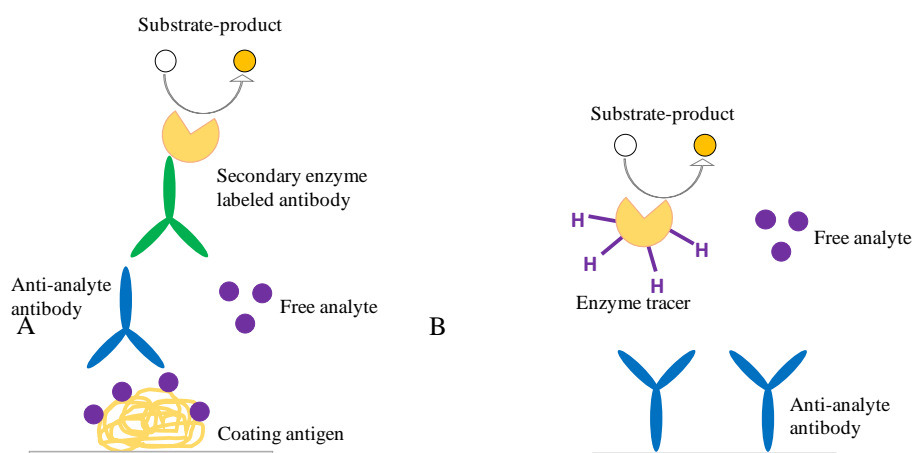


Figure 7. Scheme of the most commonly employed heterogeneous immunoassay configurations (adapted from¹¹⁶) A. Immobilized antigen format; B. Immobilized antibody format.

In both competitive configurations, the analytical signal is plotted on the ordinate (linear scale) against the concentration of the standards on a logarithmic scale, which produces a sigmoidal dose–response curve such as that represented in Figure 8. The sigmoidal curve is fitted by using the four-parameter logistic regression model. Assay sensitivity is defined as the concentration of analyte that inhibits the maximum signal by 50% (IC_{50}). The dynamic range (DR) extends from the concentration that inhibits the signal by 80 to 20%. Within this range, signal correlates linearly with analyte concentration. The working range of the dose-response curve is an important analytical feature which gives a first indication of the dynamic sensitivity of the test.¹¹⁷ The limit of detection (LOD), is the smallest concentration of the analyte that produces a signal variation that can be significantly distinguished from zero for a given sample matrix with a confidence level.

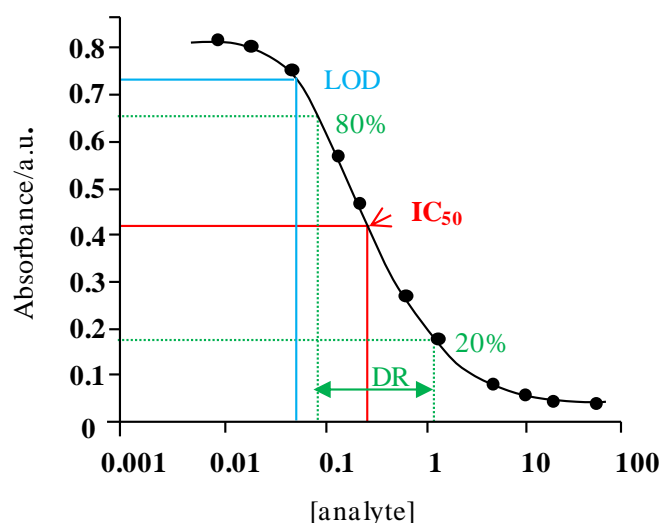


Figure 8. Dose-response curve for a competitive immunoassay.

Although there is no standardized way of defining the limit of detection (LOD), there is a general consensus in favour of selecting the dose that inhibits 10% of the maximum signal. The dose providing the blank signal plus three times the standard deviation from the mean measurement of the blank dose signal is also used to define the limit of detection.

1.6.4 Supports

Protein adsorption to plastic surfaces was first found by Catt and Tregear¹¹⁸ and since then, many different plastic surfaces have been used for the development of immunoassays. Solid supports should meet four key requirements. First, they should provide optimal binding conditions with high binding capacity. Second, the support must be suitable for mass manufacturing. This includes rapid and inexpensive production in high quantities, and ease of handling during storage as well as high reproducibility. The third requirement is to provide a surface that will not provoke denaturation of the biomolecules, as they tend to unfold, when immobilized, which often causes loss of activity. Finally, physical properties of material support must be compatible with optical, electrochemical, or other detection mode.

The first immunoassays developed in the 1970s were performed in a plastic test tube, which was replaced by microtiter plates, nitrocellulose and nylon membrane, beads of polystyrene, methyl methacrylate, and many more polymers in different presentations.

Table 10 summarizes the characteristics of the more commonly used solid phases with respect to parameters that influence their performance.

Table 10. Chemical and physical characteristic of solid phases (Adapted from^{119–121})

Solid phase	Binding force	Relative surface area	Performance characteristics
Polystyrene plates	Hydrophobic	Modest	Low background
Polystyrene (PS) beads	Hydrophobic	Moderate	Yield assays with broad dynamic ranges
Derivatized PS beads	Covalent, hydrophobic and hydrophilic	High	Less convenient to use than plates; more difficult to automate
PC, PMMA, COC, COP chips	Hydrophobic, covalent	Very high	Suitable for DNA or protein microarrays, low background
Magnetic Microparticles (Iron oxide Fe ₃ O ₄ core + gold/SiO ₂ shell)	Covalent	Very high	“Solution-phase performance” due to colloidal nature; wide dynamic range; magnetized variants make them automatable
Nitrocellulose (NC)	Hydrophobic and hydrophilic	Very high	Desorption and background problems hinder use in quantitative assays
Functionalized nitrocellulose	Hydrophobic, covalent and hydrophilic	Very high	Similar to NC but less desorption
PVDF	Hydrophobic	Very high	Very high and stable binding; may be best for immunoblotting
Celulose (paper)	Covalent	Very high	Possible to modify chemically, inexpensive, versatile
Glass slides	Covalent	Very high	Requires chemical coating for attaching the probes, low fluorescent background, inexpensive, suitable for microarraying; can break out or cut
Silicon slides and chips	Covalent	Very high	Suitable for protein microarraying
Carbon nanostructures	Covalent	Very high	Suitable for protein detection
Metallic surface (mainly Au)	Covalent	Very high	Requires chemical attachment of the probe Suitable for both protein and DNA detection Low background

The 96-well microtiter plate is frequently used in laboratories where, e.g., ELISAs are performed. The most commonly used material for microtiter plates is polystyrene, to which most proteins physically adsorb by van der Waals, hydrophobic and hydrogen-bonding interactions. The advantage of this type of immobilization is that it is very simple to perform, because it does not require any modification of the protein. Moreover, polystyrene causes little background signal and is, therefore, very popular. Plastics used for different immunoassay types have, however, some important limitations: (i) the usage of a large amount of immunoreactants, (ii) protein can be inactivated because of denaturation and steric hindrance^{122,123} and (iii) the antibody-antigen interactions are quite slow (since the volumes used are high).⁴⁸

Plastic plates have low binding capacity and low surface area to volume ratio. On the other hand, particulate solid phases are very efficient, because they become scattered throughout the reaction mixture and have a much higher surface area to volume ratio.¹²⁴

For example, magnetic beads are composed of iron oxide nanoparticles embedded in a polymeric matrix. Magnetic particles with micrometer diameters are useful for extraction or purification of biomolecules such as antibodies, proteins and nucleic acids. Also, an advantage of using magnetic microparticles is easy separation of the bound reactants to microparticles from the fluid phase containing the free molecules.^{125,126}

Membranes are the third group of solid phases which form the basis of lateral flow immunoassays (LFIA). Their adsorptive surface areas are 100–1000 times greater than those of plastic, probably due to their large internal surface. A variety of membranes exist, such as composed of cellulose nitrate ester (nitrocellulose, NC), nylon, and polyvinylidene difluoride (PVDF). Membranes, especially nylon, have a high propensity toward nonspecific binding of proteins due to their large surface area. Thus, additional blocking step is required as well as extensive washing when used in immunoassays. The principal chemical bonds between proteins and non-modified membranes are mainly hydrophobic.

Most recently, paper as the starting material for fabricating low-cost microanalytical devices (μ PADs) has been used. This material is available everywhere and is inexpensive. It can be modified chemically to incorporate a variety of functional groups that can be covalently bound to proteins, DNA, or small molecules. Bioanalytical devices using paper as a support are ideal for point-of-care diagnostics such as detection of glucose in urine¹²⁷ or liver function testing.¹²⁸

As far as microarray formats are concerned, the use of glass microscope slides has become very popular as support for attaching the probes. Currently, two major categories of microarray slides exist: gel-coated surfaces, such as polyacrylamide or agarose and non-gel-coated modified glass or plastic surfaces, such as aldehyde, poly-L-lysine, or nickel-coated slides. They are currently

the most common supports because of their easy handling, low cost, low variability, low fluorescent background and greater durability.¹²⁰

Recently, many new polymers appeared as attractive materials for microarray fabrication. For example, cyclic olefin copolymers (COCs) have attracted much attention in recent years in the fields of microfluidic engineering and biosensor technology because of their many favourable properties, such as high glass transition temperature, low auto fluorescence, optical transparency, resistance to organic solvents, low water uptake and moldability.^{129,130}

Moreover, poly(methyl methacrylate) (PMMA) is commonly used for microfluidic chips fabrication due to its optical transparency and easy chip fabrication.¹³¹

Also, polycarbonate is an attractive polymer for microarray development. Plastic disks made of this polymer (e.g. CD; DVD, BR) have the advantage of outstanding physical properties, such as impact resistance, heat stability, large surface and good protein adsorption efficiency.¹³²

1.6.5 Techniques for detection of the immunointeraction events

The radioimmunoassay, developed more than 50 years ago, was the first technique that enabled quantitative analysis of proteins (hormones) with sensitivity and selectivity.¹³³ Later, the technique was intensively used, however, the advent of nontoxic labels such as fluorescent,^{134,135} luminescent,¹³⁶ light-scattering,^{137,138} enzymes,^{139,140} and metallic labels^{141,142} has led to an explosion in the detection techniques available.

The use of such diverse labels has facilitated the extension of the analytical readout methods and led to the development of sensitive, selective and user-friendly biosensing systems, with high throughput. The most common detection systems employed in immunoassays are optical, electrochemical and the pioneer, radioactive. Table 11 shows the most common labels used in immunoassays and the typical readout methods.

Radioimmunoassays are based on competition between radiolabelled (e.g. by means of ¹²⁵I, ³H) and unlabelled antigens for limited antibody binding sites. This kind of competitive immunoassay is one of the most sensitive methods for determination of antigens (LOD~0.5 pg/mL) and the results are very reproducible.^{143,144} In the sixties, Rosalyn Yalow and Solomon Berson developed the first radioisotope immunoassay.¹³³ They determined the concentration of insulin in plasma samples by using ¹³¹I-labeled insulin as reference. This method yielded quantitative and reproducible results, leading to increased interest in this technique.

These examples show that RIAs have already successfully been used for a very long period. However, these assays have several drawbacks. Radiation may be a health hazard, special attention to handling of reagents, training of staff, and storage of waste are required. The useful

lifetime of the reagents is limited by the half-life of the isotope. Counting radioactivity requires special expensive instrumentation and is time-consuming. Therefore, other immunoassay principles, which enable similarly low limits of detection to be achieved, have become increasingly popular.

Table 11. Labels used in immunoassays

Type of label	Analytical principle/technique
Enzymes	
Peroxidase	H ₂ O ₂ /chromogen - Photometry H ₂ O ₂ /pyrogallol or luminal - Luminometry H ₂ O ₂ /KI/ ΔE (mV) - Potentiometry
Alkaline phosphatase/ β -D-Galactosidase	4-Nitrophenol - Photometry 4-Methylumbelliferone – Fluorimetry
Glucose oxidase	H ₂ O ₂ /chromogen - Photometry
Urease	NH/bromocresol purple – Photometry
Lysozyme	Cell wall fragments of <i>Micrococcus luteus</i> – Turbidimetry
Glucose-6-phosphate dehydrogenase	NADH - Photometry, fluorimetry
Fluorescent Labels	
Cy5	Fluorimetry
Alexa fluor	Fluorimetry
QDs	Fluorimetry
Coumarin derivatives	Fluorimetry
Fluorescein	Fluorimetry
Rhodamine	Fluorimetry
Europium (Eu ³⁺)	Time-resolved fluorimetry
Luminescent Labels	
Acridinium ester	Luminometry
Isoluminol derivatives	Luminometry
Particle Labels	
Latex	Nephelometry, particle counting, turbidimetry, visual assessment
Stained bacteria	Visual assessment
Erythrocytes	Visual assessment, nephelometry, turbidimetry
Radioisotopic Labels	
⁵⁷ Co, ¹²⁵ I, ³ H	Solid scintillation counting
Vesicle Labels	
Liposome	Entrapped dye (photometry), entrapped enzyme (photometry)
Colloidal Metal Labels	
Silver, gold, platinum	Emission, absorption, and fluorescence spectroscopy, atomic absorption, turbidimetry, nephelometry, electrochemical methods, anodic stripping, voltammetry

Optical immunoassays are one of the most popular protocols for bioanalysis due to the advantage of rapid signal generation and readouts. Different techniques can be used for creating an optical change, which strongly depends on label used, including fluorescence, bioluminescence or chemiluminescence. The sensitivity and selectivity of the biological sensing element offers the opportunity for development of devices for real-time analysis in complex mixtures, without the need for extensive sample pre-treatment or large sample volumes. Optical immunoassays are highly sensitive, fast, reproducible, and simple-to-operate analytical tools.

Photometric immunoassays are those that for the detection of the immunoreactions use labels that produce compounds that absorb monochromatic light. This phenomenon is applied in ELISA where diverse enzymes are used as labels which transform a substrate into a soluble coloured product. The results are quantified by an UV-vis spectrophotometer. Vast number of enzymatic immunoassays for pollutants detection has been developed, including detection of atrazine,¹⁴⁵alachlor,¹⁴⁶ sulfasalazine,¹⁴⁷ triclosan,¹⁴⁸ imidacloprid,¹⁴⁹ diuron¹⁵⁰ and many others.

In *fluorescent* detection a chemical reagent is used as a mediator to produce a fluorescent signal. The most common fluorescent labels are fluorescein, Cy5, Cy3, Alexa, BODIPYs etc., and now popular nanocrystals as quantum dots.^{151,152} The main drawback in this type of detection is the background signals that are mainly caused by light scattering from soluble molecules (Rayleigh and Raman scattering), small particles, or the solid-phase material (Tyndall scattering). Also, background fluorescence can occur due to fluorescent compounds in the sample, or impurities in the reagents. Many fluorescence ELISAs have been developed for pesticide detection, such as for quantification of atrazine,¹⁵³ diuron,¹⁵⁴ and in multiplexed formats.¹⁵⁵

Chemiluminescent methods have been applied in routine clinical analysis as well as in clinical and biomedical researches due to the relatively simple instrumentation and high sensitivity.¹⁵⁶ In general, two chemiluminescent analytical reagents are used: (1) luminol or acridinium ester; (2) horseradish peroxidase or alkaline phosphatase, both as label for enzyme immunoassay. The first technique detects directly a light flash of the chemiluminescent reagent to determine the analytes, where labels are consumed in the chemiluminescence analytical reaction. In the second way, the label is not consumed but the chemiluminescent substrates undergo a peroxidase-catalysed oxidation in the presence of a suitable oxidant. For example, immunosensors for environmental,¹⁵⁷ or food analysis^{158,159} were successfully developed.

1.7 Compact disk technology

The idea of using disk drives to monitor molecular biorecognition events on regular optical discs has received considerable attention during the last decade.¹³² Compact discs (CDs) provide inexpensive substrate materials for the preparation of microarrays, and conventional computer drives/disc players can be adapted as precise optical reading devices for signal processing.

Polycarbonate (PC) surface of a CD as an alternative substrate to glass slides or silicon wafers for the preparation of microanalytical devices can be employed. Using the characteristic optical phenomena occurring on the metal layer of a CD, researchers can develop biosensors based on optical or even advanced spectroscopic readout (interferometry or surface plasmon resonance).¹⁶⁰

CD, DVD and BD are the most commonly used compact disk formats. The readable surface is made up of areas called – “lands” and “pits” as it is shown in Figure 9. The lands and pits differ in the way they reflect or diffuse light. The areas that reflect light are known as lands, and those that diffuse or diffract the light are the pits.

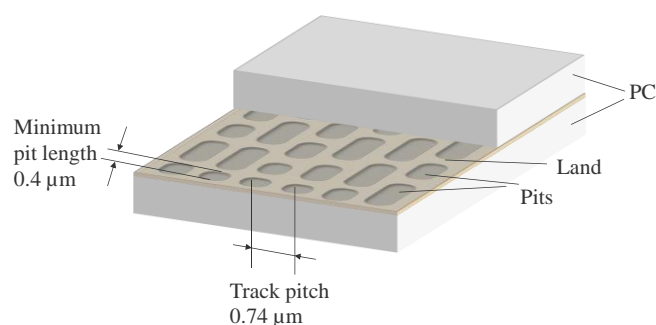


Figure 9. DVD cross section representing pits and lands.

The following paragraphs provide background information on the composition of CDs, DVDs and BDs. The schematic representation of each of disks structures is presented in Figure 10.

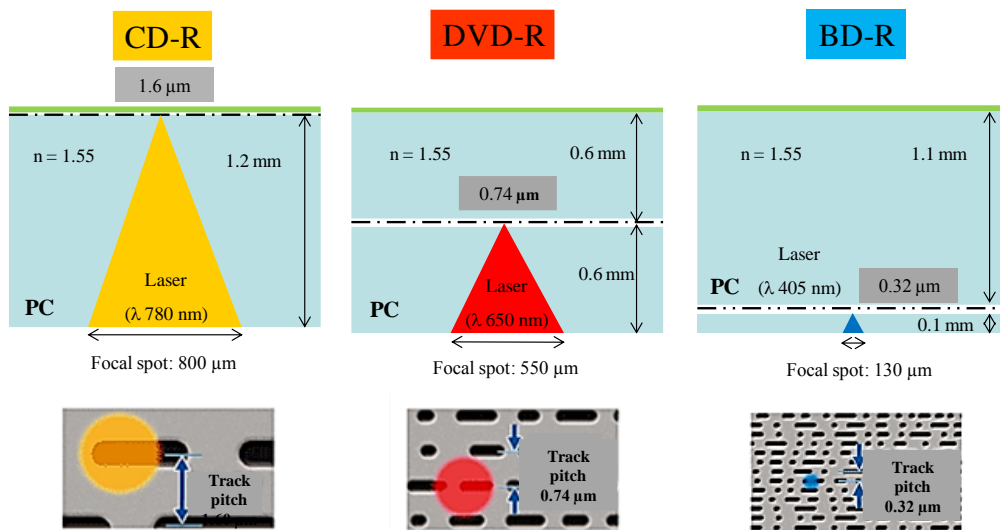


Figure 10. Characteristics of compact disks and lasers used in disk drives.

A recordable *CD* has either four or five layers with total thickness of 1.2 mm. The polycarbonate layer of a *CD-R* has a shallow groove that is used for timing and tracking in the recording process. This grooved layer is covered with a dye polymer that darkens or creates a void (creating a pseudo pit) when struck (or burned) with a recording laser beam. The disc is then coated with a reflective metallic layer as aluminium, gold, silver, etc. Next, the reflective layer is protected with a lacquer coating. Discs have also a label on top.

DVDs are composed of two 0.6-mm polycarbonate discs. One contains the laser-guiding groove and is coated with the recording dye and aluminium alloys. The other disc is a dummy polycarbonate surface that guarantees both the mechanical stability of the sandwich structure and the compatibility with the standard thickness of a *CD*. The sandwich structure also helps protect the data containing layer from scratches by the thick "dummy" disk. Compared to a *CD*'s 1.2 mm of polycarbonate, a *DVD*'s laser beam only has to penetrate 0.6 mm of plastic in order to reach the dye recording layer, which allows the lens to focus the beam to a smaller spot size to write smaller pits.

In the *Blu-ray* disc, the data layer is placed on top of a 1.1 mm thick polycarbonate. Having the data on top prevents diffraction and beam splitting from reading through the polycarbonate, thereby preventing readability problems.

All three common optical disc media (*CD*, *DVD*, and *Blu-ray*) use light from laser diodes. *DVD* uses light of 650 nm wavelength (red), as opposed to 780 nm (far-red, commonly called infrared) for *CD*. This shorter wavelength allows a smaller pit on the media surface compared to *CDs* (0.74 μm for *DVD* versus 1.6 μm for *CD*), accounting in part for *DVD*'s increased storage

capacity. In comparison, Blu-ray Disc, the successor to the DVD format, uses a wavelength of 405 nm (blue). The benefit of blue laser (405 nm) is that it has a shorter wavelength than a red laser (650 nm), making it possible to focus the laser spot with greater precision, thus it is possible to fit more data on a disc the same size as a CD/DVD.

The laser hits a semi-transparent mirror that rotates the plane of polarization of the light beams and directs the beams toward the disc surface (Figure 11). After making the divergent light rays parallel by a collimator, an objective lens focuses the laser on the disc's reflective surface. When light hits a land, it is reflected straight back towards the photodiode. When light hits a pit, it is scattered, reducing the intensity of the light that reaches the photodiode. The reflected light goes through the semi-transparent mirror that passes light in one plane but reflects light in the other plane, and strikes the photodiode. The outputs of the photodiode are then demodulated to yield the stored data.

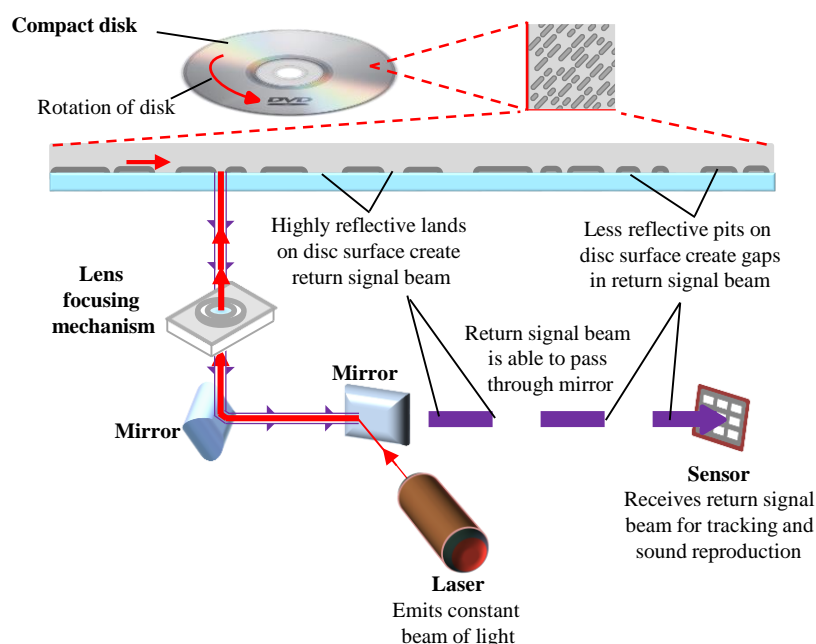


Figure 11. Schematic representation of disc reading process.

1.7.1 Analytical applications of disks as analytical platform

The current analytical applications using plastic discs as supports can be classified in two groups. One employs discs about 2-mm thickness and 12-cm diameter to accomplish the development of microfluidic-based assays for proteins and nucleic acids, in which different steps are involved. The other group is based on the use of compact discs audio-video technology for management and reading the chemical results.

1.7.1.1 Lab-on-a-CD

Lab-on-a-CD is a centrifugal device that integrates several laboratory functions on a CD-like platform. It requires only a stepper motor to provide the centrifugal forces needed for fluid manipulation. As the disc spins, centrifugal forces induced on sample fluids drive liquids radially outwards from the centre toward the edge of the disc. CD-based centrifugal methods are advantageous in many analytical situations because of their versatility in handling a wide variety of sample types, ability to gate the flow of liquids (valving), simple rotational motor requirements, ease and economic fabrication methods, and large range of flow rates attainable. Most analytical functions required for a lab-on-a-CD, including metering, dilution, mixing, calibration, separation, etc., can all be performed in a CD. Moreover, the possibility of maintaining simultaneous and identical flow rates, to perform identical volume additions, to establish identical incubation times, and to mix dynamics and detection in a multitude of parallel CD assay elements, makes the CD an attractive platform for multiple parallel assays. The platform has been commercialized by Tecan Boston for HTS,¹⁶¹ by Gyros AB to develop nanoliter-scale immunoassays and for sample pretreatment,¹⁶² by Abaxis (in a somewhat larger and less integrated rotor format compared with the CD format) for human and veterinary diagnostic blood analysis,¹⁶³ and recently by Quiagen for genetic applications.

The CD-like platform is easily adapted to optical detection methods because it is manufactured with high optical quality materials enabling absorption, fluorescence, and microscopy techniques.¹⁶⁴⁻¹⁶⁷

1.7.1.2 Compact disk technology as analytical tool

Compact disk technology is based on the use of standard disks (CDs, DVDs and BRs) as a platform for microarray fabrication and disk drive as sensitive detector to read the results.

The principle of compact disk technology was proposed by Kido *et al.*,¹⁶⁸ in 2000. In this work, low-density microarrays were performed on a polycarbonate disc for the simultaneous determination of hydroxyatrazine, carbaryl, and molinate in competitive inhibition immunoassays. The probes were printed with commercial inkjet printer in a microarray format. The resulting microspots were approximately 75 micrometres in diameter and were visualized by using an antibody labelled with a fluorescent tag and a commercially available fluorescence scanner. The results of this work suggested that compact disc-based microarray technology could give qualitative and quantitative results.

In 2002, Alexandre *et al.*¹⁶⁹ used compact disk as support to perform DNA arrays. The CD was divided into two functional areas: the external ring of the CD was used for multiparametric DNA

arrays and the inner portion was used for storing numeric information. The BioCD was used for *Staphylococcus* detection.

Also, in the same year, a DNA microarrays placed in a microchannel environment that can be read and analyzed in an optical (CD/DVD) disc drive system was developed.¹⁷⁰ In 2003, an approach to screen the recognition between small molecule ligands and biomolecules was developed.¹⁷¹

In 2006, Potyrailo *et al.*¹⁷² demonstrated quantitative chemical sensing in conventional optical disk drives by using an analog signal from the drive's photodetector. In this work, the drives not only read and write digital content to optical media, but also provide analog signals for quantitative sensor applications when sensor films are deposited onto CDs or DVDs. As there is no need of modifying the optical disks, any disk can be employed for deposition and readout of sensor films. Such a sensor platform is quite universal and can be applied for quantitative chemical and biological detection, The potential of using compact discs as high throughput screening platforms for DNA microarraying was also applied to score genetic variations of Plum pox virus.¹⁷³

A novel lead(II) detection method was described by Wang *et al.*¹⁷⁴. A standard compact disc (CD) was used as the platform to prepare DNAzyme assays and a computer drive to read out the results. A chemical surface activation was performed to attach the probes. The CDs were irradiated with UV light in the presence of ozone to generate carboxylic acid groups on the polycarbonate surface for subsequent attachment of amino-modified probes.

Recently, a lead (II) detection method by using a conventional compact disc (CD) as the platform to prepare DNAzyme assays and a standard computer drive as the readout device has been developed.¹⁷⁵

To show high-throughput capabilities of compact disk technology, high-density competitive immunoassays in microarray format were performed in both sides of compact discs. Immunoreagents were directly adsorbed on polycarbonate surface and gold or enzyme-labelled immunoglobulins were used as tracers.¹⁷⁶ Low-reflectivity compact disc were used as analytical platform for this study. The transmitted light that reached the photodiode was related to the sample concentration. The principle was demonstrated by detection of low abundant compounds, chlorpyrifos and metolachlor.

Several approaches for chemical derivatization of CD surface were developed.¹⁷⁷ The modifications consisted in amination, glutaraldehyde cross-linking of aminated polycarbonate disks, thiolation and chloromethylation. The modified disks were then used to covalently attach oligonucleotide probes (5' Cy5- labeled, 3' NH₂-ended) to discriminate single nucleotide polymorphisms.

Moreover, haptens were linked directly to polycarbonate surface of the disks.¹⁷⁸ Disks were aminated and haptens coupled through their carboxylic acid group to the amine-terminated PC surface by the DCC/NHS coupling chemistry. To prove the principle, competitive

microimmunoassays were developed for chlorpyrifos, atrazine, and 2-(2,4,5-trichlorophenoxy) propionic acid, in microarray format.

Also, oxygen plasma activation was used to chemically modify the polycarbonate surface of compact disks.¹⁷⁹ Carboxylic acid groups are generated in few seconds and by using EDC/NHS chemistry amino-modified oligonucleotide probes can be covalently attached. As proof of concept, the oxygen plasma treated interactive polycarbonate DNA microarraying platform was applied to the detection of PCR products of *Salmonella spp.*, reaching a detection limit of 2 nM that corresponds to a DNA concentration of only 1 c.f.u./mL.

The BioDVD methodology, based on a multilayer platform fabricated by radiofrequency magnetron sputtering on a pregrooved polycarbonate disc substrate was developed.¹⁸⁰ The multilayer consisted of five layers of optimal thickness of ZnS-SiO₂ to achieve the maximum change of reflected light. The intensity of the signal obtained was measured with an optical disk drive prototype. The BioDVD platform was suitable for analyzing nucleic acid hybridization, and also for antigen-antibody interactions.

Also, modification of CD surface with gold, carbon and aluminium was demonstrated.¹⁸¹ Chemical modifications were performed in order to covalently immobilize proteins. Thus, for gold substrates, self-assembled monolayers were performed by chemisorption of 11-mercaptopundecanoic acid. For aluminium modified disks, silanization with N-(trimethoxysilylpropyl)ethylenediamine triacetic acid to create a carboxylic acid functional group was performed. Carbon oxidation with oxygen plasma allowed functionalization of carbon-coated disks. To demonstrate the analytical capabilities of these platforms, microimmunoassays for the determination of chlorpyrifos were developed, reaching sensitivities in the low microgram per litre range.

Compact disks were also used for surface-enhanced Raman scattering, sputtering directly silver on CDs as a low-cost and disposable surface with potential for ultra-high sensitive detection of small molecules.¹⁸² Also, discs have been recently used for the fabrication of aluminium nanohole arrays for label-free optical biosensing¹⁸³ and as versatile substrates for releasable nanopatterned aluminium films.¹⁸⁴

The surface of Blu-ray disks was modified with SU-8 epoxy photoresist to develop new DNA microarrays.¹⁸⁵ To modified Blue-ray disks thiolated DNA probes were selectively and covalently attached to recognize specifically their complementary strand.

Surface of compact disks can be either chemically derivatized in order to attach the probes or sensing molecules can be directly adsorbed on the surface. The strategy is based on hydrophobic interactions between probes and polycarbonate, showing high immobilization yields.¹⁸⁶

Following this research line, Li *et al.*¹⁸⁷ developed bioassays performed directly on a CD in a line array format. The aim was to detect different types of biochemical recognition reactions (biotin-

streptavidin binding, DNA hybridization and protein–protein interactions) with standard optical drives.

Quantitative immunoanalysis on recordable CDs for the determination of α -fetoprotein and atrazine on four types of audio–video discs was also studied.¹⁸⁸ In this approach, both enzyme and gold nanoparticle antibody conjugates were used as reporters to modify the optical properties of the disc. The assays had a detection limit of 8.0 $\mu\text{g/L}$ for α -fetoprotein and 40 ng/L for atrazine.

In another approach, polystyrene spin-coated modified compact discs were used for the development of microarray immunoassays.¹⁸⁹ The surface did not show any optical changes, enabling to read the track without errors in a commercial CD reader. The concept was applied for the analysis of pesticide chlorpyrifos, reaching 0.96 $\mu\text{g/L}$ sensitivity.

Also, a multiplexed microimmunoassay performed on a DVD was developed.¹⁹⁰ Five different analytes (atrazine, chlorpyrifos, metolachlor, sulfathiazole and tetracycline) were simultaneously determined in natural water samples at $\mu\text{g/L}$ levels. No sample treatment or preconcentration was needed and the results were obtained in 30 min, achieving sensitivity and selectivity similar to those of the ELISA plate format.

Microimmunoassay on a DVD was developed for microcystin-LR quantification.¹⁹¹

The working principle of the biosensing platform was based on an indirect competitive microimmunoassay, where free microcystin LR competes with immobilized conjugate for specific monoclonal antibody. The results of the immunoreaction were analysed using a DVD drive, showing a sensitivity for MC-LR of 1.04 $\mu\text{g/L}$.

Moreover, using sensing films placed onto the polycarbonate surface of Super Audio CDs, Potyrailo *et al.*¹⁹² addressed the quantification of chlorine in water by a dual-wavelength approach. This was the first work demonstrating the use of disk drives for multiwavelength chemical measurements, achieving detection limits for chlorine ranging from 300 to 600 $\mu\text{g/L}$.

A duplex DNA array on a DVD platform for the simultaneous detection of *Salmonella spp.* and *Cronobacter spp.* in powder infant milk after PCR amplification as a double checking sensor system was also developed.¹⁸⁶ Also, multiplex DNA detection of food three allergens (hazelnut, peanut and soybean) on a DVD has been described.¹⁹³

In another work, two approaches under isothermal conditions: recombinase polymerase amplification (RPA) and multiple displacement amplification (MDA) were applied to a duplex assay specific for *Salmonella spp.* and *Cronobacter spp.*¹⁹⁴ Good results were obtained in terms of resistance to inhibition, selectivity and sensitivity (10^1 – 10^2 cfu/mL).

Moreover, a semi-automated DNA assay in microarray format has been described¹⁹⁵ based on the integration of an adhesive microfluidic layer onto the polycarbonate surface of conventional DVDs. The method has been applied for rapid screening of genetically modified organisms (GMOs).

Recently, Blu-ray disks were demonstrated as suitable platform for massive screening.¹⁹⁶ As a proof of concept, two sensing approaches were conducted. First one, for detection of microcystins consisted in competitive immunoassay. The second one, was a multiplex DNA hybridization test for the detection of *Salmonella typhimurium* and *Cronobacter sakazakii* in powder infant formulas. Detection limits of 0.4 µg/L for microcystin LR and 10⁰ and 10¹ cfu/mL were achieved for *Salmonella typhimurium* and *Cronobacter sakazakii*, respectively.

Also, clinical applications have been developed using compact disk technology. Disc technology in our group was employed to perform sandwich immunoassays for detection of antigens associated with infections. For example, the polycarbonate surface of DVDs was chemically modified to attach the antibodies for detection of influenza A viruses.¹⁹⁷ The inactivated virus was detected in spiked saliva samples at 29 µg/L.

Compact disk were used also to demonstrate its capability for rapid and low-cost HIV diagnostics by counting CD4+ cells isolated from whole blood.¹⁹⁸ It was shown that a commercial DVD drive with some modifications, can be turned into an improved DVD-based laser scanning microscope. The system consists of a multi-layered disposable polymer disc and a modified commercial DVD reader with rotational control for sample handling, temperature control for optimized bioassay, a photodiode array for detection, and software for signal processing and user interface.

Another practical application is the on-site determination of human chorionic gonadotropin in urine samples by Li *et al.*¹⁹⁹

Also, Avella-Oliver *et al.*²⁰⁰ has introduced for the first time ThermoChromic Etching Discs (TED) technology in the analytical field. This type of discs are mass produced and commercialized as LightScribe. Platforms compatible with TED technology are optical data recording discs (CD or DVD) containing a photochromic coating on the label side, that becomes darker when irradiated with 780 nm laser source. The work shows some possible applications of this technology, such as microarray immunoassay, immunofiltration test, solution measurements, and cell culture analysis.

Also, the possibility of performing surface plasmon resonance measurements on recordable disk platform was evaluated.²⁰¹ The author studied the feasibility of using a commercial, gold-type, compact disk as suitable platform for SPR sensing.

In 2016, an integrated device composed of micro-reactors embedded onto compact discs for real-time targeted DNA determination was developed.²⁰² The principle of the method consists of loop-mediated isothermal amplification. The detection was based on the turbidimetric or colorimetric properties of reaction solution that changed depending on the presence of target analyte.

All the presented examples show the enormous potential of Compact Disk technology in the biosensing field.

11

Objectives

II Objectives

The combination of biomolecules and nanomaterials allows the development of alternative analytical approaches with promising applications in environmental analysis. Moreover, the polycarbonate surface of audio-video discs is an interesting substrate for the development of inexpensive and easy-to-use microanalytical test. Therefore, hybrid materials, such as biomolecules conjugated with nanoparticles in combination with disposable platforms and portable detection could fill the niche in environmental screening analysis providing simple and rapid methodologies.

Multiplexed immunoassays seem to be quite challenging and has succeeded in a few cases. Therefore, there is growing interest in developing bioanalytical tools, mainly to increase the number of analysis and restrict the number of samples for subsequent more expensive measurements, thus alleviating the overall costs and speed the analysis time.

In this thesis, screening methodologies based on Compact Disk technology have been developed and optimized to conduct multiplex analysis of water pollutants in microarray format.

The main objectives set are the following:

1. To select the immunoreagents for the chosen residues of pollutants that can be integrated in a multiplex microimmunoassay.
2. To optimize the protocol for antibody immobilization on gold nanoparticles.
3. To study the optimal gold nanoparticle's size (5-250 nm) and the optimal immunoassay format and assay protocol in terms of sensitivity, selectivity, operability and cost.
4. To develop and optimize the immunoseparation step in order to improve the immunoassay sensitivity. To choose the optimal Ab-AuNPs conjugate dilution, sample volume, incubation time and resuspension volume. To compare the obtained results with those obtained without immunoseparation step.
5. To demonstrate the applicability of the methodology for spiked samples determination, and compare the results with those obtained by the reference methods.
6. To evaluate and discuss the performances of the developed methodology for the determination of residues of water pollutants.

A brief description of the analytes used are described below.

2-(2,4,5 trichlorophenoxy)propionic acid

2,4,5-TP, 2-(2,4,5 trichlorophenoxy)propionic acid, is an auxin-type herbicide that was used extensively in the past because of its effectiveness. Although use of 2,4,5-TP was banned more than 20 years ago, there is still a need to verify even trace amounts of this herbicide. The analytical procedure routinely applied to the determination of 2,4,5-TP in water, soil, and wastewater samples is EPA method 8151, consisting in solvent extraction and separation by chromatography, GC with electron capture detection or HPLC with photo-diode array-UV detection.

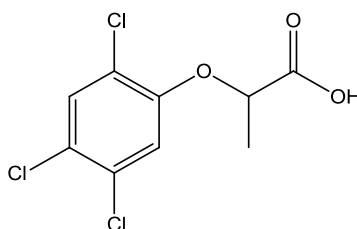


Figure 12. Chemical structure of 2-(2,4,5 trichlorophenoxy)propionic acid.

3-Phenoxybenzoic acid

Pyrethroids are a class of synthetic insecticides similar to the natural chemical pyrethrins. In the environment, pyrethroids are degraded by photolysis and 3-phenoxybenzoic acid (3-PBA) is one of the main products of pyrethroid photolysis.²⁰³ The determination of 3-PBA as a biomarker of exposure to pyrethroids is much easier than direct determination of these pesticides. Recently, McCoy et al.²⁰⁴ have developed a method based on HPLC/MS with an electrospray interface (ESI) to detect type II pyrethroids by converting them to 3-PBA. Also, GC-ECD was successfully employed for 3-PBA detection in water samples.²⁰⁵ Alternative low-cost bioanalytical approaches have been reported. Traditional ELISA tests^{204,206,207} for different matrices as well as fluorescence immunoassay have been developed.²⁰⁸

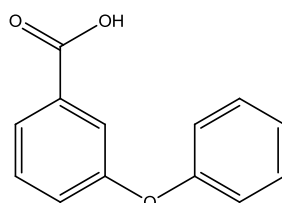


Figure 13. Chemical structure of 3-phenoxybenzoic acid.

4-Nitrophenol

4-Nitrophenol is widely present in the environment where it appears as intermediate in the synthesis of many drugs (paracetamol²⁰⁹), various pesticides as well as major degradation products of these.^{210,211} 4-Nitrophenol is thus released to the environment as a waste compound from different industrial sources, and can be found in river water.²¹² This compound is regulated as one of the priority pollutants by the US Environmental Protection Agency (EPA). The official US EPA accepted techniques are based on gas chromatography with electron capture or mass spectrometric detection.²¹³ Alternative analytical methods, particularly ELISAs, have been developed either in a simple form^{214,215} or coupled to liquid chromatography,²¹⁶ allowing very low limits of detection.

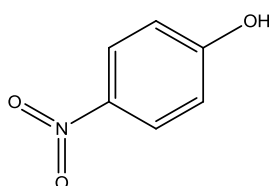


Figure 14. Chemical structure of 4-nitrophenol.

Alachlor

Alachlor, 2-chloro-2', 6-diethyl-N-methoxymethyl acetanilide, is widely used for weed control in corn and soybean production. The US EPA has classified alachlor as a group B2 carcinogen.²¹⁷ Public health concern is also related to its detection in groundwater samples collected in agricultural areas.^{218–220} The EPA has established the Method 535²²¹ for the analysis of ESA and OA degradates of chloroacetanilide herbicides in drinking water and surface water which is based on LC-MS². As far as alternative techniques are concerned, ELISA is the most common method for sensitive and rapid determination of alachlor residues.^{146,222,223} However, other types of immunoassays, such as magnetic-particle ELISA,²²⁴ or fluorescence polarization immunoassay²²⁵ have been developed.

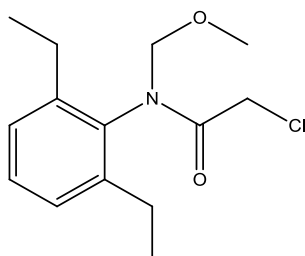


Figure 15. Chemical structure of alachlor.

Atrazine

Atrazine, 2-chloro-4-(ethylamino)-6-(isopropylamino)-s-triazine, is registered for pre- and post-emergence control of broadleaf and some grassy weeds. The chemical features of this herbicide provoke its good mobility in the aquatic media and a high persistence in the environment.²²⁶ For the determination of atrazine in water samples, EPA recommends the procedure based on GC/MS.²²⁷ Nevertheless, many other methods were developed, such as HPLC with diode-array detection,²²⁸ or and LC-MS^{2,229}

Atrazine is by far the most popular compound studied for immunoassay development. ELISAs using polyclonal²³⁰ and monoclonal²³¹ antibodies, LFIA,²³² fluorescence immunoassays,²³³ electrochemical immunosensors,^{234,235} microfluidic devices,²³⁶ conductimetric immunosensors,²³⁷ magnetic beads-based immunoassay,²³⁸ among many others, have been extensively studied.

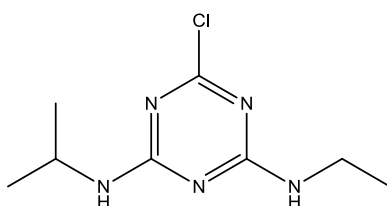


Figure 16. Chemical structure of atrazine.

Azoxystrobin

Azoxystrobin is a systemic, broad-spectrum fungicide derived from the naturally-occurring strobilurins.²³⁹ Nowadays, some studies have showed that several primary metabolites of some strobilurins are soluble in water and have a very high mobility/dissipation rates from soil/air to water and are reaching downstream aquatic ecosystems.^{240,241} Additionally, both European Pesticide Risk Assessment (EFSA) (2010) and US EPA (1997) concluded that azoxystrobin was considered as very toxic to aquatic organisms.²⁴¹ For the determination of azoxystrobin EPA recommends HPLC/UV. Recently, alternative methods, mainly based on ELISA, were developed for the determination of this fungicide.²⁴²

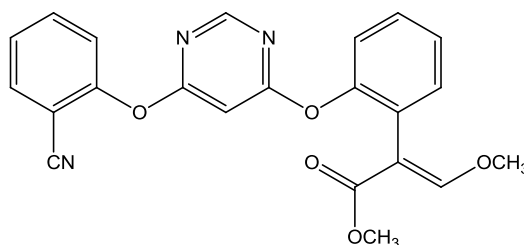


Figure 17. Chemical structure of azoxystrobin.

Chlorpyrifos

Chlorpyrifos, O,O-diethyl O-(3,5,6-trichloro-2-pyridinyl) phosphorothioate, is one of the most frequently used organophosphate pesticides in agriculture. It is a broad-spectrum insecticide commonly used to control insect and arthropod pests on agricultural and vegetable crops.

Chlorpyrifos is responsible of aquatic life toxicity due to point source discharges and agricultural discharges.²⁴³ It is moderately toxic to mammalian species, but extremely toxic to bees and a wide range of aquatic species.²⁴⁴

The determination of chlorpyrifos in water samples is generally carried out by GC-FPD,^{245–247} HPLC with UV²⁴⁸ or PDA²⁴⁹ detector, or capillary LC with UV detection.²⁵⁰ Among alternative techniques, ELISA tests^{251–253}, LFIA,²⁵⁴ fluoroimmunoassays,²⁵⁵ SPR immunosensor,²⁵⁶ have been developed.

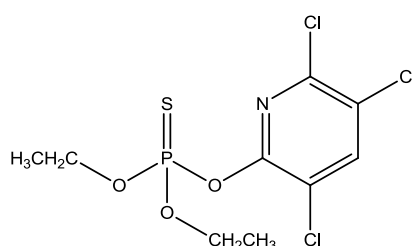


Figure 18. Chemical structure of chlorpyrifos.

Diazinon

Diazinon, O,O-diethyl- O-(2-isopropyl-6-methyl-4-pyrimidinyl)phosphorothioate, is an organophosphate pesticide used in agricultural and urban applications to control a variety of insects. Diazinon has been implicated for causing aquatic life toxicity in urban waters.²⁵⁷ Most concerns are also linked to relatively high toxicity of diazinon.²⁵⁸

The traditional analytical techniques used for the determination of diazinon are mainly GC-FID²⁵⁹ or HPLC with UV/vis detector.²⁶⁰ Among nonconventional technique used to detect diazinon residues ELISA tests are used.^{258,261,262}

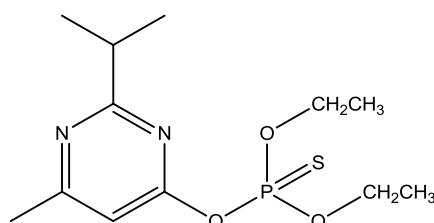


Figure 19. Chemical structure of diazinon.

Diuron

Diuron, 3-(3,4-dichlorophenyl)-1,1-dimethylurea, a substituted phenyl urea herbicide is used as a broad spectrum pre-emergence weed control in a wide variety of crops, which degraded residues are detected in ground and surface water.²⁹⁰ Standard analytical methods for detecting diuron in water samples include mainly HPLC,^{264–266} but also LC-MS,²⁶⁷ GC/MS²⁶⁸ and capillary electrophoresis.²⁶⁹ Alternative techniques, such as ELISA tests using polyclonal,¹⁵⁰ or monoclonal²⁷⁰ antibodies, fluoroimmunoassays,²⁷¹ and chemical immunosensors²⁷² have been developed. There have been as well multiplexed attempts to detect diuron and atrazine simultaneously.²⁷³

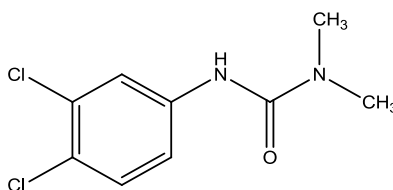


Figure 20. Chemical structure of diuron.

Endosulfan

Endosulfan, 1,4,5,6,7,7-hexachloro-8,9,10-trinorborn-5-en-2,3-ylenebismethylene, sulphite belongs to chlorinated cyclodiene (CCD) insecticides. Endosulfan presents a moderate toxicity for mammals. It is highly toxic to fish and some bird species and has been shown to have estrogenic effects on humans.²⁷⁴ More than 80 countries, including Australia, New Zealand, several West African nations, the United States of America, Brazil, and Canada had already banned it. It is still used extensively in India, China, and few other countries.

Traditional methods for determining endosulfan are based mainly on chromatographic analysis.²⁷⁵ Among non-conventional techniques the most common ones are enzymatic immunoassays.³⁰⁴

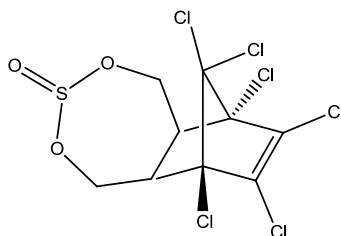


Figure 21. Chemical structure of endosulfan.

Fenthion

Fenthion is a contact and stomach organophosphorus pesticide widely used in the control of many sucking, biting pests, especially fruit flies, stem borers and mosquitoes on crops.²⁷⁷ The persistence half-life of fenthion in water under field conditions is reported to range from 3 to 21 days for various oceans and rivers.²⁷⁷

Standard methods for fenthion determination are LC-MS²⁷⁸ and GC-FTD or GC-MS.^{279,280} As far as immunoassay techniques are concerned, microtiter and dipstick ELISA tests are the most commonly employed.²⁸¹⁻²⁸³

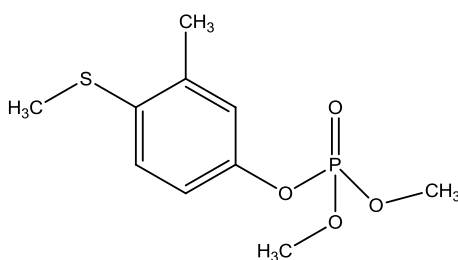


Figure 22. Chemical structure of fenthion.

Forchlorfenuron

Forchlorfenuron, 1-(2-chloro-4-pyridyl)-3-phenylurea, is a relatively new plant growth regulator extensively used in recent years for increasing fruit size in many crops, particularly in grapes and kiwifruit.²⁸⁴

Different methods based on liquid chromatography coupled to diverse detection systems, such as UV and MS, have been described for monitoring CPPU in different vegetal products.²⁸⁵⁻²⁸⁷ Among antibody-based techniques ELISA tests^{288,289} and immunochromatographic strip based on carbon nanoparticles²⁹⁰ have been developed.

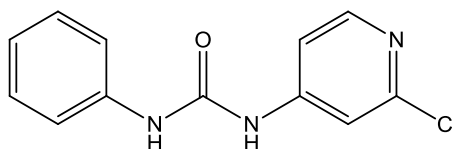


Figure 23. Chemical structure of forchlorfenuron.

Imidacloprid

Imidacloprid, 1-(6-chloro-3-pyridylmethyl)-N-nitroimidazolidin-2-ylideneamine, is a systemic insecticide used to control sucking insects in rice and other agricultural crops. Degradation caused by light or water, give rise to several products which both with imidacloprid itself may cause a threat to bees.²⁹¹

Current methods for detecting imidacloprid residues include LC methods^{319,320} and GC-MS.^{293,294} Besides, immunological methods have been developed for imidacloprid, for example ELISA²⁹⁵ or strip immunochromatographic assay.²⁹⁶ Moreover, there are commercially available immunoassay kits, for instance, antibody-coated microwell plate QuantiPlate Kit with limit of detection 0.07 µg/L.

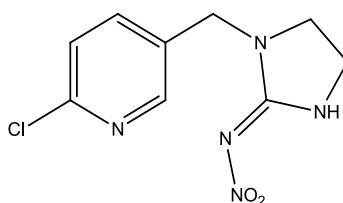


Figure 24. Chemical structure of imidacloprid.

Malathion

Malathion, O,O'-dimethyl S-(1,2-dicarbethoxyethyl) phosphorodithioate, is a nonsystemic organophosphorus insecticide and acaricide with contact, stomach, and respiratory action which inhibits acetylcholinesterase activity.²⁹⁷ In the USA, malathion has been reported in surface water at levels up to 0.18 µg/L and in drinking water at 0.1 µg/L.²⁹⁸ Reference methods for malathion determination are based on chromatographic analysis either by LC or GC methods.^{299,300} Multiresidue enantiomeric separation of organophosphorus pesticides including malathion has also been developed.^{301,302} Within alternative techniques enzymatic immunoassay have been developed.³⁰³

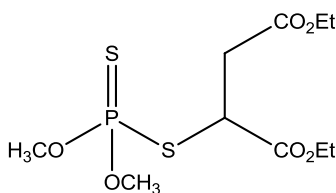


Figure 25. Chemical structure of malathion.

Pentachlorophenol

Pentachlorophenol (PCP) is an extremely hazardous pollutant, belonging to the chlorophenols group. They are by-products of a great number of manufacturing processes (production of resins, plastics, dyes, pharmaceuticals, etc.), forest and agriculture phytosanitary applications and even water chlorination.³⁰⁴ Pentachlorophenol has been classified as a B2 probable carcinogen for humans on the basis of a large body of evidence from animal toxicity studies and human clinical data.

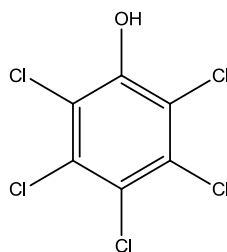


Figure 26. Chemical structure of pentachlorophenol.

Pyraclostrobin

Pyraclostrobin has eradicated, curative, and protective action against fungi both on the plant surface and within the tissues of a wide range of species. In addition, it is effective in the control of fungal diseases and promotes plant growth. Pyraclostrobin is not readily biodegradable and drinking water sources can be contaminated through run-off. It is very toxic to aquatic organisms. In humans, pyraclostrobin can cause eye damage, it is a respiratory and skin irritant, and can be absorbed through the skin.³⁰⁵

Determination of pyraclostrobin residues is mainly performed in food and animal origin commodities and entirely relied upon HPLC or GC coupled with single or tandem mass spectrometry (HPLC-MS²; GC-MS²) and ultraviolet (HPLC-UV) detection.

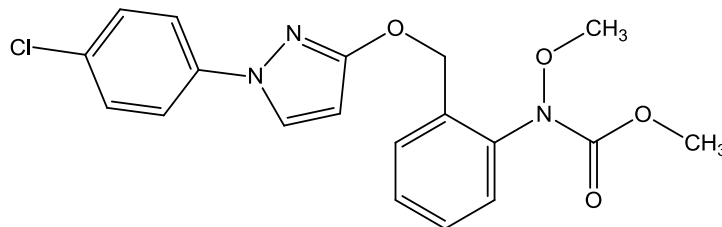


Figure 27. Chemical structure of pyraclostrobin.

Sulfasalazine

Sulfasalazine belongs to synthetic antibiotics sulphonamides that are widely used as veterinary drugs for prophylactic and therapeutic purposes.³⁰⁶ These antibiotics can be released to the environment via wastewater from animal housings,³⁰⁷ causing concern of widespread antibiotic resistant bacteria in the aquatic environment.³⁰⁸ Antibiotics are not currently covered by existing regulations on water quality but are definitively candidates for future regulation.^{309,310}

Conventional technique used to determine low levels of sulphonamides in water samples are based on LC-MS or LC-MS².³¹¹ Nonconventional techniques for sulphonamides determination are mainly applied to food samples and include immunoassays,¹⁴⁷ flow cytometric immunoassays.³¹²

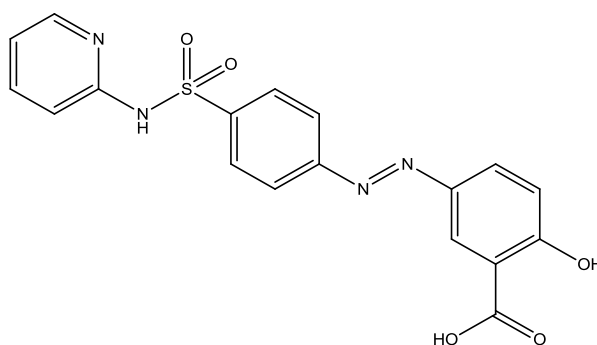


Figure 28. Chemical structure of sulfasalazine.

Triclosan

Triclosan, 5-chloro-2-(2,4-dichlorophenoxy)phenol is a broad spectrum antibacterial often used in personal care products such as soaps, deodorants, toothpastes to decrease bacterial contamination. Triclosan has been demonstrated to occur in river water samples in both North America and Europe. It undergoes bioconversion to methyl-triclosan (a more lipophilic compound), which has been demonstrated to bioaccumulate in fish.³¹³ The action of sunlight in river water has been reported to convert triclosan into dioxin derivatives³¹⁴ and raises the possibility of pharmacological dangers not envisioned when the compound was the originally utilized.

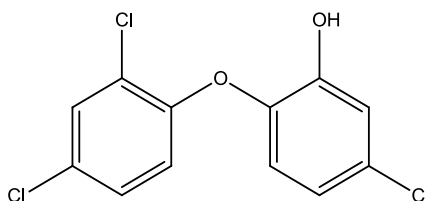


Figure 29. Chemical structure of triclosan

Considering the selected targets, and according to the EU pesticide database, the pesticides approved to be used in plant protection are: azoxystrobin, chlorpyrifos, diuron, forchlorfenuron, imidacloprid, malathion and pyraclostrobin. Pesticides not approved by current legislation are the following: alachlor, atrazine, diazinon, endosulfan, fenthion, pentachlorophenol and 2-(2,4,5-triphenoxypropionic) acid.

The biocide triclosan was banned in 2015 by European Chemical Agency (ECHA/BPC/066/2015), which states that this compound is toxic to the aquatic life and can possess endocrine disruptor properties. The EU ban on triclosan comes into effect since January 2017.

III
Materials
and
Methods

III Materials and Methods

3.1 Reagents

The analytical standards used in competitive assays were 2-(2,4,5 trichlorophenoxy)propionic acid, 3-phenoxybenzoic acid, 4-nitrophenol, alachlor, atrazine, diuron, endosulfan, imidacloprid, pentachlorophenol which were purchased from Sigma-Aldrich, chlorpyrifos, diazinon, fenthion and malathion were from Dr. Ehrenstorfer, azoxystrobin was from Syngenta AG (Basel, Switzerland), pyraclostrobin was from Riedel-de-Haen (Seelze, Germany) and forchlorfenuron from Fluka.

The stock solutions were prepared in dimethyl sulfoxide at 1.0 mg/mL.

For the preparation of coating conjugates the chemicals used for the hapten activation were: N,N'-dicyclohexylcarbodiimide (DCC), N-hydroxysuccinimide (NHS), N-acetylhomocysteine thiolactone (AHT), ovalbumin (OVA) purchased from Sigma-Aldrich. D-Salt™ Dextran Desalting Column which was used for the purification of the coating conjugates was from Thermo Scientific (Rockford, USA).

Gold nanoparticles ($\phi = 5-250$ nm) and aminated gold nanoparticles ($\phi = 5$ nm), bovine serum albumin (BSA) and human serum albumin (HSA) and Trizma base used for the preparation of gold conjugates, gold labelled anti-rabbit IgG antibody produced in goat and silver enhancer solutions (A and B) were from Sigma-Aldrich (Madrid, Spain). Gold nanorods were from Strem Chemicals (Newburyport, MA, USA). Thiol-PEG-acid ($M_w = 3073$ Da) was from Iris Biotech GmbH (Marktredwitz, Germany). 1-Ethyl-3-(3-dimethylaminopropyl)carbodiimide (EDC) was from Sigma Aldrich (Madrid, Spain). The antibody-antigen systems used in this thesis are listed in a Table 12. HiTrap Protein G HP column used to purify the polyclonal sera was purchased from GE Healthcare. DVD-R disks were purchased from CD Rohling-up GmbH, Saarbrücken, Germany.

Centrifugal filter devices used to exchange the buffer of monoclonal antibodies were from Merck Millipore (Cork, Ireland). All the buffers and solutions described above were prepared in deionized water and filtered through 0.45 μ m pore size disks.

Table 12. Systems studied for the multiplex immunoassay

#	Compound	Anti body	Coating conjugate	Reference
1	2-(2,4,5 trichlorophenoxy)propionic acid (TPA)	P	OVA-2,4-D	315
2	3-phenoxybenzoic acid (PBA)	P	OVA-3-PBA	206
3	4-nitrophenol (NPL)	P	OVA-4-NP	214
4	Alachlor (ALA)	P	OVA-metolachlor	146
5	Atrazine (ATZ)	P	OVA-2d	145
6	Azoxystrobin (AZB)	M	OVA-Azb6	316
7	Chlorpyrifos (CLP)	P	OVA-C5	252
8	Diazinon (DZN)	P	OVA- 7	258
9	Diuron (DIU)	P	OVA- MG-66B	150
10	Endosulfan (EDS)	M	OVA-CCD1	276
11	Fenthion (FNT)	P	OVA-F1	281
12	Forchlorfenuron (FCF)	M	OVA-s5	317
13	Imidacloprid (IMD)	M	OVA-1	149
14	Malathion (MLT)	P	OVA-M1	303
15	Pentachlorophenol (PCP)	P	OVA-PCP2	318
16	Pyraclostrobin (PYS)	M	OVA-PYo5	319
17	Sulfasalazine (SSZ)	P	OVA-S8	147
18	Triclosan (TCS)	P	OVA-T6	148

P: Polyclonal, M: Monoclonal

3.2 Instruments

A non-contact and quantitative liquid dispensing system was used for microarraying (AD 1500, BioDot, Inc., Irvine, CA).

For the characterization of gold conjugates a UV-vis spectrophotometer (Agilent 8453 UV-vis System) was used.

The protein concentration was determined using a NanoDrop 2000 (Thermo-Fisher, Wilmington, USA).

Zetasizer (Zetasizer Nano ZS) used to measure diameter of bare gold nanoparticles and their conjugates was from Malvern Instruments (Malvern, UK).

High frequency induction motor centrifuge (Medifriger BL-S 7001377) was from J.P. Selecta (Barcelona, España).

Fluorescence Spectrometer (LS 45) used to measure intrinsic fluorescence of the antibodies was from Perkin Elmer (Waltham, MA, USA).

3.3 Antibody purification

The sera were purified using a Protein G column. The column was coupled to UV-vis spectrophotometer to monitor the purification on-line. First, the column was equilibrated with 10 mL of phosphate buffered saline (PBS, 20 mM, pH 7.5). Then, 1.0 mL of immunized rabbit serum was added, at a flow rate of 0.7 mL/min, passing through the Protein G and allowing IgGs to bind to the immobilized protein G. Next, the column was washed with 12 mL of PBS to eliminate the unbound serum components. After that, 8.0 mL of elution buffer were added (0.1 M glycine, pH 2.7). The low-pH condition dissociates the antibody from the immobilized Protein G, and purified IgG population is recovered. The eluted solutions (1.0 mL) were collected in 1.5 mL polypropylene tubes containing 0.15 μ L of neutralizing buffer (Tris 1.0 M, pH 9.0).

Monoclonal antibodies were in saturated $(\text{NH}_4)_2\text{SO}_4$. For desalting it, centrifugal filter devices (100K) were used. The washing process was repeated 3 times. PBS 20 mM, pH 7.5 buffer was used to store the purified antibodies.

3.4 Preparation of coating conjugates

All the conjugates (exceptalachlor) were coupled covalently to carrier protein (OVA) by using the active ester method (Schneider 1992). The method consists in the activation of the free carboxylic group of the hapten and reaction with the amine groups of the carrier protein. For that, the carboxylic acid hapten (12 mg, 40 μ mol) was dissolved in 65 μ L of dry N,N-dimethylformamide (DMF). Then, 4.75 mg of N-hydroxysuccinimide (NHS) and 8.5 mg of N,N'-dicyclohexylcarbodiimide (DCC) were dissolved in 95 μ L and 170 μ L of DMF, respectively. Next, hapten solution was slowly mixed with NHS and DCC solutions. After 2 h of stirring at room temperature, the precipitated dicyclohexylurea was removed by centrifugation. Four different amounts of activated hapten (1.2 μ mol, 3 μ mol, 6 μ mol, 12 μ mol) made up to 100 μ L with DMF in order to prepare coating conjugate with different molar ratios (MR: 5.5; 14; 27; 55). The hapten solution was added slowly to 900 μ L of OVA solution (10 mg/mL; 0.22 μ mol) in 0.05 M sodium carbonate-bicarbonate buffer (pH 9.6). The reaction mixtures were stirred gently at room temperature for 2 h. After that time, the conjugates were centrifuged and the supernatant purified using desalting columns. The fractions were recollected in 20 mM PBS (pH 7.5) and the protein concentrations were measured using a NanoDrop spectrophotometer. The same procedure was employed for all haptens.

In case ofalachlor, sulfhydryl groups were introduced onto lysine residues of OVA with the thiolating agent N-acetylhomocysteine thiolactone (AHT), following the previously described

method.²²³ The protein (30 mg of OVA, 0.67 μmol) and 25 molar equivalents of AHT were dissolved in water (860 μL) at 0 $^{\circ}\text{C}$, to which metolachlor (25 equiv) dissolved in DMF (140 μL) was slowly added. Sodium carbonate-bicarbonate buffer (1.0 M, pH 11) was then added to adjust to pH 11, and the reaction mixture was stirred at 0 $^{\circ}\text{C}$ for 15 min. After 2 h of additional stirring at 50 $^{\circ}\text{C}$, the reaction mixture was neutralized and the metolachlor-protein conjugate was purified by desalting column. The fractions were collected in 20 mM PBS (pH 7.5) and the protein concentration was measured spectrophotometrically. Finally, the conjugates were stored frozen at -20 $^{\circ}\text{C}$ until use.

3.5 Gold colloid titration procedure

Colloid gold nanoparticles of different sizes (5-250 nm) were used for conjugation with purified polyclonal and monoclonal antibodies. Before conjugation, a titration experiment, to establish the minimum amount of Ab needed to saturate and stabilize colloidal gold solutions, was performed. As the adsorption is maximally achieved at, or around a pH close to the isoelectric point (pI) of the protein, the optimal pH conditions were optimized as well. The titration of colloidal gold solution was performed using 96-well plates. To each well 4 μL of buffer stock solutions (0.1 M sodium carbonate/bicarbonate (CB), pH 9.6; 0.1 M phosphate buffer (PB) pH 6.0; 0.1 M Tris, pH 8.5) were added to obtain a pH gradient. Next, 100 μL of gold nanoparticles stock to each well were added. The solution was mixed well by pipetting up and down several times. Afterwards, 2.0 μL of IgG dilutions (0-3 mg/mL) were added to each well, then mixed and incubated for 20 min. The plate was incubated on a shaker for 15 min at room temperature. Subsequently, 100 μL of 10 % NaCl were added to each well. The solution was incubated on a shaker for 30 min. Following that time, the absorbance at SPR maximum for each of AuNPs and 690 nm was measured using a UV/vis spectrophotometer. The ratio of absorbance at resonance wavelength over the absorbance at 690 nm to get a measure of aggregation was calculated. The optimal pH and protein concentration is selected by the wells where no significant aggregation is induced upon addition of NaCl as measured by an increased absorption at 690 nm and reduced absorbance at SPR max. The wells that have optimal reaction conditions were easily seen by naked eye since no major change in colour was observed.

3.6 Preparation of antibody-nanogold conjugates (Ab-AuNPs)

The following general conjugation protocol shown in Figure 30 was employed for the conjugation of proteins onto colloidal gold nanoparticles (5-250 nm). The pH of the colloidal gold solution (OD = 1) was 8.5 after the addition of few drops of 0.1 M Tris buffer, pH 8.5.

For conjugation, the optimal concentration of each antibody (10-100 μg) was diluted in 20 mM Tris buffer (pH 8.5) to get 100 μL of solution and then mixed dropwise with 1 mL of colloidal gold particles in a glass vial with rapid stirring. After 30 min, 100 μL of 10 % BSA was added for blocking residual gold surface and the mixture was incubated for another 30 min at room temperature. The mixture was then centrifuged (Table 13) at 4 °C. The pellet was resuspended in 20 mM Tris buffer (pH 8.5), centrifuged once again to remove free unconjugated antibody and the pellet dispersed up to 100 μL of pH 8.5 Tris 20 mM containing 1% BSA. The colloidal solution (OD \cong 10) was stored at 4 °C for further experiments.

The same procedure was employed for the preparation of highly concentrated gold conjugates with slight modifications. The initial volume was 5 mL (OD = 1) and the final 100 μL (OD \cong 50).

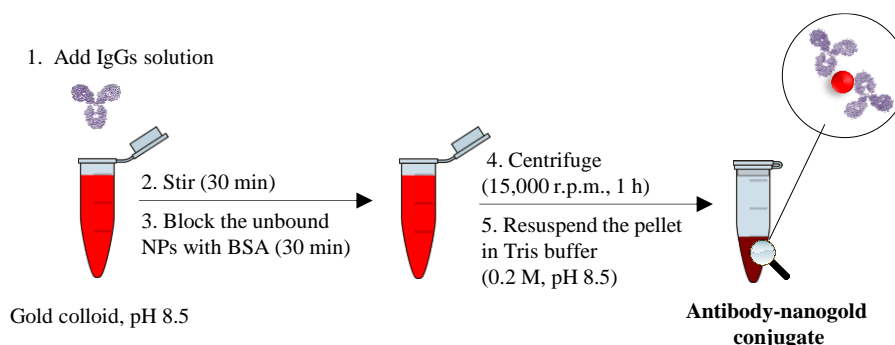


Figure 30. Antibody gold nanoparticles conjugation protocol.

Table 13. Centrifugation conditions for all studied nanoparticle sizes

Nanoparticle (nm)	Rpm	Rcf	Time (min)
5	15,000	27,670	60
10	12,000	17,700	30
20	10,000	12,290	20
50	4000	1960	20
100	2000	490	20
250	1000	120	20

The conjugates were characterized by UV-vis spectrophotometry and by Dynamic Light Scattering (DLS) and Z-potential measurements.

For UV/VIS measurements, the UV-vis spectrophotometer was used. As blanks, Milli-Q water was used for gold colloid and Tris buffer used for the gold conjugates. Gold nanoparticle solutions were monitored by measuring gold solution with: a) no antibody, b) after incubation with antibody and c) after centrifugation and re-suspension of the conjugates in storage buffer.

A Malvern Zetasizer Nano ZS DLS equipment (Malvern Instruments Ltd., Worcestershire, UK) was used to conduct all DLS measurements. The DLS system is equipped with a 633 nm He-Ne laser and an avalanche photodiode detector configured to collect backscattered light at 173°. The zeta cell and caps were cleaned with Milli-Q water. Seventy five microliters of sample was loaded into the disposable ζ -potential cuvette. The sample was held at 25 °C by a temperature controlled sample holder and allowed to equilibrate for 120 s prior to analysis. Each size measurement was determined from 10-15 runs, 10 s each. Each sample was analysed in triplicate to calculate an average and standard deviation. All DLS data were collected and analysed using Malvern Zetasizer 7.01 software.

3.7 Preparation of antibody-gold nanorod conjugates (Ab-AuNRs)

The general conjugation protocol described by Li et al.³²⁰ with slight modifications (Figure 31) was used for the conjugation of antibodies with gold nanorods (OD = 50, $\epsilon = 1.55 \cdot 10^{10}$; 40-80 nm). For anionic polymer stabilization, the CTAB was exchanged by thiolated PEG with carboxylic end. For that, 10 mL of MES buffer (0.1 M, pH 5.5), 1 mL of PEG solution (20 mg/mL) and 4 mL of gold nanorods were mixed together and the solution was sonicated for 30 min at 30 °C. The temperature was then increased to 55 °C and the nanorods dispersion was further sonicated for 60 min to enhance the ligand exchange process. Then the solution was incubated at 30 °C overnight. Afterwards the nanorods were centrifuged for 20 min. (10,000 rpm, 30 °C), the supernatant discarded and the pellet resuspended in water. The washing step was repeated once again and the nanorods resuspended in 200 μ L of water.

Once the PEGylating was finished, carboxylic groups were activated using carbodiimide chemistry. For that, 50 μ L of NHS solution (100 mg/mL in 0.1 M MES, pH 5.5), 50 μ L of MES buffer (0.1 M, pH 5.5), 206 μ L of water, 100 μ L of EDC solution (100 mg/mL in H₂O) and 94 μ L of PEGylated gold nanorods (OD = 800) were mixed and incubated at room temperature during one hour. After that time, the solution was centrifuged (10 min, 10,000 rpm, RT) to remove excess of the reagents. The pellet was suspended in MES buffer (20 mM, pH 5.5) and

centrifuged once again. Next, the pellet was resuspended in 25 μL of phosphate buffer (0.1 M, pH 8.0). Once the activation step was completed, 25 μL of gold nanorods, 75 μL of PBS buffer (10 mM, pH 8.0) and 50 μL of antibody solution (0.1 mg/mL) were mixed and incubated during 2 hours at room temperature. After that, to passivate remaining activated carboxylic groups, 5 μL of ethanolamine (10 mg/mL) were added. After 45 min, the mixture was washed three times with 10 mM PBS. As-prepared antibody-gold nanorods conjugates were stored at 4 $^{\circ}\text{C}$ for further experiments.

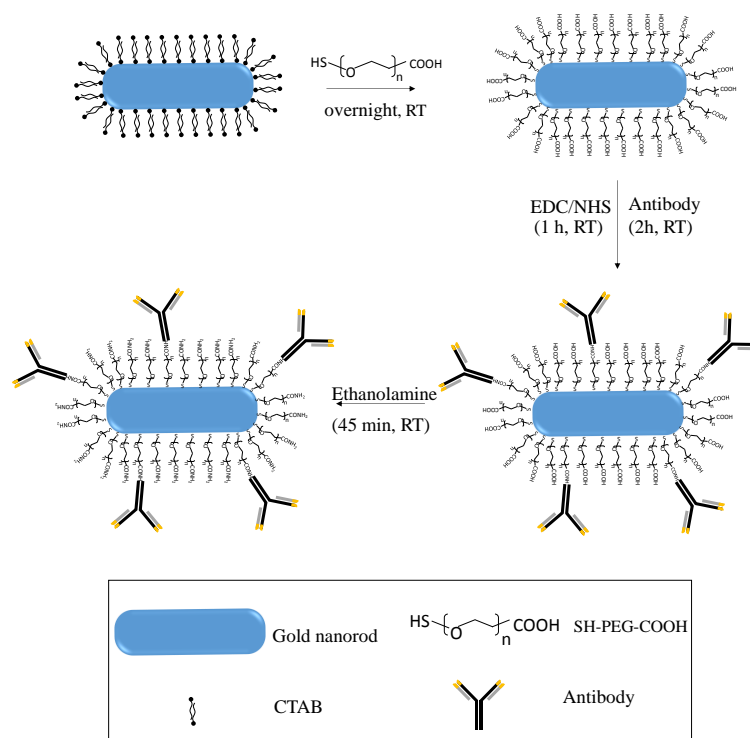


Figure 31. Antibody gold nanorods conjugation protocol.

3.8 Preparation of antigen-nanogold tracers (OVA-H-AuNPs)

The following general conjugation protocol shown in Figure 32 was employed for the conjugation of coating antigens onto colloidal gold nanoparticles. The pH of the colloidal gold solution was adjusted to 8.5 as described in section 3.6. For conjugation, the optimal concentration of each antigen (OVA-H) was diluted in 100 μL Tris buffer (pH 8.5) and then mixed dropwise with 1 mL of colloidal gold particles in a glass vial with rapid stirring. After 30 min, 100 μL of 10% HSA was added for blocking residual surface and the mixture incubated for another 30 min at room temperature. The mixture was then centrifuged (Table 13), and the supernatant discarded. The pellet was resuspended in 20 mM Tris buffer (pH 8.5), centrifuged

once again and then it was dispersed up to 100 μL of pH 8.5 Tris 20 mM containing 1% HSA. The colloidal solution was stored at 4 $^{\circ}\text{C}$ for further experiments.

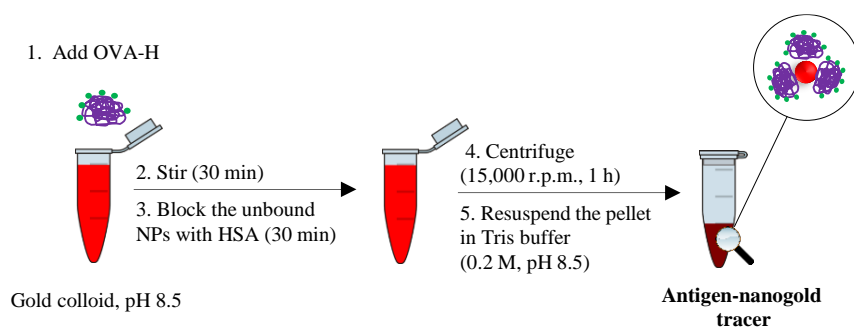


Figure 32. Coating antigen gold nanoparticles conjugation protocol.

For characterization of antigen-nanogold tracers, UV-vis measurements were carried out using UV-vis spectrophotometer. As the blank, Milli-Q water was used for gold colloid and 20 mM Tris buffer (pH 8.5) used for the gold conjugates. Gold nanoparticle solutions were monitored by measuring gold solution with: a) no coating antigen, b) after incubation with coating antigen and c) after centrifugation and re-suspension of the conjugates in storage buffer.

3.9 Preparation of hapten-nanogold tracers (H-AuNPs)

The following general conjugation protocol shown in Figure 33 was used for the conjugation of haptens with aminated gold nanoparticles. The conjugates used in this study were prepared using the active ester method. The reaction was performed in two steps. The first consisted in activation of the free carboxylic group of the hapten molecule with DCC and NHS. Briefly, 15 mg of target hapten were dissolved in 200 μL of DMF and 150 μL of DCC and NHS (final concentration was 30 mg/mL) were added slowly to hapten solution. The mixture was left to incubate for 2 h at room temperature. After that time, the solution was centrifuged to remove by-products (O-acylisourea intermediate) and supernatant used in the second step. Next, the pH of 20 μL of aminated gold nanoparticle solution adjusted to 12.0 with 10 μL of 0.1 M sodium phosphate buffer (pH 12.0). Then, the gold nanoparticles suspension was mixed with 20 μL of activated hapten and gently mixed for 2 h at room temperature. After that time, the solution was washed three times with PBS-T, pH 7.5 to remove unreacted compounds.

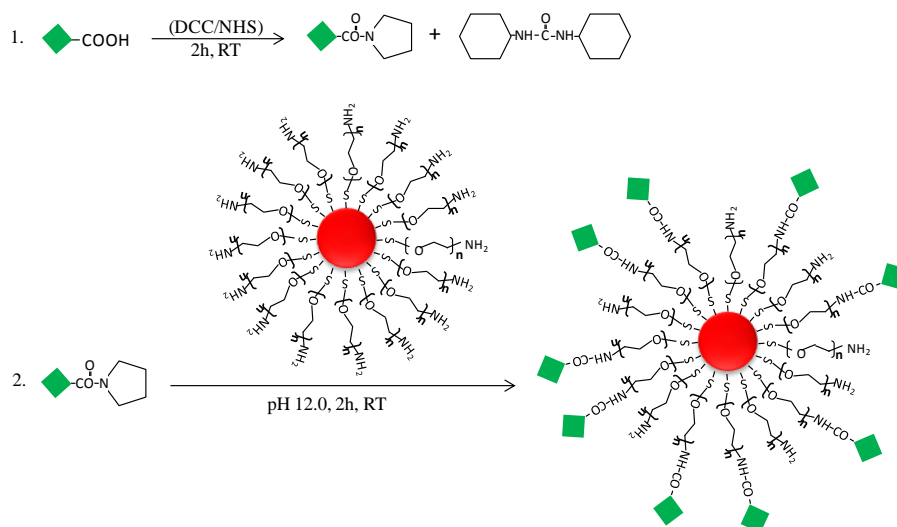


Figure 33. Scheme of the conjugation protocol for the preparation of hapten-nanogold tracers.

3.10 Microarraying

The coating conjugates and antibodies diluted in 0.1 M sodium carbonate/bicarbonate buffer were dispensed in a 384-well plate (50 μ L/well) and transferred to the disk (50 nL) in microarray format with a noncontact printing device (AD 1500 Biotdot, Inc., Irvine, CA)(Figure 34).

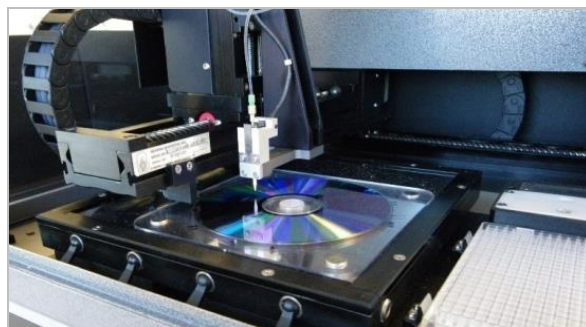


Figure 34. Non-contact printer used for microarraying.

The optimization of all the immunoassays was performed using a design shown in Figure 35. The array layout consisted in 40 arrays of 3 \times 3 spots each printed on the polycarbonate surface of the DVD-R.

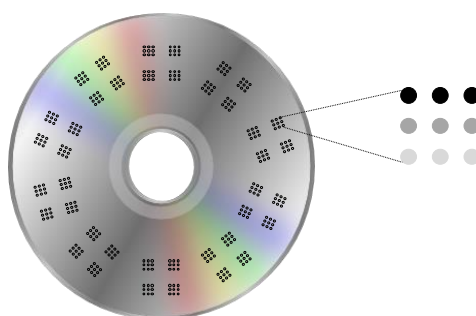


Figure 35. DVD microarray layout used for the optimization steps.

The final layout used for the multiplexed immunoassay is presented in Figure 36. The array layout consists in twenty four arrays of 7×7 spots (four replicates for each system, eight spots as positive control and one spot of negative control) printed on the polycarbonate surface of the DVD-R. Before performing the assay, disks were incubated for 16 h at 4 °C and after that washed with PBS-T and water.

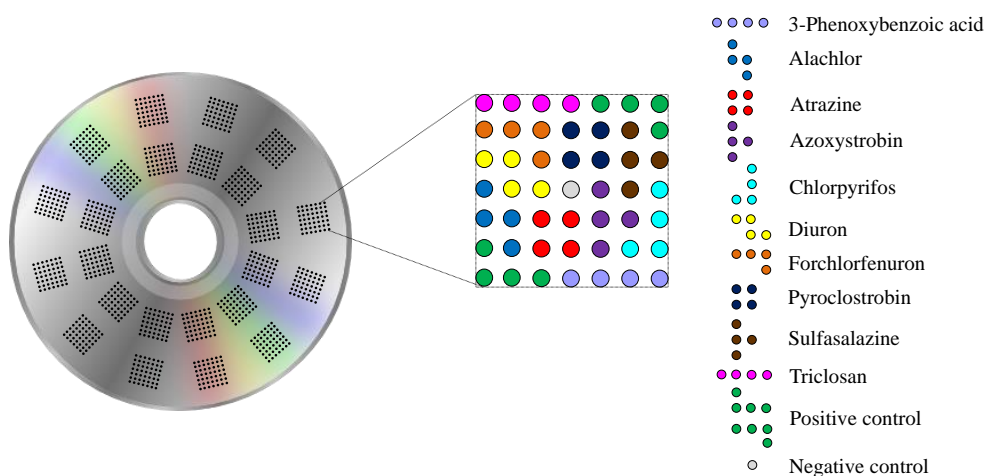


Figure 36. DVD microarray layout.

3.11 Microimmunoassay protocols

All of the described microimmunoassays were based on the principle of direct competitive format.

3.11.1 Two-step antigen-coated microimmunoassay using antibody-nanogold conjugates

The main steps of the immunoassay that was developed are schematically outlined in Figure 37. First, coating conjugate solutions, positive and negative controls were arrayed as described in section 3.11. After 16 h at 4 °C, the disk was thoroughly washed with PBS-T, rinsed with deionized water, and dried by centrifugation at 800 rpm.

For single-target assay optimization, 20 μL of antibody-gold nanoparticles conjugate solution in PBS-T, with or without analyte, was dispensed onto the array. After 25 min incubation at room temperature, the disk was washed with PBS-T and deionized water. The immunoreaction was developed by dispensing 1.0 mL of silver enhancer solution onto the disk and distributed using a dummy plastic surface. Finally, the reaction was stopped after 10 min by washing the disk with water.

For multiplexed assays, 20 μL of mixed antibody-gold nanoparticles conjugate solution (cocktail) in PBS-T, with or without analyte, were dispensed onto the array. Next, the immunoassay was performed as described above.

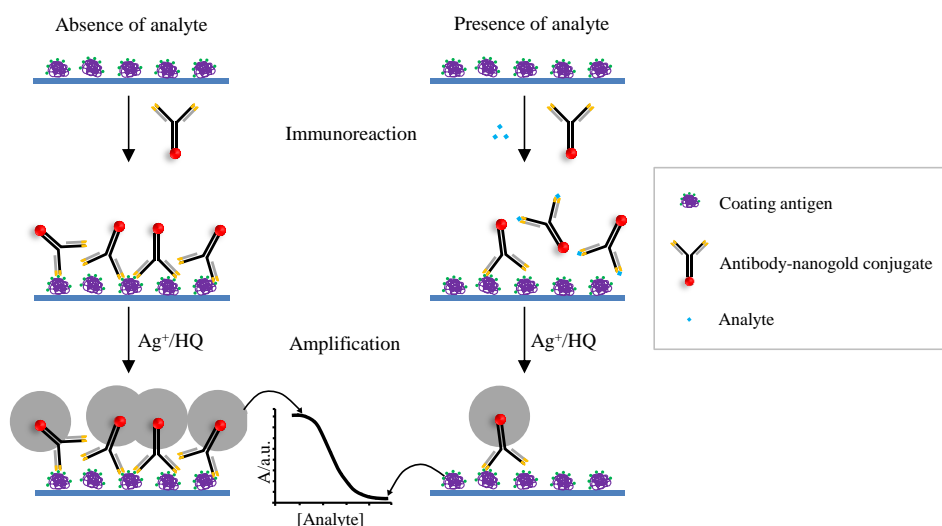


Figure 37. Scheme of the two step antigen-coated microimmunoassay using antibody-nanogold conjugate.

3.11.2 One-step antigen-coated microimmunoassay using antibody-nanogold conjugates

The main steps of the developed one-step immunoassay are outlined in Figure 38. Six different antibody-gold nanoparticles conjugates which varied according to size of gold colloid (between 5, 10, 20, 50, 100 and 250 nm) were used. For single-target assay optimization, different dilutions (without diluting, 1/2 to 1/50) for all conjugates were tested. The following steps were the same as described in section 3.12.1. Next, 20 μL of antibody-gold nanoparticles conjugate solution in PBS-T, with or without analyte, was dispensed onto the array. After 25 min incubation at room temperature, the disk was washed with deionized water. No amplification step was performed.

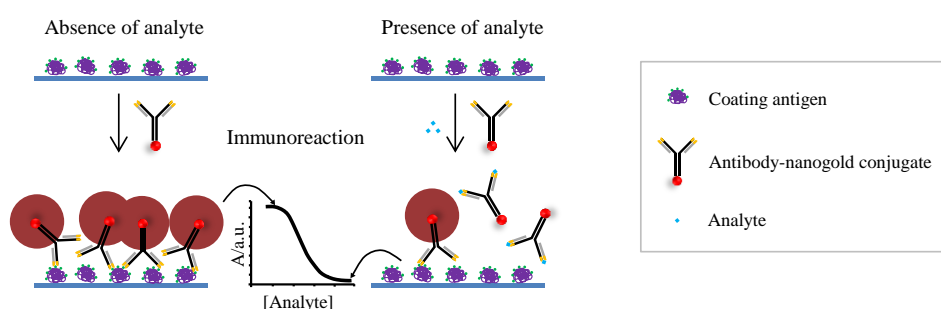


Figure 38. Scheme of one step antigen-coated microimmunoassay using antibody-nanogold conjugates.

3.11.3 One-step antigen-coated microimmunoassay using antibody-gold nanorod conjugates

First, coating conjugate solution was arrayed onto the disk. After 16 h at 4 $^{\circ}\text{C}$, the disk was thoroughly washed with PBS-T, rinsed with deionized water, and dried by centrifugation at 800 rpm.

For single-target assay optimization, the steps were performed as it is described in section 3.12.1, but using gold nanorod conjugates.

The main steps of the developed immunoassay are outlined in Figure 39.

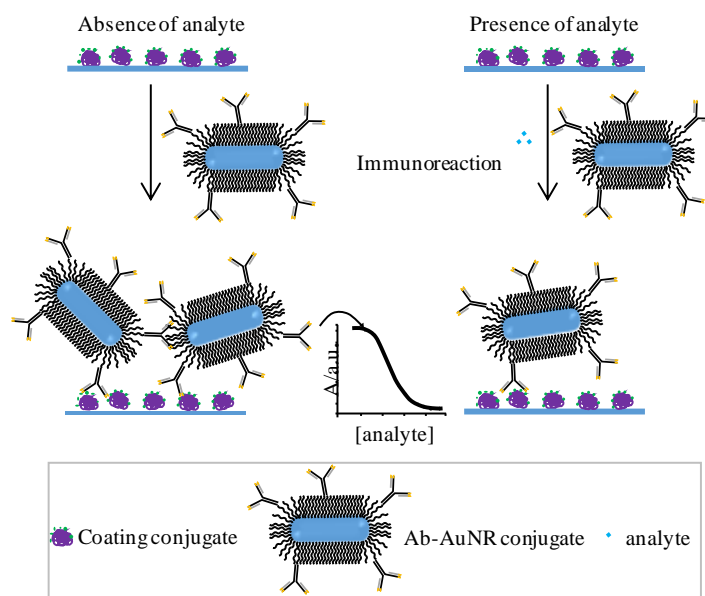


Figure 39. Scheme of the one step microimmunoassay with antibody-gold nanorod conjugate.

3.11.4 Two-step antibody-coated microimmunoassay using antigen-nanogold tracers

For the antibody-coated format, antigen-nanogold tracers were used as detector species. The main steps of the developed immunoassay are outlined in Figure 40. The immunoassay was conducted as described in section 3.12.1.

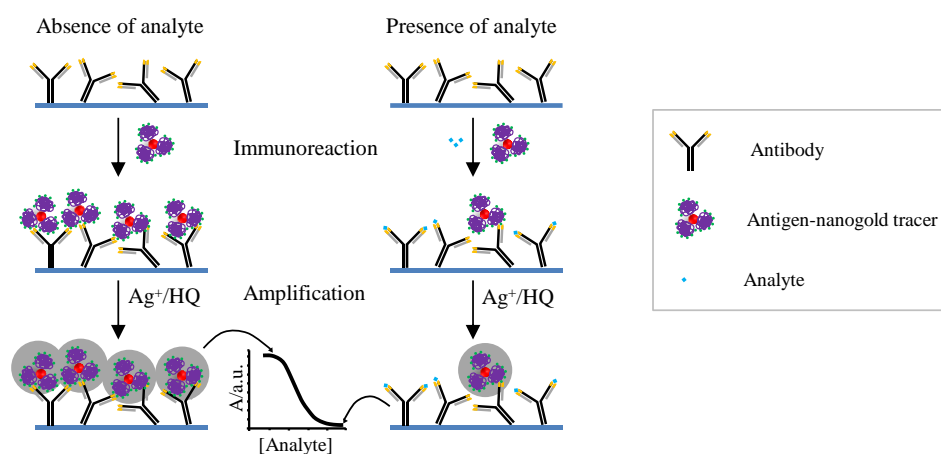


Figure 40. Scheme of the antibody-coated two-step micro immunoassay using antigen-nanogold tracer.

3.11.5 Two-step antibody-coated microimmunoassay using hapten-nanogold tracers

The main steps of the developed antibody-coated format are outlined in Figure 41. For detection, hapten-gold conjugates (AuNP-NH-H) were used as tracers. First, microarraying was performed as it is explained in section 3.11 and then immunoassay steps, using gold-hapten tracers, were performed as it is described in section 3.12.1.

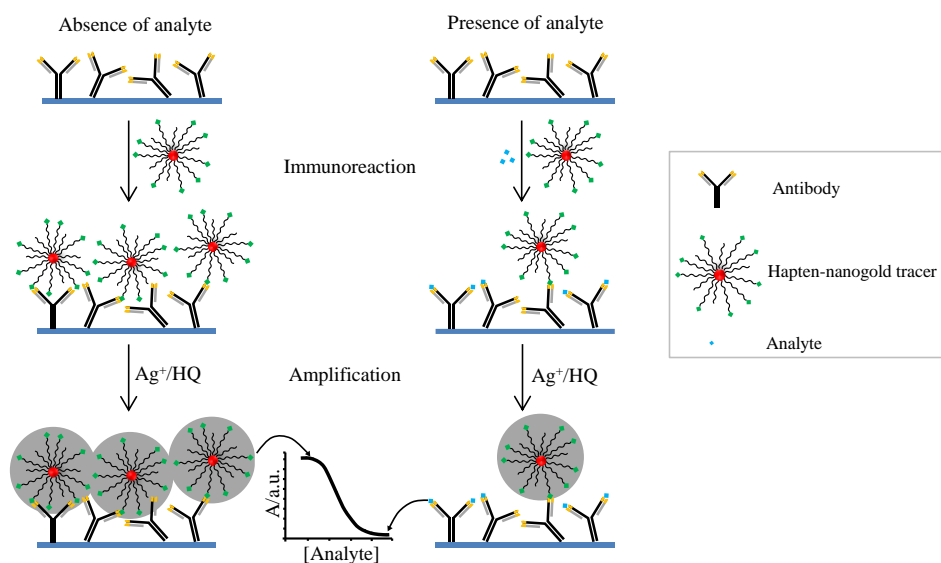


Figure 41. Scheme of two-step antibody-coated immunoassay using hapten-nanogold tracers.

3.11.6 Immunocapture microimmunoassay

The main steps of the immunocapture procedure are outlined in Figure 42.

First, 1.0 μL of antibody-gold nanoparticles conjugate (5nm) was added to 500 μL of sample, and left to incubate for 10 min at room temperature. After that time, the sample was centrifuged for 20 min at 15,000 rpm at 4 $^{\circ}\text{C}$. The supernatant was discarded and the pellet resuspended in 25 μL of PBS-T. Next, 20 μL of this suspension sample was dispensed onto the disk and incubated for 25 min. Later, the assay was developed as it is described in two-step immunoassay format.

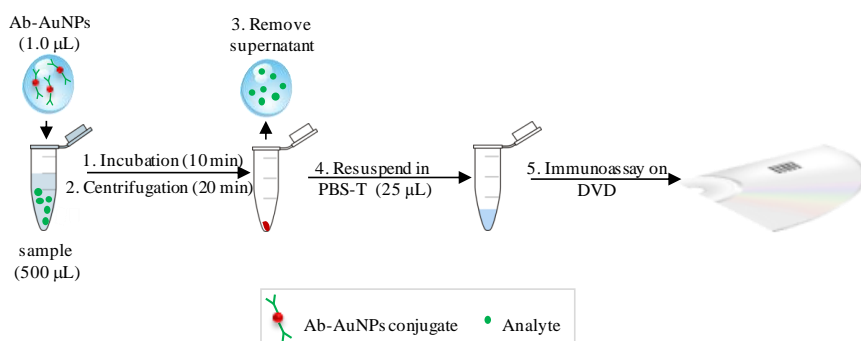


Figure 42. Scheme of the immunocapture procedure.

3.12 Analysis of water samples

The analysis of natural water samples was performed applying two-step antigen-coated microimmunoassay using antibody-nanogold conjugates (Figure 37). Before analysis, the natural water samples were conditioned with PBST (9 parts by volume of water mixture and one part by volume of 10-fold PBST). All water samples were targeted analytes free. Samples were spiked with targeted compounds at different levels, within the linearity range and determined directly. Each sample was analysed in duplicate in different disk (8 replicate spots measured per sample). The standard curves used for quantification, were the mean of 6 different plots, obtained in different days. Finally, the disk was read by the DVD drive giving quantitative results.

3.13 Compact disk scanning and data acquisition

The DVD drive used in this study was from LG Electronics Inc. (Englewood Cliffs, NJ), which was controlled by custom software (BioDisk), running on a personal computer and connected to it through a USB 2.0 universal serial bus interface. In a standard DVD driver, the disk is read by measuring the change in reflection of a polarized red laser ($\lambda = 650 \text{ nm}$). When DVD is used as a sensing platform, a recognition event that occurs on the surface (formation of an insoluble precipitate) modulates the DVD reading process. The insoluble precipitates on the surface of the DVD, interferes with the optical reflection of the metalized polycarbonate layer, and therein creates error in reading digital data from an internal layer of the DVD.

The reading mechanism of a DVD is presented in Figure 43. Let's consider two insoluble precipitate of different optical density - light grey (A) and dark grey (B). When the laser hits the light grey insoluble precipitate, most of the light is reflected back to the photodiode, as the reflection properties of the polycarbonate surface are partially modified. However, some portion of the light is scattered, thus the laser beam intensity that reaches the photodiode of the pickup is

attenuated. On the contrary, the light when laser strikes the dark grey insoluble precipitate is mostly scattered, as the optical properties of the DVD surface are drastically different. Therefore, only small portion of the incoming light reaches the photodiode, thus the reflected light intensity decreases.

The analogue signals are directly acquired from the photodiode of the DVD drive, being related to optical density of the reaction product which is inversely proportional to analyte concentration. To scan the surface of the DVD completely (10 min at 4× speed), the software simulates the writing process of a 3.8 GB size file. During the disk scanning, only signals coming from selected areas are processed for digitization, stored in the computer and convoluted into an image. BioDisk software was written in Visual C++ to control the optical disk drive, the data acquisition board (sampling rate, detector gain, spatial resolution, and scanning speed) and identifies spots with $S/N \geq 3$. To calculate the mean signal intensity of the spot, the program averages data points from a circular area of 150 μm in diameter.

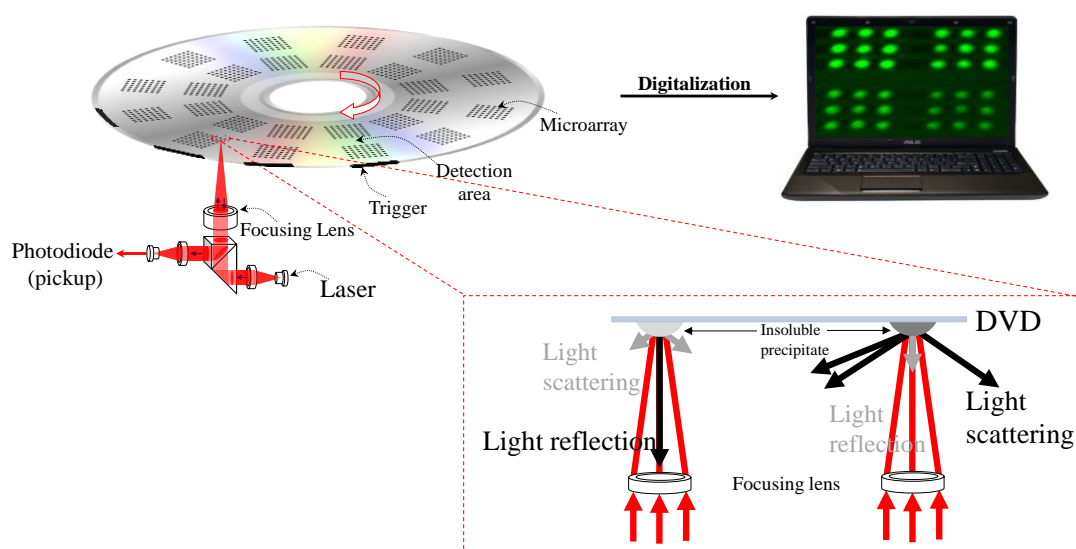


Figure 43. Scheme of the detection system.

IV
Results
and
Discussion

IV Results and Discussion

The development of multiplex screening methods based on immunorecognition event faces many problems, mainly those related to sensitivity and selectivity. Therefore, one of the crucial steps is the selection of the immunoreagents (coating conjugate, antibody, tracers, etc.), assay format (conjugate or antibody coated) and procedure (direct or indirect), incubation time, etc. In this section, the development of multiplex immunoassays will be discussed. Different tasks had to be performed in order to select the optimal parameters. First, the purification of the antibodies was conducted as it was necessary for the conjugation with gold nanoparticles. In the bioconjugation step, two important parameters were optimized, such as the pH and antibody concentration. Different sized gold nanoparticles were tested, in order to select the optimal size in terms of the signal enhancement, sensitivity and antibody amount used. Once the bioconjugates were selected, different assay formats (antibody-based, coating-antigen-based) were compared in terms of selectivity, sensitivity and reproducibility. Also, the assays performances with signal enhancement and without any amplification were evaluated. The best immunoassay was selected for developing the multiplexed assay. Finally, representative water samples were analysed to confirm the applicability of the multi-residue assay.

4.1 Purification of antibodies

All polyclonal sera were purified by affinity chromatography based on immunospecific protein G capturing IgGs column. The purification process was monitored by UV/vis spectrophotometry as described in the Materials and Methods section. Binding to protein G takes place at neutral pH, so phosphate buffered saline, pH 7.5 is used as the loading buffer. As the sample is loaded onto the column an intensive peak is observed (Figure 44). While the proteins that not bind to protein G are slowly passing through the column the peak decreases.

Elution of bound IgG is accomplished by running an acidic elution buffer. The low-pH dissociates the antibody from the immobilized protein G, and the antibodies are recovered. The use of protein G results in purification of general immunoglobulin from a crude sample. Depending on the sample source, antigen-specific antibody may account for only a small portion of the total immunoglobulin in the sample.

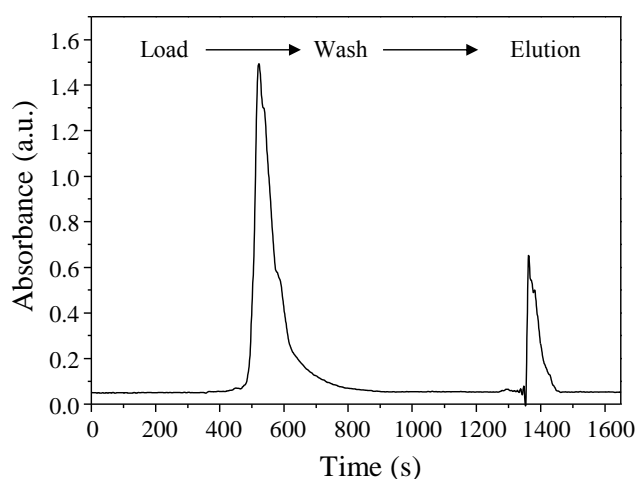


Figure 44. Elution profile for the purification of anti-atrazine serum using protein G column.

The concentrations of the purified antibodies in each fraction were determined by spectrophotometry in triplicate. For example for atrazine, the protein content in fractions 1 and 2 was negligible. The highest concentration was obtained in fractions 3 and 4 (0.82 and 0.78 mg/mL), which corresponds to the maximum in the peak as it is shown Figure 44. These two fractions were mixed together and the purified antibody (0.80 mg/mL) used for further experiments. For fractions 5 and 6 the protein concentrations were lower (0.62 and 0.40 mg/mL), which corresponds to the decreasing fraction of the elution peak.

Similarly, for 3-phenoxybenzoic acid the highest protein concentration was found in fractions 3 and 4, being 4.44 mg/mL and 3.19 mg/mL, respectively. Again, those two fractions were combined and final concentration was 3.82 mg/mL. The concentration in fractions 5 and 6 was much lower (1.59 and 1.00 mg/mL).

Also for diuron, the fractions 3 and 4 resulted in the highest protein amount. For this analyte the concentrations were 2.31 and 1.88 mg/mL in fractions 3 and 4, respectively. In fractions 5 and 6, the concentrations were lower, being 0.94 and 0.59 mg/mL, respectively. Also, in this case, fractions 3 and 4 were combined and 2.00 mg/ml solution was obtained.

The same procedure was applied for all studied antibodies. In all cases, the highest amount of protein was found in fractions 3 and 4. Usually the concentration varied between 1.0 and 4.0 mg/mL. Those fractions with the highest protein content were combined, concentration measured again and used for preparation of antibody nanogold conjugates. Antibody solutions were stored at -20 °C in small aliquots to avoid freeze/thaw cycles.

4.2 Characterization of gold nanoparticles

The intense colour of colloidal noble metal particles is due to the coherent motion of the conduction-band electrons caused by interaction with an electromagnetic field. The width of the surface plasmon absorption depends on the size and shape of the metal nanoparticle as well as on the dielectric constant of the metal itself and of the medium surrounding it.³²¹ The plasmon resonance is strongest and shifted into the visible part of the electromagnetic spectrum, which is the reason why the noble metals have historically fascinated scientists dating back as early as Faraday.

Figure 45A shows the absorption spectra of the studied colloidal AuNPs (OD = 1.0). For the 5 nm nanoparticles, the SPR wavelength value is the lowest, being 513 nm. All the SPR band values are summarized in Figure 45B. As the nanoparticles get bigger, the plasmon red shifts, therefore for 10 nm the peak of the SPR is at 517 nm, whereas for 20 nm it was found at 522 nm. When an electromagnetic wave interacts with a small sphere, a series of multipole oscillations (dipole, quadrupole, etc.) appear, which depend on the particle radius. For nanoparticles much smaller than the wavelength (< 20 nm) of the interacting light only the dipole oscillation contributes significantly to the extinction cross section, thus the band appears at lower wavelengths.

As the inset representing the colours of selected nanoparticles shows 5, 10 and 20 nm spherical gold nanoparticles are red. As it can be observed, the colour changes significantly for 50 nm gold nanoparticles turning into pink. The colour is the result of higher SPR value (535 nm), comparing to the smaller nanoparticles.

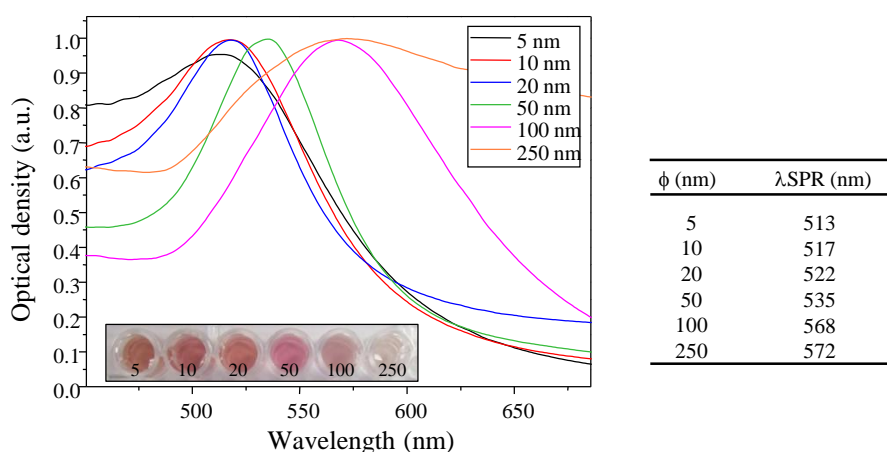


Figure 45. Surface plasmon resonance bands for studied nanoparticles. (A) Surface plasmon resonance bands for all studied AuNPs; (B) Peak SPR values.

Not only is light strongly absorbed by the plasmons, it is also Rayleigh (elastically) scattered by them, and as the particle gets larger, a larger proportion of the outgoing light is scattered, compared with that absorbed. This phenomenon is clearly observed in the inset of Figure 45 for 100 and 250 nm gold nanoparticles. These particles are opaque due to the larger portion of light that is being scattered compared with that absorbed.

The first proof of IgGs conjugation to the AuNPs, was the observation of a specific optical change in UV-visible spectrum (200-800 nm) of gold nanoparticles. UV-Vis measurements can be used to indicate adsorption of proteins onto gold with a change in absorbance peak for the nanoparticle.

As it was explained previously, due to the surface plasmon resonance of colloidal gold a strong absorbance peak between 515–570 nm is observed with λ_{max} depending on the size of the nanoparticles. As it can be seen in Figure 46, for the 5 nm colloidal gold the λ_{max} value is at 516 nm. Because nanoparticles have a high surface area to volume ratio, the plasmon frequency is exquisitely sensitive to the dielectric (refractive index) nature of its interface with the local medium. Any change to the surroundings of these particles (surface modification, aggregation, medium refractive index, etc.) lead to the shift of the plasmon band towards red. Therefore, upon addition of IgGs the plasmon band shifts 4 nm (520 nm), indicating an interaction between the gold nanoparticles and the protein and a modification of the refractive index due to the coating protein on the surface of the gold nanoparticles. After addition of BSA, the absorption peak shifts to 522 nm, showing that unreacted sites were fully blocked.

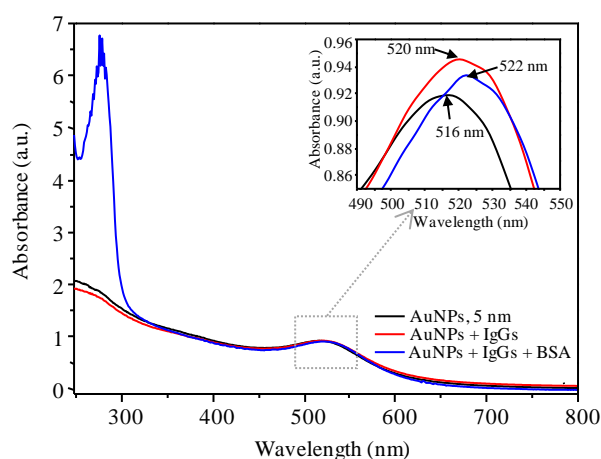


Figure 46. UV/VIS spectra of colloidal gold (5 nm) and the antibody conjugate. The inset graph shows the λ_{max} for the gold absorption peaks and the resulting red-shift upon antibody conjugation. The peak at 280 nm corresponds to protein absorption.

4.3 Optimization of antibody-gold nanoparticles conjugation

In order to prepare good quality, stable protein-gold nanoparticles several parameters should be considered. These are the isoelectric point (pI) of the protein, the pH of the reaction, the concentration of protein loaded onto the colloids, and the stability of the colloids. The optimization parameters are discussed below.

Once these nanoparticles are successfully conjugated with a layer of proteins such as antibodies, the nanoparticles can be stabilized in high salt content buffer solutions as it is schematically shown in Figure 47. The prevention of aggregation during the conjugation reaction is highly desirable, as the presence of aggregates and poor conjugates will result in a reduction of immunoactivity and poor performance of the assays. Hence, prior to immobilising the antibodies onto the nanoparticles, preliminary titrations were performed to determine the minimum amount of protein required to stabilize the gold colloids thus minimize the aggregation of the nanoparticles.

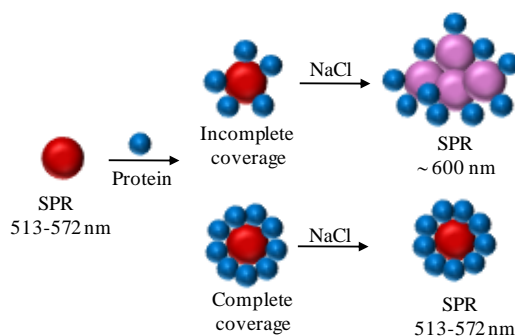


Figure 47. Scheme of the aggregation test.

Titration of the gold colloidal solution was performed through serial dilution of antibody employing the protocol outlined in *Materials and Methods* section. Where there was a sufficient amount of protein in the well the gold colloidal solution did not aggregate and therefore no major change in colour was observed. On the contrary, wells where there was insufficient protein, flocculation of the nanoparticles occurred which gave a characteristic colour change from red to blue/purple.

In Figure 48, the experimental minimal antibody concentration needed to fully cover the surface of gold nanoparticles, preventing from aggregation in high salt environment, is shown. For 5 nm nanoparticles the minimum amount of protein needed is 30 $\mu\text{g/mL}$, being the highest protein concentration used among all studied nanoparticle sizes. As the nanoparticles get bigger the amount of protein required to avoid aggregation decreases. For example, 10 nm AuNPs require only 20 $\mu\text{g/mL}$ of protein. For 20 nm AuNPs the minimum antibody concentration is remarkably

lower ($6 \mu\text{g/mL}$) being 5 times less when compared to 5 nm AuNPs. Increasing 10 times the size of 5 nm AuNPs, results in protein concentration of $2.5 \mu\text{g/mL}$ required to stabilize such gold suspension.

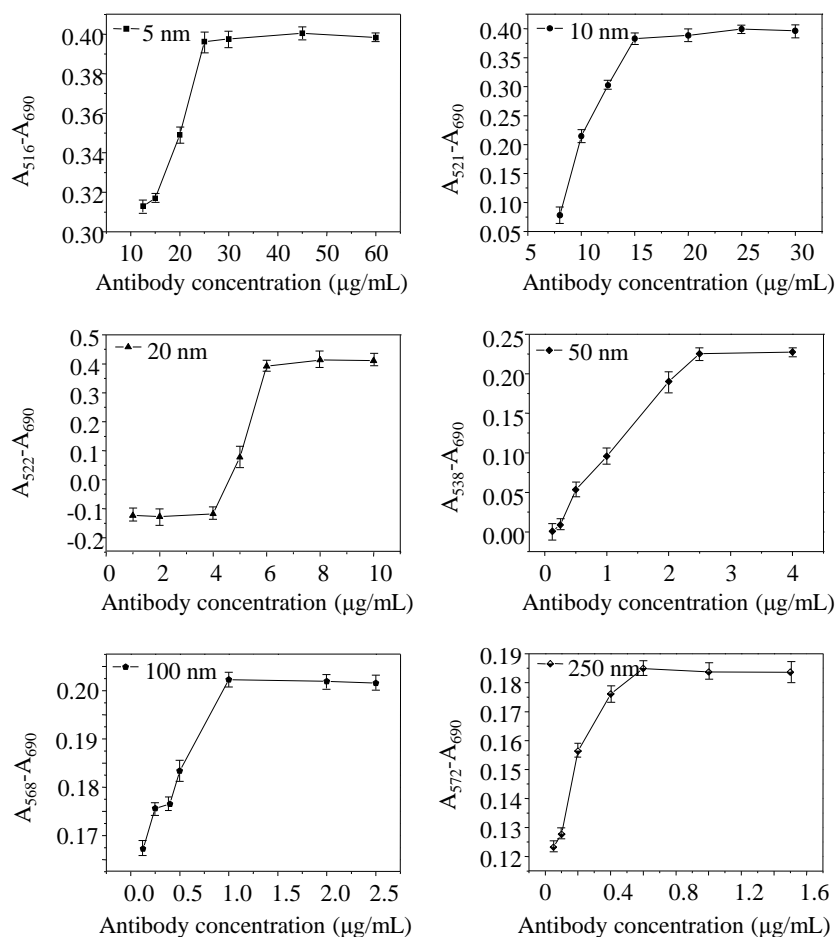


Figure 48. Gold aggregation tests performed to evaluate the minimal antibody concentration required to avoid aggregation of gold nanoparticles of different size.

For the biggest gold nanoparticles used in this work, 100 and 250 nm in diameter, the amount of protein is much lower when compared to other smaller AuNPs. As it can be observed from the Figure 48, for 100 nm there is $1.0 \mu\text{g/mL}$ of protein needed, whereas for 250 nm, 2.5 times less ($0.4 \mu\text{g/mL}$).

The results obtained from the titration experiments were used for the surface coverage calculations. The minimum concentration able to stabilize gold colloid suspensions could be logically used as parameter to determine the coverage of AuNP by estimating the antibody/AuNP ratios for each studied size.

The surface area A_{NP} , of the nanoparticles were calculated using equation 1 and assuming the nanoparticles are spherical with a radius r_{NP} .

$$A_{NP} = 4\pi r_{NP}^2 \quad (1)$$

From the calculated surface area of the gold nanoparticles, and the docking area of the IgG, the number of antibodies per nanoparticle was obtained. These calculations gave an approximate number of IgG molecules that should cover the gold nanoparticle surface.

The docking area of IgG is estimated to be 45 nm², with a molecular weight of 150 kDa. Taking 5 nm nanoparticles as an example and assuming their surface area is equal to 78.5 nm², the maximum number of antibody molecules that could be adsorbed onto the surface is 1.7. Experimentally, the minimum amount of protein that prevented aggregation of the nanoparticles was 30 µg/mL. Considering the number of nanoparticles per mL in a colloidal solution of 5 nm spherical gold nanoparticles ($5 \cdot 10^{13}$) and the number of IgG molecules ($1.2 \cdot 10^{14}$) needed to stabilize such amount of AuNPs, the gold NP/IgG molecules ratio was 2.4.

The difference between ratios (1.7 and 2.4 IgGs per nanoparticles) is due to the different methods used to calculate this relation. The first is theoretical calculation, whereas the second is experimental. Similarly, the same estimations were done for all the rest of gold nanoparticles. The results are summarized in Table 14. Consequently, larger nanoparticles need less protein to be completely covered with antibody. The surface of 50 nm diameter nanoparticles is 100-fold greater than that of the 5 nm; however the number of 5 nm nanoparticles AuNPs is 1111-fold higher than the 50 nm AuNPs. Therefore, the concentration of antibody required for complete coverage of the 5 nm AuNPs is theoretically much higher than that for 50 nm. This was proved experimentally, and for 5 nm nanoparticles the amount of protein needed for gold colloid stabilization is 12 times higher than for 50 nm diameter nanoparticles.

The average amount of protein required according to experimental results was 30% higher than the theoretical. For example, theoretically, 10 nm nanoparticles should require to cover fully the surface 14 µg/mL of protein, however, experimentally the amount of protein required was 20 µg/mL. Similarly, 50 nm nanoparticles needed higher concentrations than theoretically predicted ones.

The differences might be explained by the fact that smaller percentage of protein molecules adsorb on the surface and excess protein is needed to overcome the electrostatic repulsion between neighbouring charged proteins to a full coating of the AuNP. The experimental data was

in general in good agreement with the theoretical predictions, according to the value of IgG docking area and surface of the gold nanoparticles.

Table 14. Minimum antibody concentration needed to stabilize gold nanoparticles from aggregation and comparison between theoretical calculation and experimental results

Particle diameter (nm)	NPs/mL	Surface area per particle (nm ²)	Minimum Ab concentration (µg/ mL)		IgG/NP ratio	
			Theoretical	Experimental	Theoretical	Experimental
5	5.0·10 ¹³	78.5	21	30	1.7	2.4
10	7.7·10 ¹²	314	14	20	7	10
20	7.0·10 ¹¹	1260	5	6	28	34
50	4.5·10 ¹⁰	7850	1.9	2.5	174	223
100	5.6·10 ⁹	31400	0.97	1	698	716
250	3.6·10 ⁸	196000	0.26	0.4	4355	6691

The pH of the antibody solution, is also a key parameter to optimize the bioconjugation. Indeed, gold solutions must be kept at or slightly above the isoelectric point of the antibody.³²² Thus, for pH evaluation a series of experiments were carried out. Gold nanoparticles were conjugated with antibody at the minimum required concentration at six different pH values ranging from 6.5 to 9.5. Then, 100 µL of NaCl solution (10 %) was added and the colour of the obtained solutions was observed after 5 min. As it can be seen in Figure 49, in case of pH higher than 8.5 in all the antibody gold conjugates a small displacement of SPR was observed, which results in a decrease of absorbance ratio.

As the pH becomes more alkaline, a decrease in the ability of acidic Fab fragments to adsorb, combined with an expanding Fc, is one of the reasons for, the decrease in the number of bound IgG molecules.³²² For the majority of the studied AuNPs (5-50 nm) the optimal pH was 8.5, except for 100 and 250 nm gold nanoparticles, this displacement occurred above pH 9.0 and 8.0, respectively.

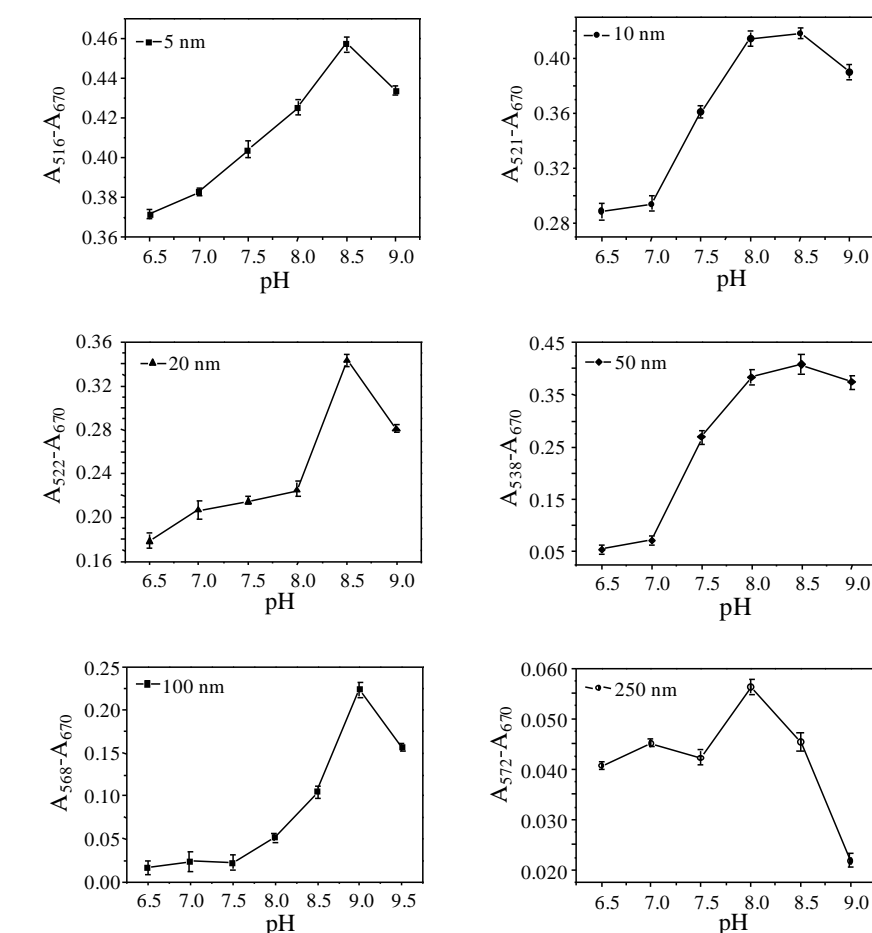


Figure 49. Optimization of pH of the conjugation for all studied AuNPs size.

The results obtained from the aggregation test and the theoretical calculations were confirmed by DLS. The results are shown in Figure 50. The nanoparticles were conjugated at two different concentrations of antibody. One being not sufficient for stabilization ($2.5 \mu\text{g/mL}$) and the other the minimal concentration needed ($30 \mu\text{g/mL}$) to saturate 5 nm gold nanoparticle surface, according to the titration experiment. IgG is a globular protein with a diameter of 2.5 nm and height of 12-14 nm, thus, a fully conjugated AuNP is expected to increase in diameter by 24–28 nm relative to the unconjugated particles if IgG is oriented perpendicular to the NP surface. The mean size in case of conjugate with $2.5 \mu\text{g/mL}$ of IgG was measured, being 15.7 ± 2.1 nm suggesting that the surface was partially covered with antibodies but not reached the saturation point. The gold conjugate prepared with the minimum concentration needed to stabilize nanoparticles showed a mean diameter of 32.6 ± 2.3 nm. These data suggest that 5 nm gold nanoparticles surface is covered by two immunoglobulin molecules if they were orthogonally oriented, what confirms the results calculated from UV-vis method.

However, as it is shown in a Figure 50C other immobilization configurations of IgG were obtained, for example immunoglobulin molecules can lie totally flat on the nanoparticle surface or at a specific angle resulting in different nanoconjugate size increases as it can be concluded from the obtained size distribution.

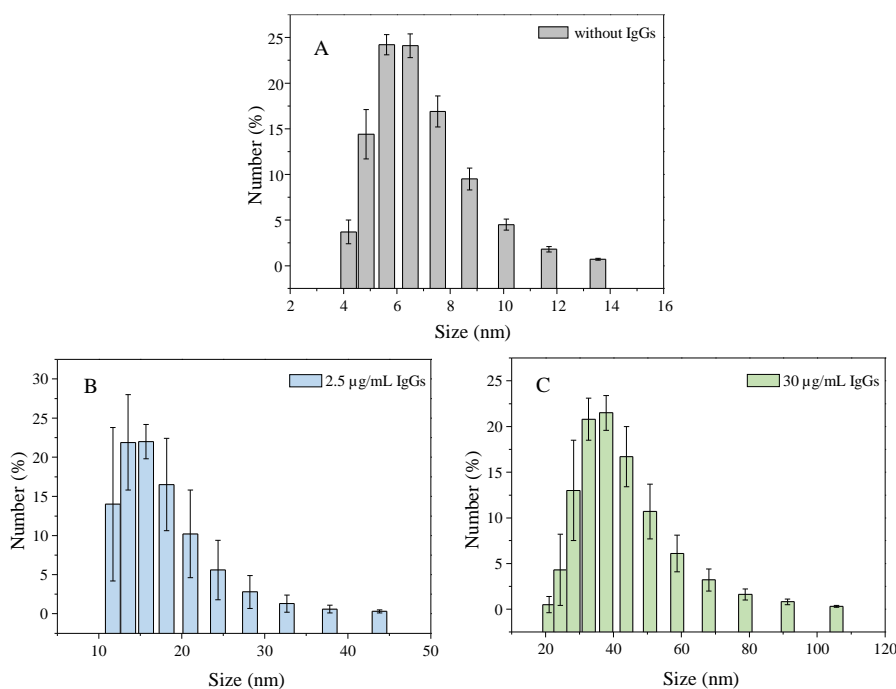


Figure 50. Size profile of AuNPs before and after incubation with antibodies (A-bare AuNPs, B-AuNPs incubated with 2.5 µg/mL of IgGs, C-AuNPs incubated with 30 µg/mL of IgGs).

4.4 Selection of the nanoparticle size

4.4.1 Two-step antigen-coated microimmunoassay using antibody-nanogold

In this section, the performances of antigen-coated microimmunoassay using the antibody-nanogold conjugates as tracer for direct detection of the antibody-antigen reaction with amplification step were evaluated. First, the optimal size of the spherical gold nanoparticles to perform direct assays was selected on the basis of signal intensity and sensitivity. As a model system, anti-atrazine IgGs were conjugated to different gold nanoparticles (diameter of 5, 10, 20, 50, 100, 250 nm) and tested by coating conjugate format (Section 3.12.1). Each of the AuNPs was conjugated with the minimal amount of the antibody, following titration experiments. Only those nanoconjugates giving acceptable signal to-noise-ratio ($S/N > 60$) corresponding to a maximum signal in absence of analyte of 10,000 arbitrary units, were considered for further

experiments. Figure 51 represents the results of the titration experiments using different sized gold nanoparticle conjugates. As it can be observed, 5 nm conjugates gave the assays with the highest signal intensity.

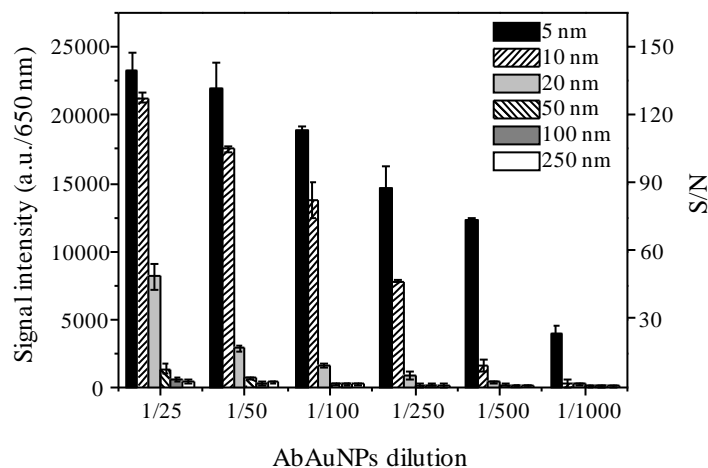


Figure 51. Titration experiment of different gold conjugates performed to evaluate the amplification yields of different sized gold nanoparticles.

Also, 10 nm nanogold conjugates and in less extension 20 nm show good amplification yields, however not as good as 5 nm nanoparticles, indicating that the nanoparticle size influences the silver amplification process.

When comparing the amount of protein needed to prepare 5, 10 and 20 nm AbAuNPs conjugates (those three showed the best amplification yields), it seems that 5 nm bioconjugate would be the less economical in terms of the IgG consume since they require the highest use of IgGs for obtaining stable conjugates. The dilution needed for developing the assay (1/500 dilution results in $S/N > 60$) are much higher than for the rest of studied gold nanoparticle sizes, thus the amount of IgGs per assay is significantly lower (0.015 $\mu\text{g}/\text{assay}$). In contrast, 10 and 20 nm gold conjugates required less amount of IgGs (20 and 6 $\mu\text{g}/\text{mL}$, respectively; Table 14) for stabilization, but higher amount of antibody, 1/100 and 1/25 dilutions, corresponding to 0.05 and 0.06 μg , for 10 and 20 nm, respectively, are used per assay.

Considering the number of gold nanoparticles in the same volume for 5, 10 and 20 nm diameter, the highest density of particles occurs for 5 nm ($5.0 \cdot 10^{13}$) and the lowest for 20 nm ($7.0 \cdot 10^{11}$), which is the result of the increase in nanoparticle diameter. For larger nanoparticles (50-250 nm) the number of nanoparticles decreases considerably. For 50 nm size AuNPs, there are around

1000 times less nanoparticles than for diameter of 5 nm, whereas for 250 nm there are only 3.6×10^8 nanoparticles (140,000 times less when compared to 5 nm).

For 5 nm AuNPs, the surface to volume ratio is much higher than for 10 or 20 nm AuNPs, resulting in a larger number of low-coordinated atoms available for interaction with silver ions, therefore the signal amplification is much more effective in terms of signal intensity obtained.

Therefore, in terms of silver enhancement performance, the less efficient silver enhancement occurs for 20 nm, due to the fact that less nucleation points are available to reduce the silver ions and transform them into solid silver. Thus, there is a need to use more concentrated antibody gold conjugate dilutions (1/100 and $> 1/25$ for 10 and 20 nm gold conjugate, respectively to reach $S/N > 60$).

Concluding, 5 nm gold nanoconjugates require less amount of antibody for the stabilization. Also, the number of nanoparticles per mL of gold suspension in comparison to other nanoconjugates of different nanoparticle sizes is higher, improving silver enhancement step and the sensitivity.

4.4.2 One-step antigen-coated microimmunoassay using antibody-nanogold

A colorimetric detection using labelled gold nanoparticles can result in the direct visual detection by the naked eye. The example of this methodology is flow immunochromatographic assay that are intended to detect the presence (or absence) of a target analyte in sample without any special and costly equipment. Based on that idea, the concept of using larger gold nanoparticles without any additional amplification step could be advantageous. For that, assays without silver amplification were performed to evaluate the effect of the nanoparticle size on signal intensity, using antibody modified gold nanoparticles (AbAuNPs; Section 3.11.2). The results of the experiment are presented in Figure 52. As it can be seen, 5 nm conjugate gave the lowest signal intensity (below 1000 a.u., $S/N = 6$) and on the contrary, the best results in terms of the signal intensity were obtained using 50 nm AbAuNPs.

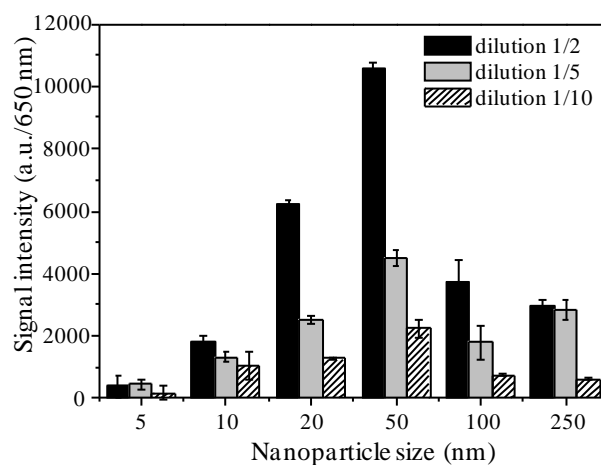


Figure 52. Titration experiment of AbAuNPs performed to evaluate their applicability in immunoassays without signal amplification.

The results are in good agreement with lateral flow immunoassays, where detection of the immunoreaction is performed by the naked eye. In this kind of assay the typical nanoparticle size is around 40 nm, as they are bright red and big enough to visualize them without any additional enhancement steps.

The number of nanoparticles per millilitre for 5 and 50 nm gold nanoparticles is $5 \cdot 10^{13}$ and $4.5 \cdot 10^{10}$, respectively. The number of antibodies per gold nanoparticle is 2 and 200 for 5 and 50 nm, respectively.

In the two step assay (5 nm), the 1/100 dilution was used, whereas in the one step assay (50 nm) 1/2 dilution was applied. Thus, it can be concluded that the number of antibodies is five times higher in the case of 50 nm. Therefore, the sensitivity for one step assay is lowered, as the limiting parameter in competitive immunoassays is the antibody concentration. To confirm that, competitive assays without any amplification step were performed for sulfasalazine and atrazine, as model analytes.

The sensitivity of the assay (IC_{50}) for atrazine was $32.6 \pm 5.4 \mu\text{g/L}$ with dynamic range varying from 6.5 to 62.6 $\mu\text{g/L}$ ($r^2 = 0.996$). Comparing these results with those of the assay using 5 nm AbAuNPs with amplification step, the sensitivity was almost 19-fold higher ($1.73 \pm 0.31 \mu\text{g/L}$). The dynamic range was from 0.18 to 8.81 $\mu\text{g/L}$ ($r^2 = 0.997$). The slope of the curves, however were very similar, being 0.74 and 0.70 for 5 and 50 nm AbAuNPs atrazine bioconjugates, respectively. For sulfasalazine the one step assay gave IC_{50} of $7.6 \pm 1.1 \mu\text{g/L}$ and the dynamic range from 0.7 to 72.3 $\mu\text{g/L}$ ($r^2 = 0.998$). The assay with silver enhancement step gave almost

110 times better sensitivity ($IC_{50} = 0.07 \pm 0.01 \mu\text{g/L}$). The slope for assay using 5 nm AbAuNPs had slightly better slope (-0.78), whereas for the one step assay the slope was 0.70.

To conclude, the best nanoparticle size is 50 nm for the one step assay as it gives the best results in terms of signal intensity and sensitivity. However, there is significant loss in assay sensitivity probably due to high antibody and nanoparticles concentration needed to establish the immunoreaction extension. This fact was observed for the studied analytes, atrazine and sulfasalazine. Therefore, the use of small nanoparticles is advantageous for setting high sensitive immunoassays. The sensitivity required by the EU Water Directives in case of small nanoparticles is easily obtained as antibody concentration used is low, thus the required sensitivity can be achieved.

4.5 Two-step antibody-coated microimmunoassay using antigen – nanogold tracers

Most of the immunoassays developed for the analysis of environmental residues are working under competitive format. This method requires the preparation of competitors, usually as labelled analyte conjugates (for direct assay format) and protein analyte conjugates (for indirect assay format).

In standard ELISAs, haptens are covalently coupled to proteins, such as BSA and OVA, when they are used as coating conjugates and to enzymes, if labelled hapten is used as tracer.

The format chosen has a strong influence on the sensitivity and selectivity of the assay.¹⁴⁵ Indirect immunoassay configurations need more incubation steps thus, they are more prone to analytical errors, whereas direct assays are carried out in a shorter time by reducing the number of steps.

The antibodies can be adsorbed onto the gold surface but coating conjugate could be used in the same manner to perform immunoassays in antibody-coated format (Section 3.11.5). In this section, the results obtained for the direct assay based on haptenized protein modified gold nanoparticles will be discussed, using atrazine as model compound.

Here, the gold nanoparticle conjugates (5 nm) with coating antigen (OVA-2d) were the signal generator and anti-atrazine antibody was immobilized on the disk surface by adsorption.

One of the important aspects in designing sensitive immunoassays is the effect of the resulting hapten-protein ratio in the conjugates. Usually, it is considered that a high ratio of immunogens increases the strength and specificity of the immune response, but for competitors a moderate value is more desirable, favouring the sensitivity of the resulting competitive immunoassay. Theoretically, when the amount of hapten in the competitor is limited there is a requirement for less analyte in solution to compete for the specific antibody.

Thus, four different coating-conjugates (prepared as described in section 3.4) were used to prepare antigen-nanogold tracers. The amount of OVA needed to stabilize the surface of 5 nm nanoparticles was 90 $\mu\text{g}/\text{mL}$. The volumes of activated hapten 2d used were: 10; 25; 50 and 100 μL which corresponds to different molar ratios (MR) coating antigen/AuNP: MR1, MR2, MR3 and MR4, respectively. With as-prepared modified gold nanoparticles titration experiments were performed. The gold coating conjugate dilutions ranged from 1/25 to 1/1000, whereas antibody concentrations were between 5 and 50 mg/L.

In order to check the performances of all prepared nanogold bioconjugates, one point competitive assays were conducted, where only one atrazine concentration was tested (1.0 $\mu\text{g}/\text{L}$) and two dilutions (1/200 and 1/1000 of OVA-2d-AuNPs). The anti-atrazine IgGs concentrations tested were 20, 30 and 40 mg/L.

Figure 53 shows the results of the one-point competitive immunoassays. The graphs A and B represent the results using 1/200 and 1/1000 dilutions of OVA-H-AuNPs, respectively.

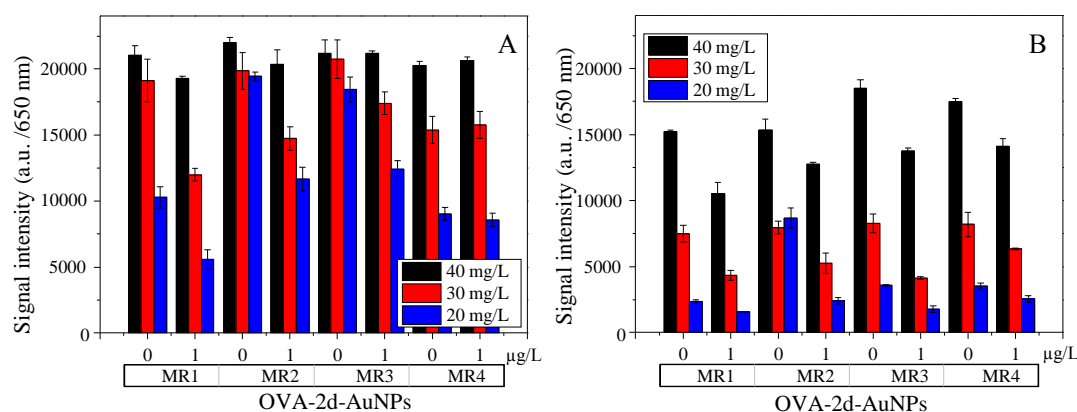


Figure 53. Evaluation of the optimal competition conditions using antigen-tracer dilutions 1/200 (A) and 1/1000 (B).

As it can be observed, for 1/200 dilution and the antibody concentration of 40 mg/L (Figure 53A), no competition was observed. The decrease of the signal caused by 1.0 $\mu\text{g}/\text{L}$ of analyte is approximately 10% for MR1 and MR2. For the other two conjugates there is no competition observed. This is probably due to the too high concentration of the coating antibody and the tracer, both being the limiting factors in this kind of the assay. If the antibody concentration is reduced, for example to 30 mg/L, sensitivity increases, however, still the inhibition of the signal is low. Here, the analyte concentration of 1.0 $\mu\text{g}/\text{L}$ inhibits 37% of the maximum signal in case of MR1 conjugate and 26% for MR2. The increase of the molar ratio results in decrease in sensitivity, as for the MR3 nanogold bioconjugate, the signal drops only 16% and for the MR4

still competition did not occur. When the antibody concentration is lowered to 20 mg/L, the sensitivity improves considerably. For the hapten-nanogold conjugate with lowest molar ratio (MR1), a 54% of the initial signal for 1.0 µg/L of atrazine analyte is observed. As usual, while the hapten concentration increases, the sensitivity is lower. For the MR2, 60% of initial signal is obtained, whereas for the MR3 is 67%. For hapten-nanogold tracer with the highest hapten density for the dilution 1/200 the competition is not observed for any of the used antibody concentrations.

The sensitivity of the assay improves when higher dilution of the antigen-nanogold tracer is used, as it is presented in Figure 53B. It can be observed that for the antibody concentration of 40 mg/L, the highest signals are obtained for all four tested coating conjugate-nanogold tracers and range between 15,000 and 18,000 a.u. when analyte is absent. In this case, the competition is observed for all of the coating conjugate-nanogold tracers and is decreasing while the molar ratio increases.

When the antibody concentration is lowered to 30 mg/L the signal drastically drops and is approximately 50% lower than for 40 mg/L. The competition in this case provokes the signal decrease of 42, 34, 50 and 22%, for MR1, MR2, MR3 and MR4 of coating conjugate-nanogold tracers, respectively. However, the intensity values are quite low ($S/N < 60$), therefore the signal range would be too low to quantify the sample with high precision. The smallest antibody concentration used for this test, 20 mg/L, gave very low signal intensity values (S/N between 14 and 22), therefore, these conditions could not be used as reliable in terms of the immunoassay precision.

As a conclusion, the two hapten-gold tracers with the highest MR did not show strong competition, therefore, for further tests only the two lower MR, being MR1 and MR2 will be evaluated.

Concerning the results obtained for the two concentration competition assays, the following conditions were tested in order to represent the complete competition curves: 30 mg/L of immobilized antibody and hapten-gold tracer 1/500 dilution. This dilution was selected since 1/200 was proved to be too low and 1/1000 gave too small signal values. The results are presented in Figure 54.

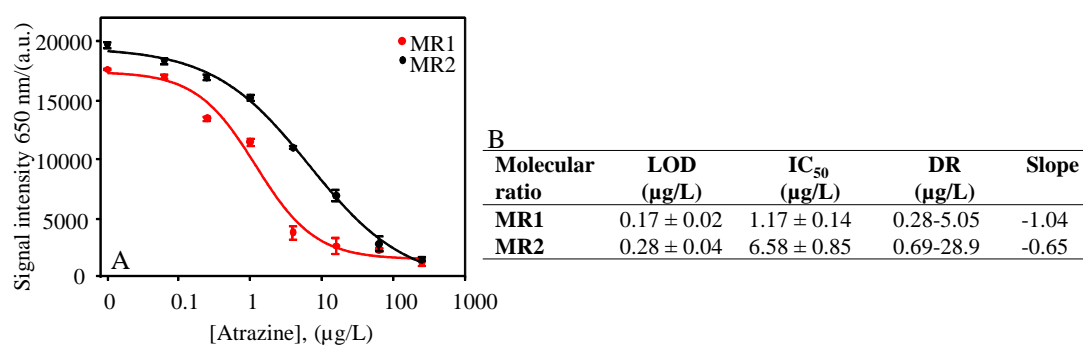


Figure 54. A. Competition curve for antigen-nanogold atrazine tracers. B. Analytical features for both assays.

As it was mentioned before, the lowest MR, the better the competition is obtained.

As it is shown in Figure 54B, the sensitivity value (IC_{50}) for the coating antigen-nanogold tracer with MR1 of haptenized protein was $1.17 \pm 0.14 \mu\text{g/L}$ with dynamic range between 0.28 to $5.05 \mu\text{g/L}$ ($r^2 = 0.998$). The assay using tracer with MR2 showed the sensitivity (IC_{50}) almost 6 times lower. The lower sensitivity of the assay is probably due to still too high amount of available hapten molecules.

Overall, the possibility of using the coating conjugates for the preparation of the tracers in the competitive immunoassays is demonstrated. The molecular ratio hapten/nanogold will strongly influence the sensitivity of the assay. The lower the concentration of the hapten molecules, the higher the sensitivity obtained. Also, the concentration of the immobilized antibody should be properly adjusted for each case individually. The presented approach showed good results in terms of assay sensitivity, however, immobilization of the antibodies directly onto the disk surface resulted in less reproducible results ($\text{RSD} \geq 15\%$), comparing to the assays where coating antigen is immobilized ($\text{RSD} \leq 10\%$).

4.6 One-step microimmunoassay using antibody-gold nanorods

Gold nanorods are also interesting nanostructures to attach antibodies, though they show lower signal amplification yields comparing to small spherical nanoparticles. However, the size of the nanorod can be tuned and even large in size nanorods are stable, whereas the large spherical nanoparticles are more prone to aggregation. Thus, as a proof of concept large nanorods (40-80 nm) were used to perform the immunoassay without any amplification step. Some important aspects of the optimization protocol will be discussed in following sections.

Gold nanospheres have one visible absorption band. On the contrary, the surface plasmon absorption of gold nanorods shows two bands: a strong long-wavelength band due to the

longitudinal oscillation of electrons and a weak short-wavelength band due to the transverse electronic oscillation. For the nanorods studied in this thesis the plasmon resonance due to the longitudinal resonance is at 650 nm, while the transverse oscillation is the reason of the appearance of the band at 524 nm.

Nanorods synthesized using CTAB are quite challenging when it comes to their functionalization, which is not as simple as it is in the case of “bare” surfaces of gold nanoparticles capped with citrate. Surface functionalization with PEG-thiols is often used to introduce a high degree of stability and biocompatibility and can be carried out simply by adding thiol-terminated PEG to centrifuged rods.

In this work, a bifunctional linker, thiol-PEG-acid, was used to attach antibodies by covalent bonding. Moreover, the use of such linker reduces the chances of aggregation or loss of solubility.

First, the concentration of the linker should be optimized in order to get stable nanorods. The IgGs bind to the carboxylic group through the free amine groups present in the immunoglobulin molecules. For that, different concentrations of thiol-PEG-acid were used (0-5 mg/mL) and then absorption spectra were measured and compared. As it is presented in the Figure 55, intensity of the absorption as well as the displacement of the SPR peak were measured. It can be seen that at concentrations below 1 mg/mL the solution is not stable as red-shift in the plasmon band is observed. At the concentration of 1.0 mg/mL, the solution is stable since there is no shift in the plasmon peak. Also, the intensity measured at SPR value is constant. Therefore, it can be concluded that SH-PEG-COOH at 1.0 mg/mL is sufficient to stabilize the gold nanorod suspension.

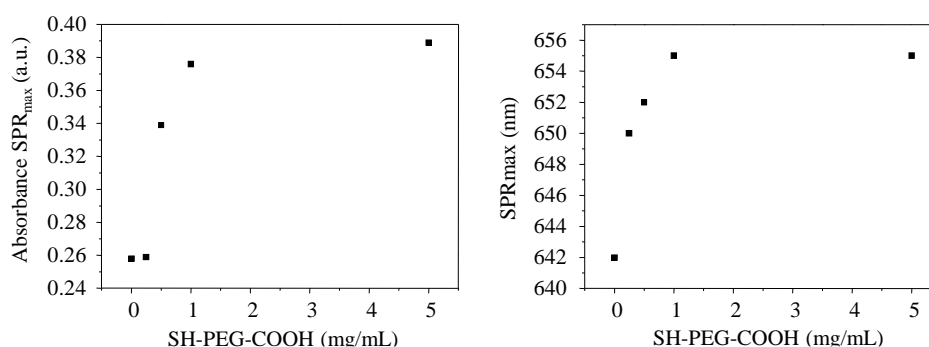


Figure 55. Optimization of the PEG concentration for nanorod stabilization. Left and right panels show the changes in the absorbance and in the SPR_{max} for different PEG concentrations, respectively.

The stabilization of the gold nanorods with thiolated PEG molecules causes the displacement of the plasmon resonance as the refractive index is changed due to the presence of the polyethylene molecules. This effect was also observed for gold spheres were upon addition of the IgGs the SPR peak was red-shifting. Figure 56 shows the displacement of the plasmon after stabilization of the gold nanorods. The observed shift is quite strong since the SH-PEG-COOH is a big molecule ($M_w = 3$ kDa). Therefore, the displacement of SPR peak of 5 nm towards red is observed.

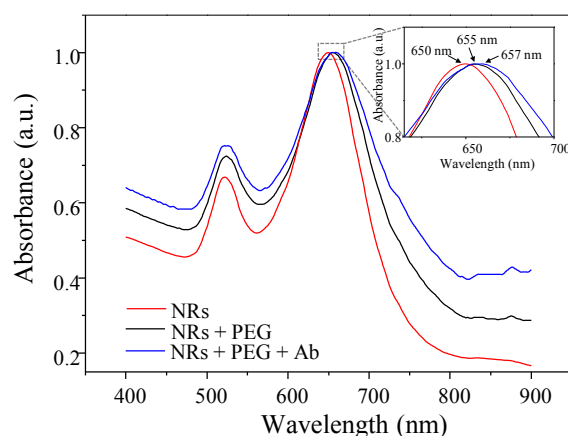


Figure 56. UV/VIS spectra of gold nanorods and the antibody conjugate. The inset graph shows the λ_{\max} for the gold absorption peaks and the resulting red-shift upon PEG and antibody conjugation.

Once the PEG layer is formed, biomolecules are covalently attached via the $-\text{NH}_2$ bond of the IgGs to the $-\text{COOH}$ terminus of the PEG molecules. The coupling of the antibodies is confirmed by measuring the SPR red-shift after the reaction as it is shown in Figure 56.

Antibody molecules have molecular weight approximately of 150 kDa, being 30 times bigger than the PEG molecule. Consequently, IgGs must show higher shifts. The reason of the small displacement is due to the proximity to gold nanorods surface. As the distance from the surface of the nanorods is larger, the plasmon resonance is less sensitive to refractive index changes, therefore only 2 nm of shift is observed (655 to 657 nm).

4.6.1 Titration experiments of the antibody-gold nanorods conjugates

In competitive immunoassay both antibody and coating conjugate concentrations play a crucial part in obtaining highly sensitive immunoassay. For this reason, it was necessary to optimize the optical density of the nanogold conjugates as well as the coating conjugate concentration. As a model compound, anti-imidacloprid antibody was used for the conjugation with gold nanorods.

Optimal coating conjugate concentration and antibody dilutions were selected by checkboard titration in a competitive format.

First, three different coating conjugate concentrations (OVA-IMD; 5, 10 and 20 mg/L) were tested against different AbNR dilutions (1/15, 1/7.5, 1/3 and 1/1.5 which correspond to OD of 30, 60, 150 and 300, respectively) to check the signal intensities.

The results are represented in Figure 57. It can be observed that antibody-nanorods at 1/15 dilution (OD = 30) gave the lowest signal intensities, ranging from 4000 (S/N = 24) to 7000 a.u. (S/N = 42), for three studied coating conjugate concentrations. These results limit the quantitative determination of the analyte with high reproducibility.

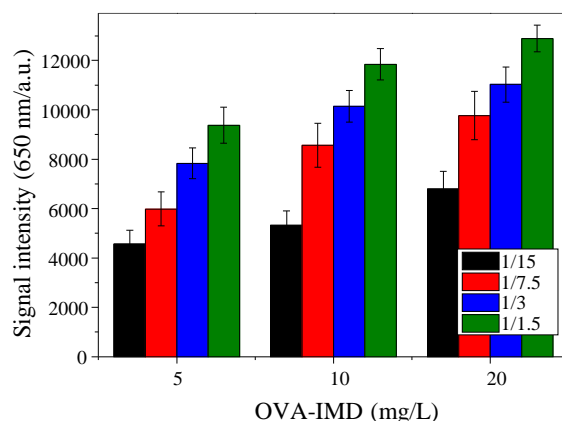


Figure 57. Titration experiment for antibody-nanorod conjugates.

The results of the assay with antibody modified gold nanorods at 1/7.5 dilution (OD = 60) were slightly better, giving higher signal intensities. The lowest signal was around 6000 a.u. (S/N = 36), whereas the higher was slightly above 10,000 a.u. (S/N = 60).

Increasing the antibody-nanorod conjugate concentration resulted in increased signals. For OD = 150 Ab-NR conjugates, the signal intensity varied between 8000 a.u. (S/N = 48) and 11,000 a.u. (S/N = 66). The highest concentration of antibody modified gold nanorods

(OD = 300), resulted in the highest intensities for all tested coating conjugate concentrations. Signal intensities ranged between 10,000 (S/N = 60) and 13,000 a.u. (S/N = 78).

4.6.2 Competitive immunoassays using antibody-gold nanorod conjugates

The titration experiments showed in previous section, serve to select the conditions for performing competitive immunoassays. The signal intensity is an important parameter in order to build a precise calibration curve, but high concentrations of antibody as well as coating conjugate can result in poor sensitivity. Therefore, it is crucial to test different conditions in order to select the best parameters to reach the highest signal inhibition. The titration experiments performed to evaluate the signal intensities that could be reached served to select the best antibody-nanorod and coating conjugates concentrations to perform competitive immunoassays. The highest signals were obtained for OD = 150 and 300 (1/3 and 1/1.5 dilutions, respectively) of antibody modified gold nanorods. Thus, these conditions were used first. However, for all three tested coating conjugate concentrations (5, 10 and 20 mg/L) no inhibition of the signal was observed. The reason is probably due to too high antibody concentrations employed. In this type of the immunoassay, no amplification step was used, as nanorods are large enough to avoid any enhancement of biorecognition event. However, as it was discussed for spherical gold nanoparticles, to reach high enough S/N ratios in order to perform a precise calibration curve, high concentration of the nanoparticles must be used. Thus, the antibody concentration is also increased, and therefore competition did not occur.

As a next step, lower antibody-nanorod conjugate concentrations were tested to check if by limiting the antibody concentration any inhibition might occur. Therefore, even if the S/N ratios did not meet the set requirements, some competitive assays were conducted. The results are presented in Figure 58.

For 10 mg/L of coating conjugate and antibody-nanorod conjugate at OD = 60 (1/7.5 dilution) an inhibition of the signal is observed. The sensitivity measured as IC_{50} , however is not very high, being $13.6 \pm 1.6 \mu\text{g/L}$. The slope of the curve is -1.3 and dynamic range 3.3-17.8 $\mu\text{g/L}$. Comparing the result with the assay performed using 5 nm antibody-gold conjugates the sensitivity is 40-times lower (IC_{50} for AuNPs was $0.32 \pm 0.06 \mu\text{g/L}$). Also, lower coating conjugate concentration was used to compare the performances and see if the sensitivity can be improved. Indeed, the sensitivity is comparable with the sensitivity obtained using spherical gold nanoparticles, and expressed as IC_{50} is $0.37 \pm 0.06 \mu\text{g/L}$. The hill slope was improved also, being -1.6 and the dynamic range is 0.13-0.27 $\mu\text{g/L}$.

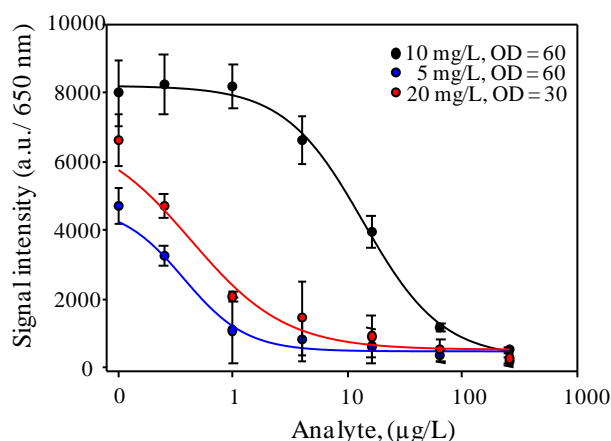


Figure 58. Antibody-gold nanorod competitive assays for imidacloprid.

The signal intensities however, are very low. The signal obtained when no analyte was present was around 4000 a.u. which corresponds to $S/N = 24$. This value is too low to obtain precise results as even small fluctuations in the signal can have considerable effect on the concentration measurements.

In the last competitive assay, 20 mg/L coating conjugate and antibody-nanorod conjugate at 1/15 ($OD = 30$) dilution were tested. These conditions were also selected according to the titration experiment performed previously. Here also the highest signal was quite low, slightly lower than 6000 a.u. ($S/N = 36$). Similarly to the assay described before, the sensitivity reached was quite high ($IC_{50} = 0.43 \pm 0.1 \mu\text{g/L}$). The slope was -1.05 and the dynamic range 0.18-0.63 $\mu\text{g/L}$. Nevertheless, the signal range is low and such assay might be more prone to error.

To conclude, the concept of using the gold nanorod as label is demonstrated. The assay works as a one-step method without any signal amplification. However, the main drawback is that the signals are quite low, affecting the reproducibility of the assay. A good point is that the results are obtained quickly so developed immunoassay could be employed as a semi-quantitative test.

4.7 Two-step antigen-coated microimmunoassay using hapten nanogold tracers

In standard ELISAs, direct assays are based on the use of antigens labelled with enzymes. Labelled antigen competes with the analyte for binding to a limited quantity of antibody. This kind of the immunoassay has advantages over indirect assays, as, there is no need of using a secondary antibody to detect the immunoreaction extension, thus the number of steps is reduced, so does the possible errors, making the analysis more reproducible.

Following the concept of direct ELISA, a direct assay using hapten nanogold tracers was performed. For that, atrazine as a model analyte was used.

The first step consisted in the optimization of the conjugation procedure between PEGylated gold nanoparticles and hapten molecules. The diameter of gold nanoparticles was 5 nm, whereas PEG was used as a linker. The PEG molecules attach through the thiol groups to gold surface leaving the amine groups available for further reactions as it is shown in Figure 59. The surface density of amine groups on the aminated gold nanoparticles is $0.5/\text{nm}^2$. For a 5 nm particle with a surface area of 78.5 nm^2 , ~ 40 amine groups per particle can be incorporated.

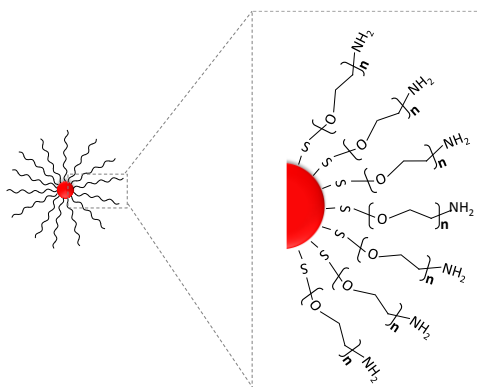


Figure 59. PEGylated gold nanoparticles.

The optimization of the conjugation consisted in the study of different pH values of the reaction solution, as well as different concentrations of the activated hapten, in order to compare the sensitivity of the immunoassays.

The pH values ranged between 7.0 and 12.0. The conjugation process did not occur satisfactorily in aqueous buffers with pH lower than twelve, as no signal was detected after running the immunoassay. Therefore, the optimal pH for the conjugation was set to 12.0.

Once the pH of the reaction was set, the influence of the hapten concentration on assay sensitivity was evaluated. First, titration experiments were performed in order to choose the best optical density of the conjugates. The concentration of the purified anti-atrazine IgGs was 5, 20 and 50 mg/L, while the tracer optical density ranged between 0.0125 and 0.5. The lowest immobilized antibody concentration (5 mg/L) did not give sufficient signal to perform the competitive assays. On the other hand, when the highest concentration (50 mg/L) was used the saturation of the signal occurred, meaning that the competitive assay would result in low sensitivity. Therefore, the concentration of 20 mg/L was set as the optimal one to perform further experiments.

Before performing the competitive immunoassays, titration experiments were conducted in order to select the optimal optical density of the tracer. Figure 60 shows the results and it can be seen, only the two highest densities (OD = 0.5 and 0.25) resulted in $S/N > 125$. However, such high tracer concentration did not allow for the competition to occur. Also, the amount of the nanogold bioconjugate is high, so the analysis would be too costly. Thus, for further experiments, lower optical densities were selected.

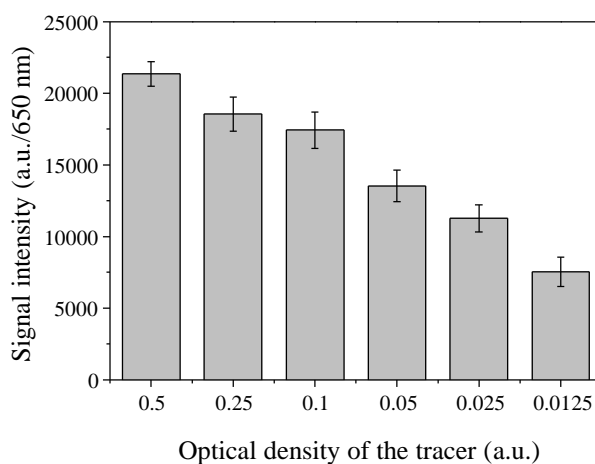


Figure 60. Titration experiments using Au atrazine hapten tracer.

Next, competitive immunoassays were performed using the lowest optical densities tested (0.0125, 0.025, 0.05 and 0.1). In case of the OD = 0.1, the competition was not observed and the signal was maintained very similar for all analyte concentrations (0-1 mg/L). The signal intensity for the tracer optical density 0.05 was quite high (~13,000 a.u.), however, in the competition (analyte concentration up to 1 mg/L) no inhibition of the signal was observed. In the case of the lowest optical density (OD = 0.0125), the signal obtained was not sufficient to perform reproducible and reliable competitive assays. Relative standard deviation in the titration experiment was the highest among all tested optical densities (RSD = 14%), whereas relative standard deviation for other cases ranged between 4 and 11%.

The tracer with an optical density of 0.025 showed high signal intensity (~11,000 a.u.), and low relative standard deviation (RSD = 8%), thus competitive immunoassays were performed. The result is presented in Figure 61.

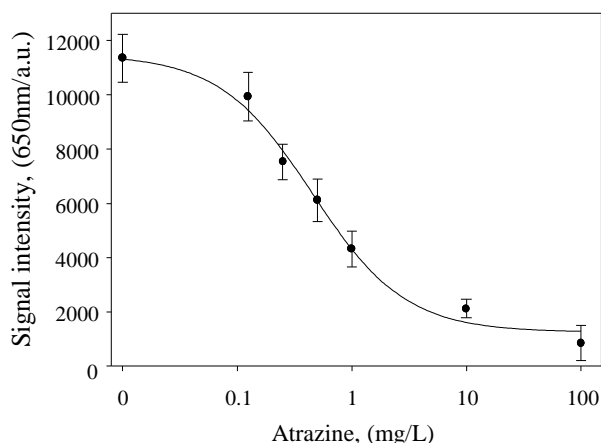


Figure 61. Competition curve for atrazine using Au-hapten tracer. The standard curves are the mean of 10 curves performed in different days and on different discs averaging four points per analyte concentration.

The sensitivity of the assay was 0.45 ± 0.08 mg/L, which is definitely not enough to meet the E.U. requirements for the determination of residues of water contaminants. The slope of the curve was quite steep, being -1.1; the LOD was set at 0.08 mg/L and the working range was 0.1-1.77 mg/L.

Despite the fact that the tracer was specific towards its own analyte, the sensitivity value obtained is an obstacle for employing this type of immunoassay based on nanorods in screening. The possible reason of the low sensitivity is the fact that the density of the hapten per gold nanorod particle is too high, resulting in high concentration of the analyte needed to reach the competition.

Overall, from all studied immunoassay types, the best results were observed for coating conjugate-based assays using 5 nm antibody labelled gold nanoparticles. Therefore, the rest of this work will focus on the development of the multiplex system for screening purposes using this reagent and format.

4.8 Optimization of the performances of microimmunoassay

The attachment of the antibodies or antigens to the surface of DVD involves non-covalent link between the hydrophobic regions of the protein and the nonpolar polycarbonate surface. Proteins including antibodies are often readily immobilized, but the coating efficiency varies from protein to protein. The coating buffer must be free of any protein other than the coating protein.

Usually, the buffer used for coating should have a pH value higher than the pI value of the protein being attached for maximum adsorption yield. In this work, ovalbumin (OVA) (molecular weight is 43 kDa and isoelectric point 4.5) was used as a coating protein to which hapten molecules were conjugated. OVA is a glycoprotein that comprises 54% of the total proteins of egg white.

Carbonate/bicarbonate buffer is one of the most often printing media used. Therefore, four buffers were tested to study the effect of the buffer concentration on immobilization of OVA-2d (2.5 mg/L). The assay consisted in testing recognition event between the antigen (OVA-2d) immobilized on the disk and anti-atrazine antibody gold conjugate, as described in section 3.12.1.

Figure 62 shows the signal intensities obtained in absence of analyte. The highest buffer concentration (0.5 M) resulted in the lowest signal (~ 9000 a.u.), whereas the lowest concentration gave the highest signal (~ 15,000 a.u.). Therefore, for all the coating conjugates used in this work, this buffer conditions were used.

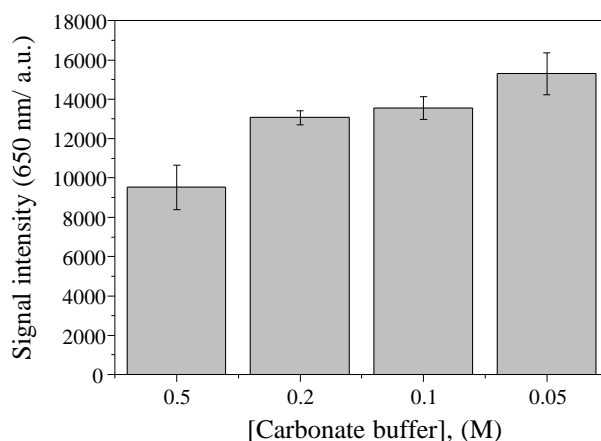


Figure 62. Signal intensities values obtained for different printing carbonate buffer concentrations.

Another factor that needs to be taken into account is sample volume. A beneficial effect of immunoassay performed in a microarray format is the reduced distance that molecules need to

travel. In the heterogeneous microarray format, the antibody–antigen reaction occurs at the solid–liquid interface, where only the reactant in the liquid phase can freely move around.

Large sample volumes may increase assay sensitivity, but they may also result in higher matrix effects and lower linearity. Sample matrix effects can be minimized by using a low ratio of the sample compared to the assay reagent in the incubation step. However, this reduces the signal level and potentially the signal-to-noise ratio, dropping the sensitivity of the assay.³²³

The use of very small volumes with associated shortened diffusion times in microscale assays should increase the reaction rate and decrease the time required to obtain high S/N ratios, resulting in overall analysis time reduction.

Therefore, different sample volumes were studied in order to evaluate the optimal one in terms of the reagent use and incubation time required to obtain high signal to noise values.

Two different approaches were compared as it is presented in Figure 63. First, using sample droplets of different volumes (Figure 63A), and second the use of cover glass slides over the microarray spots (Figure 63B).

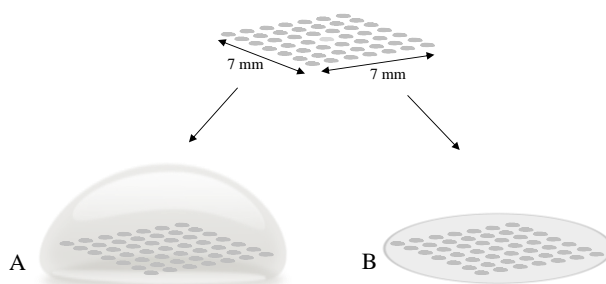


Figure 63. Different ways of applying the sample onto the microarray.

The microarray matrix is a 7 mm square with 49 mm² area, thus the sample droplet volume has to be high enough to cover all the surface containing spots. Therefore, two different volumes were checked, 100 and 200 μ L. The differences between the sample volumes used were compared for three analytes: chlorpyrifos (CLP), 3-phenoxybenzoic acid (PBA) and sulfasalazine (SSZ). Only in case of the chlorpyrifos the values of signal intensity for 100 and 200 μ L of the sample were very similar (11,150 and 11,300 a.u. for 100 and 200 μ L droplets, respectively), as it is shown in Figure 64A. Nevertheless, in the case of two other analytes, the lower droplet volume gave higher signal intensities. For PBA, the signals were 15,900 and 13,300 a.u. (19% lower), for 100 and 200 μ L, respectively, whereas for SSZ the values were 15,500 and 14,000 a.u. (10% lower). The signals for the controls as it is depicted in Figure 64B, were for 100 μ L droplets 9% higher (~17,000 a.u.), than for 200 μ L (15,500 a.u.).

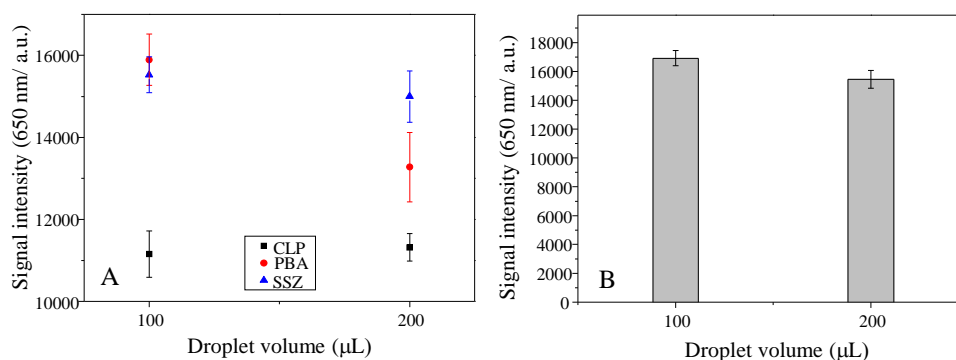


Figure 64. Comparison of signal intensities for different droplets volumes for three analytes. (A) – Signal intensities for tested analytes; (B) – Signal intensities for control (GAR-Au).

The volume of 100 μL would be the better choice if higher S/N ratio is the goal; however, such high volumes are comparable to the ones used in ELISA. Therefore, considering that one of the biggest advantages of using the immunoassays in microarray format is the reduced sample volume, the ideal solution would be the use of cover glass slides that would reduce the sample volume considerably. As a consequence, four different volumes were considered in the test regarding the use of cover glass slides to apply the sample onto the microarray matrix. The studied volumes were: 5, 10, 15 and 20 μL.

As it can be noticed in Figure 65A, the smallest sample volume (5 μL) gives the lowest signal intensity, being around 10,000 a.u. for all three studied analytes. The tendency seen in the graphs shows that as the sample volume is increased the obtained signals get higher. For chlorpyrifos, the increase is not so prominent as for other two analytes. Indeed, the difference between the lowest and the highest sample volume was approximately 1000 a.u. In the case of PBA, the difference between 5 and 20 μL was around 5000 a.u., whereas for sulfasalazine it was around 4000 a.u. According to ANOVA test, the differences between 5 μL and 20 μL for SSZ and PBA are significantly different ($F > F_{crit}$), whereas for chlorpyrifos there is no significant signal variations ($F < F_{crit}$) between different volumes. These differences are probably due to the different conditions for each of the analytes. The dilutions of antibody nanogold were 1/100, 1/100 and 1/500 for PBA, CLP and SSZ, respectively. The coating conjugates concentrations were 10, 20 and 10 mg/L, for PBA, CLP and SSZ, respectively.

On the other hand, the signal of the positive control was significantly similar (ANOVA; $F < F_{crit}$) between different sample volumes (Figure 65B).

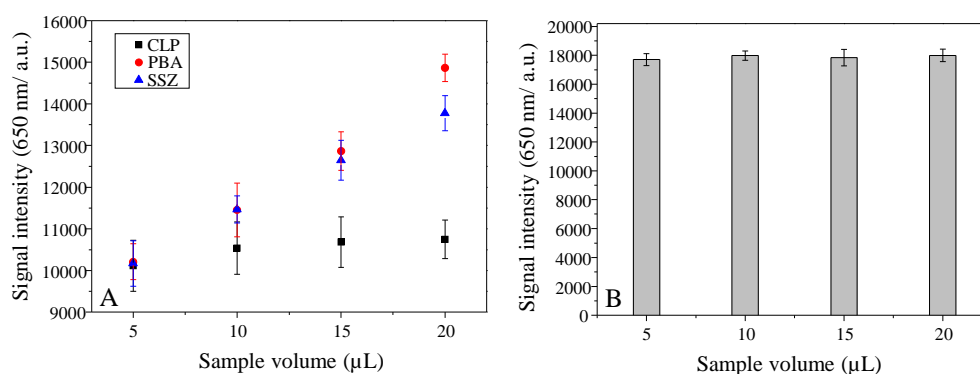


Figure 65. Comparison of signal intensities for different sample volumes using cover glass slides. (A) Signal intensities for tested analytes (A) and (B) for the positive control (GAR-Au).

Considering the fact that small sample volume would lower the overall cost of the immunoassay but at the same time should give good signal-to-noise ratios, the best sample volume was chosen to be 20 μL using cover glass slides. Comparing it with ELISA, it is 5 times less, what undoubtedly is a big advantage over this commonly used method, in terms of immunoreagent consumption.

When performing the competitive immunoassays, an important parameter that should be optimized is the immunoreaction time. The relationship between incubation times and signal generation intensity are established for a range of reagent concentrations. The goal is to achieve a high signal-to-noise ratio, not simply to maximize the signal, but also sensitivity and precision are key goals. Practical considerations also apply, for example, the incubation time needs to be acceptable. Faster assays may be achieved with higher concentrations of conjugate (enzyme-labelled antigen or antibody), but the cost and availability of the conjugate must be considered. There are usually trade-offs between desirable performance characteristics, for example, a short incubation time may result in weak signal generation, and a long incubation time may favour nonspecific signal appearance. The incubation time optimization often starts with observation of the impact of time on signal intensity and nonspecific binding. Adjusting incubation time can often be beneficial for reducing nonspecific binding.

To establish the optimal immunorecognition time, the chlorpyrifos nanogold bioconjugate was used as model system. Different incubation times, ranging between 5 to 35 min were tested. As presented in Figure 66, the signal intensity for 5 min incubation is below 6000 a.u. After 10 min, the signal reaches 7500 a.u., which is still quite low result for the performance of competitive assays. Fifteen minutes of incubation gave much higher signal (around 9500 a.u.), while incubating for 5 min more resulted in signals above 10,000 a.u. Incubation time of 20 min would be sufficient as the signal obtained is high, however, it was observed that saturation point was

reached at 25 min. Therefore, as less signal variation is involved at saturation point, the incubation during the competition step for all the analytes was set as 25 min.

Concluding, 25 min is enough for reaching the equilibrium, thus to obtain high signal intensity, maintaining the overall time of the analysis very competitive when compared with traditional ELISA test.

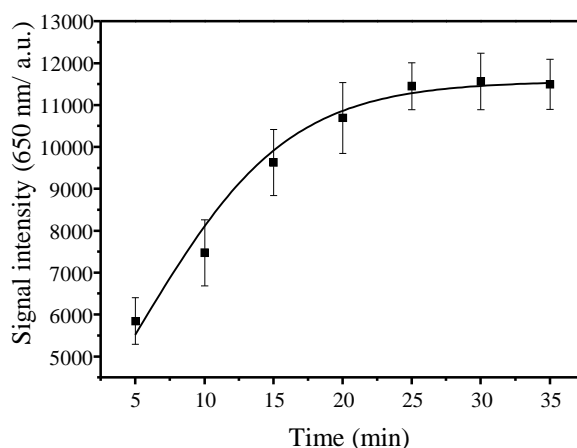


Figure 66. Optimization of the incubation time of the chlorpyrifos immunoassay.

In this work, two different signal amplification methods were compared in terms of signal intensity and the time needed to obtain detectable readouts.

Developing solutions were as follows:

- Ag^+ / hydroquinone
- Cu^{2+} /ascorbic acid

As a first raw experiment, goat anti rabbit labeled with gold nanoparticles was immobilized onto the surface of a standard DVD. Then, each of the developing solution was freshly prepared and incubated. The times studied in this experiment ranged between 5 and 30 min. As it can be observed in Figure 67A, 5 min is not sufficient to obtain the desirable intensity value. The signals obtained for silver enhancer were below 5000 a.u. ($S/N = 30$). Incubation time of 10 min gives high intensity ($\sim 17,000$ a.u.; $S/N = 102$) and very low background signal. Between 10 and 15 min the difference of signal is about 5000 a.u., but in case of 15 min incubation the background signal increased 4 times. For 20 min incubation, the signal reaches 25,000 a.u. ($S/N = 150$), whereas the background signal is increased to 3000 a.u. ($S/N = 18$). It can be clearly observed that starting from 25 min the autonucleation process begins, resulting in elevated background signals around 12,000 a.u. ($S/N = 72$) for 25 min and almost 20,000 a.u. ($S/N = 120$)

for 30 min. To conclude, incubation time of 10 min is suitable to obtain high signal intensity, maintaining very low background signal.

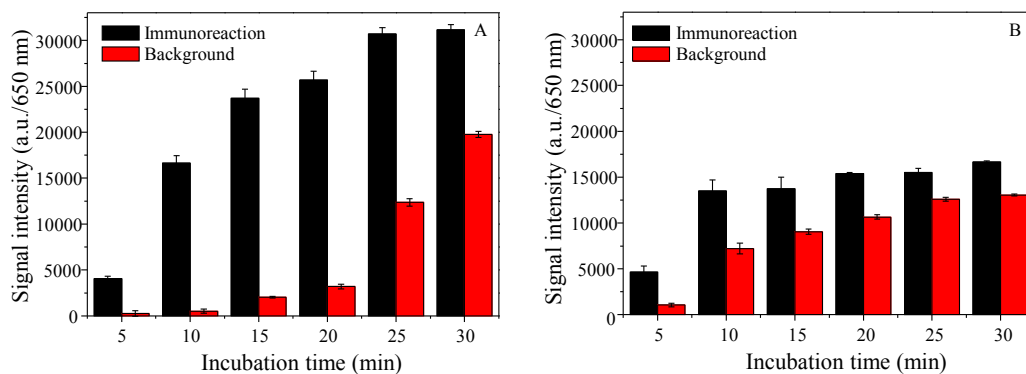


Figure 67. Analytical response of silver (A) and copper (B) enhancement reagents.

As far as copper enhancement is concerned, the solution contains ascorbic acid (0.25 M) and copper sulphate (0.5 M). Copper enhancement was successfully used in electrochemical immunoassays,³²⁴ therefore it was proposed to check its performances in microarray format.

As it is shown in Figure 67B, the signal intensity significantly increased with reaction time in the range of 5–10 min. The signal for 5 min incubation was above 4000 a.u. ($S/N = 24$), while for 10 min it was almost 14,000 a.u. ($S/N = 80$). The background also remarkably increased with longer incubation times.

The lower signal of copper enhancement is not only the matter of the amount of the precipitate but as well of its color. The reddish copper is not the optimal precipitate for the DVD laser absorption. In this case, the deposited metal will more probably only scatter the light but not absorb it. The grey precipitate of silver scatters better the laser light, as well as absorbs in all spectrum (300–800 nm), thus the signal intensity obtained is much higher. Concluding, silver enhancement is much more effective and rapid method for signal development than copper, assuring high signal intensities values with low background signal.

In the next experiment, 50 nL of a GAR-Au solution (1/800) was printed on the disc in a microarray format. The disc was washed and the signal developed using silver enhancement. The assay was performed to check how the spot size changes with the silver enhancement time. The results are shown in Figure 68.

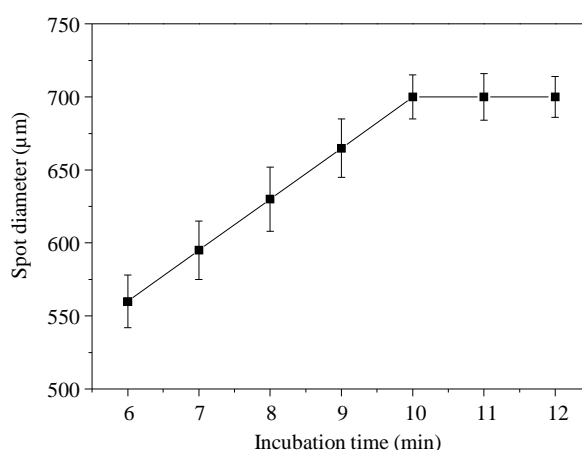


Figure 68. Spot diameter profile upon increment of development time.

As it can be observed, for the shortest time (6 min), the spot diameter is around 550 μm . A reaction time of 10 min resulted already in maximum spots diameter, as longer incubation time showed similar spot sizes. The maximum size obtained was 700 μm . This diameter is more desirable as the focal spot of the laser light used in DVD reader is of 550 μm , thus the resolution of the images obtained is better for bigger spot sizes.

As a conclusion, since multiplex detection of different analytes in a single run is the purpose of this work, a trade-off between the amplification time and the signal intensity obtained for each molecule is needed. Therefore, to obtain high enough signal intensities maintaining low background signal, the optimal time, was set to 10 minutes.

4.9 Individual calibration curves

Multiplex immunoassays involve multiple antibody/analyte pairs, each one having its own optimum performance conditions. There are several aspects that should be considered in the development of the immunoassay in microarray format. First, the signal-to-noise ratio should be high enough, in order to measure the samples with high precision. Second, the dynamic range of the immunoassay developed should cover the relevant concentration of the target analyte. Third, the assay should be reproducible and robust.

Therefore, optimal concentrations of each assay reagent must be established empirically. As the signal-to-noise ratio increases, the assay becomes more effective at measuring small amounts of antigen. The individual calibration curves should be performed and conditions optimized to ensure the highest sensitivity possible for each analyte individually. In the direct coating conjugate assay using the nanogold bioconjugates, the key immuno-microarray parameters such as coating conjugate concentration and optical density of antibody labelled gold nanoparticles

conjugate should be optimized. In competitive immunoassays, these two parameters have tremendous impact on the assay sensitivity. When the antibody concentration is too high, there will be too many binding sites available, therefore if low concentration of the analyte is measured, probably no signal inhibition will be observed. Also, too high concentration of immobilized antigen (coating conjugate) will result in high signal and will mask the competition.

Coating conjugate concentrations and antibody dilutions were selected on the basis of signal intensity, signal-to-noise ratio (S/N) by checkboard titration in a competitive format.

The coating conjugate concentrations ranged between 1.25 and 40 mg/L, whereas nanogold conjugate optical density ranged between 0.2 (dilution 1/50) and 0.02 (dilution 1/500), depending on the studied system.

The typical optimization of the immunoassay based on nanogold antibody conjugate will be discussed using atrazine system as an example. First, four different coating conjugate concentrations (1.25-10.0 mg/L) were tested using the same AbAuNPs dilution (1/500) to check the signal intensities obtained and sensitivity of the tests. The results are represented as competition curves in Figure 69.

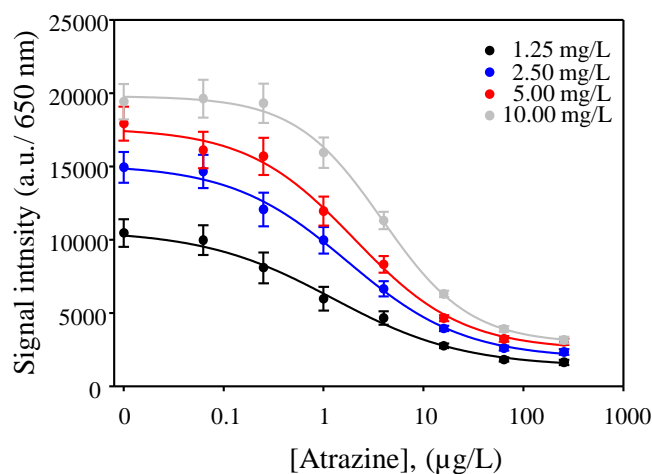


Figure 69. Influence of the coating antigen concentration on the assay sensitivity for atrazine.

As it can be observed, the higher the concentration of coating antigen the higher the signal obtained. For the lowest coating conjugate concentration (1.25 mg/L) the signal in absence of the antigen is close to 10,000 a.u. When the concentration of the immobilized antigen is doubled, the signal increases considerably (50%; from 10,000 to almost 15,000 a.u.). For 5 and 10 mg/L of coating conjugate, the signals obtained are also high, around 18,000 and 19,000 a.u., respectively, when analyte is absent. Regarding the sensitivity of the immunoassays, as it was mentioned, the

density of immobilized hapten has an important impact on the IC_{50} of the tests. The lower sensitivity value was obtained for the lowest concentration of coating conjugate ($IC_{50} = 1.24 \pm 0.14 \mu\text{g/L}$), however, the signal values within the dynamic range of the curve were quite low (between 3500 and 9000 a.u.), thus the possible errors during the quantification might be high. For the assay, when 2.5 mg/L of coating conjugate was used, the sensitivity was $1.73 \pm 0.19 \mu\text{g/L}$, which is only slightly lower (28% lower) compared to the assay when using 1.25 mg/L of coating antigen, but the signal values within the dynamic range are improved (4000-13,000 a.u.). The increase of the coating conjugate concentration from 1.25 to 2.5 did not change drastically the sensitivity, but the signal is higher, thus for quantification purposes it is more convenient, as possible errors are reduced. For the higher antigen concentrations, 5 and 10 mg/L, the sensitivity of the assay was 2.0 and 3.9 $\mu\text{g/L}$, respectively. The best results in terms of sensitivity and precision were obtained for 2.5 mg/L of coating antigen. Lower concentration resulted in higher analytical errors ($RSD \geq 15\%$) and the use of higher concentrations would result in lower sensitivity.

Once the concentration of the coating conjugate was established, different optical density of nanogold bioconjugates were tested. The optical density in case of atrazine ranged between 0.2 and 0.01, which corresponds to dilution of nanogold bioconjugate from 1/50 to 1/1000. The results are seen in Figure 70. Apart from immobilized hapten density, antibody concentration is another limiting factor in competitive immunoassays. As it can be observed, the best sensitivity was obtained for the highest dilution of antibody-nanogold (the lowest optical density – 0.01) - $IC_{50} = 0.93 \pm 0.13 \mu\text{g/L}$, however, the signals obtained are too low and does not meet criteria ($S/N \geq 60$). As it could be predicted, when antibody concentration is increased (higher optical density values), the sensitivity decreases. For nanogold conjugate dilution 1/500, the sensitivity was $1.73 \pm 0.19 \mu\text{g/L}$, whereas for 1/250 it was 1.5 times lower and equal to $2.71 \pm 0.37 \mu\text{g/L}$. The differences in the sensitivity between 1/250, 1/500 and 1/1000 dilutions are significantly meaningful as it was verified by an ANOVA test ($F > F_{\text{crit}}$). When higher optical density is employed, the number of antibody free binding sites is increasing, thus the sensitivity is becoming lower. For dilutions 1/100 the sensitivity was 4 times lower (3.81 $\mu\text{g/L}$), when compared to 10 times less concentrated antibody modified gold nanoparticles. For the highest optical density ($OD = 0.2$), the IC_{50} is almost 10 times lower (8.98 $\mu\text{g/L}$), when compared to the lowest optical density.

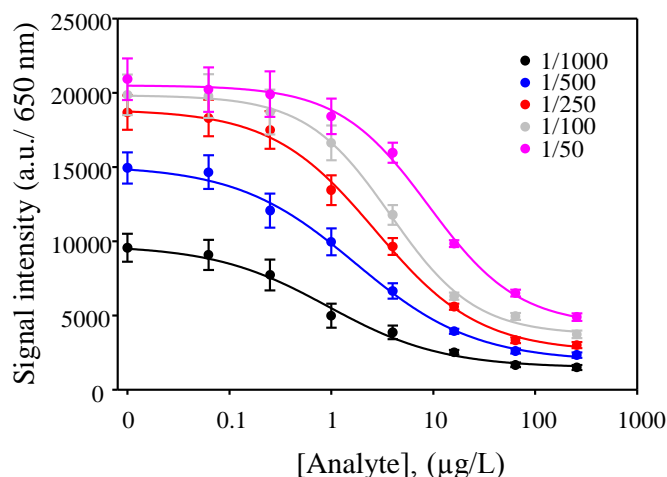


Figure 70. Influence of the nanogold bioconjugate optical density on sensitivity of the immunoassay for atrazine.

Based on those results, the optimal conditions to obtain sensitive immunoassay for atrazine detection are coating conjugate at 2.5 mg/L and AuNPs at 1/500 dilution.

Concluding, the optimization of the immunoassay conditions using antibody modified gold nanoparticles is a trade-off between the coating conjugate concentration and nanogold bioconjugate optical density in order to obtain high signals and high sensitivity, at the same time.

Similar experiments were conducted for other nine analytes. The final results are presented in Table 15. As it can be seen, for each individual analyte different concentrations of the studied parameters had to be used to obtain maximum sensitivity, with low background and no cross-reactivity towards other analytes. As it can be observed, the coating antigen concentration for majority of the studied systems is 10 or 20 mg/L of coating conjugate for the maximum sensitivity and high signal values. The lowest coating antigen concentration used was for atrazine (2.5 mg/L), whereas the highest was for triclosan (50 mg/L). For the antibody modified nanogold conjugates the typical dilution was 1/100, which was used for 50% of the studied systems. The highest dilution, meaning the lowest optical density of the gold (which corresponds to low antibody concentration) were applied for atrazine, azoxystrobin, forchlorfenuron, pyraclostrobin and sulfasalazine. The antibodies for these five analytes were highly specific and showed good titres, thus only a small antibody concentration is necessary to obtain high signals. The lowest dilution was used for alachlor, 4-nitrophenol and triclosan, meaning that the serum obtained comprised mixture of antibodies, many of them being non-specific, therefore higher antibody concentrations were necessary to obtain good signals.

The optimization of these two parameters is crucial when sensitive multiplex immunoassays in microarray format are to be developed. The antibodies cannot be treated equally as their affinity

towards analyte changes depending on the individual properties of each of them. Therefore, this step is remarkably important in fair measurement of the target analytes concentrations in real samples.

Table 15. Optimal concentration of the coating conjugates and nanogold bioconjugate dilution and its optical density for the eighteen analytes studied

Analyte	Coating conjugate (mg/L)	Gold labelled antibody	
		Dilution	Optical density
2-(2,4,5 trichlorophenoxy)propionic acid	10	1/100	0.10
3-phenoxybenzoic acid	10	1/100	0.10
4-nitrophenol	10	1/50	0.20
Alachlor	40	1/50	0.20
Atrazine	2.5	1/500	0.02
Azoxystrobin	5.0	1/500	0.02
Chlorpyrifos	20	1/100	0.10
Diazinon	20	1/100	0.10
Diuron	5.0	1/100	0.10
Endosulfan	20	1/100	0.10
Fenthion	10	1/100	0.10
Forchlorfenuron	10	1/500	0.02
Imidacloprid	10	1/250	0.04
Malathion	20	1/100	0.10
Pentachlorophenol	20	1/100	0.10
Pyraclostrobin	20	1/500	0.02
Sulfasalazine	10	1/500	0.02
Triclosan	50	1/50	0.20

4.10 Selection of the antibodies for the development of a multiplex assay

For multiplex assays, a variety of different antibody/target analyte pairs have to be mixed and the probability of unspecific recognition is more than likely. Therefore, selectivity is a crucial characteristic of antibodies to prove that multiplex immunoassay is possible. Two aspects for the development of multiplex methods should be borne in mind. In planar arrays, where systems are spatially separated not only cross-reactivity but also shared-reactivity is crucial when considering multiplexing. The concept of shared-reactivity is presented in Figure 71A. It occurs when two or more antibodies within a mixture show an affinity to an analyte or coating antigen.

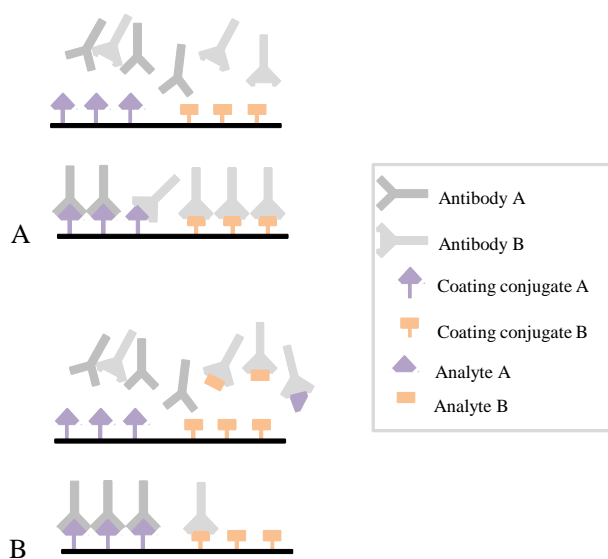


Figure 71. (A) The binding of two antibodies with shared-reactivity to one immobilized coating conjugate.(B) The binding of antibody to two different analytes. Antibody B binds to both analytes, whereas antibody A only to analyte A.

Cross-reactivity (CR) between two ligands for the same antibody describes the case in which both ligands bind to the same binding site, but with different affinities as it is shown in Figure 71B.

Antibody molecules when considering multiplexing should be exquisitely specific, and distinguish subtle differences in the structure of a compound. Otherwise, false results can be expected. Thus, each antibody should detect the target analyte and exhibit limited recognition for other compounds present in the multiplex system.

A typical experimental design in competitive immunoassays is the displacement of antigen from the complex by increasing the concentration of competing free antigen. Such curves reveal the difference in cross-reactivity and shared reactivity as it is illustrated in Figure 72. Cross-reactivity with non-specific molecules is almost always of lower affinity. Therefore, the analyte is displaced only with high concentrations of the competitor, though the displacement curve is similar to that of the specific antigen. In contrast, antigens with shared reactivity compete only for the antibodies reacting with the common epitope, and therefore, lower the bound antigen to a certain level.³²⁵

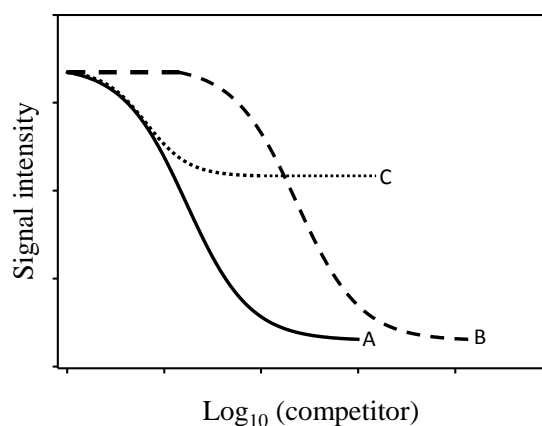


Figure 72. Effect of antigens with shared (B) or cross-reactivity (C) on the displacement of antigen from the immune complex represented as a curve A.

Considering that, the aim of this work is the development of a multi-residue screening assay on a compact disc in a microarray format, the basic concept of the microarray is the use of immobilized capture molecules in a definable location through spatial position to bind specifically to a single analyte. The presence of different capture molecules allows the simultaneous assay of multiple analytes in a complex mixture.

As the multiplex immunoassay is based on the spacial separation of the reagents, there are two key aspects to be considered, the sensitivity and the selectivity of the assay. As far as the sensitivity is concerned, the assay should be able to accurately determine the set of analytes at the lower possible concentration. To reach this goal the first task was the selection of the optimal immunoreagents to see which of the antibodies were showing shared-reactivity and cross-reactivity. As it was described in *Materials and Methods*, a set of 18 antibodies and their coating conjugates were tested in a direct format. For that, the purified antibodies (polyclonal and monoclonal) were labelled with 5 nm colloidal gold and tested by check-board titration in a competitive assay. For these experiments, the optical density of the colloidal gold solutions ranged from 0.01 to 0.4, while the concentrations of the coating conjugate varied from 0.1 to 50 mg/L.

Most of the antibodies used in this work were polyclonal (15 amongst 18 tested) and only three were monoclonal. As it is known, polyclonal antibodies are mixtures of antibodies that recognize different epitopes not only of the analyte but also chemical moieties of arm spacer or part of the protein used for immunization. On the other hand, water pollutants are mainly organic small molecules that show many similarities in chemical structure. Considering these two aspects, it was necessary to study the reactivity of nanogold antibodies against the pool of coating antigens.

For that, microarrays were printed with the 18 different coating conjugates at the optimal concentrations and titrated with the 18 specific nanogold labelled antibodies. The shared-reactivity was calculated as signal ratio and expressed in percentage in a colour coded mode. Results are shown in Table 16. There is a four colour code that represents different levels of shared-reactivity. If there was no shared-reactivity observed, the pairs antibody-coating antigen were marked as green (from 0 to 2%; signal intensity (SI) below 250). If the shared-reactivity was observed, depending on the signal intensity, different colours were used to code the percentage of the recognition. The lowest shared-reactivity was represented by yellow (2-20%; SI - 251 to 2500), for higher – orange was used (20-50%; SI – 2501-6000). The highest extent of shared-reactivity is shown as red (50-100%; SI - 6001 – 10,000 and higher).

As it can be observed from Table 16, many of the antibody nanogold conjugates showed different levels of shared-reactivity towards diverse coating antigens. Only monoclonal antibodies (AZB, FCF and PYS) were highly selective. There was no signal observed where these three antibodies were tested against the rest of coating antigens.

Table 16. Colour coded shared reactivity of antibody-functionalized nanoparticles

		Antibody-nanogold conjugates																		
		4NP	ALA	ATZ	AZB	CLP	DIU	DZN	END	FCF	FN	IMD	MLT	PBA	PCP	PYS	SSZ	TCS	TPA	
Coating antigen	4NP	+++	+	-/+	-	-	+	+	-/+	-	+	-	-/+	+	+++	-	-	+	-/+	
	ALA	++	++++	-	-	-	-	++++	+	-	+	+	-/+	-	-	-	-	-	-	-
	ATZ	+++	-	+++	-	-	-	+++	+	-	+	-	+	-	-	-	-	-	-	+
	AZB	-	-	-	+++	-	-	-	-	-	-	-	-	-	-	-	-	-	-	-
	CLP	++	-	-	-	+++	-	+++	+	-	+++	+	+	-	+++	-	-	-	-	+++
	DIU	-	-	-	-	-	+++	+	+	-	+	++	+	-	+++	-	-	-	-	++
	DZN	-	-	++	-	-/+	++	+++	+	-	+	+	+	+	+	-	+	-/+	+	+
	END	+++	+	-	-	++	+	+	+	++	++	-	+	+	-/+	-	-	++	-/+	-/+
	FCF	-	-	-	-	-	-	-	-	+++	-	-	-	-	-	-	-	-	-	-
	FNT	+	-/+	-	-	+	+	+	+	-	+++	+	+	+	+	+++	-	-	+	++
	IMD	-	-	-	-	-	-/+	+	+	-	+++	+++	+	-	++	-	-	+	+	+
	MLT	-	-	-	-	-/+	-/+	-	-	-	-/+	++	++	-	+	-	-	-/+	-/+	-/+
	PBA	++	-	-	-	-	-	+	-/+	-	+	-	+	+++	++	-	-	-	-	-
	PCP	+++	-/+	-	-	+	+	-/+	-/+	-	+	+	-/+	++	+++	-	-	+	+	+
	PYS	-	-	-	-	-	-	-	-	-	-	-	-	-	-	+++	-	-	-	-
	SSZ	-	-	-	-	-	-	-/+	-	-	+++	+	+++	-	+++	-	+++	-	+	+
TCS	++	-	-	-	-	-	-/+	+	-	-/+	+	+	-	+++	-	-	+++	+	+	
TPA	+	+	-	-	-/+	+	+	+	-	-	+	+	-	+	-	-	+	+++	+++	

Signal intensity (a.u) -: < 250; -/+ : 251-2500; + : 2501-6000; ++ : 6001-8000; +++ : 8001-10,500; ++++ : >10,501



They specifically recognized their coating antigen with high titres (signal intensities above 10,000 a.u.). The reason for such high selectivity lies in the nature of these antibodies. As they are monoclonal, the clone that shows high recognition and titre is selected amongst different clones produced, thus usually they will not show any shared-reactivity towards different coating antigens.

Also, sulfasalazine was very specific, showing shared-reactivity for only one coating antigen – diazinon (34%). Alachlor and atrazine were quite specific as well, however, showed shared-reactivity with more analytes. Anti-atrazine antibodies, for example, recognize some chemical moieties of 4NP and DZN, whereas anti-alachlor antibodies showed shared-reactivity with 4NP, END, FNT, PCP and TPA.

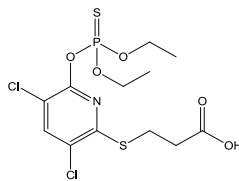
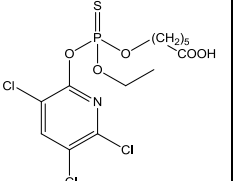
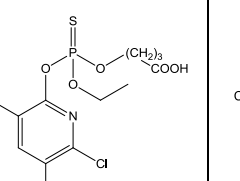
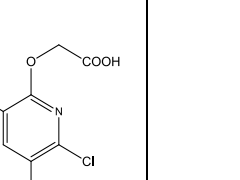
Antibodies raised towards pentachlorophenol, diazinon, fenthion or 4-nitrophenol were non-specific, presenting high degree of shared-reactivity with other antigens. Concretely, the nanogold antibody for 4-nitrophenol (4NP) specifically recognized its own coating conjugate (100%) but also reacted non-specifically with other coating antigens at different extent (2-(2,4,5-trichlorophenoxy)propionic acid, 3-phenoxybenzoic acid, alachlor, atrazine, chlorpyrifos, endosulfan, fenthion, pentachlorophenol and triclosan). The anti-4NP antibody recognizes seven of the mentioned coating conjugates almost with the same titre. This limits the simultaneous analysis of these 9 analytes along with 4NP. Pentachlorophenol, for instance, shows shared-reactivity with twelve other coating antigens, with eight of them in a very high extent (50-100%).

It is interesting to mention that PCP antibodies show higher titre towards OVA-triclopyr - coating antigen used to detect chlorpyrifos, than for its own coating antigen. Also, diazinon and fenthion both show shared-reactivity with 13 coating antigens. The reason is probably due to the fact that particular polyclonal sera comprise antibodies that recognize specific moiety of the chemical structure of the target analyte, but important amount of them also against part of the spacer arm. For instance, the spacer arm was common for diazinon, fenthion, and malathion haptens. Thus, coating antigens share the thiophosphate group and the aliphatic chain through which the carrier protein is attached, so false positive results when testing in heterologous formats might occur. Thus, it can be settled that majority of the non-specific signals are due to the similarities in hapten structures using polyclonal antibodies. Though the number of possible n-plex assays is huge, obviously as the number of analytes to be implemented increases, the chances to set up a selective multi-residue assay decreases as the non-specific signals might show up. If we consider the possibility of setting up all possible duplex assays, the number is very high. Applying sequences without repetition we get 305 duplex assays. However, as the shared-reactivity is a probable event occurring in immunoassays, the real number of duplex assays will be limited. For example, imidacloprid can be analyzed with 4NP and AZB, but it is unfeasible when SSZ or DIU

is present. Similarly, a triplex assay of ATZ, PCP and PYS can be conducted, but to analyze PCP in the presence of 4NP and PBA will result in much lower selectivity. While increasing number of analytes, the simultaneous detection is more difficult, as the compounds show many similarities in chemical structure, thus it is more likely to observe shared-reactivity. Therefore, a hypothesis that using a set of haptens with different arm spacers could be a strategy to palliate the shared reactivity issue was made.

The hypothesis was evaluated by testing gold labelled antibodies for 4-nitrophenol and TPA against a panel of four haptens for chlorpyrifos. The chemical structures of the haptens and the reactivity are shown in Table 17. The structure of hapten C1 maintains the thiophosphate moiety, having the spacer arm as an aromatic ring substituent. Haptens C2 and C3 were synthesized, respectively, by introduction of 6-aminopropionic acid and 4-aminobutanoic acid as amide linkage to the thiophosphate ester, whereas hapten C4 has the shortest spacer arm. As it is shown in Table 17, anti-chlorpyrifos antibody shows low titres for hapten C1, the only hapten with the spacer arm attached to the aromatic ring. Anti-CLP antibodies rendered high titres when using coating conjugates with haptens C2, C3 and C4 which differ only in the length of the spacer arm.

Table 17. Reactivity for gold labelled 4NP, TPA and CLP antibodies

	Coating conjugate			
	C1	C2	C3	C4
Antibody functionalized nanoparticle				
CLP (IC ₅₀ ; µg/L)	-/+	++++ (1013)	++++ (474)	++++ (2.71)
4NP	++	-	++++	++
TPA	++	++++	++++	+++

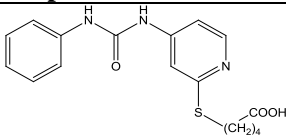
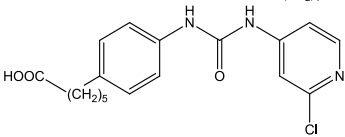
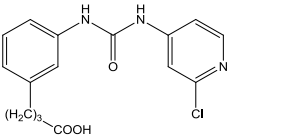
Signal intensity (a.u): < 250; -/+ : 251-2500; +: 2501-6000; ++: 6001-8000; +++: 8001-10,500; +++++: >10,501

On the other hand, both 4NP and TPA antibodies recognize the coating antigens of chlorpyrifos at different extent. Antibodies against 4NP did not recognize hapten C2, whereas TPA antibodies showed nonspecific signal for all tested coating antigens. The highest titres were observed for hapten C2 and C3 (signal intensity above 10,000 a.u.), whereas for hapten C1 and C4 the signal intensities were slightly lower but still high (around 6000-7000 a.u.). Antibodies for 4NP showed

the highest shared-reactivity towards coating conjugate with hapten C3 (more than 10,000 a.u. of signal obtained), whereas for haptens C1 and C5 the signal was lower (around 5000-6000 a.u.). The 4NP antibodies did not recognize the coating antigen with hapten C2, thus it would be possible to integrate this analyte into multiplex detection. However, the sensitivity for chlorpyrifos is drastically lowered when using hapten C2 ($IC_{50} = 1.01 \pm 0.15$ mg/L), while the sensitivity using hapten C4 is three orders of magnitude higher (2.71 ± 0.30 μ g/L).

The hypothesis was also evaluated by studying the influence of three forchlorfenuron haptens against diuron antibody. Both diuron and forchlorfenuron belong to the family of phenylurea pesticides, however, in forchlorfenuron, the chloropyridine ring makes the difference between this compound and other urea derivatives. Therefore, three different haptens functionalized at different positions were tested as it is presented in Table 18. The only hapten that was not recognized by diuron antibody was the hapten s5, which contains the spacer arm (5-methoxy-5-oxopentylmercaptol group) at the C-2 position of the pyridine ring. In addition, the ureido group, a chemical moiety that usually plays a fundamental role in the molecular recognition of this kind of compounds, retains unchanged, and the titre of forchlorfenuron antibody was high when tested against the OVA-s5 conjugate.

Table 18. Forchlorfenuron hapten structures

Hapten	Hapten structure
s5	
p6	
m6	

The shared reactivity values for haptens m6 and p6 with diuron antibody was 26 and 34%, thus they could not be used as coating antigens for forchlorfenuron assay. The assay with the highest sensitivity, was obtained using hapten s5 (0.16 μ g/L), whereas for the m6 and p6, the results were very similar, giving IC_{50} values of 0.32 and 0.27 μ g/L, respectively.

In general, the replacement of the hapten in the coating antigen allows eliminating the shared reactivity of the antibody, thus more analytes could be integrated in a multiplex assay, though in some cases the assay loses the sensitivity to detect the analyte at low μ g/L level. This means that the multi-residue analysis can be tailored to ones need, by adding, replacing or eliminating the analytes

depending on the particular purpose, as long as there are no interferences between other targets. Therefore, though it is possible to avoid non-specific recognition, both the sensitivity and selectivity of the assay limit the development of a multi-residue analysis by the selected immunoassay format.

Antibody-nanogold conjugates against structurally similar compounds require making several considerations. So the challenge in this work was to integrate the maximum number of analytes for multi-residue assay using both polyclonal and monoclonal antibodies with sensitivity at the low $\mu\text{g/L}$. Taken into consideration these challenges, a 10-plex assay, including the simultaneous determination of 3-phenoxybenzoic acid, alachlor, atrazine, azoxystrobin, chlorpyrifos, diuron, forchlorfenuron, pyraclostrobin, sulfasalazine and triclosan was set.

The specific recognition of each antibody only its own coating antigen is presented in Figure 73. As it is shown, each antibody-nanogold conjugate is specific towards its own coating conjugate, showing no reactivity with other protein-hapten conjugates.

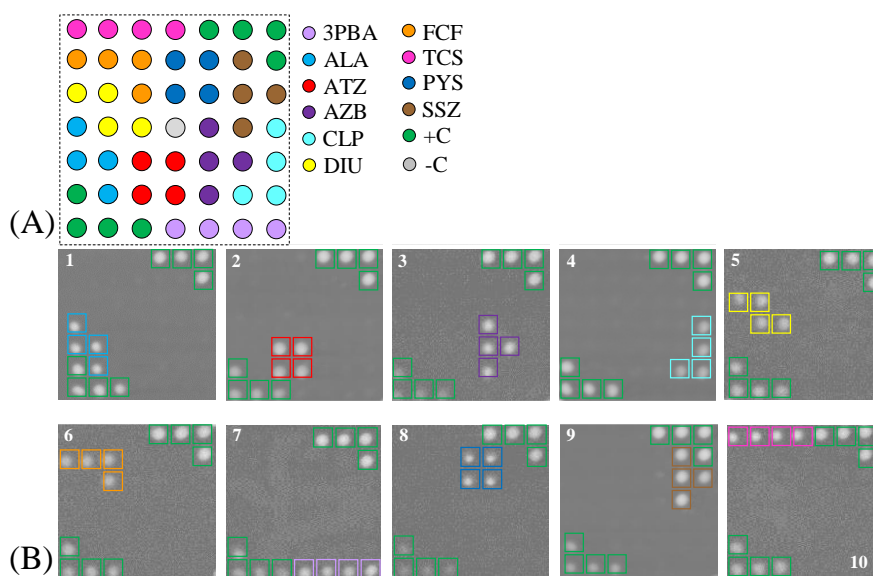


Figure 73. A) Layout of the 10-plex immuno multi-residue assay. B) Images showing the selectivity of antibody-nanogold conjugates. (1. Alachlor; 2. Atrazine; 3. Azoxystrobin; 4. Chlorpyrifos; 5. Diuron; 6. Forchlorfenuron, 7. 3-Phenoxybenzoic acid, 8. Pyraclostrobin; 9. Sulfasalazine, 10. Triclosan).

Each panel (from 1 to 10) represent the test were all coating antigens were printed at the optimal concentrations and only one antibody-nanogold conjugate was tested to check its selectivity.

As it is shown, the spots correspond to the immunorecognition between the antibody-nanogold conjugate to the coating antigen. Also, both controls gave positive results, meaning that the recognition took place correctly. It is interesting to notice that the first control (BSA + KLH) in each particular case gives different signal intensities. This topic will be explained in detail in another section related to the assay controls.

The full selectivity is very important since a lack of it could provoke false positives, thus limiting its use as a screening methodology. Though the number of possible combinations of a 10-plex assay using 18 antibody-functionalized nanoparticles is huge, the selectivity was the main limitation to integrate a larger number of systems. The 10-plex system was not the only possible multiplex configuration. For example, when pentachlorophenol has to be analyzed, five other targets (alachlor, atrazine, azoxystrobin, forchlorfenuron and pyraclostrobin) can be included forming a 6-plex immunoassay. Similarly, a 7-plex can be constructed from such analytes as 3-phenoxybenzoic acid, 4-nitrophenol, atrazine, azoxystrobin, forchlorfenuron, imidacloprid, and pyraclostrobin. Also, smaller multiplex immunotests could be performed. For instance, triplex assays can be conducted in such configurations: atrazine, pentachlorophenol and pyraclostrobin; 4-nitrophenol, imidacloprid and forchlorfenuron; sulfasalazine, endosulfan andalachlor. Similarly, many other triplex or duplex assays can be set. Three examples of the different array layouts are presented in Figure 74.

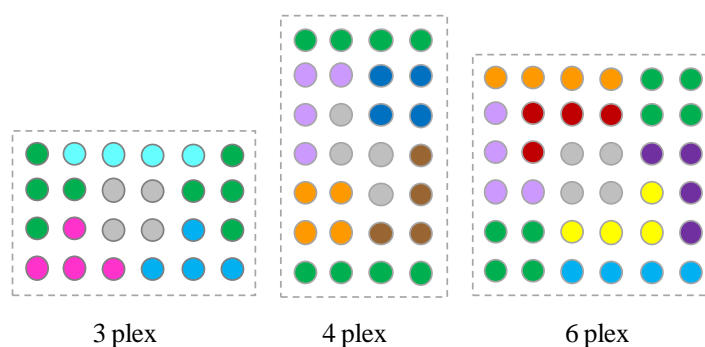


Figure 74. Alternative array configurations (Green and grey arrays correspond to positive and negative controls, respectively).

For example, the 3-plex array could be used to detect MLT, AZB and FCF, or any other three analytes that are free of shared and cross-reactivity. The 6-plex assay would be suitable for the determination of AZB, END, FCF, PBA and PYS.

Not always it is of interest to analyze many different analytes within the same sample, thus the possibility to arrange the number of the analytes according to the specific purpose is a big asset of this approach. Moreover, the arrangement of the microarray matrixes on the disc could be designed in such a way that all eighteen analytes would be analysed in parallel but not simultaneously within the same array. The presented approach shows great flexibility and the ability to analyse mixture of compounds of different families, such as pesticides, herbicides, antibiotics and bactericides, what fulfils the requirements for multi-residue screening and for on-site monitoring.

Recognition of different haptens by a single antibody is not the only problem that has to be faced during multiplex optimization. In order to fully characterize all systems in terms of their selectivity it is crucial to calculate cross-reactivity (CR) between analytes and structurally related compounds. This study was carried out with five main structurally similar compounds used as competitors for each of the ten selected analytes. Table 19 shows the cross-reactivity found by the two-step antigen-coated microimmunoassay using antibody-nanogold conjugates, expressed in percentage of the IC_{50} for each analyte. As it can be seen, the majority of the analytes show only small percentage of cross-reactivity towards some structurally similar compounds. A weak cross-reactivity was observed for alachlor assay by structurally related compounds such as acetochlor (2.2%), butachlor (1.9%), and alachlor oxanilic acid (13.8%). Thus, the developed immunoassay for alachlor was highly specific against the main chloroacetanilides and their metabolites. In case of atrazine, the immunoconjugate carries free chlorine and an isopropyl group in its structure that explains the high recognition observed with derivatives bearing one (atrazine) or two (propazine) isopropyl groups. The high cross-reactivity of propazine seems to be an inherent property of all antibodies raised for atrazine. Cross-reactivity which often exceed 100% could be observed in most polyclonal antibodies.³²⁶ Additionally, the chlorine group seems to be essential for this antibody for good hapten recognition, because no reactivity or only an extremely weak one was observed for triazines lacking this atom as for example, prometryn and ametryn. For chlorpyrifos, assay selectivity was evaluated using a set of organophosphorus insecticides and metabolites because of their similar structure to chlorpyrifos. Interferences were observed for chlorpyrifos-methyl (50%) and chlorpyrifos-oxon (46%). Chlorpyrifos-methyl is not a troublesome interfering, as it is present in many commercial chlorpyrifos formulations. On the other hand, the cross-reactivity to TCP is negligible. Since this is the main chlorpyrifos metabolite, it is possible to determine specifically chlorpyrifos in water.

The most unspecific was the anti-diuron antibody, which cross-reacts with the studied arylurea herbicides. Diuron cross-reacts quite strongly with monuron (64%) and to lower extent with linuron (30%) and monolinuron (25%). This fact could be used as an advantage to detect presence of the compounds from the same family using only one class specific antibody. Among the compounds tested for cross-reactivity for 3-phenoxybenzoic acid, 4-fluoro-3-phenoxybenzoic acid (FPBA), 4-hydroxy-3-PBA, and 3-phenoxybenzaldehyde have significant responses at values of 72%, 105%, and 77%, respectively. However, these metabolites are unlikely present at levels that would make an impact on the results. Other metabolites such as permethrin and esfenvalerate do not cause any interference in the assay up to concentrations tested (10,000 $\mu\text{g/L}$).

Table 19. Cross-reactivity values for structurally related compounds in the ten-plex immunoassay

Compound	IC₅₀ (µg/L)	CR (%)	Compound	IC₅₀ (µg/L)	CR (%)
Alachlor*	2.48	100	Forchlorfenuron	0.16	100
Metolachlor	496	0.4	Thidiazuron	0.81	20
Acetochlor	99.0	2.2	Diphenylurea	>10000	< 0.01
Butachlor	108	1.9	KIN	>10000	< 0.01
Propachlor	496	0.4	<i>Trans</i> -Zeatin	>10000	< 0.01
AOA	35.0	13.8	6-BAP	>10000	< 0.01
Atrazine	1.73	100	3-Phenoxybenzoic acid	1.9	100
Propazine	1.48	110	FPBA	2.6	72
Terbutylazine	7.21	20	4-hydroxy-3-PBA	1.8	105
Simazine	8.81	16	3-phenoxybenzaldehyde	2.4	77
Ametryn	12.8	11	Cypermethrin	>10000	< 0.01
Prometryn	20.1	7	Fenvalerate	>10000	< 0.01
Azoxystrobin	0.88	100	Pyraclostrobin	1.78	100
Kresoxim-methyl	>10000	> 0.01	Dimoxystrobin	> 0.01	> 0.01
Dimoxystrobin	>10000	> 0.01	Picoxystrobin	> 0.01	> 0.01
Picoxystrobin	>10000	> 0.01	Azoxystrobin	> 0.01	> 0.01
Trifloxystrobin	>10000	> 0.01	Trifloxystrobin	> 0.01	> 0.01
Pyraclostrobin	>10000	> 0.01	Kresoxim-methyl	> 0.01	> 0.01
Chlorpyrifos	2.71	100	Sulfasalazine	0.07	100
Chlorpyrifos-methyl	5.42	50	Sulfathiazole	3.71	1.6
Chlorpyrifos-oxon	5.89	46	N ⁴ -Phtalylsulfathiazole	4.00	1.4
Bromophos-methyl	10.84	25	Sulfapyridine	12.0	0.5
Bromophos-ethyl	677.5	0.4	Sulfamethoxazole	86.0	0.07
TCP	>10000	0.01	Sulfadiazine	120	0.05
Diuron	3.52	100	Triclosan	182	100
Monuron	5.50	64	Methyl-triclosan	>3033	<6
Linuron	11.7	30	2,4-Dichlorophenol	>10000	0.03
Monolinuron	14.1	25	2,5-Dichlorophenol	>10000	0.03
Fenuron	352	1	Nitrofen	>10000	0.03
Neburon	0.25	1400	BDE conger 28	444	41

*In bold target molecules

The selectivity of the assay for sulfasalazine was determined against different compounds. As it is shown, negligible CR values lower than 0.1% were obtained for most of the sulphonamides tested. Only sulfathiazole and phtalylsulfathiazole showed CR values in the range from 1 to 1.5%. These results indicate that the developed immunoassay is specific for sulfasalazine and confirm that the hapten used for immunization is valuable for eliciting high-affinity antibodies suitable for the specific detection of sulfasalazine at the low µg/L. Assay selectivity for triclosan was evaluated using a set of chlorophenols, polybrominatedbiphenyl ethers (BDEs), the metabolite methyltriclosan, nitrofen, and oxyfluorfen, as their structures are quite similar to that of triclosan. As noted the interferences were negligible for most of the tested compounds (< 0.03%). Thus, the developed immunoassay is specific for triclosan discerning this compound to the main triclosan metabolite - methyl triclosan and different chlorophenols. Besides, the

structurally related herbicide nitrofen did not show cross-reactivity with triclosan. Only one of the compounds (BDE congener 28) showed a high cross-reactivity (41%) with triclosan. However, the low concentrations found in wastewaters for this compound (<1.4 ng/L) indicate that this would not be a real interference.

On the other hand, monoclonal antibodies against azoxystrobin and pyraclostrobin were specific. Cross reactivity values with structurally similar compound were in both cases always below 0.01. On the contrary, forchlorfenuron showed certain cross-reactivity with thidiazuron (20%), which would allow to use this antibody for the determination of this compound.

Also, cross-reactivity studies were performed using the analytes corresponding to the 10-plex assay. For that, different concentrations of each analyte (0.1, 1.0 10 and 100 µg/L) were tested against the other nine to check any possible cross-reactivity between them. First, no cross-reactivity was observed when the concentration of the analytes was within the working ranges. However, when azoxystrobin, forchlorfenuron and pyraclostrobin were present at 100 µg/L, a slight signal decrease was found for ALA, ATZ, DIU, PBA, SSZ and TCS systems (< 10%). Such small decrease of signal intensity could overestimate the concentration of these analytes. However, the presence of such amount of fungicides is rare in water samples and in the case of being present at 100 µg/L, and due to the elevated assay sensitivity the problem could be overcome by diluting the sample.

4.11 Multiplex calibration curves

In the *in-situ* measurements, where fast assesment of the contamination is demanded, the turnaround time should be short, in order to take any adequate action. Usually, samples are run in batches with freshly-prepared standard curves made by diluting a standard solution. But it is advantageous to analyze samples without performing the full calibration curve. This would shorten the analysis time and allow for high-throughput analysis. To achieve that, one of the possibilities is to build a *master calibration curve*. To create it, 6 to 10 standards are used performing many replicates. Generally, at least 20 “replicates” for each standard are used to establish the master calibration curve. Commonly, 4 Parameter Logistic (4PL) nonlinear regression model is used for curve-fitting.

The calibration curves obtained for the simultaneous determination of the ten selected analytes are shown in Figure 75. The standard curves are the mean of 20 curves performed in different days and on different discs. As it can be seen, for the majority of the analytes the highest signal was around 12,000 a.u., with some exceptions such as for sulfasalazine that it was around 16,000 a.u and for azoxystrobin was slightly above 17,000 a.u. For all of the analytes included in

10-plex, the signal-to-noise ratio was higher than 60, showing clear decrease of the signal in the competitive assay. High signals ensure lower errors and improve the quantification accuracy. The relative standard deviation values along the whole calibration curve were below 10%.

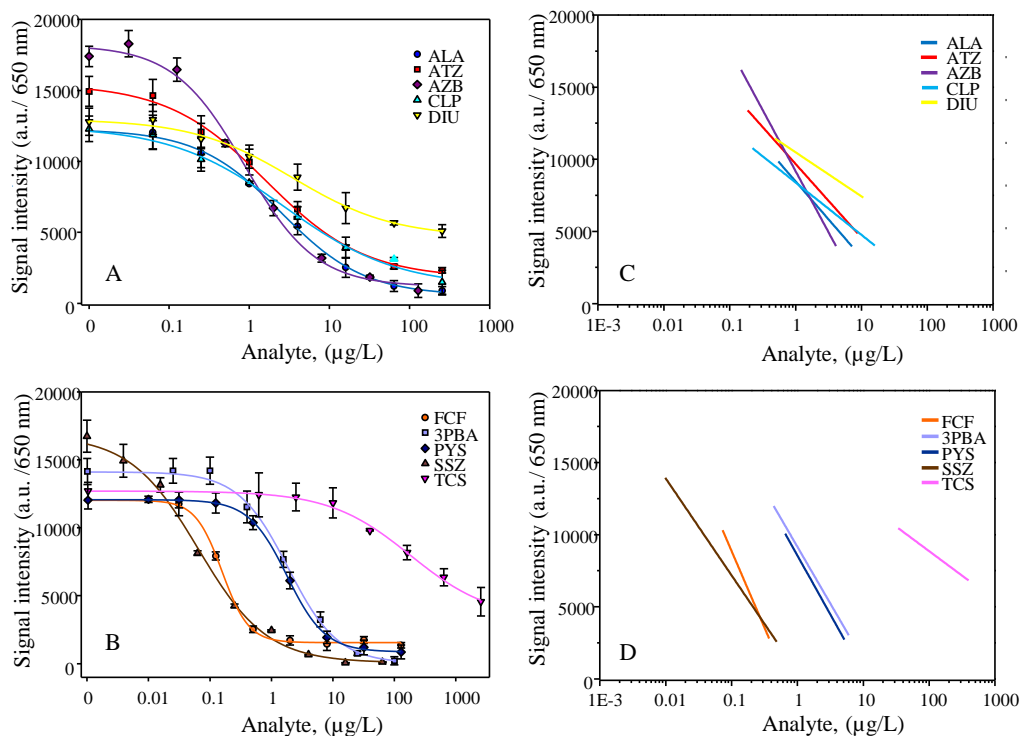


Figure 75. Competition curves for the 10-plex assay. Panel A and B represent sigmoidal curves, whereas panels C and D show the linear working ranges for 10-plex assays.

Table 20 outlines all the analytical features of 18 tested compounds. As it can be seen, limit of detection for sulfasalazine is very low (3 ng/L), which is extremely important, as this veterinary drug is regarded as one of the emerging micropollutants.¹⁶ Thus, having a methodology able to detect traces of this compound in environmental samples can contribute to the legislation update in the future. Also, forchlorfenuron showed very low limit of detection (0.06 $\mu\text{g/L}$), and it should be also mentioned the remarkably steep slope of the curve (-2.0). Such steep slope allows precise and accurate quantitative measurements to be performed. Very steep slope is also observed for pyraclostrobin (-1.4), which showed good sensitivity ($\text{IC}_{50} = 1.78 \mu\text{g/L}$). The sensitivity of the multiplex assay for the majority of the analytes integrated in 10-plex assay gave similar sensitivities which were in the low range of $\mu\text{g/L}$. For example, for 3PBA, ALA, ATZ, CLP, DIU and PYS the IC_{50} values were 1.86, 2.48, 1.73, 2.71, 3.52 and 1.78 $\mu\text{g/L}$, respectively. These results are very interesting as alachlor, atrazine, chlorpyrifos and diuron are listed as priority pollutants under EU Water Framework Directive.

Table 20. Limit of detection (LOD; IC₁₀), sensitivity (IC₅₀), working range (WR), slope, and linear regression coefficient (r²) for all tested analytes

Analyte	LOD (µg/L)	IC ₅₀ (µg/L)	WR (µg/L)	slope	r ²
2-(2,4,5-trichlorophenoxy) propionic acid (TPA)	0.07	1.23 ± 0.22	0.14 - 5.54	-0.93	0.999
3-Phenoxybenzoic acid	0.24	1.86 ± 0.27	0.39 - 6.04	-1.07	0.996
4-Nitrophenol (4NP)	10.9	72.7 ± 21.2	13.5 - 349	-0.97	0.986
Alachlor (ALA)	0.21	2.48 ± 0.24	0.35 - 7.21	-0.83	0.998
Atrazine (ATZ)	0.14	1.73 ± 0.31	0.18 - 8.81	-0.74	0.997
Azoxystrobin (AZB)	0.11	0.88 ± 0.11	0.15 - 4.12	-0.97	0.997
Chlorpyrifos (CLP)	0.11	2.71 ± 0.36	0.22 - 16	-0.61	0.995
Diazinon (DZN)	102	627 ± 33	85 - 1895	-0.86	0.974
Diuron (DIU)	0.36	3.52 ± 0.94	0.49 - 10.7	-0.68	0.994
Endosulfan (END)	1.8	20.2 ± 1.6	5.3 - 37.3	-0.56	0.993
Fenthion (FTN)	1.7	8.4 ± 2.1	2.3 - 34.3	-0.77	0.996
Forchlorfenuron (FCF)	0.06	0.16 ± 0.01	0.06 - 0.52	-2.00	0.999
Imidacloprid (IMD)	0.08	0.32 ± 0.06	0.14 - 0.52	-1.58	0.999
Malathion (MLT)	5.8	15.1 ± 2.4	7.52 - 41.4	-1.32	0.967
Pentachlorophenol (PCP)	1.0	14.2 ± 3.1	2.1 - 25.3	-0.72	0.999
Pyraclostrobin (PYS)	0.39	1.78 ± 0.06	0.46 - 5.14	-1.4	0.999
Sulfasalazine (SSZ)	0.003	0.070 ± 0.011	0.004 -	-0.78	0.998
Triclosan (TCS)	12	182 ± 70	34 - 397	-0.65	0.995

For alachlor, atrazine, and diuron the maximum allowable concentration (MAC) set by this legislation are within working ranges obtained by the developed methodology. The values of MAC for these compounds are 0.7, 2.0, and 1.8 µg/L, for alachlor, atrazine and diuron, respectively. For chlorpyrifos, the maximum allowable concentration is quite low (0.1 µg/L). The limit of detection of the immunoassay for chlorpyrifos reaches of 0.1 µg/L, therefore, the compound can be detected at such low level however, some further confirmation by standard method would be necessary. From all ten analytes, the lowest sensitivity was obtained for triclosan (IC₅₀ = 182 µg/L). The reason of that could be the low affinity of the antibodies towards the analyte molecules, which could be solved by using antibodies showing higher affinity.

Overall, the best sensitivity and selectivity was obtained for the two-step antigen-coated immunoassay using antibody-nanogold conjugates. It is also worth mentioning that the mixture of antibody-nanogold conjugates gave similar sensitivity to that corresponding to single assays under the same working conditions. This fact allows using different combinations of antibodies for the determination *a la carte* residues of contaminants.

Also, competitive assays and corresponding curves were conducted for the 8 analytes that were not included in the 10-plex. As it was explained before, it was not possible to integrate them into the multiplex detection. However, different configurations of the multi-analyte system are possible, thus it was important to see their performances. The calibration curves for the rest of analytes are presented in Figure 76. As it can be observed, imidacloprid system shows the best performances in terms of sensitivity (IC_{50} is equal to $0.32 \mu\text{g/L}$), reaching a limit of detection of $0.08 \mu\text{g/L}$. This result is important as imidacloprid was included in a first watch list of emerging contaminants in the aquatic environment.

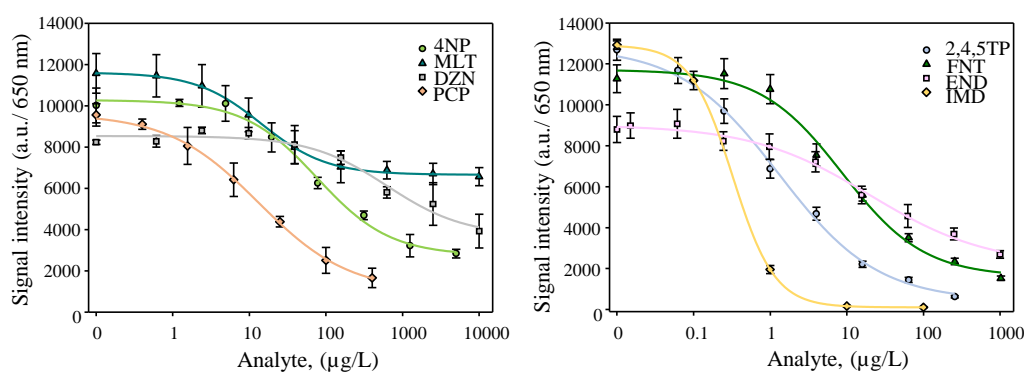


Figure 76. Competitive curves for eight analytes that were not included in the 10-plex assay.

Moreover, on the priority list there is also one more compound studied in this work, endosulfan. The maximum allowable concentration for this compound set by the directive is $0.01 \mu\text{g/L}$. The limit of detection of the assay on DVD is drastically higher ($LOD = 1.8 \mu\text{g/L}$). In this case, the microimmunoassay on disc is a tool with not enough sensitivity to monitor residues of this compound in water.

Also, 2-(2,4,5-trichlorophenoxy) propionic acid showed very good sensitivity with limit of detection and IC_{50} at 0.07 and $1.23 \mu\text{g/L}$, respectively. The rest of the analytes showed sensitivity in the $\mu\text{g/L}$ range. For example, the midpoint of the curve for pentachlorophenol is at $14.2 \mu\text{g/L}$, whereas for fenthion $8.4 \mu\text{g/L}$. Nevertheless, these systems could be used for assays where only binary response is needed, thus fast assessment of contaminated and pollutant free samples could be conducted. The positive samples however would be analysed using a more sensitive confirmatory technique or preconcentrating the analytes.

On the other hand, the matrix layout was designed in such a way, that also simple visual detection can be performed. As we can observe in Figure 77, each system has its own characteristic pattern. As it is seen, by knowing the spatial location of each analyte it is very easy to directly identify which analyte is present in the sample. Thus, if we look at the forchlorfenuron (orange L-shape design) it is clear that this analyte is present at concentration below $1.0 \mu\text{g/L}$,

since the intensity of the spots is very low. Similar observing can be done for sulfasalazine, the other analyte that showed very high sensitivity. Both analytes demonstrate that, obviously using high sensitive antibodies, either monoclonal (FCF) or polyclonal (SSZ) is the key parameter in obtaining good results. On the contrary, in the case of the triclosan (pink upper left line), it is impossible to differentiate, by naked eye, the analyte concentrations up to $16\ \mu\text{g/L}$. In order to obtain quantitative results, disk reading and data analysis must be performed.

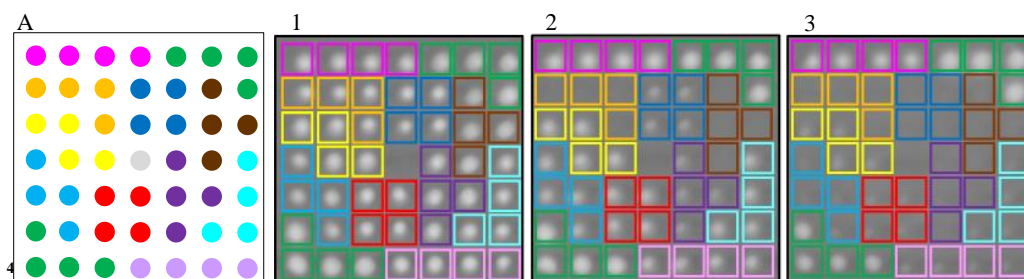


Figure 77. Images of the 10-plex microimmunoassay after reading the disk. Panel A represent the matrix layout, whereas panels 1, 2 and 3 show the spots intensity. The concentration of the mixture analytes in panels 1, 2 and 3 is 0, 1.0 and $16.0\ \mu\text{g/L}$, respectively; see Figure 36 for the layout.

4.12 Study of the assay controls

Best practices in immunoassay performance should always be taken into consideration in order to obtain high quality data. However, the presence of quality controls helps to identify samples for which the data characteristics are significantly different than the majority. Nevertheless, systematic variation may be the result of the experimental process itself. Therefore, it is important to employ in the detection system, adequate controls in order to ensure reproducible results.

In the present work, to verify the reproducibility of the multiplex immunoassay, two positive controls were included in the array. The first comprises a mixture of KLH/BSA and the second anti-rabbit IgG–gold solutions as it is presented in Figure 78. The positive controls were positioned on the corners of the array and consisted of four spots, whereas the negative control was a single spot placed in the centre of the matrix. In practice, the spots of lower left and upper right corners of the array should always be present, but the spot of the centre of the array empty.

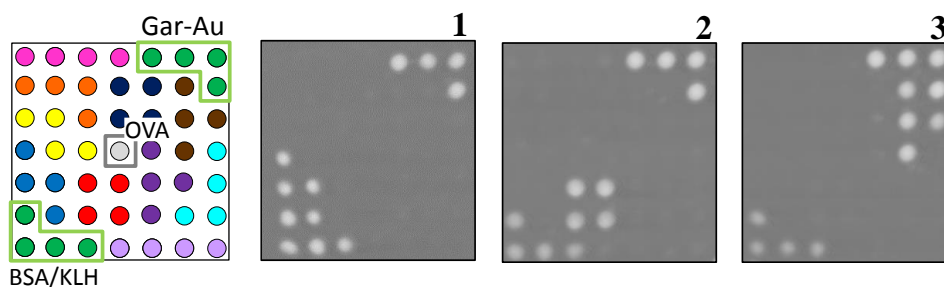


Figure 78. Comparison of the signal intensities of first step control for individual assays (1 – alachlor; 2 – atrazine; 3 – sulfasalazine) in absence of analyte.

For the production of the antibodies used in this work, different immunizing proteins were used. The antibodies included in the 10-plex immunoassay were immunized using either BSA or KLH protein, as it is outlined in Table 21. For seven of the analytes included in 10-plex assay, the protein used for immunogen preparation was bovine serum albumin, whereas for rest of them, keyhole limpet hemocyanin.

The role of the KLH/BSA solution was to control the first step of the assay and relied on the ability of the antibodies to specifically recognize the immunogenic carrier proteins. As it can be observed in the Figure 78, for single assays, the intensity of the first positive control differs depending on the analyte, due to the different titres against the carrier protein. For example, for alachlor and atrazine, the carrier protein was KLH, however, during the production of the antibodies, the number of IgG molecules that recognize the protein moieties varies, and thus different signal intensities are obtained. Moreover, the optical density of antibody-nanogold conjugate for these two analytes is also different (for ALA 0.2, whereas for ATZ 0.02), showing that the atrazine antibody titre against KLH is much higher than the one of alachlor. In case of sulfasalazine, the carrier protein is BSA and the optical density of nanogold bioconjugates is 0.02, indicating that the antibody is specific, therefore shows low titre against BSA.

Table 21. Immunizing proteins used for the preparation of the antibodies integrated in 10-plex immunoassay

Analyte	Carrier protein
Alachlor	KLH
Atrazine	KLH
Azoxystrobin	BSA
Chlorpyrifos	BSA
Diuron	BSA
Forchlorfenuron	BSA
3-phenoxybenzoic acid	BSA
Pyraclostrobin	BSA
Sulfasalazine	BSA
Triclosan	KLH

The second positive control, anti-rabbit IgG–gold was used to provide information about the amplification step, this signal being used as inter and intra-disc calibrator.

In order to determine intra- and interdisc relative standard deviation of positive controls, 20 discs were tested, each one with 20 arrays and 3 replicates per array, a total of 1200 spots being averaged. Figure 79 shows the signal variability between 20 different disks. Each point corresponds to average signal value of twenty arrays (80 points). Analysis of variance (ANOVA) showed that there are no significant differences among the control values ($F < F_{\text{crit}}$; $F = 1.25$ and $F_{\text{crit}} = 3.59$). The intradisc RSD varied from 5% to 12% whereas the interdisc RSD ranged from 3% to 8%, indicating their suitability.

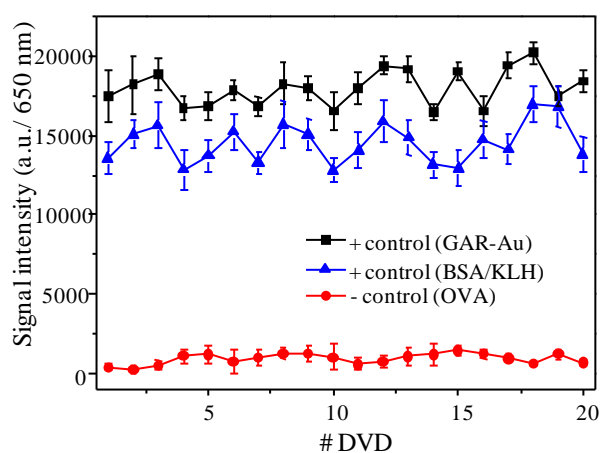


Figure 79. Signal variability for the second positive control (GAR-IgG-Au).

Also, a negative control (OVA) was integrated in the array to corroborate the selectivity of the assays. As it is presented in Figure 79, the negative control values ranged between 244 and 500 a.u., which correspond to signal-to-noise ratio of 1.5 to 3, being very similar to disk background noise.

The implementation of controls is necessary to ensure the quality of the obtained data. The positive controls in this work showed good performances such as low signal variability between the disks. Thus, results from different days and different disks provide assurance that the results of assay are reproducible.

4.13 Study of the antibody-gold nanoparticles stability

The stability of bioreagents is essential if they are to produce consistently accurate results with confidence. For the nanogold bioconjugates prepared in this work, their stability upon time should be determined. Stability of the reagent indicates its ability to maintain expected, and consistent, performance over time without degradation. Stability testing for nanogold bioconjugates should consider antibody activity drift over time, which will be observed by the signal intensity changes.

For that, 3 batches of the antibody modified gold conjugates were prepared and their activity, measured as the signal obtained after antibody-antigen immunoreaction, was studied. This test was performed for a period of 24 weeks as it is shown in Figure 80. The initial signal is slightly above 18,000 a.u. which is maintained up to 13 weeks (Student's t-test, 0.05 threshold level). However, signal variation is observed. The difference during 13 weeks between the highest and the lowest intensity value is 12%. After that time, a significant loss in the activity is observed, following a kinetic degradation of first order ($k_{\text{deg}} = -0.045 \pm 0.04 \text{ week}^{-1}$). The signal values are gradually lowered and the intensity values at week 24 are around 10,000 a.u., being 44% lower than initial intensity. Despite the signal loss, those conjugates can be used for sensing, as long as absolute values are compared.

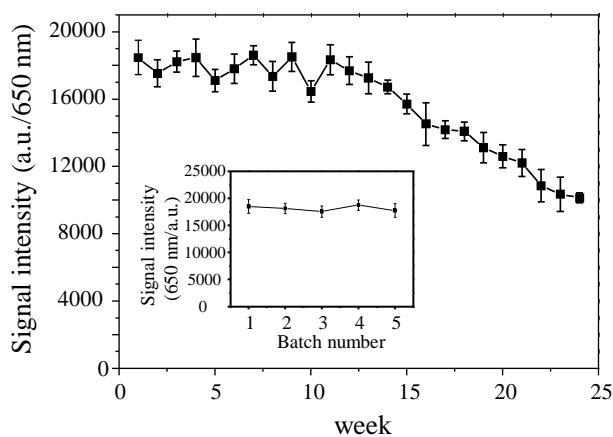


Figure 80. Time stability profile of the nanogold bioconjugates and batch to batch variability.

Another important aspect is the batch to batch variability, since it can affect the signals obtained in competitive assays, thus the sensitivity of the test. Therefore, the preparation of the nanogold antibody conjugates is a crucial step in high reproducibility of the method. Different batches of the antibody modified gold nanoparticles were routinely checked in terms of the optical density and any differences between the batches were corrected to obtain desired initial OD values.

Regarding the variability between batches, as it is shown in the inset of Figure 80, the signal variation was less than 7%, showing good quality assurance in nanogold bioconjugates production.

These results point out the limited shelf life of the nanogold bioconjugates. Considering that the conjugates were stored at room temperature with minimum precaution, three months period is appropriate and meets the requirement of a reliable reagent.

4.14 Immunocapture microimmunoassay

The conceptual principle of this approach is simple and is schematized in Figure 42 (section 3.12.6). The antibodies attached to gold nanoparticles act as capture specie to specifically bind the antigen molecules in solution. As the immunoreaction event occurs much faster in the liquid phase, rather than in a heterogeneous format, the antigen molecules bind faster to the gold labelled antibodies. Next, the unbound antigen molecules are removed by centrifugation. Then, the immunocomplexes are detected on a previously pre-coated DVD with haptenized protein. The recognition event is amplified using silver enhancer solution in case when small nanoparticles are used. Also, an immunocapture assay is performed without amplification step, when 50 nm nanogold bioconjugates are applied.

In order to fully characterize the immunocapture procedure, different parameters were optimized. In the following section, optimization will be described in detail.

4.14.1 Selection of the optimal conditions for homogeneous immunocapture step

The selection of the sample volume and optical density of the nanogold bioconjugate were the parameters optimized. As a model compound, chlorpyrifos was chosen. First, optimal conditions were selected for antibody modified 5 nm nanoparticles. For these experiments, several AbAuNPs dilutions were studied varying both the antibody nanogold (0.25, 0.5 and 1 μL) and the final volume (10, 25 and 50 μL). The optical density of the studied dilutions ranged between 0.05 and 1.0. The solutions without analyte were centrifuged, supernatant discarded and then resuspended in the initial volume. For comparison purposes, the assay was also performed using the same AbAuNPs dilutions directly dispensed on the disc without centrifugation. The assay was performed as described in section 3.12.6. The results are presented in Figure 81.

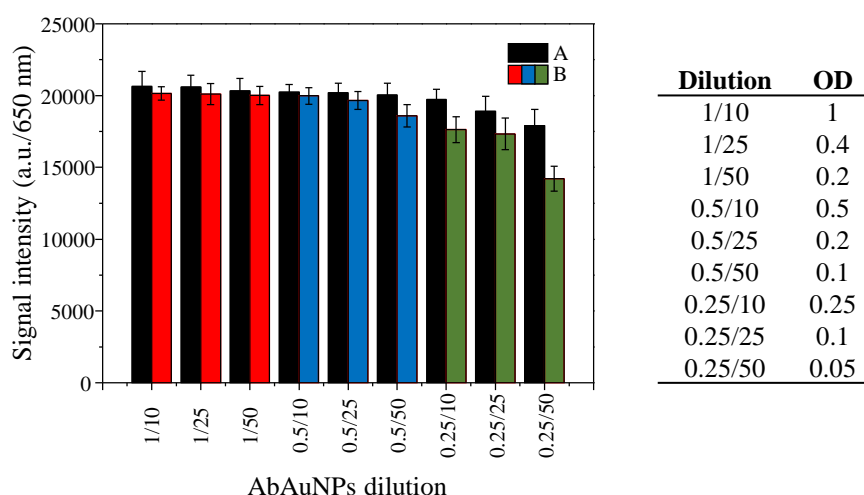


Figure 81. Recovery of the signals after centrifugation of the samples (A: without centrifugation, B: after centrifugation).

As it is observed, for the highest nanogold volume used (1.0 μL) and for all three tested volumes (10, 25 and 50 μL), the signals were similar to those obtained without centrifugation (close to 100%). The signal differences before and after centrifugation are within the standard deviation. Using 0.5 μL , for two smaller volumes (10 and 25) the signal recovery was 98%, whereas for 50 μL , 93% of the signal intensity was recovered. For the lowest nanogold volume (0.25 μL), the loss of the signal is slightly higher with a recovery ranging from 80% to 89% for 50 and 10 μL , respectively. Such significant decrease in the signal intensity is probably due to the loss of gold nanoparticles after the centrifugation.

As a next step in optimization of the immunocapture procedure, competitive immunoassays were performed. As it was demonstrated, the best recovery of the signal after centrifugation was achieved using 0.5 and 1.0 μL of the nanogold conjugate, diluted in 25 μL as the final volume (1/25 and 0.5/25).

Two approaches were compared in terms of immunoassay sensitivity. One consisted in preincubating the antibody modified gold nanoparticles with analyte for 10 min in solution out of the disk and then, disposed onto the disk. This assay is named PI. Similarly, the solution was preincubated during 10 min, and then centrifuged and resuspended with 25 μL PBS-T (assay IC). In the IC approach immunocapture concept was employed. The results are shown in Figure 82.

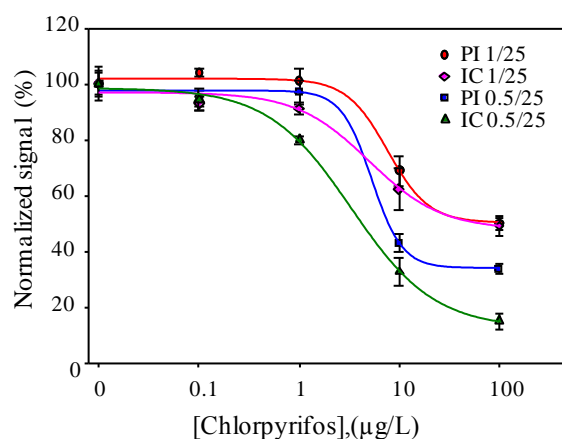


Figure 82. Comparison of the sensitivity between assays with pre-incubation step (PI) and using immunocapture concept (IC).

As it can be observed, the lower dilution (1/25) of the Ab nanogold conjugate gave lower sensitivity in both assays. The assay with only preincubation step was insensitive to low concentrations up to 1.0 µg/L, since no signal decrease or inhibition was observed. On the contrary, for the assay with immunocapture step (IC), the signal inhibition of 8% is observed for 0.1 µg/L. The midpoint of the curve (IC_{50}) for the PI approach was set at 7.7 µg/L, whereas for the immunocapture assay, 5.0 µg/L.

Since in competitive immunoassays the limiting factor is the antibody concentration and as the optical density of the solution was high (1/25), the sensitivity obtained was quite low compared to that shown for the 10-plex approach.

The higher dilution tested (0.5/25) resulted in better sensitivity. In both cases, the assays were sensitive to small analyte concentration of 0.1 µg/L, giving similar signal inhibition (5%). However, for the immunocapture step the signal decrease for 1.0 µg/L was slightly higher (80% of the maximum signal), whereas for preincubation step assay, the signal was 95% of the initial value. For the assay with only preincubation step, the sensitivity (IC_{50}) obtained was 5.3 µg/L, whereas for the immunocapture step, 3.3 µg/L. However, the sensitivity obtained using immunocapture step gave similar results than the standard assay without any preincubation as it is presented in Table 20 (in Section 4.11). The improvement of the assay as it was explained in the introduction of this Chapter could be achieved by reducing the antibody concentrations which should result in higher occupancy of the binding sites of the antibody.

As it was demonstrated, lowering the volume of the Ab nanogold conjugate provokes the loss of the initial signal, thus a preconcentration would be a solution. For that, the experiment was conducted diluting the nanogold conjugate up to 500 µL. Three different Ab nanogold volumes were tested (0.25, 0.5 and 1.0 µL). Figure 83 shows the signal obtained for different optical

density of gold nanoconjugates. The figures correspond to signal obtained after the centrifugation step and resuspension to a smaller volume (25 μL). As it can be observed, similarly to previous assay, increase of the optical densities resulted in higher signals, obtained for dilutions 1/100, 0.5/100 and 0.25/100. The higher the sample volume, the lower signals were obtained. Nevertheless, after centrifugation and resuspension in much smaller volume, are high enough for quantification. The remarkable change was observed when 1.0 μL of nanogold conjugates was used. For example, for dilution 1/500 (which corresponds to $\text{OD} = 0.02$), the signal was increased from 7000 and 17,000 a.u., without and after centrifugation, respectively.

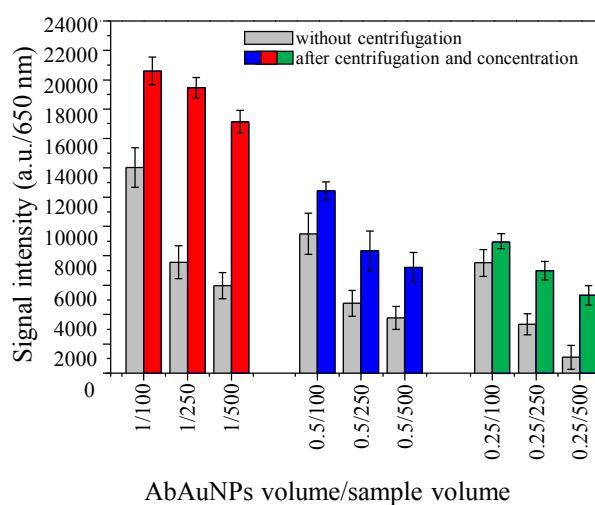


Figure 83. Signal intensity profile for different nanogold bioconjugate-sample volume ratios.

For the lower Ab gold nanoparticles volumes, the signal after centrifugation was higher, but the increase of the intensity was much lower compared to signal obtained using 1.0 μL . The reason is probably due to the non-quantitative recovery of the gold nanoparticles after the centrifugation step. For the lowest nanogold conjugate volume (0.25 μL), the signals even after centrifugation were quite low. The highest signal was 9000 a.u. ($S/N = 54$), with important error figures ($\text{RSD} > 15\%$). Therefore, a trade-off between nanogold bioconjugate consumption and signal intensity and sensitivity had to be made in order to get maximum sensitivity along with low reagent consumption.

4.14.2 Competitive assays using immunocapture step

It was demonstrated before that the lowest volume of nanogold gave the highest irreproducibility. Thus, only two volumes of AbAuNPs were tested (0.5 and 1.0 μL), the ones that gave better signal recovery results in previous experiments. The immunoreaction volumes were 100, 250 and 500 μL . After centrifugation, the nanogold conjugates were resuspended in 25 μL . The curves are presented in Figure 84.

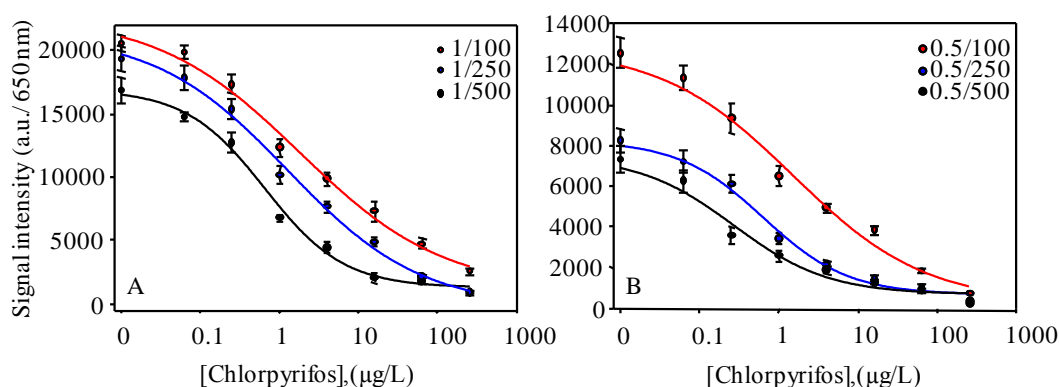


Figure 84. Competitive assays in immunocapture format. Curves obtained using 1.0 μL (A) and 0.5 μL (B) of nanogold conjugate.

For 0.5 μL , the signal values obtained were considerably lower compared to 1.0 μL of nanogold. The highest signal intensity was around 12,000 a.u. For the dilution 0.5/250 and 0.5/500, the recovery of the signal was not sufficient. The signals were too low, being around 7000-8000 a.u., which corresponds to signal-to-noise ratio of 40-45, respectively. As it was mentioned in previous chapters, the optimal S/N ratio should be 60, in order to have enough signal in the dynamic range. The sensitivity expressed as IC_{50} for the assay using 0.5/500 dilution was 0.27 $\mu\text{g/L}$ and for the 0.5/250 dilution the midpoint of the curve was at 0.64 $\mu\text{g/L}$. This value is very similar to the value obtained using 1/500 dilution (0.65 $\mu\text{g/L}$). However, as far as the signals are concerned, assay using 0.5/250 dilution gave half lower signal compared to that obtained with 1/500 dilution. In terms of the signal intensity, the best results were obtained for the assay using 0.5/100 dilution (12,000 a.u., S/N = 69). Midpoint of the curve was at 1.53 $\mu\text{g/L}$, however 2-times lower than in case of 1/500 dilution.

As it can be observed, better recovery of the Ab nanogold was obtained for 1.0 μL of AbAuNPs, which is displayed as higher intensity signals, ranging between 17,000 and 21,000 a.u. As it could be predicted, the lower the optical density (1/500), the better the sensitivity obtained. The sensitivity of the assay was 1.82 $\mu\text{g/L}$, 1.63 $\mu\text{g/L}$ and 0.65 $\mu\text{g/L}$, for the 1/100, 1/250 and 1/500 dilutions, respectively.

To select the optimal conditions a trade-off should be made, as different parameters are important when optimizing an immunoassay. The crucial parameters in this case are sensitivity and the nanogold consumption. The latter one also decides about the reproducibility of the immunoassay, as the recovery of the signal plays an important role. Taking into account these aspects, the conditions selected are 1.0 μL of antibody modified gold nanoparticles and 500 μL of the sample. These conditions gave a good balance between high signal intensity ($S/N \sim 100$), sensitivity ($IC_{50} = 0.65 \mu\text{g/L}$), and reproducibility ($RSD < 10\%$).

As a next step, immunocapture concept was applied for the chlorpyrifos detection. This approach consisted in preincubating the sample for 10 min, at selected conditions, concentrating the solution and performing the detection. Simultaneously, a standard immunoassay was also conducted to compare the sensitivity, previously described in 10-plex optimization (Figure 38). This assay consisted in mixing the nanogold bioconjugate with the sample and then directly applying the solution onto the precoated disk. The AbAuNPs was used at 1/100 dilution. Also, the assay consisting only in preincubation (10 min) of the sample with nanogold was evaluated. The results are presented in Figure 85.

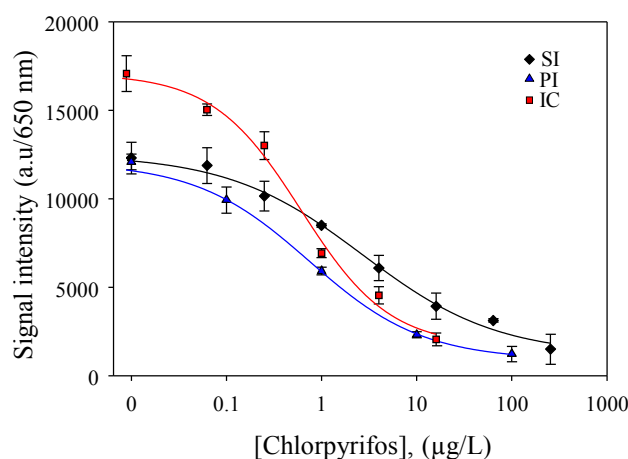


Figure 85. Competitive curves for chlorpyrifos for different immunoassay approaches (SI – standard immunoassay; PI – preincubation immunoassay, IC – immunocapture step) for chlorpyrifos.

As seen in Figure 85, it can be seen that the best sensitivity was obtained for the immunocapture approach. The sensitivity expressed as IC_{50} is $0.65 \mu\text{g/L}$ with LOD equal to $0.06 \mu\text{g/L}$. The dynamic range of this approach was $0.11\text{--}3.6 \mu\text{g/L}$ and hill slope -0.93 as it is shown in Table 22.

The standard immunoassay that was used for 10-plex measurements is less sensitive as the IC_{50} is 2.71 $\mu\text{g/mL}$. The dynamic range was wider ranging from 0.22 to 15.95 $\mu\text{g/L}$, but the slope was -0.61 which is less steep than for IC assay.

Preincubating the sample improves the sensitivity as it was demonstrated for the third approach. Here the IC_{50} was 0.74 $\mu\text{g/mL}$ with the slope of -0.72. Comparing to the standard assay the sensitivity was 3.6-times better. Nevertheless, none of these assays reached the sensitivity of the immunocapture approach.

The immunocapture approach showed better performances than standard immunoassay format. This simple step allows working with low antibody concentrations, thus the sensitivity can be considerably improved. The advantage of the method is also the fact that, the same conditions could be used for different analytes, so the immunoassay optimization could be reduced. Also, important assets of the method are low consumption of the antibody nanogold and no need for sophisticated equipment.

Table 22. Analytical parameters of chlorpyrifos immunoassays for immunocapture, preincubation and standard immunoassay approaches with signal amplification

Parameter	IC	PI	SI
S/N_{\max}	98	64	70
IC_{50} ($\mu\text{g/L}$)	0.65 ± 0.07	0.74 ± 2.3	2.71 ± 0.47
DR ($\mu\text{g/L}$)	0.11 ± 3.6	0.31 ± 11.5	0.22 – 15.95
slope	-0.93	-0.72	-0.61
r^2	0.995	0.996	0.995

The immunocapture approach was also tested for the assay without signal amplification. For that, 50 nm nanogold bioconjugates were used. As a model compound anti-pyraclostrobin monoclonal antibody was selected. The idea consisted in preincubating the sample, as it was described above, centrifugation, concentration and detection. Here, the signal could be observed through deposition of gold nanoparticles on the disk surface.

As a first step, different optical densities of the gold were tested. As it was already stated in section 4.4, there is necessary to use high optical density nanogold bioconjugate solutions to get high signals without any amplification step. Therefore, the volume of the antibody modified gold nanoparticles was 5.0 μL , whereas the sample volume ranged between 50 and 500 μL . These

conditions were tested for the samples in absence and at analyte concentration of 1.0 $\mu\text{g/L}$. The results are shown in Figure 86.

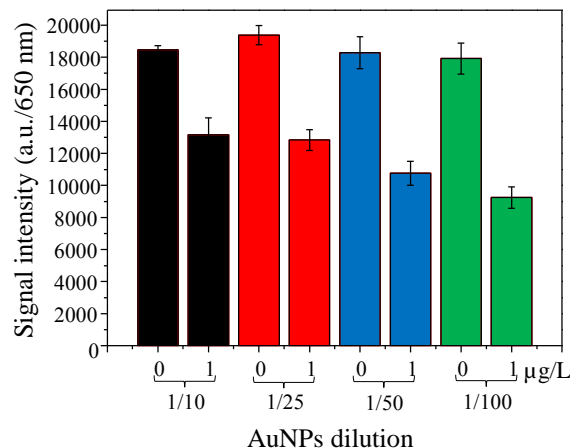


Figure 86. Pyraclostrobin titration experiments to evaluate the optimal AuNPs dilution for immunocapture step.

As it was demonstrated in the immunocapture approach with signal amplification, low antibody concentration in the preincubation step, improves the sensitivity of the assay. This statement is confirmed also in the immunocapture without signal enhancement. For the 1/10, 1/25 and 1/50 dilutions, 1.0 $\mu\text{g/L}$ of pyraclostrobin inhibited the maximum signal in 28%, 34% and 41%, respectively. The best results for the competitive assay were obtained for the 1/100 dilution, observing an inhibition of 52% of maximum signal. These results were confirmed by performing full calibration curve applying the immunocapture step. Also, to compare the results, a standard one step assay was performed. In the immunocapture step, after the centrifugation, the nanogold was resuspended up to 10 μL , in order to have high optical density solution. As it was demonstrated already, to obtain the best results in a one-step assay, 1/1 (v/v) is the best dilution. The competitive curves are presented in Figure 87.

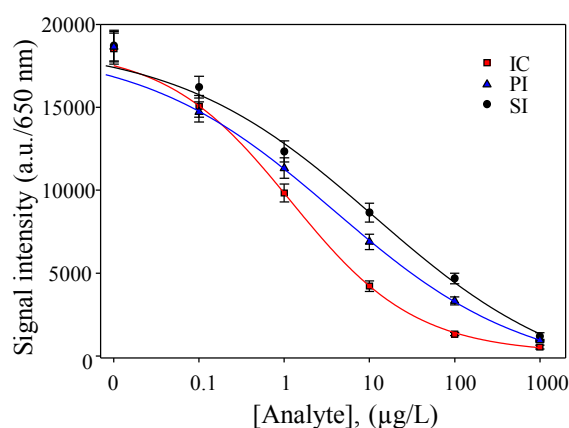


Figure 87. Calibration curves for three different one step immunoassays approaches (SI – standard immunoassay; PI – preincubation immunoassay, IC – immunocapture step).

Similarly to immunocapture assay with signal amplification, the lowest sensitivity showed the standard one step immunoassay (Table 23). The IC_{50} was being $11.9 \mu\text{g/L}$ with the slope of the curve -0.38 . The reason of such low sensitivity is due to the high concentration of the antibody molecules, as high optical density of the nanogold bioconjugates is required. By applying the preincubation step, the sensitivity was considerably improved. The IC_{50} value for this assay was $3.8 \mu\text{g/L}$, being 3-times higher than for one step standard assay. Also, the slope of the curve was slightly improved (-0.41). Nevertheless, none of these assays could reach the sensitivity obtained when immunocapture step was introduced. Here, the sensitivity was almost 10- and 3-times better when compared to the standard (SI) and preincubation (PI) assays, respectively. The midpoint of the curve corresponds to $1.23 \mu\text{g/L}$ and the slope was -0.58 .

Table 23. Comparison of analytical parameters for standard immunoassay and immunocapture without signal amplification

Parameter	IC	PI	SI
S/N_{\max}	103	103	100
IC_{50} ($\mu\text{g/L}$)	1.23 ± 0.19	3.81 ± 0.28	10.6 ± 1.98
DR ($\mu\text{g/L}$)	0.14 - 11.6	0.21 - 70.0	0.47 - 127.1
slope	-0.58	-0.41	-0.38
r^2	0.997	0.997	0.998

Immunocapture approach showed good performances in both described assays. The sensitivity was improved comparing to the standard assay that was applied for 10-plex analysis. This simple idea allows for using the nanogold bioconjugates as both capture agents and signal tags. Also, depending on the gold nanoparticles size used the immunocapture approach could be performed with signal enhancement and without amplification. Overall, the immunocapture approach is a simple method that does not require any expensive equipment showing utility for immunoassay sensitivity improvement.

4.15 Determination of the potential of the developed methodology. Analysis of water samples

The suitability of the multiplex method based on the antibody labeled gold nanoparticles for the determination of residues of ten micropollutants in water was evaluated. For this, fifteen different fortified natural water samples were prepared because it is nearly impossible to get real samples with all the selected residues targets. In parallel, the same samples were analyzed by a validated laboratory using the reference methods.

The spiked levels are given in Table 24 together with the recovery values (R; %). As it can be seen, for the samples 1, 2 and 3 there was an overestimation of the alachlor concentration, as the recoveries for this analytes were 136, 129 and 122%, respectively. Also, in sample 1 two analyte concentrations were slightly underestimated: atrazine that gave the recovery value of 77% and azoxystrobin – 78%. In sample two, low recoveries were obtained for chromatographic analysis of four from six analytes. Those analytes were alachlor, atrazine, azoxystrobin and pyraclostrobin. The recoveries for these analytes ranged between 70 and 75%.

For the sample 3, the recovery results using chromatographic analysis also resulted in underestimation of analyte concentrations. The low recoveries were obtained for alachlor, diuron, azoxystrobin and pyraclostrobin. Surprising results were obtained for diuron, where the recoveries using immuno-disk were much higher (R = 138%), whereas chromatographic analysis resulted in very low recovery of diuron sample, being only 34%. Also, using the immunoassay methodology, pyraclostrobin and atrazine concentrations found in sample 3 were lower than expected (R= 61% and 73%, respectively).

Samples 4, 5 and 6 contain residues of six analytes: ALA, ATZ, DIU, SSZ, PBA and CLP. The recovery values for alachlor in samples 4, 5 were also high, being 137 and 144%, respectively. Chromatographic analysis resulted in very low recovery for this analyte in sample 6 (R = 46%), whereas for the immunoassay method, the recovery was within acceptable range. Also, using standard analytical method, the concentrations of chlorpyrifos in samples 4 and 5 were underestimated (recoveries of 67 and 65% for samples 4 and 5 respectively). On the contrary, using the proposed method chlorpyrifos recoveries for samples 4 and 5, were within acceptable

recovery range. Also, recovery value for diuron in sample 6, was slightly higher, being 129%. Moreover, the results obtained using immunoassay method resulted in slightly underestimated values (71 and 73%).

In case of sample 7, the only problematic analyte in terms of the sensitivity was triclosan. The spiked concentration was 2.0 µg/L, which by proposed immunoassay cannot be analysed as limit of detection for this analyte is 12 µg/L, while chromatographic analysis gave underestimated recovery result (R = 67%). Such underestimated result was also obtained for sample 9.

In samples 8 and 9 chromatographic analysis gave overestimated recovery results for sulfasalazine (129 and 134%, respectively), whereas the recoveries for the immunoassay method were in the good concentration range. Also, forchlorfenuron concentration was slightly low using immunoassay approach (R = 72%). In samples 10, 11 and 12 all the 10 analytes were analysed simultaneously.

Table 24. Results obtained for the immuno multi-residue^a and chromatographic^b analysis (GC-MS or HPLC-MS) of spiked water sample

	Added ($\mu\text{g/L}$)	Found ($\mu\text{g/L}$)		Recovery (%)			Added ($\mu\text{g/L}$)	Found ($\mu\text{g/L}$)		Recovery (%)			Added ($\mu\text{g/L}$)	Found ($\mu\text{g/L}$)		Recovery (%)	
Sample	1						2						3				
ALA	2	^a 2.71 ± 0.48	^b 1.70 ± 0.25	136 ^a	85 ^b		1	1.29 ± 0.41	0.75 ± 0.15	129	75		0.5	0.61 ± 0.09	0.33 ± 0.10	122	66
ATZ	4	4.12 ± 1.04	3.08 ± 0.22	103	77		2	2.22 ± 0.54	1.44 ± 0.30	111	72		1	0.73 ± 0.20	0.82 ± 0.16	73	82
DIU	8	8.42 ± 0.86	6.82 ± 1.11	105	85		4	4.81 ± 0.72	3.40 ± 0.21	120	85		2	2.75 ± 0.58	0.67 ± 0.21	138	34
AZB	1	1.14 ± 0.16	0.78 ± 0.12	114	78		0.5	0.55 ± 0.06	0.37 ± 0.12	110	74		0.25	0.28 ± 0.04	0.18 ± 0.06	112	72
FCF	0.5	0.59 ± 0.05	0.42 ± 0.11	118	84		0.25	0.27 ± 0.04	0.20 ± 0.08	108	80		0.125	0.14 ± 0.09	0.09 ± 0.01	112	72
PYS	2	1.80 ± 0.28	1.69 ± 0.31	90	85		1	0.61 ± 0.11	0.70 ± 0.18	61	70		0.5	0.41 ± 0.05	0.44 ± 0.12	72	88
Sample	4						5						6				
ALA	2	2.73 ± 0.65	2.40 ± 0.31	137	120		1	1.44 ± 0.23	1.10 ± 0.28	144	110		0.5	0.51 ± 0.06	0.23 ± 0.15	102	46
ATZ	4	2.83 ± 0.12	3.29 ± 0.45	71	82		2	1.46 ± 0.25	1.68 ± 0.19	73	84		1	0.97 ± 0.13	0.83 ± 0.17	97	83
DIU	8	6.71 ± 0.52	7.96 ± 0.92	84	100		4	4.87 ± 0.36	4.12 ± 0.44	122	103		2	2.57 ± 0.63	2.03 ± 0.10	129	102
SSZ	2	1.95 ± 0.14	2.14 ± 0.33	98	107		1	0.92 ± 0.26	1.06 ± 0.11	92	106		0.5	0.46 ± 0.21	0.50 ± 0.04	92	100
PBA	4	4.41 ± 0.02	3.45 ± 0.56	110	86		2	2.64 ± 0.39	2.03 ± 0.28	132	102		1.00	1.17 ± 0.54	1.34 ± 0.17	117	134
CLP	2	2.36 ± 0.41	1.34 ± 0.41	118	67		1	0.99 ± 0.28	0.65 ± 0.16	99	65		0.5	0.66 ± 0.16	0.37 ± 0.07	132	74
Sample	7						8						9				
AZB	1	0.86 ± 0.19	0.87 ± 0.16	86	87		0.5	0.47 ± 0.16	0.47 ± 0.09	94	94		0.25	0.29 ± 0.07	0.25 ± 0.09	116	100
FCF	0.5	0.48 ± 0.20	0.57 ± 0.12	96	114		0.25	0.34 ± 0.05	0.28 ± 0.03	136	112		0.125	0.09 ± 0.03	0.13 ± 0.02	72	104
PYS	2	2.06 ± 0.53	1.84 ± 0.28	103	92		1	1.21 ± 0.45	0.93 ± 0.09	121	93		0.5	0.59 ± 0.29	0.43 ± 0.12	118	86
SSZ	2	2.15 ± 0.11	2.80 ± 0.20	108	140		1	1.11 ± 0.25	1.29 ± 0.11	111	129		0.5	0.46 ± 0.11	0.67 ± 0.07	92	134
TCS	2	< LOD	1.33 ± 0.16	-	67		1	< LOD	0.78 ± 0.14	-	78		0.5	< LOD	0.38 ± 0.09	-	76

Table 24. Results obtained for the immuno multi-residue^a and chromatographic^b analysis (GC-MS or HPLC-MS) of spiked water sample

Sample	10				
ALA	2	2.68 ± 0.39	1.33 ± 0.24	134	67
ATZ	4	3.80 ± 0.62	3.13 ± 0.49	95	78
DIU	8	8.93 ± 0.61	7.74 ± 0.96	112	97
AZB	1	1.20 ± 0.18	0.87 ± 0.11	120	87
FCF	0.5	0.63 ± 0.05	0.50 ± 0.06	126	100
PYS	2	1.66 ± 0.44	1.90 ± 0.18	83	95
PBA	4	4.00 ± 0.53	3.28 ± 0.53	100	82
CLP	2	1.46 ± 0.35	1.29 ± 0.28	73	64
SSZ	2	1.92 ± 0.61	2.83 ± 0.29	96	142
TCS	2	< LOD	1.33 ± 0.14	-	66
Sample	13				
AZB	1	0.99 ± 0.18	0.93 ± 0.08	99	93
FCF	0.5	0.44 ± 0.19	0.56 ± 0.06	88	112
PYS	2	2.50 ± 0.53	2.04 ± 0.18	125	102
PBA	4	4.82 ± 0.61	3.57 ± 0.47	121	89
CLP	2	2.21 ± 0.19	1.39 ± 0.19	111	70
SSZ	2	2.36 ± 0.16	3.46 ± 0.61	118	173
TCS	2	< LOD	1.32 ± 0.15	-	66

11				
1	1.34 ± 0.16	0.75 ± 0.13	134	75
2	2.34 ± 0.73	1.47 ± 0.68	117	74
4	3.76 ± 0.56	4.06 ± 0.62	94	102
0.5	0.43 ± 0.08	0.48 ± 0.06	86	96
0.25	0.33 ± 0.03	0.26 ± 0.01	132	104
1	0.65 ± 0.07	0.84 ± 0.05	65	84
2	1.58 ± 0.16	2.07 ± 0.11	79	104
1	1.16 ± 0.31	0.74 ± 0.22	116	74
1	1.04 ± 0.41	1.17 ± 0.33	104	117
1	< LOD	0.67 ± 0.25	-	67
14				
0.5	0.41 ± 0.04	0.51 ± 0.03	82	102
0.25	0.29 ± 0.02	0.27 ± 0.01	116	108
1	0.82 ± 0.18	0.99 ± 0.09	82	99
2	2.38 ± 0.34	1.73 ± 0.21	119	87
1	1.26 ± 0.31	0.79 ± 0.28	126	79
1	0.85 ± 0.27	1.91 ± 0.16	85	191
1	< LOD	0.72 ± 0.22	-	72

12				
0.5	0.61 ± 0.13	0.31 ± 0.08	122	62
1	0.92 ± 0.22	0.74 ± 0.13	92	74
2	2.75 ± 0.49	1.98 ± 0.38	138	99
0.25	0.23 ± 0.14	0.23 ± 0.14	92	92
0.125	0.11 ± 0.01	0.12 ± 0.01	88	96
0.5	0.52 ± 0.11	0.47 ± 0.12	104	94
1	1.19 ± 0.25	1.38 ± 0.24	119	138
0.5	0.55 ± 0.12	0.37 ± 0.12	110	74
0.5	0.58 ± 0.24	0.69 ± 0.14	116	138
0.5	< LOD	0.39 ± 0.11	-	78
15				
0.25	0.14 ± 0.06	0.24 ± 0.03	56	96
0.125	0.11 ± 0.04	0.13 ± 0.01	88	104
0.5	0.42 ± 0.08	0.49 ± 0.07	84	98
1	1.32 ± 0.43	0.85 ± 0.11	132	85
0.5	0.62 ± 0.12	0.40 ± 0.08	124	80
0.5	0.57 ± 0.09	1.40 ± 0.03	114	280
0.5	< LOD	0.38 ± 0.06	-	76

In sample 10, alachlor and forchlorfenuron concentrations in spiked sample were overestimated using the proposed methodology (134 and 126% for ALA and FCF, respectively). The chromatographic analysis resulted in underestimated recovery values for alachlor (67%), atrazine (78%), chlorpyrifos (64%) and triclosan (66%). Low recovery was also obtained for chlorpyrifos using immunoassay approach (73%).

In sample 11, the recovery results for alachlor and forchlorfenuron are very similar to those in sample 10. Both analytes showed higher recovery results (134 and 132%, respectively). Similarly, triclosan analysed by chromatographic method gave low recovery results (67%). Also, low recovery was obtained for pyraclostrobin (65%) and 3-phenoxybenzoic acid (79%), using immunoassay approach. Underestimation of the concentrations found was also observed for alachlor, atrazine and chlorpyrifos using chromatographic method. For these analytes recoveries were between 74 and 75%.

When it comes to sample 12, alachlor again gave acceptable recovery results (122%) using the immuno-disk method, while standard analytical method resulted in underestimation of the alachlor concentration (62%). Overestimation of the analyte concentrations was also observed for diuron (13%, immunoassay method), 3-phenoxybenzoic acid and sulfasalazine (both 138%) performing the chromatographic analysis, whereas low recoveries were obtained for atrazine, chlorpyrifos and triclosan (recoveries between 74 and 78%).

Samples 13, 14 and 15 consisted in seven analytes: AZB, FCF, PYS, PBA, CLP, SSZ and TCS. For sample 13, two of the seven compounds analysed gave slightly high recovery results using the proposed method. Those analytes were pyraclostrobin and 3-phenoxybenzoic acid and the recovery results were 125 and 121%, respectively. Similarly to other samples, in this one triclosan concentration using chromatographic analysis was underestimated (R = 66%). Also, chromatographic analysis for chlorpyrifos resulted in low recovery (70%).

For sample 14, only chlorpyrifos gave high recovery result – 126% when analysed by immunoassay approach. Standard analytical method for chlorpyrifos and triclosan resulted in underestimated recovery values (79 and 72%, respectively).

In sample 15, three analytes were overestimated. Two of them by using multi-residue immunodisk: 3-phenoxybenzoic acid and chlorpyrifos, giving recovery values of 132 and 124%, respectively. The third compound that was overestimated was sulfasalazine analysed by standard method, which concentration was remarkably high. The spiked concentration was 0.5 µg/L and the result obtained was almost three times higher (1.4 µg/L), giving recovery of 280%. Only one analyte in sample 15 was underestimated when analysed by immunoassay approach – azoxystrobin which gave recovery of 56%. Low recovery was also obtained for triclosan using the standard analytical method (76%).

Overall, 80% of the spiked concentrations were successfully determined ($80\% \leq R \leq 120\%$). Moreover, 13% of the samples concentrations were found to be significantly different but not incoherent ($70\% < R < 80\%$ and $120\% < R \leq 130\%$). Five samples amongst 99 evaluated were overestimated ($R > 130\%$), whereas only one sample was underestimated ($R < 70\%$). Besides, blank samples without pesticide spiking were involved in the analysis and detected values were significantly lower than the assay detection limits in all cases, suggesting that no false positives were observed.

In case of GC-MS analysis, seven samples were overestimated ($R > 130\%$), whereas twelve were underestimated ($R < 70\%$). In general, the proposed method is in a good agreement with the reference methodology. It definitely cannot compete with gold standard methods in terms of high-throughput, however as a fast, cost-effective alternative approach can serve as a good solution for remote quality control.

The task of developing multiplex immunoassay platforms is hard and requires sensitive immunoreagents. Described in this Thesis methodology, that offers analysis of ten chemically different analytes is a first attempt described in the literature. Similar works have been published^{327,328}, however none of them achieved such high multiplex level. This shows the possible impact in the field of environmental monitoring if this approach was brought to the market.

The disk used for water sample analysis (Figure 37) contains 24 arrays of 49 spots each, corresponding to ten analytes and assay controls. The calibration curves were prepared by performing the competitive assays within the working ranges (four concentrations) of the analytes, in order to obtain the linear part of the curve. Thus, 20 samples were simultaneously analyzed.

In traditional ELISA, one 96-well plate enable the determination of only one analyte in 40 samples in duplicate. In the developed microimmunoassay, one disk allows for the determination of 20 samples, thus to analyze 40 samples, 2 disks are necessary. However, in each sample ten different analytes can be measured simultaneously. To analyze the same number of analytes by ELISA, 10 plates are required. To estimate the cost of the assay, a price of 1000 and 300 € is calculated for an antibody and coating antigen solutions set at 1.0 mg/mL, respectively. The cost of a commercial ELISA kit is approximately 500 euros. The analysis of all studied analytes is possible as long as commercial kits are available. One ELISA kit allows for the determination of 40 samples of one analyte in duplicate. The cost per samples is approximately 12,5 euros, thus to analyze ten different compounds the price is 125 euros.

For one immunoassay on disk, 15 μ L of coating antigen per analyte (20 mg/L) are necessary to spot 96 droplets (24 arrays \times 4 spots) of 50 nL each. In total, 300 μ L of coating antigens are necessary for

spotting two disks. The cost is less than 1 cent of euro. As far as the antibody is concerned, for the preparation of antibody-nanogold conjugates only 30 µg/mL of antibody is required. The conjugates are further diluted. Considering that 1/100 dilution is used the amount of antibody-nanogold conjugate prepared allows the analysis of 500 samples, which corresponds to 20 disks. Thus, antibody at 1.0 mg/mL allows for 16,000 assays. The cost for each analyte is thus 6 cents, so for 10 analytes is 60 cents. The silver enhancement step cost for 1 disk is 80 cents. The overall reagent cost can be estimated as 1.5 euros per disk.

To conclude, the proposed microimmunoassay on compact disk using antibody-nanogold conjugates is an advantageous screening technique. It allows to analyze simultaneously different analytes at reasonable cost. Nevertheless, the confirmatory analysis is necessary, but the amount for samples for further more detailed analysis can be considerably reduced.

In the developed microimmunoassay, in each array ten analytes can be determined simultaneously, in total 200 assays can be performed in one disk in 35 min, offering high-throughput analysis in short time.

This information is important as quick assessment of contaminated sites where rapid response is required in order to take appropriate actions. The methodology is also very competitive compared to chromatographic methods, because it can be easily adapted to on-site analysis. Also, there is no need of sample preparation prior to analysis, nor pre-concentration steps, making it highly suitable as a on-site monitoring tool.

In conclusion, these results show that proposed methodology based on the antigen-coated format using antibody-nanogold conjugates combined with compact disk technology has a huge potential for being applied as a multi-residue method for water contamination monitoring.

✓

Conclusions

V Conclusions

In this Thesis, practical screening immunoassay methods have been developed to determine simultaneously residues of multiple analytes in water samples with a minimum sample treatment. The limiting factor in creating a multiplex platform when antibody-antigen binding is concerned is cross-reactivity and shared reactivity. Among eighteen systems studied, ten were successfully implemented in a multiplex assay.

The developed approach as proof of concept shows some important advantages, such as flexibility to design the assay. As each antibody can be functionalized individually, there is a possibility of “on-demand” adapting the immunoassay for the detection of emerging or little-known pollutants. Also, depending on the particular interests of the end users, the nature of the water pollution or the legislation requirements, the preparation of the appropriate cocktail solutions and working in different multiplexed configurations, is possible as well.

The present multi-residue methodology may be a very useful alternative for screening not only the targeted compounds but also structurally related ones. Other advantage is the possibility to determine analytes with specific chemical characteristics that is non-viable by the current reference techniques in a single assay, in a short time and *in situ*, using also the same detection system.

The compact disk technology was used for the development of the screening system. This approach is based on using commercial disks as microimmunoassay platform and disk-drive as detector. The platform used for microarray development was a standard DVD disk. There are several advantages of using DVD as platform for immunoanalysis. First, the number of spots possible to immobilize on a single disk (12 cm in diameter gives 94 cm² of working surface) can reach thousands. In this way, many different samples can be analyzed simultaneously in replicates on the same disk, including also calibration standards. Second, polycarbonate shows good properties for passive immobilization of sensing probes in high-density. Finally, their cost efficiency makes them attractive for many low-budget analytical devices, as the price of regular disc is approximately €0.10 to €0.25.

Disk drive is used as a chemical detector providing sensitive, compact, user-friendly detection mode. DVD drives achieve a sharp focus using a 650 nm wavelength laser, with a high numerical aperture giving high optical resolution and signal-to-noise ratios. Market price of high optical resolution drives is between €20 and €300, which makes this consumer electronics an interesting cost-effective analytical tool. Moreover, its size makes it suitable for on-site measurements. DVDs along with a high-precision optical disk drive are a perfect combination for sensitive and affordable methodology for diverse analytical purposes.

All the developed immunoassays were based on the use of gold nanoparticles with different size and shape. Spherical gold nanoparticles present simple probe conjugation protocol and can be used with or without amplification step depending on their size.

For the assays with signal amplification, the best results in terms of sensitivity were obtained using 5 nm nanogold bioconjugates, as the nanogold catalytic properties of silver precipitation improve due to high surface-to-volume ratio.

Larger gold nanoparticles can be used without any amplification step, but the assay sensitivity is lower due to high antibody and nanoparticles concentration needed to detect the immunoreaction. The optimal size of gold nanoparticles for one-step microimmunoassay giving high signal-to-noise ratio and sensitive results was 50 nm.

As alternative to large spherical gold nanoparticles, gold nanorods were tested without amplification step. This assay works well in a competitive format; however the sensitivity obtained is much lower when compared with 5 nm spherical gold nanoparticles. Still, the immunoassay with gold nanorods used as label could serve as a semi-quantitative method for yes or no response.

For the selection of the final immunoassay format, different approaches were tested in order to choose the best one in terms of sensitivity and selectivity. All assays relied on direct recognition of the antibody-antigen event. The studied assays were coating-antigen and antibody-coated formats. Within the coating antigen approach, antibodies were immobilized on the surface of gold nanoparticles via physical adsorption in case of spherical nanoparticles and via covalent attachment for gold nanorods.

For the antibody-coated format, two different assays were designed and optimized. In both assays gold tracers were prepared. The first one consisted in immobilizing coating conjugate onto the spherical gold nanoparticles, whereas the second approach comprises the covalent attachment of hapten molecules through covalent bonds. The results showed that using coating antigen modified gold nanoparticles the sensitivity achieved was similar to that obtained using antibody modified gold nanoparticles. However, the prepared gold nanoparticle-hapten tracers showed much lower sensitivity. Nevertheless, such antibody-immobilized immunoassays could be used as a binary system to detect higher pollutant concentrations.

Overall, the use of nanogold conjugates is very interesting and promising approach. Considering that the number of steps is reduced to either one or two, and in comparison to the indirect detection, the reproducibility of the assays is better, reducing the errors associated to the signal amplification step. Also, antibodies of different nature such as mono, polyclonal and recombinant can be used simultaneously in the same multiplex assay without the need of different secondary detection markers. Furthermore, as it was presented in our paper reference 334, a mixture of

modified nanogold conjugates (antibody and haptized protein) can be used for performing simultaneous assays under different formats. This result is very interesting since allows approaching the integration of different types of assays in a single platform using the same detection system. For instance, both competitive and non-competitive assays, for small (e.g. pesticides, toxins, antibiotics) and large (e.g. biomarkers, proteins, bacteria) organic molecules, respectively can be integrated and performed in the same disc using the disc drive as detector, keeping the assay sensitivity and selectivity.

In general, the gold sol labelling procedure is very simple and does not affect generally the biochemical activity of the labelled compound. Moreover, the bioconjugates were stable for a considerable period of time such as three months.

A promising approach to improve the readout sensitivity of microimmunoassays based on used of gold nanoparticles as both capture and detection species is demonstrated. The immunocapture microimmunoassay allows increasing the sensitivity one order of magnitude compared with the standard assay. Apart from an increase in sensitivity, this approach has several other advantages over existing methods. First of all, low sample and nanogold bioconjugate consumption make it very competitive to standard immunoassays where high amounts of reagents are required. The nanogold bioconjugates preparation is simple. Also, it is possible to concentrate the nanogold using simply a centrifuge, thus increasing the signal without additional cost. Moreover, the analysis does not require a secondary label to develop the signal, resulting in faster and likely to perform throughput analysis. The presented approach shows high versatility as it was performed using small and large gold nanoparticles, using signal enhancement or without any amplification step.

The other types of nanoparticles such as colloid silver could be successfully used and detection performed on more suitable platform such as Blu-ray, showing the flexibility of the concept. The use of such sensing technology is of great analytical interest for various sensing and biosensing applications where antibody modified nanoparticles may be involved.

To summarize, sensitive and selective screening methodologies based on compact disc technology were developed as a proof of concept, able to determine simultaneously chemically different water contaminants, showing promising future in the field of water screening techniques. The great advantage of the methodology is definitely the versatility, selectivity and sensitivity achieved for many different analytes. The majority of the immunoassays developed is suitable for use as a screening method according the E.U. Water Framework Directive, but the performances could be improved in case of using immunoreagents developed for this purpose.

Also, a big asset is the small sample and reagents volume requirement. Overall, good analytical outcome, high-throughput, analysis price together with the speed of compact disk technology

makes this system a good approach for fast and reliable qualitative and quantitative screening of pollutant residues in water samples.

This is an essential approach for facing the European Union critical problem of the chemical water pollution. Only having this type of methodology is possible to know in time and at reasonable economical cost, the information needed to take the necessary controlling correcting action.

VI

References

VI References

- (1) European Environment Agency, *SOER 2015, Freshwater quality*; 2015.
- (2) *Climate Change, impacts and vulnerability in Europe 2012. EEA 12/2012*; European Environment Agency, 2012.
- (3) Stokstad, E.; Grullon, G. *Science (80-.)*. **2013**, *341*, 730–731.
- (4) http://ec.europa.eu/eurostat/statistics-explained/index.php/Pesticide_sales_statistics.
- (5) Regulation (EC) No 1107/2009 of the European Parliament and of the Council of 21 October 2009 concerning the placing of plant protection products on the market.
- (6) Mesquita, R. B. R.; Rangel, A. O. S. S. *Anal. Chim. Acta* **2009**, *648*, 7–22.
- (7) Buchanan, I.; Liang, H. C.; Khan, W.; Liu, Z.; Singh, R.; Ikehata, K.; Chelme-Ayala, P. *Water Environ. Res.* **2009**, *81*, 1731–1816.
- (8) Peters, K.; Bundschuh, M.; Schäfer, R. B. *Environ. Pollut.* **2013**, *180*, 324–329.
- (9) Sánchez-Avila, J.; Tauler, R.; Lacorte, S. *Environ. Int.* **2012**, *46*, 50–62.
- (10) *Water Frame Directive – directive 2000/60/EC of the parliament and of the council, Official Journal of the European Communities L 327/1, of 23 October 2000, establishing a framework for Community action in the field of water policy*; 2010; Vol. 429.
- (11) Petrie, B.; Barden, R.; Kasprzyk-Hordern, B. *Water Res.* **2014**, *72*, 3–27.
- (12) Norman Network. Network of reference laboratories, research centers and related organizations for monitoring of emerging environmental substances. <http://www.norman-network.net/>.
- (13) Kasprzyk-Hordern, B.; Baker, D. R. *Sci. Total Environ.* **2012**, *423*, 142–150.
- (14) López-Serna, R.; Kasprzyk-Hordern, B.; Petrović, M.; Barceló, D. *Anal. Bioanal. Chem.* **2013**, *405*, 5859–5873.
- (15) Hughes, S. R.; Kay, P.; Brown, L. E. *Environ. Sci. Technol.* **2012**, *47*, 661–677.
- (16) Gros, M.; Petrović, M.; Ginebreda, A.; Barceló, D. *Environ. Int.* **2010**, *36*, 15–26.
- (17) Baker, D. R.; Kasprzyk-Hordern, B. *Sci. Total Environ.* **2013**, *454–455*, 442–456.
- (18) Carvalho, R. N.; Ceriani, L.; Ippolito, A. *JRC Technical Report: Development of the first Watch List under the Environmental Quality Standards Directive water policy*; Joint Research Centre; Institute for Environment and Sustainability; Water Resources Unit, 2015.
- (19) Greenwood, R.; Mills, G. A.; Roig, B. *Trends Anal. Chem.* **2007**, *26*, 263–267.
- (20) EPA US Environmental Protection Agency, <https://www.epa.gov/sdwa>.
- (21) Wilkowska, A.; Biziuk, M. *Food Chem.* **2011**, *125*, 803–812.
- (22) Lazartigues, A.; Fratta, C.; Baudot, R.; Wiest, L.; Feidt, C.; Thomas, M.; Cren-Olivé, C. *Talanta* **2011**, *85*, 1500–1507.
- (23) Wiest, L.; Buleté, A.; Giroud, B.; Fratta, C.; Amic, S.; Lambert, O.; Pouliquen, H.; Arnaudguilhem, C. *J. Chromatogr. A* **2011**, *1218*, 5743–5756.
- (24) Filho, A. M.; dos Santos, F. N.; Pereira, P. A. D. P. *Microchem. J.* **2010**, *96*, 139–145.
- (25) Rodrigues, F. D. M.; Mesquita, P. R. R.; de Oliveira, L. S.; de Oliveira, F. S.; Menezes Filho,

- A.; de P. Pereira, P. A.; de Andrade, J. B. *Microchem. J.* **2011**, *98*, 56–61.
- (26) Lavagnini, I.; Urbani, A.; Magno, F. *Talanta* **2011**, *83*, 1754–1762.
- (27) Bedendo, G. C.; Jardim, I. C. S. F.; Carasek, E. *Talanta* **2012**, *88*, 573–580.
- (28) Boonchiangma, S.; Ngeontae, W.; Srijaranai, S. *Talanta* **2012**, *88*, 209–215.
- (29) Wang, Y.; You, J.; Ren, R.; Xiao, Y.; Gao, S.; Zhang, H.; Yu, A. *J. Chromatogr. A* **2010**, *1217*, 4241–4246.
- (30) Malik, A. K.; Blasco, C.; Picó, Y. *J. Chromatogr. A* **2010**, *1217*, 4018–4040.
- (31) Fernández-Alba, A. R.; García-Reyes, J. F. *Trends Anal. Chem.* **2008**, *27*, 973–990.
- (32) García-Chao, M.; Agruña, M. J.; Flores Calvete, G.; Sakkas, V.; Llompart, M.; Dagnac, T. *Anal. Chim. Acta* **2010**, *672*, 107–113.
- (33) Pirard, C.; Widart, J.; Nguyen, B. K.; Deleuze, C.; Heudt, L.; Haubruge, E.; De Pauw, E.; Focant, J.-F. *J. Chromatogr. A* **2007**, *1152*, 116–123.
- (34) Dagnac, T.; Garcia-Chao, M.; Pulleiro, P.; Garcia-Jares, C.; Llompart, M. *J. Chromatogr. A* **2009**, *1216*, 3702–3709.
- (35) Pérez-Parada, A.; Colazzo, M.; Besil, N.; Geis-Asteggiane, L.; Rey, F.; Heinzen, H. *J. Chromatogr. A* **2011**, *1218*, 5852–5857.
- (36) de Pinho, G. P.; Neves, A. A.; de Queiroz, M. E. L. R.; Silvério, F. O. *Food Control* **2010**, *21*, 1307–1311.
- (37) Rawn, D. F. K.; Judge, J.; Roscoe, V. *Anal. Bioanal. Chem.* **2010**, *397*, 2525–2531.
- (38) Yu, S.; Xu, X. *Rapid Commun. Mass Spectrom.* **2012**, *26*, 963–977.
- (39) Castillo, M.; González, C.; Miralles, A. *Anal. Bioanal. Chem.* **2011**, *400*, 1315–1328.
- (40) Lacorte, S.; Guiffard, I.; Fraisse, D.; Barceló, D. *Anal. Chem.* **2000**, *72*, 1430–1440.
- (41) Stamatis, N.; Hela, D.; Triantafyllidis, V.; Konstantinou, I. *Sci. World J.* **2013**.
- (42) Allan, I. J.; Vrana, B.; Greenwood, R.; Mills, G. A.; Roig, B.; Gonzalez, C. *Talanta* **2006**, *69*, 302–322.
- (43) Justino, C. I. L.; Duarte, K. R.; Freitas, A. C.; Panteleitchouk, T. S. L.; Duarte, A. C.; Rocha-Santos, T. A. P. *Trends Anal. Chem.* **2016**, *80*, 293–310.
- (44) Díaz-González, M.; Gutiérrez-Capitán, M.; Niu, P.; Baldi, A.; Jiménez-Jorquera, C.; Fernández-Sánchez, C. *Trends Anal. Chem.* **2016**, *77*, 186–202.
- (45) <https://water.usgs.gov/admin/memo/QW/qw92.09.html>.
- (46) Rassaei, L.; Marken, F.; Sillanpää, M.; Amiri, M.; Cirtiu, C. M.; Sillanpää, M. *Trends Anal. Chem.* **2011**, *30*, 1704–1715.
- (47) Hayat, A.; Marty, J. L. *Sensors* **2014**, *14*, 10432–10453.
- (48) Dankwardt, A. In *Encyclopedia of Analytical Chemistry*; Meyers, R. A., Ed.; John Wiley & Sons Ltd: Chichester, 2006; pp. 1–27.
- (49) Porstmann, T.; Kiessig, S. T. *J. Immunol. Methods* **1992**, *150*, 5–21.
- (50) Palchetti, I.; Mascini, M. *Analyst* **2008**, *133*, 846–854.
- (51) Lagarde, F.; Jaffrezic-Renault, N. *Anal. Bioanal. Chem.* **2011**, *400*, 947–964.

- (52) Song, S.; Wang, L.; Li, J.; Fan, C.; Zhao, J. *Trends Anal. Chem.* **2008**, *27*, 108–117.
- (53) Rodriguez-Mozaz, S.; Alda, M. J. L. De; Marco, M.-P.; Barceló, D. *Talanta* **2005**, *65*, 291–297.
- (54) Sassolas, A.; Prieto-Simón, B.; Marty, J.-L. *Am. J. Anal. Chem.* **2012**, *3*, 210–232.
- (55) <http://www.epa.gov/wastes/hazard/testmethods/sw846/online/index.htm>.
- (56) M. Kramer, P. *Rapid Chemical and Biological Techniques for Water Monitoring. Immunochemical Methods*; Gonzalez, C.; Quevauviller, P.; Greenwood, R., Eds.; John Wiley & Sons Ltd, 2009.
- (57) Díaz-González, M.; Gutiérrez-Capitán, M.; Niu, P.; Baldi, A.; Jiménez-Jorquera, Cecilia Fernández-Sánchez, C. *Trends Anal. Chem.* **2016**, *77*, 186–202.
- (58) Rebe Raz, S.; Haasnoot, W. *Trends Anal. Chem.* **2011**, *30*, 1526–1537.
- (59) Desmet, C.; Blum, L. J.; Marquette, C. A. *Anal. Chem.* **2012**, *84*, 10267–10276.
- (60) Ma, H.; Mao, K.; Li, H.; Wu, D.; Zhang, Y.; Du, B.; Wei, Q. *J. Mater. Chem. B* **2013**, *1*, 5137–5142.
- (61) Herranz, S.; Marazuela, M. D.; Moreno-Bondi, M. C. *Biosens. Bioelectron.* **2012**, *33*, 50–55.
- (62) Guo, Y.-R.; Liu, S.-Y.; Gui, W.-J.; Zhu, G.-N. *Anal. Biochem.* **2009**, *389*, 32–39.
- (63) <http://www.google.com/patents/US20050250141>.
- (64) Guo, Y.; Tian, J.; Liang, C.; Zhu, G.; Gui, W. *Microchim. Acta* **2013**, *180*, 387–395.
- (65) Wang, X.; Mu, Z.; Shangguan, F.; Liu, R.; Pu, Y.; Yin, L. *J. Hazard. Mater.* **2014**, *273*, 287–292.
- (66) Bai, W.; Zhu, C.; Liu, J.; Yan, M.; Yang, S.; Chen, A. *Environ. Toxicol. Chem.* **2015**, *34*, 2244–2249.
- (67) Sara Rodriguez-Mozaz, M. J. L. de A.; Barceló, D. *Achievements of the RIANA and AWACSS EU Projects: Immunosensors for the Determination of Pesticides, Endocrine Disrupting Chemicals and Pharmaceuticals*; 2009.
- (68) Barzen, C.; Brecht, A.; Gauglitz, G. *Biosens. Bioelectron.* **2002**, *17*, 289–295.
- (69) Rodriguez-Mozaz, S.; Reder, S.; Lopez De Alda, M.; Gauglitz, G.; Barceló, D. *Biosens. Bioelectron.* **2004**, *19*, 633–640.
- (70) Tomizaki, K. Y.; Usui, K.; Mihara, H. *ChemBioChem* **2005**, *6*, 782–799.
- (71) Köhler, G.; Milstein, C. *Nature* **1975**, *256*, 495–497.
- (72) Newman, D. J.; Henneberry, H.; Price, C. P. *Ann. Clin. Biochem.* **1992**, *29*, 22–42.
- (73) Algar, W. R.; Tavares, A. J.; Krull, U. J. *Anal. Chim. Acta* **2010**, *673*, 1–25.
- (74) Rousserie, G.; Sukhanova, A.; Even-Desrumeaux, K.; Fleury, F.; Chames, P.; Baty, D.; Oleinikov, V.; Pluot, M.; Cohen, J. H. M.; Nabiev, I. *Crit. Rev. Oncol. / Hematol.* **2010**, *74*, 1–15.
- (75) Ekimov, A. I.; Onushchenko, A. A. *JETP Lett* **1981**, *34*, 345–349.
- (76) Zhang, H.; Liu, L.; Li, C.-W.; Fu, H.; Chen, Y.; Yang, M. *Biosens. Bioelectron.* **2011**, *29*, 89–96.

- (77) Zekavati, R.; Safi, S.; Hashemi, S. J.; Rahmani-Cherati, T.; Tabatabaei, M.; Mohsenifar, A.; Bayat, M. *Microchim. Acta* **2013**, *180*, 1217–1223.
- (78) Trapiella-Alfonso, L.; Costa-Fernandez, J. M.; Pereiro, R.; Sanz-Medel, A. *Talanta* **2013**, *106*, 243–248.
- (79) Rotello, V. *Nanoparticles. Building Blocks for Nanotechnology.*; Springer, 2004.
- (80) Faraday, M. *The Bakarian Lecture - Experimental Relations of Gold (and other Metals) to Light*; 1857.
- (81) Thompson, D. *Gold Bull.* **2007**, *40*, 2–4.
- (82) Shipway, A. N.; Katz, E.; Willner, I. *Chemphyschem* **2000**, *1*, 18–52.
- (83) Rothenberg, E.; Kazes, M.; Shaviv, E.; Banin, U. *Nano Lett.* **2005**, *5*, 1581–1586.
- (84) Urban, A. S.; Lutich, A. A.; Stefani, F. D.; Feldmann, J. *Nano Lett.* **2010**, 4794–4798.
- (85) Taton, T. A.; Mirkin, C. A.; Letsinger, R. L. *Science (80-.)*. **2000**, *289*, 1757–1760.
- (86) Li, C.; Shuford, K. L.; Park, Q.-H.; Cai, W.; Li, Y.; Lee, E. J.; Cho, S. O. *Angew. Chemie* **2007**, *119*, 3328–3332.
- (87) Seo, D.; Yoo, C. II; Chung, I. S.; Park, S. M.; Ryu, S.; Song, H. *J. Phys. Chem. C* **2008**, *112*, 2469–2475.
- (88) Kim, F.; Connor, S.; Song, H.; Kuykendall, T.; Yang, P. *Angew. Chemie Int. Ed.* **2004**, *43*, 3673–3677.
- (89) Seo, D.; Ji, C. P.; Song, H. *J. Am. Chem. Soc.* **2006**, *128*, 14863–14870.
- (90) Wang, Z.; Zhang, J.; Ekman, J. M.; Kenis, P. J. A.; Lu, Y. *Nano Lett.* **2010**, *10*, 1886–1891.
- (91) Mie, G. *Ann. Phys.* **1908**, *330*, 377.
- (92) Tokonami, S.; Yamamoto, Y.; Shiigi, H.; Nagaoka, T. *Anal. Chim. Acta* **2012**, *716*, 76–91.
- (93) Link, S.; Wang, Z. L. *J. Phys. Chem. B* **1999**, *103*, 3529–3533.
- (94) P. K. Jain, I. H. El-Sayed, M. A. E.-S. *Nano Today* **2007**, *2*, 18–29.
- (95) Vigderman, L.; Khanal, B. P.; Zubarev, E. R. *Adv. Mater.* **2012**, *24*, 4811–4841.
- (96) Chen, H.; Shao, L.; Li, Q.; Wang, J. *Chem. Soc. Rev.* **2013**, *42*, 2679–2724.
- (97) Daniel, M.-C.; Astruc, D. *Chem. Rev.* **2004**, *104*, 293–346.
- (98) Doria, G.; Conde, J.; Veigas, B.; Giestas, L.; Almeida, C.; Assuncao, M.; Rosa, J.; Baptista, P. *V. Sensors* **2012**, *12*, 1657–1687.
- (99) Gole, A.; Dash, C.; Ramakrishnan, V.; Sainkar, S. R.; Mandale, A. B.; Rao, M.; Sastry, M. *Langmuir* **2001**, *17*, 1674–1679.
- (100) Geoghegan, W. D. *J. Histochem. Cytochem.* **1988**, *36*, 401–407.
- (101) Putman, C. A. J.; de Grooth, B. G.; Hansma, P. K.; van Hulst, N. F.; Greve, J. *Ultramicroscopy* **1993**, *48*, 177–182.
- (102) Hermann, R.; Walther, P.; Müller, M. *Histochem. Cell Biol.* **1996**, *106*, 31–39.
- (103) Roth, J. *Histochem. Cell Biol.* **1996**, *106*, 1–8.
- (104) He, H.; Xie, C.; Ren, J. *Anal. Chem.* **2008**, *80*, 5951–5957.
- (105) Sperling, R. A.; Parak, W. J. *Philos. Trans. A. Math. Phys. Eng. Sci.* **2010**, *368*, 1333–1383.

- (106) Haes, A. J.; Hall, W. P.; Chang, L.; Klein, W. L.; Van Duyne, R. P. *Nano Lett.* **2004**, *4*, 1029–1034.
- (107) Riboh, J. C.; Haes, A. J.; McFarland, A. D.; Ranjit Yonzon, C.; Van Duyne, R. P. *J. Phys. Chem. B* **2003**, *107*, 1772–1780.
- (108) Haes, A. J.; Chang, L.; Klein, W. L.; Duyne, R. P. Van. *J. Am. Chem. Soc.* **2005**, *127*, 2264–2271.
- (109) Huang, T.; Nallathamby, P. D.; Gillet, D.; Xu, X.-H. N. *Anal. Chem.* **2007**, *79*, 7708–7718.
- (110) Wilchek, M.; Bayer, E. A. *Anal. Biochem.* **1988**, *171*, 1–32.
- (111) Smith, D. S.; Eremin, S. A. *Anal. Bioanal. Chem.* **2008**, *391*, 1499–1507.
- (112) Goryacheva, I. Y.; Eremin, S. A.; Shutaleva, E. A.; Suchanek, M.; Niessner, R.; Knopp, D. *Anal. Lett.* **2007**, *40*, 1445–1460.
- (113) Wang, L.; Zhu, Y.; Xu, L.; Chen, W.; Kuang, H.; Liu, L.; Agarwal, A.; Xu, C.; Kotov, N. A. *Angew. Chemie Int. Ed.* **2010**, *49*, 5472–5475.
- (114) Guo, L.; Xu, Y.; Ferhan, A. R.; Chen, G.; Kim, D. H. *J. Am. Chem. Soc.* **2013**, *135*, 12338–12345.
- (115) Wang, C.; Yu, C. *Rev. Anal. Chem.* **2013**, *32*, 1–14.
- (116) Shan, G.; Lipton, C.; Gee, S. J.; Hammock, B. D.; Lee, P. W. *Handbook of Residue Analytical Methods for Agrochemicals: Immunoassay, biosensors and other nonchromatographic methods*; Lee, P. W., Ed.; John Wiley & Sons, Ltd.: Chichester, 2002.
- (117) Hennion, M.-C.; Barceló, D. *Anal. Chim. Acta* **1998**, *362*, 3–34.
- (118) Catt, K.; Tregear, G. W. *Science* **1967**, *158*, 1570–1572.
- (119) Butler, J. E. *Methods* **2000**, *22*, 4–23.
- (120) Kusnezow, W.; Hoheisel, J. D. *J. Mol. Recognit.* **2003**, *16*, 165–176.
- (121) Hahm, J. *Sensors* **2011**, *11*, 3327–3355.
- (122) Butler, J.; Ni, L.; Nessler, R.; Joshi, K.; Suter, M.; Rosenberg, B.; Chang, J.; Brown, W.; Cantarero, L. *J. Immunol. Methods* **1992**, *150*, 77–90.
- (123) Butler, J.; Brown, W.; KS, J.; Chang, J.; Rosenberg, B.; Voss, E. *Mol Immunol* **1993**, *30*, 1165.
- (124) Helfe, S. L. *Food Technol.* **1995**, *49*, 102–107.
- (125) de la Escosura-Muñiz, A.; Maltez-da Costa, M.; Merkoci, A. *Biosens. Bioelectron.* **2009**, *24*, 2475–2482.
- (126) Kourilov, V.; Steinitz, M. *Anal. Biochem.* **2002**, *311*, 166–170.
- (127) Lankelma, J.; Nie, Z.; Carrilho, E.; Whitesides, G. M. *Anal. Chem.* **2012**, *84*, 4147–4152.
- (128) Pollock, N. R.; Rolland, J. P.; Kumar, S.; Beattie, P. D.; Jain, S.; Noubary, F.; Wong, V. L.; Pohlmann, R. A.; Ryan, U. S.; Whitesides, G. M. *Sci. Transl. Med.* **2012**, *4*, 152ra129.
- (129) Sung, D.; Shin, D. H.; Jon, S. *Biosens. Bioelectron.* **2011**, *26*, 3967–3972.
- (130) Raj, J.; Herzog, G.; Manning, M.; Volcke, C.; MacCraith, B. D.; Ballantyne, S.; Thompson, M.; Arrigan, D. W. M. *Biosens. Bioelectron.* **2009**, *24*, 2654–2658.

- (131) Pipatpanukul, C.; Amarit, R.; Somboonkaew, A.; Sutapun, B.; Vongsakulyanon, A.; Kitpoka, P.; Srihirin, T.; Kunakorn, M. *Vox Sang.* **2016**, *110*, 60–69.
- (132) Morais, S.; Puchades, R.; Maquieira, Á. *Anal. Bioanal. Chem.* **2016**, *408*, 4523–4534.
- (133) Yalow, B. R. S.; Berson, S. A. *J Clin Invest* **1960**, *39*, 1157–1175.
- (134) Ullman, E. F.; Schwarzberg, M. *J. Biol. Chem.* **1976**, *251*, 4172–4178.
- (135) Zuk, R. F.; Rowley, G. L.; Ullman, E. F. *Clin. Chem.* **1979**, *25*, 1554–1560.
- (136) Kricka, L. J. *Clin. Chem.* **1991**, *37*, 1472–1481.
- (137) Antony, T.; Saxena, A.; Roy, K. B.; Bohidar, H. B. *J. Biochem. Biophys. Methods* **1998**, *36*, 75–85.
- (138) Thakkar, H.; Davey, C. L.; Medcalf, E. A.; Skingle, L.; Craig, A. R.; Newman, D. J.; Price, C. P. *Clin. Chem.* **1991**, *37*, 1248–1251.
- (139) Engvall, E.; Perlmann, P. *Immunochemistry* **1971**, *8*, 871–874.
- (140) Organon, N. V. *Febs Lett.* **1971**, *15*, 232–236.
- (141) Seydack, M. *Biosens. Bioelectron.* **2005**, *20*, 2454–2469.
- (142) Saha, K.; Agasti, S. S.; Kim, C.; Li, X.; Rotello, V. M. *Chem. Rev.* **2012**, *112*, 2739–2779.
- (143) Coates, J. E.; Lam, S. F.; McGaw, W. T. *Clin. Chem.* **1988**, *34*, 1545–1551.
- (144) Ma, Z.; Gingerich, R. L.; Santiago, J. V.; Klein, S.; Smith, C. H.; Landt, M. *Clin. Chem.* **1996**, *42*, 942–946.
- (145) Gascón, J.; Oubiña, A.; Ballesteros, B.; Barceló, D.; Camps, F.; Marco, M.-P.; González-Martínez, M. A.; Morais, S.; Puchades, R.; Maquieira, Á. *Anal. Chim. Acta* **1997**, *347*, 149–162.
- (146) Casino, P.; Morais, S.; Maquieira, Á. *Environ. Sci. Technol.* **2001**, *35*, 4111–4119.
- (147) Pastor-Navarro, N.; Gallego-Iglesias, E.; Maquieira, Á.; Puchades, R. *Anal. Chim. Acta* **2007**, *583*, 377–383.
- (148) Brun, E. M.; Bonet, E.; Puchades, R.; Maquieira, Á. *Environ. Sci. Technol.* **2008**, *42*, 1665–1672.
- (149) Lee, J. K.; Ahn, K. C.; Park, O. S.; Kang, S. Y.; Hammock, B. D. *J. Agric. Food Chem.* **2001**, *49*, 2159–2167.
- (150) Schneider, P.; Goodrow, M. H.; Gee, S. J.; Hammock, B. D. *J. Agric. Food Chem.* **1994**, *42*, 413–422.
- (151) Schobel, U.; Barzen, C.; Gauglitz, G. *Fresenius. J. Anal. Chem.* **2000**, *366*, 646–658.
- (152) Frasco, M. F.; Chaniotakis, N. *Anal. Bioanal. Chem.* **2010**, *396*, 229–240.
- (153) Reimer, G. J.; Gee, S. J.; Hammock, B. D. *J. Agric. Food Chem.* **1998**, *46*, 3353–3358.
- (154) Sharma, P.; Gandhi, S.; Chopra, A.; Sekar, N.; Raman Suri, C. *Anal. Chim. Acta* **2010**, *676*, 87–92.
- (155) Mastichiadis, C.; Kakabakos, S. E.; Christofidis, I.; Koupparis, M. A.; Willetts, C.; Misiako, K. *Anal. Chem.* **2002**, *74*, 6064–6072.
- (156) Kricka, L. . *Anal. Chim. Acta* **2003**, *500*, 279–286.

- (157) Marquette, C. A.; Blum, L. J. *Talanta* **2000**, *51*, 395–401.
- (158) Heyries, K. A.; Loughran, M. G.; Hoffmann, D.; Homsy, A.; Blum, L. J.; Marquette, C. A. *Biosens. Bioelectron.* **2008**, *23*, 1812–1818.
- (159) Marquette, C. A.; Coulet, P. R.; Blum, L. J. *Anal. Chim. Acta* **1999**, *398*, 173–182.
- (160) Citartan, M.; Gopinath, S. C. B.; Tominaga, J.; Tang, T.-H. *Analyst* **2013**, *138*, 3576–3592.
- (161) The LabCD-ADMET System from Tecan. <http://www.tecan-us.com/us-index.htm>.
- (162) <http://www.gyros.com/>.
- (163) Abaxis. <http://www.abaxis.com/>.
- (164) Madou, M.; Zoval, J.; Jia, G.; Kido, H.; Kim, J.; Kim, N. *Annu. Re. Biomed. Eng.* **2006**, *8*, 601–628.
- (165) Honda, N.; Lindberg, U.; Andersson, P.; Hoffmann, S.; Takei, H. *Clin. Chem.* **2005**, *51*, 1955–1961.
- (166) Gustafsson, M.; Hirschberg, D.; Palmberg, C.; Jornvall, H.; Bergman, T. *Anal. Chem.* **2004**, *76*, 345–350.
- (167) Puckett, L. G.; Dikici, E.; Lai, S.; Madou, M.; Bachas, L. G.; Daunert, S. *Anal. Chem.* **2004**, *76*, 7263–7268.
- (168) Kido, H.; Maquieira, Á.; Hammock, B. D. *Anal. Chim. Acta* **2000**, *411*, 1–11.
- (169) Alexandre, I.; Houbion, Y.; Collet, J.; Hamels, S.; Demarteau, J.; Gala, J.; Remacle, J. *Biotechniques* **2002**, *33*, 435–439.
- (170) Barathur, R.; Bookout, J.; Sreevatsan, S.; Gordon, J.; Werner, M.; Thor, G.; Worthington, M. *Psychiatr. Genet.* **2002**, *12*, 193–206.
- (171) Clair, J. J. La; Burkart, M. D. *Org. Biomol. Chem.* **2003**, *1*, 3244–3249.
- (172) Potyrailo, R. A.; Morris, W. G.; Leach, A. M.; Sivavec, T. M.; Wisnudel, M. B.; Boyette, S. *Anal. Chem.* **2006**, *78*, 5893–5899.
- (173) Morais, S.; Marco-Molés, R.; Puchades, R.; Maquieira, Á. *Chem. Commun.* **2006**, 2368–2370.
- (174) Wang, Z.; Li, R. X. *Nanoscale Res. Lett.* **2007**, *2*, 69–74.
- (175) Wang, H.; Ou, L. M. L.; Suo, Y.; Yu, H.-Z. *Anal. Chem.* **2011**, *83*, 1557–1563.
- (176) Morais, S.; Carrascosa, J.; Mira, D.; Puchades, R.; Maquieira, Á. *Anal. Chem.* **2007**, *79*, 7628–7635.
- (177) Bañuls, M.-J.; García-piñón, F.; Puchades, R.; Maquieira, Á. *Bioconjugate Chem.* **2008**, *19*, 665–672.
- (178) Tamarit-López, J.; Morais, S.; Bañuls, M.-J.; Puchades, R.; Maquieira, Á. *Anal. Chem.* **2010**, *82*, 1954–1963.
- (179) Tamarit-López, J.; Morais, S.; Puchades, R.; Maquieira, Á. *Bioconjug. Chem.* **2011**, *22*, 2573–2580.
- (180) Gopinath, S. C. B.; Awazu, K.; Fons, P.; Tominaga, J. *Anal. Chem.* **2009**, *81*, 4963–4970.
- (181) Brun, E. M.; Puchades, R.; Maquieira, Á. *Anal. Chem.* **2013**, *85*, 4178–4186.
- (182) Song, Y.; Luo, D.; Ye, S.; Hou, H.; Wang, L. *Appl. Surf. Sci.* **2012**, *258*, 2584–2590.

- (183) Barrios, C. A.; Canalejas-Tejero, V.; Herranz, S.; Urraca, J.; Moreno-Bondi, M. C.; Avella-Oliver, M.; Maquieira, Á.; Puchades, R. *Biosensors* **2015**, *5*, 417–431.
- (184) Barrios, C. A.; Canalejas-Tejero, V. *Nanoscale* **2015**, *7*, 3435–3439.
- (185) Peris, E.; Banuls, M.-J.; Puchades, R.; Maquieira, Á. *J. Mater. Chem. B* **2013**, *1*, 6245–6253.
- (186) Arnandis-Chover, T.; Morais, S.; Tortajada-Genaro, L. A.; Puchades, R.; Maquieira, Á.; Berganza, J.; Olabarria, G. *Talanta* **2012**, *101*, 405–412.
- (187) Li, Y.; Wang, Z.; Ou, L. M. L.; Yu, H. *Anal. Chem.* **2007**, *79*, 426–433.
- (188) Morais, S.; Tamarit-López, J.; Carrascosa, J.; Puchades, R.; Maquieira, Á. *Anal. Bioanal. Chem.* **2008**, *391*, 2837–2844.
- (189) Tamarit-López, J.; Morais, S.; Puchades, R.; Maquieira, Á. *Anal. Chim. Acta* **2008**, *609*, 120–130.
- (190) Morais, S.; Tortajada-Genaro, L. A.; Arnandis-Chover, T.; Puchades, R.; Maquieira, Á. *Anal. Chem.* **2009**, *81*, 5646–5654.
- (191) Morais, S.; Tamarit-López, J.; Puchades, R.; Maquieira, Á. *Environ. Sci. Technol.* **2010**, *44*, 9024–9029.
- (192) Potyrailo, R. a.; Morris, W. G.; Wroczynski, R.; Hassib, L.; Miller, P.; Dworken, B.; Leach, A. M.; Boyette, S.; Xiao, C. *Sensors Actuators B Chem.* **2009**, *136*, 203–208.
- (193) Tortajada-Genaro, L. A.; Santiago-Felipe, S.; Morais, S.; Gabaldón, J. A.; Puchades, R.; Maquieira, Á. *J. Agric. Food Chem.* **2012**, *60*, 36–43.
- (194) Santiago-Felipe, S.; Tortajada-Genaro, L. A.; Morais, S.; Puchades, R.; Maquieira, Á. *Food Chem.* **2015**, *174*, 509–515.
- (195) Tortajada-Genaro, L. A.; Santiago-Felipe, S.; Amasia, M.; Russom, A.; Maquieira, Á. *RSC Adv.* **2015**, *5*, 29987–29995.
- (196) Arnandis-Chover, T.; Morais, S.; González-Martínez, M. Á.; Puchades, R.; Maquieira, Á. *Biosens. Bioelectron.* **2014**, *51*, 109–114.
- (197) Bañuls, M.-J.; González-Pedro, M.-V.; Puchades, R.; Maquieira, Á. *Anal. Methods* **2012**, *4*, 3133.
- (198) Ramachandraiah, H.; Amasia, M.; Cole, J.; Sheard, P.; Pickhaver, S.; Walker, C.; Wirta, V.; Lexow, P.; Lione, R.; Russom, A. *Lab Chip* **2013**, *13*, 1578–1585.
- (199) Li, X.; Shi, M.; Cui, C.; Yu, H. *Z. Anal. Chem.* **2014**, *86*, 8922–8926.
- (200) Avella-Oliver, M.; Morais, S.; Carrascosa, J.; Puchades, R.; Maquieira, Á. *Anal. Chem.* **2014**, *86*, 12037–12046.
- (201) Fontana, E. *Appl. Opt.* **2004**, *43*, 79–87.
- (202) Santiago-Felipe, S.; Tortajada-Genaro, L. A.; Carrascosa, J.; Puchades, R.; Maquieira, Á. *Biosens. Bioelectron.* **2016**, *79*, 300–306.
- (203) Matsuo, N.; Mori, T. *Environmental Behavior of Synthetic Pyrethroids.*; Springer, 2012; Vol. 314.
- (204) McCoy, M. R.; Yang, Z.; Fu, X.; Ahn, K. C.; Gee, S. J.; Bom, D. C.; Zhong, P.; Chang, D.;

- Hammock, B. D. *J. Agric. Food Chem.* **2012**, *60*, 5065–5070.
- (205) Lin, C.-H.; Ponnusamy, V. K.; Li, H.-P.; Jen, J.-F. *Chromatographia* **2012**, *76*, 75–83.
- (206) Shan, G.; Wengatz, I.; Stoutamire, D. W.; Gee, S. J.; Hammock, B. D. *Chem. Res. Toxicol.* **1999**, *12*, 1033–1041.
- (207) Ahn, K. C.; Gee, S. J.; Kim, H.-J.; Aronov, P. A.; Vega, H.; Krieger, R. I.; Hammock, B. D. *Anal. Bioanal. Chem.* **2011**, *401*, 1285–1293.
- (208) Han, J.-H.; Kim, H.-J.; Sudheendra, L.; Hass, E. A.; Gee, S. J.; Hammock, B. D.; Kennedy, I. M. *Biosens. Bioelectron.* **2013**, *41*, 302–308.
- (209) Călinescu, O.; Badea, I. A.; Vlădescu, L.; Meltzer, V.; Pincu, E. *J. Chromatogr. Sci.* **2012**, *50*, 335–342.
- (210) Sorrano, T. M.; Sultatos, L. G. *Toxicol. Lett.* **1992**, *60*, 27–37.
- (211) Anderson, P. N.; Eaton, D. L.; Murphy, S. D. *Fundam. Appl. Toxicol.* **1992**, *18*, 221–226.
- (212) House, W. A.; Leach, D.; Long, J. L. A.; Cranwell, P.; Smith, C.; Bharwaj, L.; Meharg, A.; Ryland, G.; Orr, D. O.; Wright, J. *Sci. Total Environ.* **1997**, *194/195*, 357–371.
- (213) Munch, J. W. *EPA Method 528. Determination of phenols in drinking water by solid phase extraction and capillary column gas chromatography with large volume injection and chemical ionization tandem mass spectrometry (GS/MS)*; 2000.
- (214) Li, Q. X.; Zhao, S.; Gee, S. J.; Kurth, M. J.; Seiber, J. N.; Jps, B. D. H. *J. Agric. Food Chem.* **1991**, *39*, 1685–1692.
- (215) Oubiña, A.; Ballesteros, B.; Galve, R.; Barcelo, D.; Marco, M. *Anal. Chim. Acta* **1999**, *387*, 255–266.
- (216) Kramer, P. M.; Qing, X. L.; Hammock, B. D. *J. AOAC Int.* **1994**, *77*, 1275–1287.
- (217) EPA. *2011 Edition of the Drinking Water Standards and Health Advisories 2011 Edition of the Drinking Water*; 2011.
- (218) Isensee, A. R.; Helling, C. S.; Gish, T. J.; Kearney, P. C.; Coffman, C. B.; Zhuang, W. *Chemosphere* **1988**, *17*, 165.
- (219) Pereira, W. E.; Rostad, C. E.; Leiker, T. J. *Anal. Chim. Acta* **1990**, *228*, 69–75.
- (220) Holden, L. R.; Graham, J. A.; Whitmore, R. W.; Alexander, W. J.; Pratt, R. W.; Liddle, S. K.; Piper, L. L. *Environ. Sci. Technol.* **1992**, *26*, 935–943.
- (221) Borton, C.; Golden, A. B. S. *EPA Method 535 : Detection of Degradates of Chloroacetanilides and other Acetamide Herbicides in Water by LC/MS/MS*; pp. 1–5.
- (222) Feng, P. C. C.; Horton, S. R.; Sharp, C. R. *J. Agric. Food Chem* **1992**, *40*, 211–214.
- (223) Feng, P. C. C.; Wratten, S. J.; Horton, S. R.; Sharp, C. R.; Logusch, E. W. *J. Agric. Food Chem.* **1990**, *38*, 159–163.
- (224) Gascón, J.; Martinez, E.; Barceló, D. *Anal. Chim. Acta* **1995**, *311*, 357–364.
- (225) Nartova, Y. V.; Ermolaeva, T. N.; Fleisher, M. R.; Abuknesha, R.; Eremin, S. A. *J. Anal. Chem.* **2008**, *63*, 499–505.
- (226) Erickson, L. E.; Lee, K. H.; Sumner, D. D. *Crit. Rev. Environ. Control* **1989**, *19*, 1–14.

- (227) EPA. *Method 523 : Determination of Triazine Pesticides and their Degradates in Drinking Water by Gas Chromatography/Mass Spectrometry (GC/MS)*; 2011.
- (228) Dopico, M. S.; González, M. V; Castro, J. M.; González, E.; Pérez, J.; Rodríguez, M.; Calleja, A. *J. Chromatogr. Sci.* **2002**, *40*, 523–528.
- (229) Cahill, M. G.; Caprioli, G.; Stack, M.; Vittori, S.; James, K. J. *Anal. Bioanal. Chem.* **2011**, *400*, 587–594.
- (230) Wortberg, M.; Kreissig, S. B.; Jones, G.; Rocke, D. M.; Hammock, B. D. *Anal. Chim. Acta* **1995**, *304*, 339–352.
- (231) Schneider, P.; Hammock, B. D. *J. Agric. Food Chem.* **1992**, *40*, 525–530.
- (232) Shim, W.-B.; Yang, Z.-Y.; Kim, J.-Y.; Choi, J.-G.; Je, J.-H.; Kang, S.-J.; Kolosova, A. Y.; Eremin, S. a; Chung, D.-H. *J. Agric. Food Chem.* **2006**, *54*, 9728.
- (233) Seidel, M.; Dankbar, D. M.; Gauglitz, G. *Anal. Bioanal. Chem.* **2004**, *379*, 904–912.
- (234) Zacco, E.; Galve, R.; Marco, M. P.; Alegret, S.; Pividori, M. I. *Biosens. Bioelectron.* **2007**, *22*, 1707–1715.
- (235) Ramón-Azcón, J.; Valera, E.; Rodríguez, A.; Barranco, A.; Alfaro, B.; Sanchez-Baeza, F.; Marco, M.-P. *Biosens. Bioelectron.* **2008**, *23*, 1367–1373.
- (236) Yakovleva, J.; Davidsson, R.; Bengtsson, M.; Laurell, T.; Emnéus, J. *Biosens. Bioelectron.* **2003**, *19*, 21–34.
- (237) Valera, E.; Ramón-Azcón, J.; Sanchez, F.-J.; Marco, M.-P.; Rodríguez, Á. *Sensors Actuators B Chem.* **2008**, *134*, 95–103.
- (238) Tudorache, M.; Tencaliec, A.; Bala, C. *Talanta* **2008**, *77*, 839–843.
- (239) Bartlett, D. W.; Clough, J. M.; Godwin, J. R.; Hall, A. A.; Hamer, M.; Parr-Dobrzanski, B. *Pest Manag. Sci.* **2002**, *58*, 649–662.
- (240) Belden, J.; McMurry, S.; Smith, L.; Reilley, P. *Environ. Toxicol. Chem.* **2010**, *29*, 2477–2480.
- (241) Food European Safety Authority. *Conclusion on the peer review of the pesticide risk assessment of the active substance azoxystrobin*; 2010.
- (242) Parra, J.; Mercader, J. V; Agulló, C.; Abad-Somovilla, A.; Abad-Fuentes, A. *Anal. Chim. Acta* **2012**, *715*, 105–112.
- (243) Banks, K. E.; Hunter, D. H.; Wachal, D. J. *Environ. Int.* **2005**, *31*, 351–356.
- (244) Tomlin, C. D. . *The Pesticide Manual: A World Compendium.*; Tomlin, C.D.S, E., Ed.; 11th ed.; The British Crop Protection Council: Surrey, U.K., 1997.
- (245) EPA. *EPA Method 622. The Determination of Organophosphorus Pesticides in Municipal and Industrial Wastewater.*
- (246) Tiwari, M. K.; Guha, S. *Environ. Monit. Assess.* **2013**, *185*, 8451–8463.
- (247) Samadi, S.; Sereshti, H.; Assadi, Y. *J. Chromatogr. A* **2012**, *1219*, 61–65.
- (248) Li, C.; Chen, L.; Li, W. *Microchim. Acta* **2013**, *180*, 1109–1116.
- (249) Seebunrueng, K.; Santaladchaiyakit, Y.; Soisungnoen, P.; Srijaranai, S. *Anal. Bioanal. Chem.* **2011**, *401*, 1703–1712.

- (250) Cháfer-Pericás, C.; Herráez-Hernández, R.; Campíns-Falcó, P. *J. Chromatogr. A* **2007**, *1141*, 10–21.
- (251) Tang, J.; Zhang, M.; Cheng, G.; Li, A.; Lu, Y. *J. Environ. Sci. Heal. Part B Pestic. food Contam. Agric. wastes* **2008**, *43*, 707–712.
- (252) Brun, E. M.; Garcés-García, M.; Puchades, R.; Maquieira, Á. *J. Agric. Food Chem.* **2005**, *53*, 9352–9360.
- (253) Cho, Y. A.; Lee, H.; Park, E. Y.; Lee, Y. T.; Hammock, B. D.; Ahn, K. C.; Lee, J. K. *Bull. Korean Chem. Soc.* **2002**, *23*, 481–487.
- (254) Kim, Y. A.; Lee, E.-H.; Kim, K.-O.; Lee, Y. T.; Hammock, B. D.; Lee, H.-S. *Anal. Chim. Acta* **2011**, *693*, 106–113.
- (255) Chen, Y. P.; Ning, B.; Liu, N.; Feng, Y.; Liu, Z.; Liu, X.; Gao, Z. X. *J. Environ. Sci. Heal. , Part B Pestic. food Contam. Agric. wastes* **2010**, *45*, 508–515.
- (256) Mauriz, E.; Calle, A.; Lechuga, L. M.; Quintana, J.; Montoya, A.; Manclús, J. J. *Anal. Chim. Acta* **2006**, *561*, 40–47.
- (257) Lee, G. F.; Jones-Lee, A. *Water Quality Control TMDL Goals for Urban Stormwater Runoff OP Pesticide-Caused Aquatic Life Toxicity*; 1999.
- (258) Brun, E. M.; Garcés-García, M.; Escuin, E.; Morais, S.; Puchades, R.; Maquieira, Á. *Environ. Sci. Technol.* **2004**, *38*, 1115.
- (259) Bavcon, M.; Trebse, P.; Zupancic-Kralj, L. *Chemosphere* **2003**, *50*, 595–601.
- (260) Rahiminejad, M.; Shahtaheri, S. J.; Ganjali, M. R.; Forushani, A. R.; Golbabaei, F. *Iran. J. Environ. Heal. Sci. Eng.* **2009**, *6*, 97–106.
- (261) Zaruk, D.; Comba, M.; Struger, J.; Young, S. *Anal. Chim. Acta* **2001**, *444*, 163–168.
- (262) Hoeve, W.; Wynberg, H.; Jones, W. T.; Harvey, D.; Ryan, G. B.; Reynolds, P. H. S. *Bioconjug. Chem.* **1997**, *8*, 257–266.
- (263) Lapworth, D. J.; Goody, D. C. *Environ. Pollut.* **2006**, *144*, 1031–1044.
- (264) Lin, H.-H.; Sung, Y.-H.; Huang, S.-D. *J. Chromatogr. A* **2003**, *1012*, 57–66.
- (265) Muñoz de la Peña, A.; Mahedero, M. C.; Bautista-Sánchez, A. *J. Chromatogr. A* **2002**, *950*, 287–291.
- (266) Ozhan, G.; Ozden, S.; Alpertunga, B. *J. Environ. Sci. Heal. Part B Pestic. Food Contam. Agric. Wates* **2005**, *40*, 827–840.
- (267) Li, Y.; George, J. E.; McCarty, C. L.; Wendelken, S. C. *J. Chromatogr. A* **2006**, *1134*, 170–176.
- (268) Carabias-Martínez, R.; García-Hermida, C.; Rodríguez-Gonzalo, E.; Soriano-Bravo, F. E.; Hernández-Méndez, J. *J. Chromatogr. A* **2003**, *1002*, 1–12.
- (269) Dinelli, G.; Vicari, a; Catizone, P. *J. Chromatogr. A* **1996**, *733*, 337–347.
- (270) Karu, A. E.; Goodrow, J. M. H.; Schmidt, D. J.; Hammock, B. D.; Bigelowl, M. W. *J. Agric. Food Chem.* **1994**, *42*, 301–309.
- (271) Sharma, P.; Kukkar, M.; Ganguli, A. K.; Bhasin, A.; Suri, C. R. *Analyst* **2013**, *138*, 4312–

- 4320.
- (272) Sharma, P.; Sablok, K.; Bhalla, V.; Suri, C. R. *Biosens. Bioelectron.* **2011**, *26*, 4209–4212.
- (273) Ciumasu, I. M.; Krämer, P. M.; Weber, C. M.; Kolb, G.; Tiemann, D.; Windisch, S.; Frese, I.; Kettrup, A. A. *Biosens. Bioelectron.* **2005**, *21*, 354–364.
- (274) Soto, A. M.; Chung, K. L.; Sonnenschein, C. *Environ. Health Perspect.* **1994**, *102*, 380–383.
- (275) Mukherjee, I.; Gopal, M. *J. Chromatogr. A* **1996**, *754*, 33–42.
- (276) Manclús, J. J.; Abad, A.; Lebedev, M. Y.; Mojarrad, F.; Micková, B.; Mercader, J. V.; Primo, J.; Miranda, M. A.; Montoya, A. *J. Agric. Food Chem.* **2004**, *52*, 2776–2784.
- (277) Díaz, T. G.; Cabanillas, A. G.; Soto, M. D. L.; Ortiz, J. M. *Talanta* **2008**, *76*, 809–814.
- (278) Molina, C.; Grasso, P.; Benfenati, E.; Barceló, D. *J. Chromatogr. A* **1996**, *737*, 47–58.
- (279) Lambropoulou, D. A.; Albanis, T. A. *J. Chromatogr. A* **2001**, *922*, 243–255.
- (280) Lambropoulou, D. A.; Sakkas, V. A.; Hela, D. G.; Albanis, T. A. *J. Chromatogr. A* **2002**, *963*, 107–116.
- (281) Brun, E. M.; Garcés-García, M.; Puchades, R.; Maquieira, Á. *J. Immunol. Methods* **2004**, *295*, 21–35.
- (282) Cho, Y. A.; Kim, Y. J.; Hammock, B. D.; Lee, Y. T.; Lee, H.-S. *J. Agric. Food Chem.* **2003**, *51*, 7854–7860.
- (283) Kim, Y. J.; Cho, Y. A.; Lee, H.-S.; Lee, Y. T. *Anal. Chim. Acta* **2003**, *494*, 29–40.
- (284) Kim, J. G.; Takami, Y.; Mizugami, T.; Beppu, K.; Fukuda, T.; Kataoka, I. *Sci. Hortic. (Amsterdam)*. **2006**, *110*, 219–222.
- (285) Ferrer, I.; Thurman, E. M.; Fernández-Alba, A. R. *Anal. Chem.* **2005**, *77*, 2818–2825.
- (286) Valverde, A.; Aguilera, A.; Ferrer, C.; Camacho, F.; Cammarano, A. *J. Agric. Food Chem.* **2010**, *58*, 2818–2823.
- (287) Kobayashi, M.; Takano, I.; Tamura, Y.; Tomizawa, S.; Tateishi, Y.; Sakai, N.; Kamijo, K.; Ibe, A.; Nagayama, T. *Shokuhin Eiseigaku Zasshi*. **2007**, *48*, 148–152.
- (288) Suárez-Pantaleón, C.; Esteve-Turrillas, F. a; Mercader, J. V; Agulló, C.; Abad-Somovilla, A.; Abad-Fuentes, A. *Anal. Bioanal. Chem.* **2012**, *403*, 2019–2026.
- (289) Suárez-Pantaleón, C.; Mercader, J. V; Agulló, C.; Abad-Somovilla, A.; Abad-Fuentes, A. *J. Agric. Food Chem.* **2010**, *58*, 8502–8511.
- (290) Suárez-Pantaleón, C.; Wichers, J.; Abad-Somovilla, A.; van Amerongen, A.; Abad-Fuentes, A. *Biosens. Bioelectron.* **2013**, *42*, 170–176.
- (291) Rancan, M.; Sabatini, A. G.; Achilli, G.; Galletti, G. C. *Anal. Chim. Acta* **2006**, *555*, 20–24.
- (292) Kookana, R. S. *J. Chromatogr. A* **1997**, *787*, 271–275.
- (293) K, S. A.; Srivastava, M. K.; Patel, D. K.; Mudiam, M. K. R.; Srivastava, L. P. *J. Environ. Res. Dev.* **2012**, *7*, 643–651.
- (294) Navalón, A.; González-Casado, A.; El-Khattabi, R.; Vilchez, J. L.; Fernández-Alba, A. R. *Analyst* **1997**, *122*, 579–581.
- (295) Lee, J. K.; Ahn, K. C.; Park, O. S.; Kang, S. Y.; Hammock, B. D. *J. Agric. Food Chem.* **2001**,

- 49, 2159–2167.
- (296) Xu, T.; Gong, Q.; Li, H.; Wang, J.; Li, Q. X.; Shelver, W. L.; Li, J. *Talanta* **2012**, *101*, 85–90.
- (297) Windham, G. C.; Titenko-Holland, N.; Osorio, A. M.; Gettner, S.; Reinisch, F.; Haas, R.; Smith, M. *Am. J. Ind. Med.* **1998**, *33*, 164–174.
- (298) WHO/SDE/WSH/03.04.103. *Malathion in Drinking-water Background document for development of WHO Guidelines for Drinking-water Quality*; 2004.
- (299) Beeson, M. D.; Driskell, W. J.; Barr, D. B. *Anal. Chem.* **1999**, *71*, 3526–3530.
- (300) Kristenson, E. M.; Haverkate, E. G.; Slooten, C. J.; Ramos, L.; Vreuls, R. J.; Brinkman, U. A. *J. Chromatogr. A* **2001**, *917*, 277–286.
- (301) García-Ruiz, C.; Álvarez-Llamas, G.; Puerta, Á.; Blanco, E.; Sanz-Medel, A.; Marina, M. L. *Anal. Chim. Acta* **2005**, *543*, 77–83.
- (302) Fidalgo-Used, N.; Blanco-González, E.; Sanz-Medel, A. *Talanta* **2006**, *70*, 1057–1063.
- (303) Brun, E. M.; Garcés-García, M.; Bañuls, M. J.; Gabaldón, J. A.; Puchades, R.; Maquieira, Á. *Environ. Sci. Technol.* **2005**, *39*, 2786–2794.
- (304) Rodriguez, I.; Cela, R. *Trends Anal. Chem.* **1997**, *16*, 463–475.
- (305) *Pyraclostrobin ELISA (Microtiter Plate). Enzyme-Linked Immunosorbent Assay for the Determination of Pyraclostrobin in Water and Wine Samples. Abraxis, Product No. 50070*; 2012.
- (306) Marzo, A.; Dal Bo, L. *J. Chromatogr. A* **1998**, *812*, 17–34.
- (307) Kümmerer, K. *J. Environ. Manage.* **2009**, *90*, 2354–2366.
- (308) Oberlé, K.; Capdeville, M.-J.; Berthe, T.; Budzinski, H.; Petit, F. *Environ. Sci. Technol.* **2012**, *46*, 1859–1868.
- (309) Kostopoulou, M.; Nikolaou, A. *Trends Anal. Chem.* **2008**, *27*, 1023–1035.
- (310) Seifrtová, M.; Nováková, L.; Lino, C.; Pena, A.; Solich, P. *Anal. Chim. Acta* **2009**, *649*, 158–179.
- (311) Fontanals, N.; Marcé, R. M.; Borrull, F. *J. Chromatogr. A* **2011**, *1218*, 5975–5980.
- (312) de Keizer, W.; Bienenmann-Ploum, M. E.; Bergwerff, A. A.; Haasnoot, W. *Anal. Chim. Acta* **2008**, *620*, 142–149.
- (313) Balmer, M. E.; Poiger, T.; Droz, C.; Romanin, K.; Bergqvist, P.-A.; Müller, M. D.; Buser, H.-R. *Environ. Sci. Technol.* **2004**, *38*, 390–395.
- (314) Latch, D. E.; Packer, J. L.; Stender, B. L.; VanOverbke, J.; Arnold, W. A.; McNeil, K. *Environ. Toxicol. Chem.* **2005**, *24*, 517–525.
- (315) Morais, S.; Casino, P.; Marín, M. L.; Puchades, R.; Maquieira, Á. *Anal. Bioanal. Chem.* **2002**, *374*, 262–268.
- (316) Parra, J.; Mercader, J. V.; Agulló, C.; Abad-Somovilla, A.; Abad-Fuentes, A. *Toxicol. Lett.* **2012**, *210*, 240–247.
- (317) Suárez-Pantaleón, C.; Mercader, J. V.; Agulló, C.; Abad-Somovilla, A.; Abad-Fuentes, A. *J. Agric. Food Chem.* **2008**, *56*, 11122–11131.

-
- (318) Noguera, P.; Maquieira, Á.; Puchades, R.; Brunet, E.; Carramolino, M. M.; Rodríguez-Ubis, J. *C. J. Environ. Monit.* **2002**, *4*, 442–448.
- (319) Mercader, J. V.; Suárez-Pantaleón, C.; Agulló, C.; Abad-Somovilla, A.; Abad-Fuentes, A. *J. Agric. Food Chem.* **2008**, *56*, 7682–7690.
- (320) Li, J. L.; Day, D.; Gu, M. *Adv. Mater.* **2008**, *20*, 3866–3871.
- (321) Link, S.; El-Sayed, M. A. *Annu. Rev. Phys. Chem.* **2003**, *54*, 331–366.
- (322) Geoghegan, W. D. *J. Histochem. Cytochem.* **1988**, *36*, 401–407.
- (323) He, J. *Practical Guide to ELISA Development*; Fourth Edi.; Elsevier Ltd, 2011.
- (324) Dungchai, W.; Siangproh, W.; Chaicumpa, W. *Talanta* **2008**, *77*, 727–732.
- (325) Tijssen, P. *Practice and Theory of Enzyme Immunoassays*; Science, Elsevier, 1985.
- (326) Dunbar, B.; Riggle, B.; Niswender, G. *J. Food Agric. Chem* **1990**, *38*, 433–437.
- (327) Lan, M.; Guo, Y.; Zhao, Y.; Liu, Y.; Gui, W.; Zhu, G. *Anal. Chim. Acta* **2016**, *938*, 146–155.
- (328) Wang, F.; Wang, H.; Shen, Y.-D.; Li, Y.-J.; Dong, J.-X.; Xu, Z.-L.; Yang, J.-Y.; Sun, Y.-M.; Xiao, Z.-L. *J. Agric. Food Chem.* **2016**, *64*, 8054–8061.
- (329) Dobosz, P.; Morais, S.; Puchades, R.; Maquieira, Á. *Biosens. Bioelectron.* **2015**, *69*, 294–300.